



Dottorato di Ricerca in Ambiente Salute e Processi Ecosostenibili

XXII Ciclo

RHEOLOGY OF HIGHLY-CONCENTRATED-IN-OIL EMULSIONS

S.S.D. ING-IND/24
PRINCIPI DI INGEGNERIA CHIMICA

Coordinatore del Dottorato

Prof. Bruno DE CINDIO

Supervisore

Prof. Bruno DE CINDIO

Dottoranda

Francesca Romana LUPI

Introduction	1
Chapter 1 – General overview and state of the art	3
Introduction.....	3
1.1. An introduction to general definitions of colloids and emulsions	5
1.1.1. Droplet size distribution.....	7
1.1.2. Statistical Models.....	9
1.2. Emulsions rheology	12
1.2.1. Dynamic regime: small amplitude oscillatory tests	13
1.2.2. Flow behaviour: from diluted to concentrated emulsions	16
1.3. Emulsifiers and surfactants characteristics	22
1.4. Structured emulsions: an overview.....	23
1.4.1. Structured O/W emulsions.....	24
1.4.2. Structured W/O emulsions for food applications	26
1.4.3. Gelled emulsions	32
1.5. Crude oil emulsification.....	32
1.5.1. O/W unstructured emulsion for crude oil transportation	33
1.5.2. Crude water-in-oil emulsions.....	35
1.5.3. SARA components of crude oil: effect on emulsions properties	36
1.5.4. Environmental impact	38
Conclusions.....	39
References.....	39
Chapter 2 – Isoenergetic emulsification: rheology and droplet size distribution	50
Abstract	50
2.1. Introduction.....	48
2.1.1. Different methods of emulsification: a general overview	47
2.1.2. DSD measurement and statistic analysis	55
2.2. Materials and methods	57
2.2.1. Emulsions preparation	57
2.2.2. Mixing conditions	58
2.2.3. Rheological characterisation	59
2.2.4. Microscopic characterisation: DSD	59
2.3. Results and discussion.....	61
2.3.1. Droplet size distribution: choice of the best fitting model	61
2.3.2. Droplet size distribution: physical meaning	63

2.3.3. Rheological characterisation: viscosity	65
Conclusions.....	69
References.....	70
Chapter 3 – Stability of concentrated O/W emulsions: a microscopic and rheological analysis	75
Abstract	75
3.1. Introduction.....	75
3.2. Materials and Methods	81
3.2.1. Rheological characterisation	83
3.2.2. Microscopic characterisation: DSD	84
3.2.3. Oil extraction procedure	85
3.3. Results and discussion.....	85
3.3.1. Dilution effect on the DSD results.....	85
3.3.2. STSTs: effect of oil characteristics.....	86
3.3.3. STSTs: effect of oil fraction.....	92
3.3.4. LTSTs.....	98
Conclusions.....	102
References.....	103
Chapter 4 – Effect of waxes addition on rheological properties of O/W concentrated model emulsions.....	108
Abstract	108
4.1. Introduction.....	108
4.2. Materials and Methods	110
4.2.1. Materials	110
4.2.2. Batch emulsification.....	111
4.2.3. Flow emulsification	112
4.2.4. Rheological characterisation	113
4.3. Results and discussion.....	114
4.3.1. Oil and wax mixture	114
4.3.2. Batch produced emulsions.....	114
4.3.3. In-flow produced emulsions.....	114
Conclusions.....	117
References.....	117
Chapter 5 – Structuring water phase: olive oil emulsions as puff pastry shortening replacer.....	120
Abstract	120

5.1. Introduction.....	120
5.1.1. Puff pastry and shortenings	121
5.1.2. Structured emulsions: a brief introduction.....	123
5.1.3. Interaction between the more common hydrocolloids and emulsions characteristics	125
5.2. Materials and Methods	126
5.2.1. Samples ingredients and identification.....	126
5.2.2. Samples preparation	128
5.2.3. Rheological characterisation	129
5.3. Results and Discussion	131
5.3.1. Rheological characterisation of commercial margarines.....	131
5.3.2. Rheological characterisation of the W/O emulsions.....	133
5.3.3. Rheological characterisation of the O/W emulsions.....	139
Conclusions.....	144
References.....	145
Chapter 6 – Structuring oily phase: water in olive oil emulsions as puff pastry shortening replacer	149
Abstract	149
6.1. Introduction.....	150
6.1.1. Margarine and margarine substitutes: a state of the art	150
6.1.2. W/O emulsions with cocoa butter	154
6.2. Materials and methods	157
6.2.1. Samples ingredients and identification.....	157
6.2.2. Samples preparation	157
6.2.3. Rheological characterisation	158
6.2.4. Microscopy tests	161
6.2.5. Study of the phases placement.....	161
6.3. Results and discussion.....	162
6.3.1. Oily phase rheological characterisation	164
6.3.2. Emulsions rheological characterisation	166
6.3.3. Microstructural characterisation	173
Conclusions.....	174
References.....	175
Conclusions	179
List of publications	181

This PhD thesis could not have been written without the expert advice of my academic supervisor, Prof. Bruno de Cindio, who taught me to be a good professional and a better person. I also have to thank Dr. Noemi Baldino, Dr. Domenico Gabriele and Dr. Massimo Migliori (in alphabetic order!) for their technical and human support (thank you Massimo and Mimmo for proofreadings!). I am also very grateful to Prof. Crispulo Gallegos Montes and the members of the 'Laboratorio de Ingeniería de Fluidos Complejos', Universidad de Huelva (Spain), for the wonderful months spent together and the professional support for the study of crystallised emulsions. Special thanks also to Dr. Cesare Oliverio Rossi for the NMR tests and oil composition measurements presented in Chapter 3. Finally, I would like to thank 'Soavegel S.r.l.' for the collaboration on structured emulsions study.

Introduction

In the present PhD thesis the rheological and microscopic study of highly-concentrated-in-oil emulsions (with an oily phase percentage > 50%) is reported. The increasing importance of this subject is emphasised by the industrial request to improve research and development in order to find new materials for different applications. It is worth noticing that the high concentration of one phase does not imply that it is dispersed in the other, but there are many cases (i.e. W/O emulsions like margarines) in which the continuous phase is the main constituent of the emulsion.

To this purpose, the thesis was developed by subdividing the main subject into two opposites parts: the first one deals with unstructured and concentrated low viscous O/W emulsions, while the second one examines structured emulsions considering the structuration of both the water phase (W/O ‘gelled emulsions’ and O/W emulsions) and the oily phase (W/O emulsions). Aiming at transferring the obtained results to real industrial problems, two different case studies were taken into account: the first one is the crude oil transportation in pipelines promoting the production of concentrated O/W emulsions, while the second one is the formulation and production optimisation of a new-*trans-fats-free* puff pastry shortening replacer.

As far as the first case study is concerned, crude oil emulsification in water is a reliable method to decrease the fluid viscosity for its transportation in pipelines, leading to a cost reduction and energy saving technique. A practical demonstration of crude oil emulsification realised to improve its transportation, was successfully carried out with the highly viscous oil of the field in the Orinoco River region of Venezuela. The surfactant-stabilised emulsion is a new liquid fuel, trade name Orimulsion, that can be fed directly to an electric power plant, thereby strongly reducing particulate emission.

In regard to the second case study, structured emulsions are mostly used in foodstuffs engineering and production. Emulsions like margarines used in puff pastry production derive their consistency from a fat crystal network obtained with a certain amount of fully saturated triglycerides (TAGs). Traditionally TAGs saturation is performed by hydrogenation from which *cis* and *trans* isomers (TFAs) can be obtained. In particular TFAs promote the development of atherosclerosis and a predisposition to coronary heart

disease and other not well-known risks. The importance of designing healthy everyday foods without trans-fats can be clearly understood looking at the recent literature: in the last “International Symposium of Food Rheology and Structure”, Zurich, 15-18 June 2009, many interesting works have been published in the proceedings.

Thus, apart from the first chapter, which is a state-of-art literature review of the examined subject, the arrangement of the thesis consists of other five chapters, structured as scientific papers.

As already said, in the first chapter a state-of-the-art review is presented, focusing on a general overview of emulsions main characteristics in the first part, and giving a detailed summery of the two case studies in the second part. Chapters 2, 3 and 4 deal with the first case study, while chapters 5 and 6 treat the second case study.

Chapter 2 reports the study of the emulsification of model concentrated O/W emulsions performed with an isoenergetic criterion, and examining the effect of the specific power of mixing on the rheological and droplet size characteristics of the samples. The stability of the same kinds of emulsions was studied in Chapter 3, analysing differences and analogies of two different destabilisation tests: a long-term and an accelerated short-term one. In Chapter 4 a batch and a flow induced emulsification process was studied in order to simulate the pipeline behaviour of model crude oil-in-water emulsions with paraffin waxes added. Chapters 5 presents the production of structured W/O gelled emulsions and O/W emulsions in which the water phase was thickened by different hydrocolloids (wheat flour, κ -carrageenan and Xanthan gum). Finally in Chapter 6 the formulation and process optimisation of W/O crystallised emulsions with a structured oily phase is reported.

Chapter 1 – General overview and state of the art

Introduction

Emulsion is a heterogeneous system that consists of two immiscible phases one of which is dispersed in the other in the form of droplets. The dispersed phase, belonging to the phases disposition, can be oily, forming O/W emulsions, or aqueous forming W/O emulsions (or even multiple O/W/O or W/O/W).

The aim of the present PhD thesis is a rheological and microscopic characterisation of different kinds of emulsions prepared with a high concentration ($\geq 50\%$) of the oily phase. Persistent interest in the comprehension of peculiarities of the rheological properties of emulsions is determined by the challenge posed by numerous and unexpected effects observed in the flow of emulsions. This interest is also strongly motivated by the problems of industry, which produces and consumes many hundred thousand tons of emulsions of various content, properties and functions. The fundamental

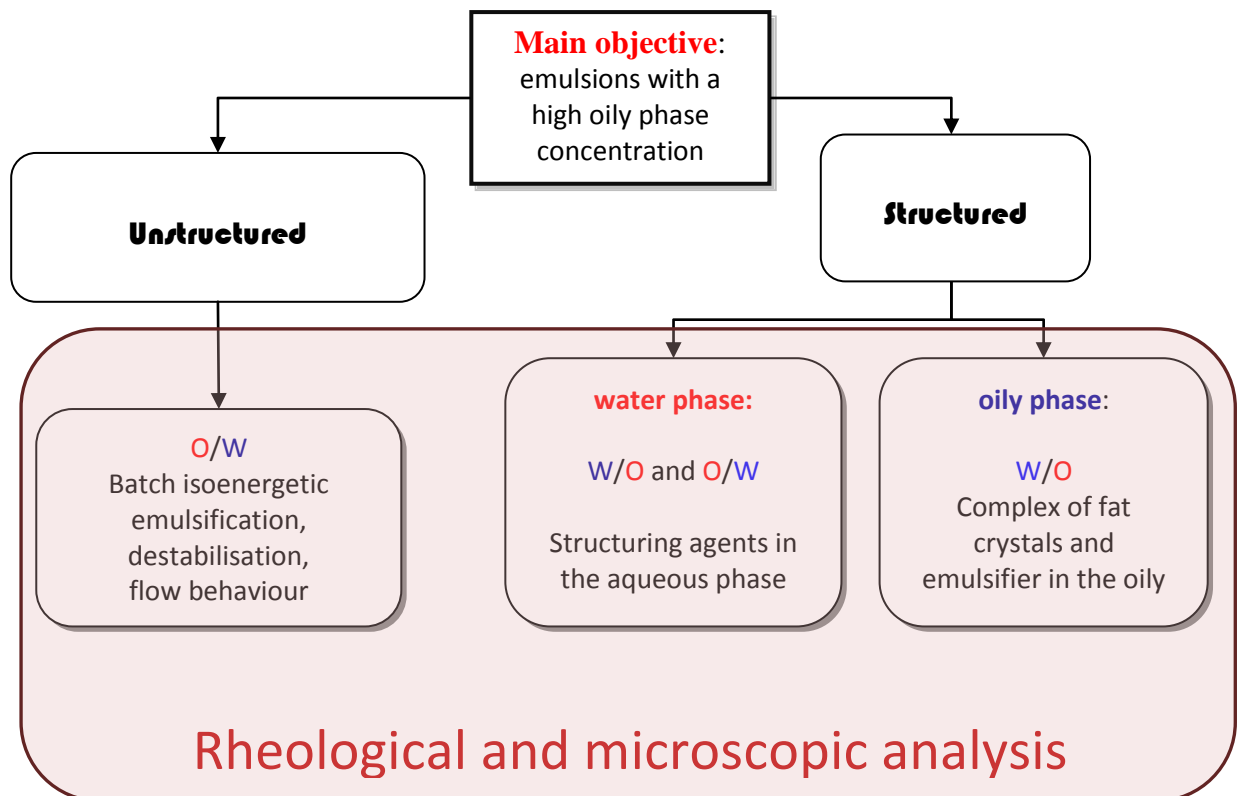


Figure 1.1: Schematic representation of the thesis work

reasons for unexpected and new effects in the behaviour of emulsions is mainly due to the abundance of chemical compounds and the variation of their nature in composing these multi-component materials. If one considers the raw materials involved in emulsions

production, it is obvious that from an economical point of view the biphasic systems in which a greater relative amount of oily phase is used are much more interesting with respect to the aqueous diluted systems, because of the higher added value of the fat phase. The emulsions with a high concentration of oily phase may vary from a rheological point of view from highly structured solid-like emulsions to liquid unstructured systems. The structuration can be achieved by creating a network connecting the rheological unities (droplets) structuring the external phase and reaching different results and degree of structuration. The unstructured emulsions on the contrary are characterised by the absence of interconnection between droplets. Thus, the entire work is mainly focused on two different and opposite case studies whose importance in industrial processes is increasingly important. The first case study concerns the realisation and, in some cases, the destabilisation of low viscous unstructured and highly concentrated O/W emulsions for heavy crude oil transportation aiming at reduce the viscosity and consequently the pressure drops in pipelines of the starting crude oil; the second, on the contrary, concerns the progressive structuration of olive oil emulsions as shortening replacers for puff pastries production. This second objective has been reached structuring the water phase in both the W/O and the O/W system and, finally, structuring the oily phase in W/O emulsions with a fat crystallisation process. In order to summarize the whole work, a scheme of the thesis work is sketched in figure 1.1.

The first case study is discussed in chapters 2, 3 and 4 of the thesis, in which first of all an isoenergetic emulsification is studied (Chapter 2). Then, the destabilisation study of apparent Newtonian emulsions is considered comparing two different destabilisation tests: a long-term and an accelerated short-term one (Chapter 3). Finally, a batch and a flow induced emulsification process are studied in order to simulate the pipeline behaviour of model crude oil-in-water emulsions with paraffin waxes added (Chapter 4). The other two chapters deal with the production of W/O and O/W emulsions with a structured water phase and W/O emulsions with a structured oily phase (Chapters 5 and 6).

The two case studies proposed were chosen considering their great importance in emulsions industries: it can, in fact, be affirmed that huge efforts are addressed in the research of those problems. The first case study is becoming crucial for the crude oil industry: the piping of crude oil in the form of oil-in-water emulsion is becoming a widespread application because of the current large amount of heavy oil extracted from wells. This determines an increase of pumping costs and great energy consumption with consequent environmental impact as a consequence of the higher oil viscosity. Heavy oils

viscosity may range widely from 0.1 Pa·s to 100 Pa·s, [[Wakabayashi, 1997](#); [Ahmed et al., 1999](#); [Quiñones-Cisneros et al., 2005](#)], also showing shear thinning behaviour, depending upon type and amount of minor components (such as waxes, resins, asphaltenes, sand or possibly hydrates).

A more detailed overview is proposed in paragraph 1.5 of the present chapter.

The second case study is a typical food industry challenge. The growing request for healthy foods demanded by the consumer is pushing research to substitute dangerous and unhealthy additives with better known and natural ingredients. The importance of designing healthy everyday foods without trans-fats can be clearly understood looking at the recent literature. In the last “International Symposium of Food Rheology and Structure” (Zurich, 15 – 18 June 2009), a lot of interesting works have been published in the proceedings: an example is the plenary lecture given by Ian T. Norton [[Norton, 2009](#)]. Thus, the problem of substituting trans-fatty acids in margarine (W/O emulsions) is a huge problem treated differently by research. A detailed review in the literature of this matter is proposed in paragraph 1.4 of this chapter.

In the present chapter a general overview of emulsions properties and characteristics is presented, showing the main differences between W/O or O/W emulsions and their possible applications in food industries and concentrated O/W emulsions and their applications for crude oil transportation. Regarding food applications, an introduction about both W/O and O/W structured emulsions is also reported. In the next paragraph is presented a general preamble on emulsions characteristics as well as the most important definition of colloid science such as the droplet size distribution concept.

1.1. An introduction to general definitions of colloids and emulsions

The greater part of heterogeneous systems is composed of a continuous medium having one or more dispersed phases. Some examples of these systems are:

- O/W emulsions (mayonnaise, lubricant oils, milk) with a droplet dimension that varies from 0.5 to 5 μm
- W/O emulsions (butter, margarines, food creams) with a droplet dimension that varies from 1 to 3 μm
- asphalt in water emulsions with a droplet dimension that varies from 2 to 7 μm
- polymeric systems with a droplet dimension that varies from 1 to 2000 μm

- spores as dispersed globules in an heterogeneous phase with a droplet dimension $> 4 \mu\text{m}$
- minerals dispersed in a water phase as a fluid vector.

If the dimensions of the dispersed phase are bigger than those indicated, a single heterogeneous system could not be considered, but rather two different systems.

Thus, it is necessary to make a distinction amongst the various systems. If the dispersed particles are liquid the system is an emulsion, if they are solid with a dimension bigger than $1 \mu\text{m}$, it is a suspension, and finally, if the dispersed particles are one dimension smaller than $1 \mu\text{m}$ the system is a dispersion. Dispersions are *colloidal* systems with a mean diameter between 1 nm and $1 \mu\text{m}$, for which we have to consider *Van der Waals-London forces*, *thermal agitation motion*, *hydrodynamic forces* and *field forces* [Riley, 2005].

A *colloid* is a molecule or a polymolecular particle dispersed in a medium with, at least in one direction, a dimension roughly between 1 nm and $1 \mu\text{m}$: fibres in which only two dimensions are in this range, and thin films, in which one dimension is in this range, may also be classified as colloidal. This is the same range that, in a *colloidal system*, establishes the distance between its discontinuities [<http://old.iupac.org/>].

The size limits given above can vary in some cases since they will depend to some extent on the properties under consideration [Vincent, 2005].

The name *dispersed phase* for the particles should be used only if they have essentially the properties of a bulk phase of the same composition. An important parameter that identifies the volumetric composition of emulsions is the *dispersed phase volume fraction* or ϕ , equal to the volume of emulsion droplets (V_D) divided by the total volume of the emulsion (V_E): $\phi = V_D/V_E$.

The greater importance of the volumetric concentration with respect to the mass concentration is due to the flow field that is influenced by the dimension of the dispersed phase and is not affected by its weight. There is also an upper limit for this concentration that depends on the shape, dimensions and droplet size distribution. Moreover, there are no differences between emulsions and suspensions if the parameter ϕ is considered: the disturbance to the hydrodynamic field remains the same, and in both cases flocs or agglomerates can be formed.

In an emulsion liquid, droplets and/or liquid crystals are dispersed in a liquid and the droplet diameter often exceeds the limits for colloids in size. Thus, emulsions are often made by these immiscible systems, usually water and oil. An emulsion is denoted by the

symbol O/W if an organic liquid (an “oil”) is dispersed in a continuous aqueous solution phase and by W/O if the continuous phase is oil. More complicated emulsions are called multiple emulsions. An example is the double O/W/O emulsion in which oil droplets contained within aqueous droplets are dispersed in a continuous oil phase [Pal, 2007].

Emulsions are very important for a large number of industrial applications. They are widely employed in food applications [Friberg and Larsson, 1976, McClements, 1999] related to their rheological behaviour (e.g. creaminess, thickness, smoothness, spreadability, pourability and flowability), such as milk, ice creams, dairy emulsions [Gabriele et al., 2009], butter, margarine, fruit beverages [Buffo and Reineccius, 2002], soups, cake batters, mayonnaise, cream liqueurs, sauces, desserts, salad cream, and coffee whitener. O/W emulsions are also a good method for heavy crude oil transportation [Saniere et al., 2004], and W/O emulsion can accidentally be formed in oil spill tragedies [Fingas and Fieldhouse, 2004].

W/O and O/W emulsions are also involved in pharmaceutical cream production [Masmoudi et al., 2006] and for cosmetics [Förster and Herrington, 1998], for which they have to be strongly stable (years) and have to show a shear thinning, predominately elastic behaviour and low yield stress. According to Eccleston (1997) the importance of emulsions and dispersions in cosmetics is mostly centred on their ability to deliver their therapeutic properties by acting as vehicle drugs and a cosmetic agent to the skin. Moreover, rheological properties of creams, often obtained by adding a polymeric thickener [Miller et al. 1999], can be distinguished between cosmetic agent (drug or cosmetic agent remain on the surface of the skin), or therapeutic agent (in this case the drug penetrates the stratum corneum). Thus, emulsion formulation has to guarantee skin safety and non-irritant properties, and has to be able to incorporate co-solvents, antioxidants and so on. Another industrial application of emulsions is polymerisation, mostly for rubber production. Owing to the increasing necessity to reduce the environmental impact, this method has attracted more interest because it avoids the use of hazardous solvents [do Amaral, 2004].

1.1.1. Droplet size distribution

The dimension of droplets in biphasic systems is very important for understanding their rheological properties. If droplets have more or less the same dimension, the emulsion is ‘*monodisperse*’ while if droplet size differs from an average value, the emulsion is

'polydisperse'. An important characteristic of colloids is the polydispersity of their size. Pure science tends to study model monodisperse systems, but in practical applications a large polydispersity can sometimes bring better properties to the system, for example, preferable rheological properties [Vincent, 2005]. In particular, if the *droplet size distribution* of emulsions is almost *monomodal*, all droplets are characterised by an average size and a standard deviation or a polydispersity degree; if, on the contrary, the emulsion is *bimodal* it is characterised by two different groups of droplets, each distinguished by an average droplet size diameter (see figure 1.2).

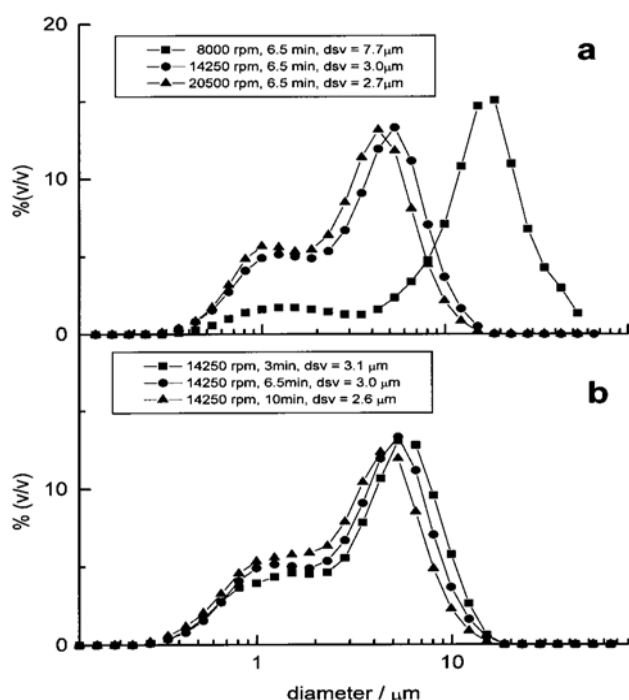


Figure 1.2: an example of droplet particle size bimodal distribution with (a) agitation speed and (b) emulsification time for lupin protein-stabilized emulsions

In a monomodal emulsion, the average diameter that characterises the dimensional distribution of the system can be determined as belonging to the analysis approach used for its estimation. Analysis of polydisperse emulsions using osmotic pressure measurements gives information about their mean length diameter, whereas light-scattering, sedimentation and optical microscopy measurements give information about their surface diameter.

It is often convenient to represent the size of the droplets in a polydisperse emulsion by the mean diameter $\langle d \rangle$, which is a measure of the central tendency of the distribution, and the standard deviation σ , a measure of the width of the distribution.

In the following table a list of the different ways of expressing the mean droplet diameter of a polydisperse emulsion is reported [McClements, 1999].

Diameter	Symbol	Definition	Equation	Reference
Lenght	\bar{d} or d_L	$d_L = \sum n_i d_i / \sum n_i$	[1.1.1]	McClements, 1999
Surface Area	d_S	$d_S = \sqrt{\sum n_i d_i^2 / \sum n_i}$	[1.1.2]	McClements, 1999
Volume	d_V	$d_V = \sqrt[3]{\sum n_i d_i^3 / \sum n_i}$	[1.1.3]	McClements, 1999
Volume Surface Area	d_{VS} or d_{32}	$d_{VS} = \sqrt{\sum n_i d_i^3 / \sum n_i d_i^2}$	[1.1.4]	McClements, 1999 Comas et al., 2006 Quintana et al., 2002 Hemmingsen et al., 2006
Mean Volume	d_{43}	$d_{43} = \sqrt[4]{\sum n_i d_i^4 / \sum n_i d_i^3}$	[1.1.5]	Hénaut et al., 2009 Ye and Singh, 2006

Table 1.1: mean droplet diameters definition

The data analysis for droplet size distribution determination is based on simple statistic model. First of all is pretty convenient to present data as the number frequency (eq. 1.1.6) or the volume frequency (eq 1.1.7).

$$f_i = \frac{n_i}{N} \quad [1.1.6]$$

$$\phi_i = \frac{v_i}{V} \quad [1.1.7]$$

where n_i is the number of droplets in each size class, N is the total number of droplets, v_i is the volume of the droplets in the i -th size class and V is the total volume of all the droplets in the emulsion. Other useful representations (figure 1.3) of the particle size distribution are the *distribution function* $F(d_i)$, and the *cumulative function* $C(d_i)$. The (number) distribution function is constructed so that the area under the curve between two droplet sizes (d_i and $d_i + \delta d_i$) is equal to the number of droplets (n_i) in that size range. This relationship can be used to convert a histogram to a distribution function or vice versa. The cumulative function represents the percentage of droplets that are smaller than d_i . The resulting curve has an S-shape which varies from 0 to 100% as the particle size increases. The particle size at which half the droplets are smaller and the other half are larger is known as the median droplet diameter (d_m) [McClements, 1999].

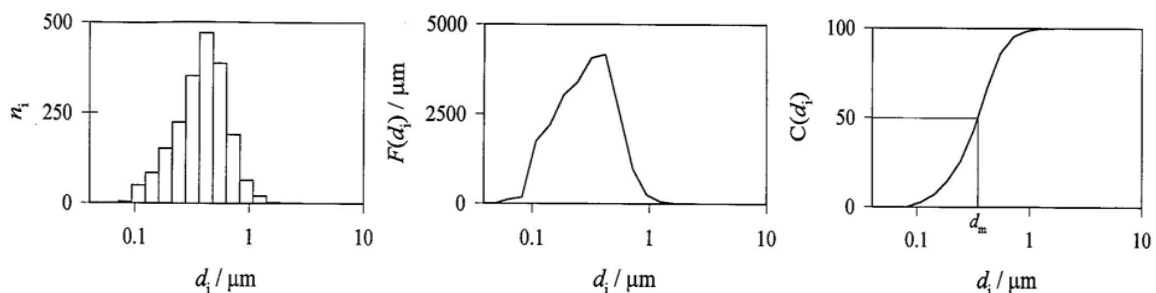


Figure 1.3: particle size distribution representation

1.1.2. Statistical Models [McClements, 1999]

The droplet size distribution can be modelled with a mathematical model that describes the full data with a small number of parameters. At the thermodynamic equilibrium, one of the most used models to interpret data is the well-known “Gaussian distribution” or “normal distribution” that describes the whole data as they are symmetrical about the mean droplet size \bar{d} with a standard deviation σ . The Gaussian probability density function $f(d)$ is:

$$f(d) = \frac{1}{\sigma\sqrt{2\pi}} \exp\left[-\frac{(d-\bar{d})^2}{2\sigma^2}\right] \quad [1.1.8]$$

If a distribution behaviour is considered, like the one shown in figure 1.4 [McClements, 1999], which describes the functionality of a Gaussian and a log-normal distribution with the standard deviation at a fixed mean droplet diameter ($\bar{d} = 1 \mu\text{m}$), it can be assumed that $f(d)\delta d$ is the fraction of emulsion droplets which lies within the size interval d and $d + \delta d$ (equivalent to the number distribution function). The number of droplets in each size group can be calculated from the relation $n_i = N \cdot f(d) \cdot \delta d$. Most (~68%) of the droplets fall within one standard deviation of the mean ($\bar{d} \pm \sigma$), while the vast majority (~99.7%) fall within three standard deviations ($\bar{d} \pm 3\sigma$). Only two parameters are needed to describe the particle size distribution of an emulsion that can be approximated by a normal distribution, the mean and the standard deviation.

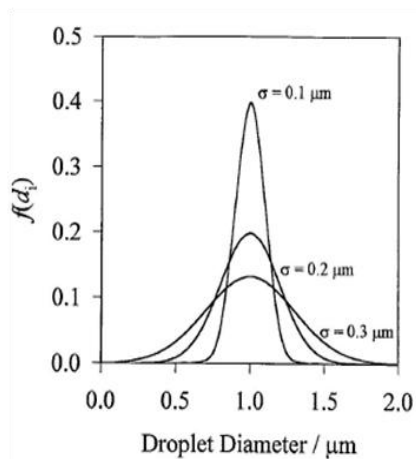


Figure 1.4: Normal (or Gaussian) distribution

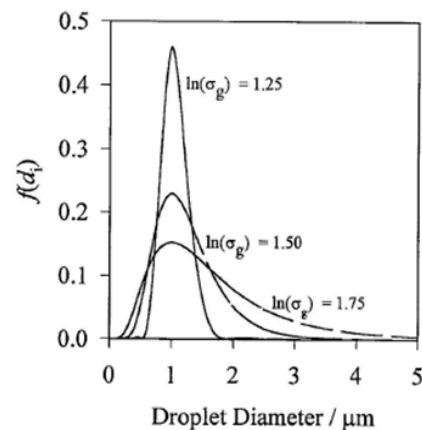


Figure 1.5: Log-normal distribution

where $\ln(\sigma_g) = \sigma_{\ln}$ is the standard deviation of the lognormal model.

Distributions may be symmetric or asymmetric. A symmetric distribution has a vertical axis of symmetry passing through its mode, and as noted above, in such distributions the mean, median, and mode all lie at the same point. Very few real distributions are

symmetric, most having more material on one side of the mode than the other. Such distributions are said to be *skewed*; if the ‘tail’ of the distribution is on the large side of the mode, the distribution is said to be *positively skewed* or *skewed to the right*. If the ‘tail’ is on the small side of the mode, the distribution is said to be negatively skewed or skewed to the left [Washington, 1992].

These particular data sets can be interpreted as a log-normal distribution (figure 1.5).

$$f(d) = \frac{1}{d \cdot \sigma_{ln} \cdot \sqrt{2\pi}} \exp \left[\frac{-(\ln d - \bar{d}_g)^2}{2\sigma_{ln}^2} \right] \quad [1.1.9]$$

where $f(d)\delta(\bar{d}_g)$ is the fraction of emulsion droplets which lies within the size interval between \bar{d}_g and $\bar{d}_g + \delta(\bar{d}_g)$, and \bar{d}_g and σ_{ln} are the geometric mean and its standard deviation given by the following equations:

$$\bar{d}_g = \sum n_i \ln d_i / N \quad [1.1.10]$$

$$\sigma_{ln} = \sqrt{\sum [n_i (\ln d_i - \bar{d}_g)^2] / N} \quad [1.1.11]$$

Owing to the relevance of the droplet size distribution, many techniques are described in the literature for analysis such as optical microscopy, scanning electron microscopy (SEM), transmission electron microscopy (TEM), light scattering, ultrasound spectrometry, nuclear magnetic resonance (NMR) [Franco et al., 1998, Gabriele et al., 2009, Egelanddal et al., 2001, Pal, 1998]. Microscopy is quite easy to use and it is considered the traditional method; electron microscopy (SEM or TEM) is a powerful tool able to give information on morphology of droplets and air bubble and on the microstructure of the sample; light scattering methods, based on the scattering of light by particles, is widely used for droplet sizing, however, it can be used only if emulsions are dilute (typical volume fraction lower than 1%) and transparent; ultrasound spectrometry can be applied to concentrate emulsions without sample pre-treatment, but errors can be produced by the presence of gas bubbles; NMR techniques are largely adopted to characterise emulsion systems, particularly to determine droplet size distribution. It can be used to study opaque and concentrated systems and results are not affected by possible contaminants (e.g. gas bubble or suspended solids) [Gabriele et al., 2009].

1.2. *Emulsions rheology* [Barnes et al., 1989]

Heterogeneous systems are theoretically and experimentally difficult to study. The worldwide method adopted to characterise these systems is a homogeneous approach, where the effect of the heterogeneity on the response of the system is analysed.

The theory of classical elasticity studies the mechanical properties of elastic solids, according to which, following the Hooke law, the stress is always proportional to the strain (for little values of strain) but it does not depend on the shear rate. On the contrary, the theory of the classical hydrodynamic studies the properties of viscous liquids following the Newton law, for which the stress is always proportional to the shear rate but it is not a function of the deformation. These are linear laws, which assume direct proportionality between stress and strain, or strain rate, whatever the stress. Within this linear framework, a wide range of rheological behaviour can be accommodated. However, this framework is very restrictive. The range of stress over which materials behave linearly is invariably limited, and the limit can be quite low. In other words, material properties such as rigidity modulus and viscosity can change with the applied stress, and the stress need not be high. The change can occur either instantaneously or over a long period of time, and it can appear as either an increase or a decrease of the material parameter. However, a lot of different materials can behave in an intermediate way between solids and liquids. In fact, if a very wide range of stress is applied over a very wide spectrum of time, or frequency, liquid-like properties can be observed in solids and solid-like properties in liquids. It follows therefore that difficulties can arise when an attempt is made to label a given material as a solid or a liquid. The term 'viscoelasticity' is used to describe behaviour which falls between the classical extremes of Hookean elastic response and Newtonian viscous behaviour. If the relationship between stress and deformation can be described by linear differential equations with constant coefficients, the considered material is linear *viscoelastic*, and the rapport between stress and deformation is not related to the stress intensity [Ferry, 1980]. The constitutive equation of a linear viscoelastic material is [Tanner, 1985]:

$$\underline{\underline{\tau}}(t) = \int_{-\infty}^t f(t-t') \underline{\underline{C}}_t^{-1}(t') dt' \quad [1.2.1]$$

where $\underline{\underline{\tau}}$ is the stress tensor, $\underline{\underline{C}}_t^{-1}$ is the inverse of the Cauchy deformation tensor, $f(t-t')$ a memory function. The linearity is based on the principle that the effects of following

variations on the deformation are additives, and can be added to give as a result the total stress of eq. [1.2.1].

1.2.1. Dynamic regime: small amplitude oscillatory tests

The rheological characterisation of a material should be based on properties that do not belong to the deformation history: this can be achieved by applying an asymptotic cinematic where the response to a sollicitation is not affected by the deformation history [Ferry, 1980]. Amongst the possible approaches, the one that allows both the solid and liquid behaviour to be determined is the ‘viscoelastic approach’. In order to obtain this useful information, small amplitude oscillation tests are a very important instrument. When a viscoelastic material is submitted to an oscillating strain, the response is not exactly in phase with the sollicitation (behaving like a solid) or completely out of phase with a phase angle of 90° (behaving like a liquid), but it behaves in an intermediate way [Steffe, 1996]. Thus, if the material is submitted to a monodimensional shear strain [Ferry, 1980]

$$\gamma = \gamma_0 \sin \omega t \quad [1.2.2]$$

where γ_0 is the amplitude of the strain, ω is the frequency of oscillation, and t the time, the response is

$$\tau = \tau_0 \sin(\omega t + \delta) \quad [1.2.3]$$

where τ_0 is the amplitude of the shear stress and δ , the phase angle, is a measurement parameter of the prevalence of the solid behaviour with respect to the liquid one: if δ tends to 0, the material is solid-like, and if δ tends to 90° is liquid-like. Manipulating the two equations [1.2.2] and [1.2.3], we obtain

$$\tau = \gamma_0(G' \sin \omega t + G'' \cos \omega t) = G' \gamma + \frac{G''}{\omega} \dot{\gamma} \quad [1.2.4]$$

$$G' = \frac{\tau_0}{\gamma_0} \cos \delta \text{ and } G'' = \frac{\tau_0}{\gamma_0} \sin \delta \quad [1.2.5]$$

G' is the elastic modulus or storage modulus and it is function of frequency. It indicates the accumulated energy in the material for each deformation cycle, while the G'' function of the frequency also, is the viscous modulus or loss modulus, a measurement of the energy lost for the viscous dissipation for each deformation cycle. Another popular material function used to describe viscoelastic behavior is the tangent of the phase shift or phase angle which is also a function of frequency

$$\tan \delta = \frac{G''}{G'} \quad [1.2.6]$$

This parameter is directly related to the energy lost per cycle divided by the energy stored per cycle. Since $0 \leq \delta \leq \pi/2$, $\tan \delta$ can vary from zero to infinity.

Rheological properties of emulsions are very important for their stability evaluation and most of all for their processability.

Emulsion rheology depends upon various factors. One of the most important works about the link between process variables and rheological characteristics of emulsions was published by Pal (1998).

In the case of diluted to moderate-concentrated emulsions, he assumes the moduli G' and G'' as a function of seven variables for O/W emulsions having negligible Coulombic and van der Waals interactions: frequency (ω), continuous phase viscosity (η_c), droplet radius (R), concentration of droplets (number density n), interfacial tension ($\gamma_{o/w}$) and thermal energy (KT).

He showed the study of moduli G' and G'' with the variables after a scaling analysis as:

$$G' / \omega \eta_c = f(\kappa, \phi, N_{Ca}, N_{Pe}) \quad [1.2.7]$$

$$G'' / \omega \eta_c = f(\kappa, \phi, N_{Ca}, N_{Pe}) \quad [1.2.8]$$

where κ is the viscosity ratio η_d / η_c , $\phi = 4\pi n R^3 / 3$ is the volume fraction of the dispersed phase, $N_{Ca} = \frac{\omega \eta_c R}{\gamma_{o/w}}$, the capillary number, is the ratio of the stress exerted on a droplet by the

flow and the Laplace pressure $\frac{2\gamma_{o/w}}{R}$.

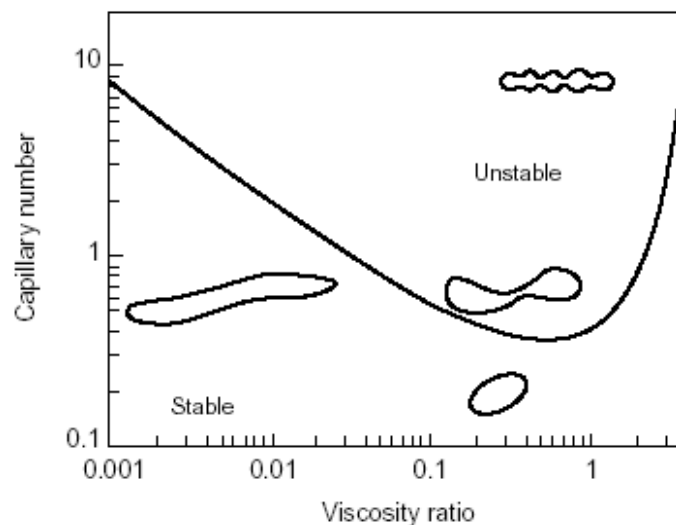


Figure 1.6: N_{Cacr} (solid line) for drop rupture in a shear flow as a function of the viscosity ratio

As shown in figure 1.6 [Langevin et al., 2004], if N_{Ca} is larger than a critical value $N_{Ca_{cr}}$, the drop splits into two smaller droplets (Taylor problem). Moreover, the other dimensionless number is $N_{Pe} = \frac{\omega\eta_c R^3}{KT}$ the Peclet Number, that can be neglected if droplet diameter is bigger than $1 \mu\text{m}$ and Brownian motion can be ignored. In a simple shear flow particles can be subjected to a revolutionary motion at a constant angular velocity equal to $\frac{\dot{\gamma}}{2}$ if Brownian motion can be neglected. Even if not presented in the equations [1.2.7, 1.2.8], the suspended spherical particle's motion can be evaluated by a dimensionless number called Brenner number or rotational Peclet number: $N_{Pe_r} = N_{Br} = \frac{\dot{\gamma}}{2D_r}$ where D_r is the revolutionary diffusion coefficient. In the case of non-spherical particles, their motion can be characterised by alternatively accelerations and decelerations: if $N_{Pe_r} \ll 1$ the rotation is Brownian and, consequently, the droplet size distribution is random. This situation can be encountered only in the case of slow flows. If $N_{Pe_r} \gg 1$ the rotation is controlled by the flow field.

For moderate concentrated emulsions $G' / \omega\eta_c$ and $G'' / \omega\eta_c$ are function of κ , ϕ and N_{Ca} .

For high concentrated emulsions ($\phi > 0.7$) the rheological properties of the emulsions are controlled by the network structure of thin films of continuous-phase. For the systems in which $\phi > 0.712$, the scaling analysis of the elastic modulus demonstrate the functionality of the modulus only with the capillary number and ϕ , as found by Princen and Kiss [Pal, 1998]:

$$G' / \omega\eta_c = 1.769 N_{Ca}^{-1} \phi^{1/3} (\phi - 0.712) \quad [1.2.9]$$

Therefore it does not belong to the viscosity ratio. Thanks to Pal's work, it can also be concluded that scaling of viscoelastic properties with respect to the droplet size has to be done plotting storage and loss moduli against ω/R^3 , as he investigated using two different emulsions, a monomodal and a bimodal one.

Apart from the relationship between rheological properties and variables involved, a great number of works have been written in order to study the rheological properties of emulsions. The general behaviour of concentrated and highly flocculated O/W emulsions follows a gel-like behavior, characterized by G' being about one order of magnitude higher than G'' within the experimental frequency range for different food emulsions (mayonnaise, salad dressings and so on) [Romero et al., 2008].

The occurrence of a region where a very low-frequency dependence for G' can be observed has been related to the formation of an elastic structural network that confers a high stability to the emulsion [Franco et al., 1995].

According to [Romero et al. \(2002\)](#), the complex modulus G^* , evaluated as $G^* = (G'^2 + G''^2)^{1/2}$, increases with the frequency, showing a progressive solid-like behaviour of the investigated concentrated bitumen in water emulsions. An important conclusion of Romero's work is that at any frequency, the magnitude of viscoelastic parameters (G^* , and G') increases with the bitumen volume fraction in the emulsion, while at a frequency of 1 Hz, G'' is constantly major than G' , indicating a predominant viscous response of emulsions below $\phi = 0.6$. The changes observed in the rheological behaviour of emulsions with bitumen volume fraction is due to the steric interactions between the chains of non-ionic emulsifier molecules adsorbed on adjacent droplets. At low volume fractions (<0.60), droplets behave as undeformed hard spheres, separated by a distance (h) larger than twice the thickness (δ) of the surfactant adsorbed layer ($h > 2\delta$). The rheological parameters of these emulsions increased when the mean droplet diameter decreased, and when the length of the ethylene oxide chains increased. In the case of crude oil emulsion, when $\phi > 0.7$ micelles change their shape from spherical to polyhedrons because the more stable spherical shape cannot be maintained: this causes changes in rheological properties of emulsions [[Welch et al., 2006](#)].

1.2.2. Flow behaviour: from diluted to concentrated emulsions [[McClements, 1999](#)]

Together with oscillatory tests, other measurements are very important for emulsions characterisation. These measurements are not performed in asymptotic cinematic conditions, and consequently they do not give information about the material characteristics, but are strictly dependent on the flow conditions applied. Nevertheless, the obtained information is very useful because it allows the study of the material behaviour even in extreme conditions, when it flows or breaks., The most used among them are flow curves and creep tests. In the flow curves test the sample is submitted to a flow field in a simple shear flow, measuring its viscosity versus shear rate. In a creep test, material is subjected to a constant stress and the corresponding strain is measured as a function of time.

Regarding the relation of the emulsions viscosity with the applied variables, the flow behaviour of emulsions is generally approached by the open literature starting from the rheology of diluted suspensions of noninteracting rigid spheres, and complicating the system for nonrigid, nonspherical, and/or interacting droplets.

The viscosity of a liquid increases upon the addition of rigid spherical particles that disturb the normal flow of the fluid, causing greater energy dissipation due to friction. If the Brownian motions can be neglected, the well-known Einstein equation relates the viscosity of a diluted suspension (particle concentration up to 5%) of rigid spheres to its composition [Toda and Furuse, 2006]:

$$\eta_r = 1 + 2.5\phi \quad [1.2.10]$$

where, η_r is the relative viscosity given as the ratio of the emulsion viscosity and the viscosity of the liquid surrounding the droplets (η_0), and ϕ is the volume fraction of the suspended solutes or particles assumed to be spherical.

An important parameter is the *intrinsic viscosity*, expressed as

$$[\eta] = \frac{\eta/\eta_0 - 1}{\phi} \quad [1.2.11]$$

For rigid spherical particles, the intrinsic viscosity tends to 2.5 as the volume fraction tends to zero. For nonspherical particles or for particles that swell due to the adsorption of solvent, $[\eta]$ is larger than 2.5, whereas it may be smaller for fluid particles. Emulsions usually contain fluid droplets. In the presence of a flow field, the liquid inside the droplet is caused to circulate because it is dragged along by the liquid continuous phase that flows past the droplet. The greater the viscosity of the fluid within a droplet, the more it acts like a rigid sphere, and therefore the higher the viscosity of the system.

The equation that can be applied for noninteracting spherical droplets with a dispersed phase viscosity η_d is:

$$\eta = \eta_0 \left[1 + \left(\frac{\eta_0 + 2.5\eta_d}{\eta_0 + \eta_d} \right) \phi \right] \quad [1.2.12]$$

also known as *Taylor equation*. If $\eta_d/\eta_0 \gg 1$, the equation evolve to the [1.2.10], whilst if $\eta_d/\eta_0 \ll 1$ starting from the limit case of air bubbles in a foam, the system viscosity is given by

$$\eta = \eta_0(1 + \phi) \quad [1.2.13]$$

It could be expected that for an emulsion the bulk viscosity should be somewhere between these two extreme, but the effect of the emulsifier layer on the droplets surface cannot be neglected. In fact the emulsifier molecules form a viscoelastic membrane that retards the transmittance of the tangential stress from the continuous phase into the droplet and therefore hinders the flow of the fluid within the droplet.

A very important factor that can be common in both suspensions and emulsions are the electroviscous effects, which can be primary, secondary or tertiary [Rubio-Hernández et al., 2000]. The *primary electroviscous effect* justifies the viscosity increase due to the presence

around the particle of a double electric layer that is distorted as an effect of the flow field. The electrical double layer is due to the presence of electrical charges on the droplet surface that give stability to the system and creates an electrostatic field that then affects the ions in the bulk of the liquid. This electrostatic field, in combination with the thermal motion of the ions, creates a counter charge, and thus screens the electric surface charge. The net electric charge in this screening diffuse layer is equal in magnitude to the net surface charge, but has the opposite polarity. As a result the complete structure is electrically neutral. Some of the counter-ions might specifically adsorb near the surface and build an inner sub-layer, or so-called *Stern layer* [Riley, 2005]. The formed ionic layer gives an increase of the hydrodynamic volume enhancing the viscosity of the system. The various equations describing the primary electroviscous effect of dilute suspensions can all be expressed in the form:

$$\eta = \eta_0[1 + 2.5(1 + p)\phi] \quad [1.2.14]$$

where p is the primary electroviscous coefficient which is a function of the charge on the particle. It can be noticed that for $p = 0$, the equation [1.2.14] becomes the [1.2.10] [Rubio-Hernández et al., 2000].

The *secondary electroviscous effect* is generally considered more important than the primary; it is caused by an electrostatic interparticle interaction which results from the overlap of the electrical double layers of neighboring particles. The contribution to the viscosity of the suspension is proportional to the square of the volume fraction. The *tertiary electroviscous effect* is due to a change in the size or shape of the particle due to pH change or salt adding.

The previously shown equations are valid for spherical droplets. The effect of particle shape on suspension viscosity is sketched in figure 1.7: at low shear rates, the particles rotate freely in all directions, but as the shear rate increases, they become more and more aligned with the flow field. This causes a reduction in the viscosity with increasing shear rate.

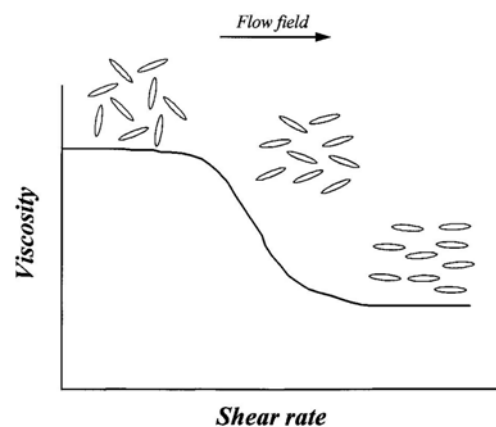


Figure 1.7: effect of the shape of particle on the flow curve of biphasic systems

As mentioned before, the orientation of a spheroid particle in a flow field is governed by a balance between the hydrodynamic forces (that favour alignment of the particles) and its rotational Brownian motion.

The relative importance of these two different forces is expressed in terms of Peclet number, that, for a simple shear flow can be expressed as

$$Pe = \frac{\dot{\gamma}KT}{8\pi\eta r^3} \quad \text{for rigid sphere} \quad [1.2.15]$$

$$Pe = \frac{3\dot{\gamma}KT}{32\pi\eta b^3} \quad \text{for circular disks} \quad [1.2.16]$$

$$Pe = \frac{3\dot{\gamma}KT}{8\pi\eta r^3} (\ln 2r_p - 0.5) \quad \text{for long thin rods} \quad [1.2.17]$$

in which a and b are the major and the minor axis of a spheroid and $r_p = a/b$.

Likewise, the flow behaviour of emulsions with the imposed shear rate can be interpreted considering the particle flocculation under the influence of the shear field.

The particles can be arranged in different “organisations” that can be stable, metastable and unstable. *Aggregates* are stable systems of particles clusters that can be separated only by chemical reactions. *Flocculates* are metastable systems of particles organised in flocs that can be temporary disrupted by an external cause. As can be seen in figure 1.8, an emulsion that contains flocculated droplets exhibits shear thinning behavior because the flocs are deformed and disrupted in the shear field.

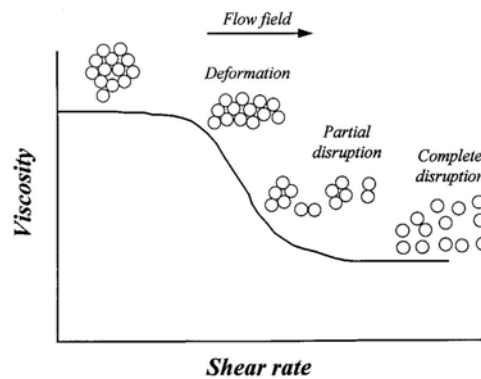


Figure 1.8: effect of the shear rate on the disruption of floc particles

The size, shape, and structure of flocs largely determine the rheological behavior of diluted suspensions of flocculated particles. Flocs formed by the aggregation of emulsion droplets often have structures that are fractal. The effective volume fraction (ϕ_{eff}) of a fractal floc is related to the size of the floc and the fractal dimension D by the following expression:

$$\phi_{eff} = \phi \left(\frac{R}{r} \right)^{3-D} \quad [1.2.18]$$

where r is the droplet radius and R is the floc radius. In nature, flocs are three-dimensional structures, and so D ranges from 1 to 3: the higher the fractal dimension, the more compact

the floc structure. The viscosity of a diluted emulsion containing fractal flocs can therefore be established by substituting this expression into the equation [1.2.10]:

$$\eta = \eta_0(1 + [\eta]\phi_{eff}) = \eta_0[1 + [\eta]\phi(R/r)^{3-D}] \quad [1.2.19]$$

If it is assumed that the flocs are approximately spherical, then $[\eta] = 2.5$.

Finally, *agglomerates* are unstable systems that can be definitively disrupted by an external cause. All the equations presented are referred to diluted emulsions or suspensions. At low concentrations, hydrodynamic interactions are mainly between pairs of particles, but as the concentration increases, three or more particles may be involved. As the concentration increases, the measured viscosity becomes larger than that predicted by the Einstein equation because these additional hydrodynamic interactions lead to a greater degree of energy dissipation. The Einstein equation can be extended to account for the effects of these interactions by including additional volume-fraction terms

$$\eta = \eta_0(1 + a\phi + b\phi^2 + c\phi^3 + \dots) \quad [1.2.20]$$

For a diluted suspension of rigid spherical particles, the value of a is 2.5, whilst for moderate concentrated suspensions $b = 6.2$ for rigid spherical particles. The value of all constants a , b , c , etc. can be determined either experimentally or theoretically, but it's extremely difficult to evaluate mathematically the value of higher order terms (c, d and so on) because of the complexity of the mathematical treatment of interactions among three or more particles. Therefore an empirical approach is employed worldwide to fit the experimental data.

Even the inclusion of the term ϕ^2 does not allow to overcome $\phi=0.20$ at every value of b . In fact the viscosity increase is much higher than how predicted by the equation [1.2.20]. One of the reasons for this particular behaviour is due to the friction between the particles that draw near progressively with the increase of the dispersed phase volume fraction. Therefore, with the increase of ϕ , the viscosity starts to increase up to a limit value $\phi = \phi_{max}$ where the viscosity tends to infinite [Pal, 1998] as shown in figure 1.9.

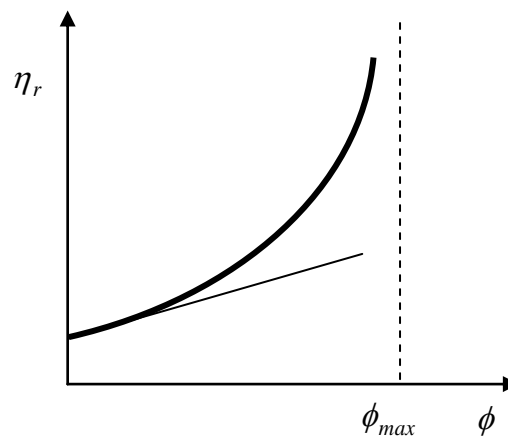


figure 1.9: relative viscosity versus concentration

In his work Brinkman (1952) developed an equation for concentrated suspension, where the viscosity of emulsion with spherical surface droplets were described as [Dan and Jing, 2006]:

$$\eta = \eta_0(1 - \phi)^{-2.5} \quad [1.2.21]$$

In the 1943, Eilers used bitumen emulsions and produced an empirical correlation for Newtonian behaviour

$$\eta_r = \left[1 + \left(\frac{2.5\phi}{1 - a_E\phi}\right)\right]^2 \quad [1.2.22]$$

where $1.28 < a_E < 1.30$ [Dan and Jing, 2006].

Other equations have been written starting from the [1.2.19], but *Pal and Rhodes* (1989) took into account the non-Newtonian behavior of high concentration emulsions, developing one of the most important correlations for to predict the viscosity of Newtonian and non-Newtonian emulsions.

$$\eta_r = (1 - K_0 K_f(\gamma)\phi)^{-2.5} \quad [1.2.22]$$

The model accounts for the flocculation of dispersed droplets and hydration effect. K_0 is the hydration factor and may vary from one emulsion system to another system depending upon the nature of emulsifier; and $K_f(\gamma)$ represents a flocculation factor used for non-Newtonian emulsions only.

Apart from those equations that give a power dependence between viscosities and ϕ , exponential correlations can also be applied; the simplest one is the Richardson equation [Dan and Jing, 2006]:

$$\eta_r = e^{k\phi} \quad [1.2.23]$$

In which k is a correlation constant.

An evolution of the [1.2.23] was then proposed adding a system dependent parameter A :

$$\ln(\eta_r) = A + k\phi \quad [1.2.24]$$

Both A and k can have a dependence from temperature, expressed in the following equation:

$$\ln(\eta_r) = k_1 + k_2 T + k_3 \phi + k_4 T \phi \quad [1.2.25]$$

Where the k_i coefficients are shear rate dependant.

Starting from the Taylor equation, *Pal* (2000) suggested a new equation for predicting the relative viscosity of concentrated emulsions

$$\eta_r \left[\left(\frac{2\eta_r + 5K}{2 + 5K} \right) \right]^{3/2} = (1 - K_0\phi)^{-5/2} \quad [1.2.26]$$

Where $K = \eta_{drop}/\eta_0$ and K_0 is a factor that takes into account the presence of adsorbed surfactant on the surface of the droplets, and it is a constant for a given system but may vary from one emulsion system to another.

Apart from these important models, emulsion viscosity is moreover strictly correlated to their stability [Mat et al., 2006] and their flow behaviour is a consequence of packing degree of internal phase and dimensional distribution of droplets. It is in fact well known that *viscosity of emulsions decreases if droplet size increases and if polydispersity increases as well* [Ford et al., 1997]. All emulsions can in fact be categorised in stable, unstable and meso-stable. The first ones show viscoelastic properties and their viscosities are usually greater than the pure oil. With time stable emulsions increase their viscosities

1.3. Emulsifiers and surfactants characteristics

The multiphase system can be stabilised, delaying coalescence, introducing an emulsifying agent or a surfactant adsorbed through the disperse phase droplet surface. Emulsifiers are amphiphilic molecules (with a hydrophilic head and a lipophilic tail) that adsorb at the interface lowering the surface tension and allowing a stabilisation of droplets. Adsorption is associated with significant energetic changes since the free energy of a surfactant molecule located at the interface is lower than that of a molecule solubilised in either bulk phase. True surfactants are distinguished by an ability to form oriented monolayers at the interface (here air/water or oil/water) and, most importantly, self-assembly structures (micelles, vesicles) in bulk phases. Finally, another characteristic of surfactants is their ability to form liquid crystalline phases (or lyotropic mesophases) when their aqueous concentration exceeds approximately 40% [Eastoe, 2005].

Four basic classes therefore emerge as:

1. the anionics and cationics, which dissociate in water into two oppositely charged species (the surfactant ion and its counterion)
2. the non-ionics, which include a highly polar (non-charged) moiety, such as polyoxyethylene ($-\text{OCH}_2\text{CH}_2\text{O}-$) or polyol groups
3. the zwitterionics (or amphoteric), which combine both a positive and a negative group

Some other classes have been studied in the last few years, such as the catanionics (both anionic and cationic surfactant that precipitate forming catanionic crystals that stabilize emulsions) [Schelero et al., 2009], bolaforms (composed of two hydrophilic heads linked by one or several hydrophobic chains) [Sateg  et al., 2004], gemini (or dimeric) surfactants (made up of two identical amphiphilic moieties connected at the level of head groups by a

spacer) [Zhou et al., 2009] and polymeric and polymerisable surfactants (that combine the self-assembling properties of conventional surfactants with the chemical reactivity of vinyl monomers) [Schwering et al., 2008]. Emulsifier concentration and chemistry [Guo et al., 2006, Sajjadi, 2006] are important characteristics for emulsion rheology and stability [Zaki, 1997]. Surfactant molecules can self-aggregate forming micelles and their formation as spherical droplets minimizes the free energy in the system. Surfactant in fact reduces the surface free energy required to increase any interfacial area, according to the energy equation $\Delta G = \gamma \Delta A$ [Abismaïl et al., 1999].

The surfactant concentration at which single surfactant molecules start to self-aggregate at the bulk phase forming micelle structures, is called *critical micelle concentration* (cmc). Spherical micelles have a characteristic size, and thus the increasing surfactant concentration increases the number of spherical micelles, not the size that could be varied by changing the speed of mixing during emulsification process [Ahmed et al., 1999, Bibette et al., 1999].

A fundamental parameter for choosing the proper emulsifier that can stabilise the wanted emulsion is the HLB value. The *Hydrophilic–lipophilic Balance* is generally expressed as an empirical equation based on the relative proportions of hydrophobic and hydrophilic groups within the molecule. A general empirical equation that associates a constant with the different hydrophilic and hydrophobic groups is [Eastoe, 2005]:

$$\text{HLB} = [(n_{\text{H}} \times H) - (n_{\text{L}} \times L)] + 7 \quad [1.3.1]$$

where H and L are constants assigned to hydrophilic and hydrophobic groups respectively, and n_{H} and n_{L} the number of these groups per surfactant molecule.

Generally low HLB value (< 10) can stabilize W/O emulsions, whilst a high HLB value stabilizes O/W emulsions [Salager et al., 2004].

The effect of the emulsifier is moreover very important for the viscosity of the emulsion. Sherman (1959) reviewed all the articles in which there was a relation between emulsion viscosity and emulsifier concentration. His conclusion is generally that as emulsifier concentration increases, emulsion viscosity increases in a nonlinear manner with respect to inner phase volume fraction.

1.4. Structured emulsions: an overview

As shown in the first paragraph of the thesis, the study of emulsions prepared with a high oily phase concentration has been separated into the analysis of structured and

unstructured system for different uses. The basic knowledge about the structural properties of an emulsion is progressing, but the inherent complexity of such materials permanently raises a variety of fundamental questions at the frontier between physics, chemistry and biology. Three phenomena of potential relevance to the formulation of novel functional and structured systems are the *droplet attractive interactions*, the *formation of a polymer network* in the continuous phase and the *heat induced gelation of stabilized emulsions*. As already mentioned, droplet size and polydispersity are fundamental for emulsions rheology and stability. Recently structuring of both the dispersed and continuous phase has become an issue for the production of special materials [Rodríguez-Abreu and Lazzari, 2008]. A structured emulsion is a complex multiphase system characterised by interdroplet interactions that can be realised in different ways. One way is the progressive concentration of the internal dispersed phase until the maximum packing degree is almost reached. Moreover, a structuration of emulsions can be achieved by adding different agents to the continuous phase [Gabriele et al., 2009]. In food emulsions, if water is the continuous phase, it can be structured by polysaccharides or proteins or hydrocolloids in general. Their main effect is based on the control of the rheology of the aqueous continuous phase located in the gaps between the dispersed droplets. In this case a structured emulsion can be imagined as an *entangled polysaccharide network* and the buoyancy force acting on each droplet is insufficient to overcome the yield stress of the surrounding gel [Leal-Calderon et al., 2007]. This last conclusion is always true for diluted emulsions, but for moderately concentrated emulsions (30_{v/v}% oil) the evolving microstructure of the emulsion is highly heterogeneous. In the following paragraphs an overview of the state of the art for structured emulsions in food systems is presented.

1.4.1. Structured O/W emulsions

Structured O/W emulsions are mostly used in foodstuffs engineering and production, and in fact the literature works about this subject are mostly addressed to the food emulsions study. For O/W emulsions, the important function of many hydrocolloid ingredients as a structuring/thickening/gelling agent in the aqueous medium is well recognised, in conjunction with added ‘weighting agents’ to match the densities of oil and aqueous phases. If water is the continuous phase, as already said, it can be structured by polysaccharides or proteins [Gabriele et al., 2009].

Xanthan gum is especially effective for its stabilizing role. For low oil volume fractions the simple rheological control mechanism is most effective; in fact individual droplets are separately immobilized in an entangled biopolymer network, and the small buoyancy force acting on each droplet is hardly sufficient to overcome the effective yield stress of the surrounding weak gel-like biopolymer matrix. Theoretically, a yield stress of just 10^2 Pa is sufficient to prevent the creaming of individual dispersed droplets in the size range below $10\ \mu\text{m}$ [Dickinson, 2009]. For concentrated emulsions, emulsion stability and rheological characteristics strictly belong to the total amount of hydrocolloids in the aqueous phase. For very low concentrations (less than $0.1_{\text{w/w}}\%$ for Xanthan Gum), the added hydrocolloid has a destabilizing property because of the depletion flocculation induced by the nonadsorbing hydrocolloid causes enhanced serum separation of the emulsion [Dickinson, 2009, Blijdenstein et al., 2004 a]. In fact, the addition of polysaccharides like Dextran [Blijdenstein et al., 2004 b] or gum Arabic for beverages emulsions [Chanamai and McClements, 2006], which do not adsorb at the emulsion droplets, can induce a depletion interaction between the emulsion droplets and an increase in viscosity of the aqueous phase [Blijdenstein et al., 2004 b]. But at higher added hydrocolloid concentrations (still $<0.1_{\text{w/w}}\%$ for xanthan gum), when the depletion interactions are stronger, creaming is inhibited due to the viscoelastic character of the interconnected regions of emulsion droplets that have become flocculated into a gel-like network. Aiming at enhancing the viscosity of an emulsion, also the shape of the droplets have a crucial role in the rheological characteristics of emulsions and suspension. Marti et al. (2005) studied the effect of replacing part of the spherical particles in a non-Brownian suspension by fiber-shaped particles, finding a dramatic increases in the zero shear viscosity as a function of the mixing ratio and overall particle concentration; an evident increase in the relative viscosity η_r with the increase of fibre disperse particles with respect to the round shaped ones has been found. Similarly Walther et al. (2005) investigated the possibility of deforming κ -carrageenan solution drops in sunflower oil under shear flow in a smooth narrowing deformation channel of a fast continuous flow process by quenching the system up to the gelling temperature. Therefore, they “froze” the droplet in a ellipsoid shape obtained by varying the flow conditions (and Capillary number) with the possibility of modifying the rheological properties of the emulsion or suspension.

Those systems, called “gelled emulsions” show a very interesting behaviour, allowing an emulsions in a suspension of non-spherical droplets to be converted.

1.4.2. Structured W/O emulsions for food applications

Structuring W/O emulsions is a well-known technique for producing margarine or shortenings as a very important ingredient for cooking or for the industrial pastries production.

The margarine fabrication process follows different production steps aiming at obtain W/O emulsions with a dispersed phase ratio minor than 20_{w/w}%. With a fat percentage less than 80_{w/w}% W/O emulsions, called “spreads”, cannot be considered as margarines, but they can be commercialized as spreading shortenings [Borwankar, 1992].

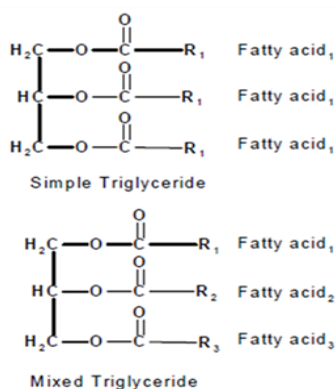


Figure 1.10: simple and mixed triglycerides: in the first one molecule is composed by three equal fatty acids

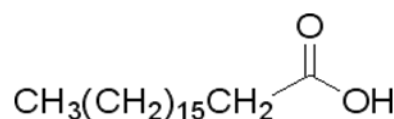


Figure 1.11: stearic acid

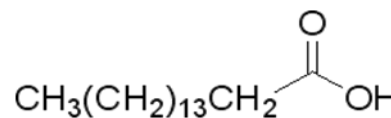


Figure 1.12: palmitic acid

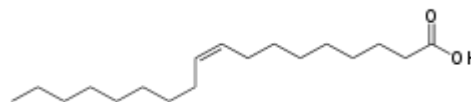


Figure 1.13: oleic acid

The taste of margarines and food spreads is due to water-soluble flavors, oil soluble flavors and salt in the water phase [Blanco Muñoz, 2004]. The rheological characteristics are given by the high melting point of saturated fats into the oily phase; crystals interact and form a three-dimensional network surrounding water droplets and stabilizing the biphasic system, giving a hard gel-like character to these foods.

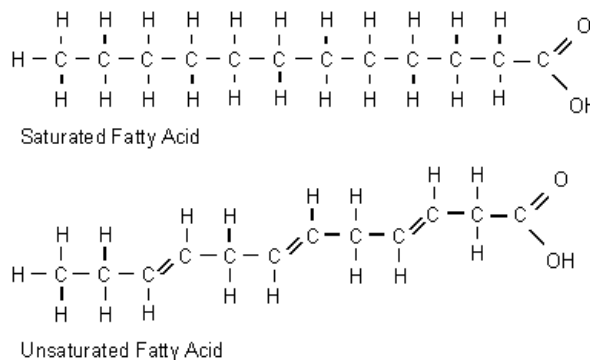


Figure 1.14: chemical structure of fatty acids: unsaturated fatty acids have at least one double bound

The high consistency of margarine is obtained with a certain amount of fully saturated triglycerides (triacylglycerol or TAGs) that allow a better molecular interaction and, as a consequence, a better packing (see figure 1.14) giving a more ordered structure. In general, fats containing a majority of saturated fatty acids (SFA) are solid at room temperature, and those containing mostly unsaturated fatty acids (oils) are usually liquid at room temperature [Ghotra et al., 2002].

The hardening of the oily phase has to be achieved to reach the optimal consistence of the final emulsion, three different methods are currently employed in food process industries:

- partial hydrogenation of vegetable oils
- catalytic interesterification of vegetable oils and completely saturated fats
- addition of solid fats materials to the starting liquid oil

The most used technique amongst those listed before, is the catalytic hydrogenation of double bounds of the unsaturated fatty acids chains. Industrial hydrogenation of vegetable oil (fish oil occasionally) is a process performed with a three phase (gas–solid–liquid) system generally carried out in a batch autoclave over nickel based catalyst as a slurry at 110–190°C, 30–70 psi H₂ pressure, with 0.01– 0.15_{w/w}% Ni [Singh et al., 2009]. The process may imply the movement of double bonds in their positions on the fatty acid carbon chain, producing positional and geometrical isomers, *trans* fatty acids (TFAs, figure 1.15), dangerous for consumers' health.

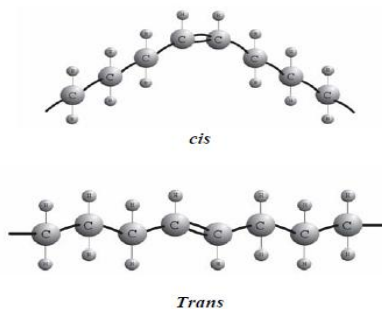


Figure 1.15: *cis*- and *trans*- configuration of a fatty acid

Different data indicates that TFAs are not metabolically equivalent to the natural *cis* isomers and that they promote the development of atherosclerosis and predispose to coronary heart disease and other not well known risks [Blanco Muñoz, 2004]. Their formation can be minimized by increasing pressure, decreasing temperature, and increasing agitation to address mass transfer limitations. Precious metal catalysts are active at considerably lower temperatures and can thus produce less TFA as compared to conventional Ni catalysts, but they cannot completely avoid their formation. The order of catalytic activity of precious metal catalysts is Pd>Rh>Pt>Ru [Singh et al., 2009].

The negative effects that TFAs have on consumers' health led the research to find other way aiming at produce high viscous and structured emulsions as a regular margarine replacer.

An alternative process that does not produce TFA is catalytic interesterification between a fully hydrogenated fat and a natural *trans*-free vegetable oil [Criado et al. 2007, Hee Lee et al., 2008]. Interesterification is an exchange of fatty acid between the two TAG molecules participating in this reaction, thereby causing a rearrangement of the FA residues in both of these molecules (figure 1.16).

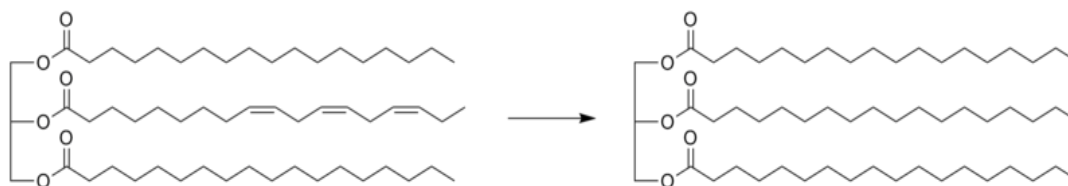


Figure 1.16; a triglyceride with a PUFA (linolenic acid) at the sn-2 position which is replaced by a saturated fatty acid (stearic acid) via interesterification.

This reaction can be intramolecular if the exchange of FA happens between two chains in the same TAG molecule or extramolecular if two TAGs are involved. Therefore, the saturated fatty acids chains of fully hydrogenated tag source can substitute the unsaturated chains of TAGs naturally presents in the vegetable oil. These rearrangements are accompanied by a concomitant change in the properties of the original physical mixture. The final properties of the semi-solid fat product are strongly influenced by both the relative proportions of reactants in the original starting mixture and the type of catalyst used. Normally in this process, a chemical catalyst such as sodium metal or sodium alkoxide is used to promote acyl migration among glyceride molecules, but its toxicity lead the research to use different enzymes to promote the reaction. Macrae (1983) suggested to use lipases to produce useful glyceride mixtures which cannot be obtained by conventional chemical interesterification processes. Kim et al. (2009) use the same enzyme, immobilized on silica granules in order to interesterificate olive oil with palm stearin.

If the oily phase is continuous, the structure of the final biphasic system could be improved by adding fat crystals, while if the water phase is the continuous one, upon cooling, the spherical shape of the warm dispersed droplets which is controlled by surface tension evolves into a rough surface due to the formation of irregularly shaped/oriented crystals. Moreover, crystals located near the oil/water interface can protrude into the continuous phase and when such crystals are present within the thin films separating two droplets, they may pierce the film and bridge the surface causing the partial coalescence of the droplets and, as a consequence, the gelling of the system [Leal-Calderon et al.,

2007]. In the case of W/O emulsions, as already mentioned, one of the method that could be applied to enhance their mechanical characteristics is the addition of hard fats in the oily liquid phase with an opportune emulsifier and stabilizing agent. [Jahaniaval \(2005\)](#) in his patent suggests a recipe of preparation of healthy margarine and butter substitutes based on liquid oils (at room temperature) like olive oil and phospholipids as stabilizers. The final consistence of the resulting margarine is increased by mixing at high temperature the oil and added hard fat like cotton stearin, palm and canola stearins and intermediate melting point triglycerides such as intersterified fat, cocoa butter or cocoa butter substitution and or any fractionated fat with melting point of 34-40 °C. [Skogerson et al. \(2007\)](#) propose an interesting patent relating to a glyceride emulsifier with an elevated di-glyceride portion, which is especially useful in preparing puff pastry products. Mono- and di-glycerides of fatty acids are a very common emulsifier widely employed in the food industry, produced by the reaction of glycerol with vegetal oil and fats, whose composition strictly depends on the characteristics of the starting fruit from which the oil is obtained [[Clogston et al., 2000](#)]. This emulsifier is lipophile and its HLB value, about 3.7, should allow the formation of W/O emulsions [[Constantinides & Yiv, 1994](#); [Friberg, 1997](#)]. Commercial mono- and di-glycerides usually contain 40-60% mono-glycerides, 38-45% di-glycerides, 8-12% tri-glycerides, and 1-7% free glycerol. In accordance with their patent, the authors suggest increasing di-glyceride portion (on a weight basis) preferably to about 75% by vacuum distillation, with the remaining mono-glyceride portion being about 10% and the triglyceride portion of the order of 15%. Therefore, the resulting W/O emulsion recipe could be prepared by admixing, on a w/w basis, from about 10% to about 16% of the HiDi emulsifier, from about 55% to about 65% of vegetable oil, and from about 13% to about 25% of saturated fat.

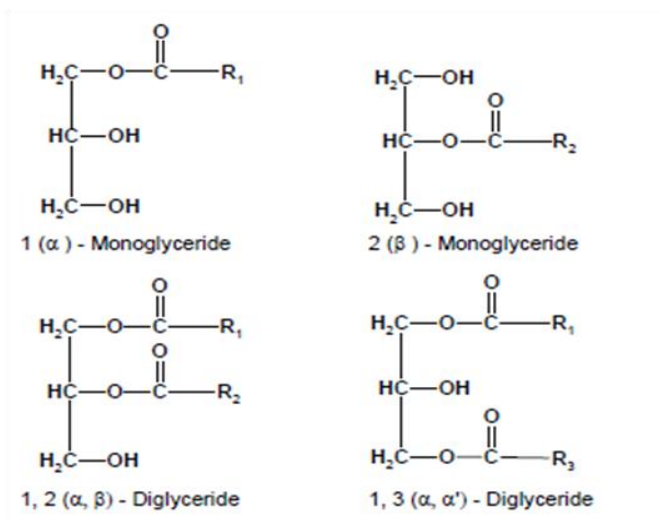


figure 1.17: diagram of mono and di-glycerides

The presence of fat crystals is very interesting for their stabilising properties. When water droplets are dispersed in an oily phase with a certain quantity of added hard fats, the emulsion is stabilized by fat crystals disposed at the interface like a Pickering emulsion [Rousseau, 2000]. The wetting behavior of particles at the interface is described by *contact angles* which are related to the surface tension of each of the three interfaces by Young's equation:

$$\gamma_{(o/w)}\cos\theta = \gamma_{(o/s)} - \gamma_{(w/s)} \quad [1.4.1]$$

where θ is the contact angle measured through the water phase and $\gamma_{(o/w)}$, $\gamma_{(o/s)}$ and $\gamma_{(w/s)}$ are the interfacial tensions of the oil/water, oil/solid and water/solid interfaces, respectively. $\gamma_{(o/w)}\cos\theta$ is also known as the adhesion tension.

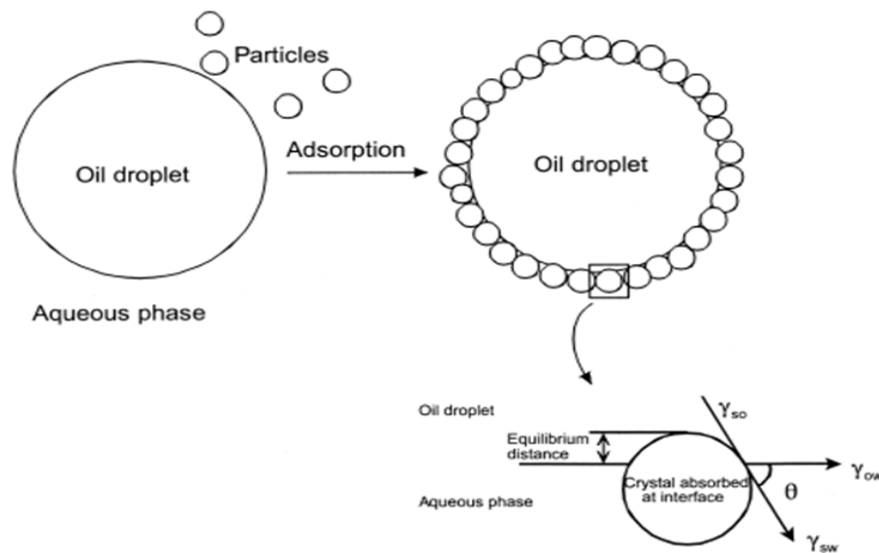


Figure 1.18; contact angle of a water/oil/crystal system for an O/W emulsion

A graphic representation of the contact angle is showed in figure 1.18 for an O/W emulsion. With a contact angle at the solid/water/oil interface across the water phase smaller than 90° , the particles stabilize O/W emulsions. With contact angles greater than 90° , the particles stabilize a W/O emulsion. If the particles used are completely wetted by one of the two phases (contact angle 180°), they become fully dispersed in that phase and any stabilizing effect is negated. With a 90° contact angle a crystal is equally wetted by the oil and aqueous phases. In conclusion, for O/W emulsions, the contact angle should be 60° - 70° for optimal stability.

Fat crystals are expected to contribute to the stability of margarine emulsions if they are preferentially wetted by the oil phase ($0^\circ < \theta < 90^\circ$), but they give instability if they are preferentially wetted by the water phase ($90^\circ < \theta < 180^\circ$) [Johansson et al., 1995].

For system where one of the phases is apolar, the Young's equation becomes:

$$\gamma_{(o/w)} \cos\theta = -\gamma_{(o/w)} + C + I_{(s/w)} \quad [1.4.2]$$

where

$$C = 2 \left(\sqrt{\gamma_o^d} - \sqrt{\gamma_w^d} \right) \left(\sqrt{\gamma_o^d} - \sqrt{\gamma_s^d} \right) \quad [1.4.3]$$

γ_o^d is the dispersion force of the oily phase, γ_w^d the dispersion force of the aqueous phase, γ_s^d the dispersion force of the particle phase and $I_{(s/w)}$ the energy term due to the stabilization by polar forces. [Johansson et al. \(1995\)](#) studied the wetting of tristearin and fully hydrogenated palm stearin fat crystals by investigating a comprehensive selection of emulsifiers (lecithins, mono-glycerides and their esters, ethoxylated emulsifiers) and considering the influence of factors, such as polymorphism, temperature and oil type.

In the schematic picture in figure 1.19, the stabilization mechanism of fat particles linked to the emulsifier molecules is shown: belonging to [Garti et al. \(1998\)](#) emulsifier are the molecular bridges that facilitates the adsorption of molecular wetting agents.

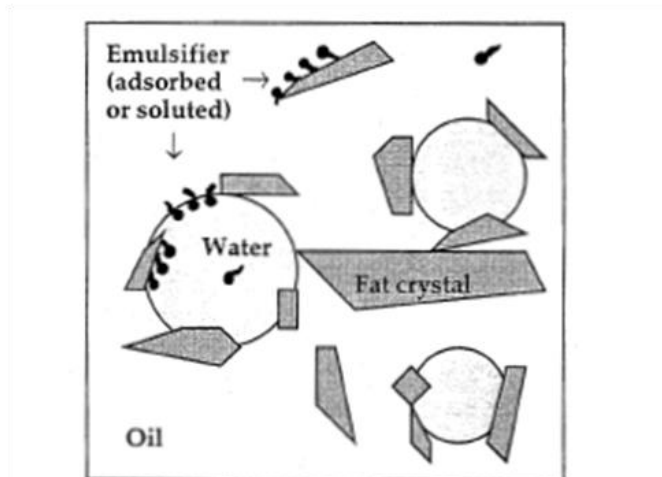


Figure 1.19; [Garti et al, 1998]. A schematic picture of margarine structure: interaction between water droplets, fat crystals and emulsifier

The most common triglycerides used to enhance the consistency of the oily phase of W/O emulsions for shortenings production by the addition of hard fats is palm stearin or fully hydrogenated tristearin [[Garti et al. 1998](#), [Johansson et al. 1995](#), [Ramli et al. 2008](#)]. As already mentioned, [Jahaniaval \(2005\)](#) proposed the adding of cocoa butter or cocoa butter equivalents aiming at produce margarines or shortenings. [Norton J. et al. \(2009\)](#) produced stable W/O emulsions with cocoa butter using a high shear mixer or bench-scale margarine line (scraped surface heat exchanger and a pin stirrer) in order to produce a low fat dietary milk chocolate. The authors obtained fully emulsified emulsions with the polymorphic form $\beta(V)$ required for good eating qualities.

The importance of organogels on emulsions' characteristics have been well exposed by [Marangoni \(2009\)](#). He introduced organogels as an organic liquid entrapped within a thermo-reversible, three-dimensional gel network formed by the self assembly of a relatively low concentration of organogelator (concentration 0.5-2%) molecules into long crystalline fibres, thus called Self-assembled fibrillar network (SAFIN). The best known organogelators are TAGs, DAGs, MAGs, fatty acids, fatty alcohols, waxes, wax esters, sorbitan monostearate, or mixture of fatty acids and fatty alcohols, lecithin and sorbitan tristearate and phytosterols and oryzanol. These organogels have numerous potential different functionalities, included the increasing in the consistency of the final product, replacement of saturated and trans- fats, the stabilisation of emulsions and the ability to control the rate of nutraceutical release [[Frasch-Melnik et al. 2009](#)]. [Bot et al. \(2009\)](#), for example, suggest the use of a mixture of γ -oryzanol with β -sitosterol to form a network of tubules in oil that may be an alternative to the network of small crystallites of triglycerides occurring in regular oil structures. The resulting gel melts at a temperature in which the tubules vanish, and the sitosterol can be replaced by different sterols in tubules.

1.4.3. Gelled emulsions

The rheological properties of emulsions can be changed, improving for instance their consistency, also producing the so-called 'gelled emulsions'. In the case of W/O emulsions, the gelled emulsions are produced by an internal gelling water phase that deforms for an imposed shear rate effect. [Walther et al. \(2005\)](#) investigated the deformation of κ -carrageenan aqueous solution drops in sunflower oil under shear flow in a fast continuous flow process by quenching the system up to the gelling temperature. The deformed gelled droplets remain in an ellipsoid shape obtained by varying the flow conditions with the possibility of modifying the rheological properties of the emulsion or suspension.

Those systems show a very interesting behaviour, allowing an emulsions in a suspension of non-spherical droplets to be converted.

1.5. *Crude oil emulsification*

In the following paragraphs a general overview of the second case study proposed in this *PhD* thesis is proposed. As mentioned before, the study of unstructured and concentrated

emulsions are really important for crude oil transportation in conventional pipelines. Moreover, a brief general introduction to water-in-crude oil emulsions is also presented even if these systems aren't directly treated in the present work.

1.5.1. O/W unstructured emulsion for crude oil transportation

Conventional pipelining is not suitable for transporting heavy crude from the reservoir to the refinery because of the high viscosities involved [Ahmed et al., 1999]. The pressure drop in pipes has to be as low as possible in order to limit pumping costs and travel long piping distances: in the case of heavy oils, the pressure drop increases as viscosity increases and pumping single oil-phase becomes economically disadvantageous [Al-Roomi et al., 2004]. An extensive literature has been written in order to solve the important problem of the transportability of bituminous oil, and also some patents were published in the U.S.A.: Briggeman and Black (2002) proposed the injection of a gas or a combination of gases (CO₂ alone or with N₂) at high pressure in order to reduce oil viscosity. Kane's patent (1969) suggests to add an aqueous solution of non-ionic surfactants into the pipeline in order to create O/W emulsion. Allen and Chien (1978) in their U.S. patent proposed the injection of water (with no surfactant) at 32°F followed by mixing until the inversion point W/O to O/W is reached in order to extract oil from the deep of the well and then to transport crude.

Apart from these techniques, other interesting methods have been successfully tested up to a on-the-field application:

- Core Annular Flow
- Partial upgrading
- Thermal treatment
- Oil Dilution

Emulsions and core annular flow are based on the apparent viscosity reduction effect using water as continuous or dispersed phase in the first one and as lubricating layer in the second one.

Core annular flow, in particular, appears as a layer of water acting as lubricant surrounding the central coaxial oil core. Owing to the thin layer of water, the wall pressure drops approaches those realised in a pipe completely full of water [Gosh et al., 2009, Sotgia et al., 2008, Bannwart, 2001, Bensakhria et al., 2004, Angeli and Hewitt, 1999].

Partial upgrading uses refinery systems, like hydrotrating, to break molecules and reduce crude oil viscosity for its transportability in pipelines, also avoiding the pre-treatment before refinery processing. The aim of partial upgrading is to increase the H/C ratio, using fluidised or fixed bed reactors with Co/Mo and Ni/Mo catalysts [Strausz et al., 1999]. Dehkissia et al. (2004 a) investigated catalytic (FeS, MoS₂) and noncatalytic hydrovisbreaking for Doba heavy crude oil. They found that the treated crudes and the syncrudes (mixtures of untreated and treated crudes) were observed to exhibit non-elastic viscous Newtonian behaviour over the temperature range typical of crude transportation via pipeline.

In order to reduce crude viscosity, another promising technique is based on heat treatments: in this systems viscosity decreases as temperature increases, as usual for other different systems [Durand, 2007]. An application is working in Alaska, where the Alyeska pipeline transports crude oil at approximately 50°C [Saniere et al., 2004].

Dilution exploits low viscosity liquids to diluted heavy oils and lower the viscosity of the whole system [Gateau et al., 2004]. Different liquids are used to reduce heavy crudes viscosities: until the end of the 80's condensates were the most important alternative, but in the last 20 years light oils and naphtha have been successful employed. The last one is in fact the best solution because of its high reusability and good compatibility with asphaltenes naturally presents in heavy crudes (condensates cannot dissolve asphaltenes and flocculation may occur).

Amongst these important techniques, the emulsions production is the one considered in this PhD thesis. The scenario of available technology is wide enough and between different basic ideas, emulsions pumping (up to 75_{v/v}% of oil in water) [Langevin et al., 2004] and separation in situ, is one of the most diffused [Fournanty et al. 2008, Saniere et al., 2004, Nädler and Mewes, 1996, Dehkissia et al., 2004 b].

Emulsions can be water in oil W/O [Fingas and Fieldhouse, 2003 a, 2004, 2009], oil in water (O/W), named “inverse” emulsion, or multiple and complex double emulsion [Pal, 2007].

O/W and W/O emulsions can be desirable or not belonging to their occurrence. For heavy oil transportation, oil sand flotation process or in order to enhance oil recovery in situ, emulsions are O/W and their formation improve all processes involving crude. In the case of fuel oil emulsions (sea spill), emulsification occurring in the well-head, and so on, water is the dispersed phase and emulsification is undesired [Mat et al., 2006].

Packing degree, droplet size and distribution of disperse phase strongly affect viscosity value and rheological behaviour of emulsions [Pal, 2000] can be controlled as a consequence.

After transportation, oil must be separated from water, destabilising the emulsifying film around water droplets. The de-emulsification process starts from flocculation or aggregation of droplets, followed by coalesce and separation of the two phases and it can be obtained using different methods: from gravitational separation of oil in large settling chambers to chemical emulsifier addition, increasing temperature, or applying electrical field [Kokal, 2005]. Thermal treatments is discouraging because of its high environmental impact even if also the use of emulsions generates the problem of water treatment after the phases separation in the refinery.

1.5.2. Crude water-in-oil emulsions

During the production phase of conventional heavy oils, emulsification occurs when crude oil is mixed with produced formation water or injected water in reservoir, at well bore, in pipelines, and at surface facilities. If the dispersed phase is water, these systems are unwanted because they cause high pressure drops due to their high viscosity involved [Al-Sahhaf et al., 2009].

When crude is spilled at sea, oil emulsification occurs (producing W/O emulsions) and this leads to important changing of its characteristics due also to the evaporation of the most volatile components [Nordvik et al., 1996].

W/O emulsions, often called ‘chocolate mousse’ or ‘mousse’ are stable if water cut is between 60 and 80% [Fingas and Fielhouse, 2003 b], and can form spontaneously. The big viscosity increase related to these emulsions compromises crude transportation. In fact, if oil is the continuous phase, both density and viscosity of crude usually increase their values. The density of a typical crude oil is about 0.80 g/ml, while a W/O emulsions can reach a density value of about 1 g/ml and viscosity can increase up to 1000 times [Fingas and Fieldhouse, 2004]. As a consequence W/O breakup is necessary, and the most useful methods employed to obtain crude and discharge water are heating and/or adding an emulsion breaker. Kristiansen et al. (1996) studied emulsions obtained with different crudes, BCF-17 oil, rich of asphaltenes and intermediate waxes content, and ANS, intermediate in both waxes and asphaltenes content. They found that W/O emulsions formed from ANS were broken by Breaxit 7877 with a faster rate than BCF-17: this

implies that different oils form emulsions whose breakage depends on crude characteristics. Moreover, they concluded that heat alone could slowly break emulsion, but its action is improved by the contemporary use of emulsion breaker. A different and preventive way to avoid the production of stable W/O emulsions is the removal of asphaltenes from crudes by using silica columns [Lee, 1999].

Fingas and Fieldhouse (2003 b) classify W/O emulsions in four clearly defined states, established by their stability over time, their appearance, and by rheological measurements. The states are stable water-in-oil emulsions, mesostable water-in-oil emulsions, entrained water, and unstable water-in-oil emulsions.

In one of his earlier review, Fingas (1995) explained the formation mechanism of W/O emulsions as the rate of water incorporation promoted by the wind speed and the fraction of water in oil. Moreover, the viscosity of the mixture was described as an exponential function of the fraction of water in oil initially and at the end of incorporation.

Anyway, the rate of emulsion formation was assumed to be first-order with time, but the simple model proposed cannot be used for very stable or unstable emulsions, whose formation is promoted by their content of asphaltene and resin forming stable films at the oil and water interface. This model, introduced before extensive work on emulsion physics took place, has been substituted by a prediction of the tendency and the formation of emulsions based on empirical data [Fingas et al., 1999].

1.5.3. SARA components of crude oil: effect on emulsions properties

The notable stability of emulsions is related to the content of asphaltenes, resins, waxes and inorganic solids, elsewhere called SARA fractions.

SARA components of crude are saturates (S), aromatics (A), resins (R), and asphaltenes (A). Asphaltenes and resins consist of condensed aromatic rings with others atoms like sulphur, nitrogen and oxygen; they are soluble in toluene and precipitate in the presence of aliphatic solvents [Hannisdal et al., 2007]. Asphaltenes are present in crude oils in the form of colloidal dispersed particles. Their aggregates accumulate in pipelines just below the pour point of the crude oil due to the release of low molecular weight paraffins. This can cause the deposition of the materials blocking the crude oil into the pipelines. Some authors suggest to avoid this phenomenon by adding different dispersant to prevent asphaltene precipitation during petroleum transportation: Atta et al. (2008) employ

poly(ethylene acrylic acid) (PEAA), which is used as a plastic waste modified through chemical grafting with alkanols and phenol.

In the case of emulsion promotion, asphaltenes interact with resins forming interfacial films surrounding droplets that are protected against coalescence. The resins are polar and non volatile, they are soluble in n-pentane, n-heptane and aromatic solvents and insoluble in methanol and propanol. Resins' H/C ratio is lower compared to the aromatics, but much higher compared to the asphaltenes, so they contain less aromatic than asphaltenes, that are presumed to be maturation products of resin [Mat et al., 2006].

The formation of asphaltenes aggregates covered by aromatic resins, stabilises emulsion; asphaltenes and resins have acidic and basic groups, so the pH value of water used to produce emulsion can influence the mechanical characteristics of stabilising film. McLean and Kilpatrick, (1997) studied, for example, a molecular model that put in relation different crude solvency parameters to the stabilising properties of interfacial film. It is known moreover that water-in-oil emulsions are stabilised by asphaltenes only when they are in their point of incipient flocculation, maybe because they form finely dispersed aggregates that interact with the interface stabilising it [McLean and Kilpatrick, 1997].

Waxes are natural components of high viscous crude oil, and their precipitation under certain conditions in conventional crude transportation, can cause serious damages to conventional pipelines. These high molecular weight alkanes, solid at room temperature, can be grouped into microcrystalline ($>C_{40}$) or macrocrystalline ($<C_{40}$) [Than et al., 1999]. In the case of emulsion formation, waxes can coadsorb at the oil/water interface improving the stability. Natural waxes are mixtures of esters and frequently also contain hydrocarbon [Mat et al., 2006]. They are esters of long-chain (C_{16} and above), monohydric (one hydroxyl group), or alcohols with long-chain (C_{16} and above) fatty acids. Lee (1999) reports that for a Kuwait crude oil, an asphaltenes concentration of 0.01 g/ml did not produce a stable water-in-oil emulsion, but stability is improved when waxes (0.05 g/ml) are added; a consequent conclusion is that waxes cannot act as emulsifier by themselves, but they are good stabilisers for both O/W and W/O emulsions. For the same sample a concentration of asphaltenes containing 0.03 g/ml produced stable emulsions with no waxes!

Also resins alone could act as emulsifiers, but the best result is obtained when both resins and asphaltenes are used.

Porphyrins (organic components containing a metal, generally nickel and vanadium) are indicated by Lee as another type of emulsifiers, and their contribution was in the

formation of water-in-oil emulsions; the possible explication of this result is maybe due to the orientation of these molecules that probably orient at the oil-water interface forming a barrier for coalescence.

The water used to produce emulsions (both O/W and spontaneous W/O) contain clay particles and organic-clay particulates; their important characteristic is the contemporary hydrophobic and hydrophilic behaviour, that allows them to act as stabilisers [Lee, 1999]. Inorganic particles stabilise emulsion, producing the so-called “Pickering emulsions”. According to Langevin et al. (2004), emulsions are stable if droplet diameter is 10 μm or less, therefore, the particles that make their contribution to the stability should not be greater than 1 μm . Emulsion stability increases with a decrease in particle size, and if their contact angle with the interface is close to 90° , irreversible adsorption occurs. Moreover coalescence rate strongly decreases if a particles monolayer completely surrounds droplets, and if their concentration is high enough to form multilayers, stability is improved. If particles are hydrophilic O/W emulsions are stabilised, and if they are dried and in presence of asphaltenes they stabilise W/O emulsions.

1.5.4. Environmental impact

As Kokal found [Kokal, 2005] for Saudi Arabian crude, emulsions are W/O at approximately 80% water cut, but a phase inversion takes place if this threshold is overcome. Due to the big increase of viscosity, the W/O emulsification has to be avoided, while on the contrary if oil is the inner phase of emulsion, we can improve crude transportation reducing pressure drops in pipes. A practical demonstration of crude oil emulsification realised to improve its transportation, was successfully carried out with the highly viscous oil of the field in the Orinoco River region of Venezuela [Shigemoto et al., 2007, Salager et al., 2001]. The surfactant-stabilised emulsion (0.15% of additive surfactant) of oil in water so realised (70_{v/v}% of bituminous oil) is a new liquid fuel, trade name Orimulsion, whose disadvantage is a high concentration of sulphur and heavy metals. However, the price of Orimulsion is lower than traditional crude oil, so the expenses of investment for reducing environmental impact would be completely recovered over a few year period. Emulsification can also avoid problems involving environmental impact.

If emulsions like Orimulsion are directly fed to electric power plant [Wang and Fingas, 1996], heavy fuel oil (HFO) are burned in droplets forms both as a disperse phase or

continuous phase [Ocampo-Barrera et al., 2001, Ballester et al., 1995]. In the case of O/W emulsion, particulate emission is strongly reduced using a distillate oil, and the range of emissions reduction is between 50 and 90% for heavy fuel oil [Ballester et al., 1995].

1.6. Conclusions

In the present PhD thesis the study of highly-concentrated-in-oil emulsions is treated. The work has been divided into two arguments: the production of unstructured low viscous systems and the structuration of emulsified systems performed by the progressive structuration of both the internal and the external phase. Two different industrial case studies have been chosen in order to develop the whole work: first of all the characterisation of O/W model emulsions for crude oil transportation is studied and then the production of W/O and O/W emulsions as shortening replacer for puff pastry manufacture is proposed.

In the present chapter a general overview and state of the art of the analysed subject has been treated, focusing on colloids and emulsions main characteristics in the first part, and specifying the particular problems involving the two case studies in the second part. Thus, a detailed description of unstructured and structured emulsions for foodstuff production and crude oil transportation has been given.

References

- Abismaïl B., Canselier J.P., Wilhelm A.M., Delmas H., Gourdon C., (1999). *Emulsification by ultrasound: drop size distribution and stability*, Ultrasonics Sonochemistry 6, 75-83.
- Ahmed N. S., Nassar A. M., Zaki N. N., Gharieb H. K., (1999). *Formation of fluid heavy oil-in-water emulsions for pipeline transportation*, Fuel, 78, 593-600
- Allen J.C., Chien S.F., (1978). *Method for decreasing resistance to flow of crude oil up from a well or through a pipeline*, United States Patent No. 4,126,182
- Al-Roomi Y., George R., Elgibaly A., Elkamel A., (2004). *Use of a novel surfactant for improving the transportability/transportation of heavy/viscous crude oils*, Journal of Petroleum Science & Engineering 42, 235-243

- Al-Sahhaf T. A., Fahim M. A., Elsharkawy A. M., (2009). *Effect of Inorganic Solids, Wax to Asphaltene Ratio, and Water Cut on the Stability of Water-in-Crude Oil Emulsions*, Journal of Dispersion Science and Technology, 30, 597-604
- Angeli P., Hewitt G.F. (2000). *Flow structure in horizontal oil-water flow*, International Journal of Multiphase Flow 26, 1117-1140
- Atta A. M., Elsockary M. A., Kandil O. F., Mohamed Z. M., (2008). *Using of modified plastic waste based on Poly(ethylene-co-acrylic acid) grafts to solve transportation problem of petroleum crude oil*, Journal of Dispersion Science and Technology, 29, 7- 19
- Ballester J. M., Fueyo N., Dopazo C., (1995). *Combustion characteristics of heavy oil-water emulsions*, Fuel 75, 695-705
- Bannwart A. C., (2001). *Modeling aspects of oil-water core-annular flows*, Journal of Petroleum Science and Engineering 32, 127-143
- Barnes H.A., Hutton J.F., Walters K. (1989). *An Introduction to Rheology*. Elsevier Science Publishers B.V., Amsterdam, NL
- Bensakhria A., Peysson Y., Antonimi G. (2004). *Experimental study of the pipeline lubrication for heavy oil transport*, Oil & Gas Science and Technology, 59, 523-533
- Bibette J., Leal Calderon F., Poulin P., (1999). *Emulsions: basic principles*, Rep. Prog. Phys. 62, 969–1033
- Blanco Muñoz M. A. (2004), *Olive oil in food spreads*, Grasas y Aceites 55, 92-94
- Blijdenstein T.B.J., Veerman C., van der Linden E., (2004) a. *Depletion–Flocculation in Oil-in-Water Emulsions Using Fibrillar Protein Assemblies*, Langmuir, 20, 4881-4884.
- Blijdenstein T.B.J., Zoet F.D., van Vliet T., van der Linden E., van Aken G.A., (2004) b. *Dextran-induced depletion flocculation in oil-in-water emulsions in the presence of sucrose*, Food Hydrocolloids 18, 857–863
- Borwankar R.P., Frye L. A., Blaurock A.E., Sasevich F.J., (1992). *Rheological characterization of melting of margarines and tablespreads*, Journal of food engineering 16, 55-74
- Bot A., den Adel R., Roijers E. C., Regkos C., (2009). *Non-triglyceride structuring of edible oils: tubules in sterol + γ -oryzanol-based organogels*, Proceeding of the 5th

International Symposium on Food Rheology and Structure, Zurich 15- 18 June, 224-228

Briggeman W.H., Black J. J., (2002). *Method and system for reducing the viscosity of crude oil*, United States Patent No. US 6,491,053 B1

Buffo R. A., Reineccius G. A., (2002). *Modeling the rheology of concentrated beverage emulsions*, Journal of Food Engineering 51, 267-272

Chanamai R. and McClements D.J, (2006). *Depletion Flocculation of Beverage Emulsions by Gum Arabic and Modified Starch*, Journal of Food Science, 66, 457 - 463

Clogston J., Rathman J., Tomasko D., Walker H., Caffrey M. (2000), *Phase behaviour of a monoacylglycerol (Myverol 18-99K)/water system*, Chemistry and Physics of Lipids 107, 191-220

Comas D.I., Wagner J.R., Tomás M.C., (2006). *Creaming stability of oil in water (O/W) emulsions: Influence of pH on soybean protein–lecithin interaction*, Food Hydrocolloids 20, 990–996

Constantinides, P. P., Yiv S. H. (1994). *Particle size determination of phase-inverted water-in-oil microemulsions under different dilution and storage conditions*, International Journal of Pharmaceutics 115, 225-234

Criado M., Hernández-Martín E., López-Hernández A., Otero C., (2007). *Enzymatic interesterification of extra virgin olive oil with a fully hydrogenated fat: characterization of the reaction and its products*, Journal of American Oil Chemistry Society, 84,717–726

Dan D. , Jing G., (2006). *Apparent viscosity prediction on non-Newtonian water in crude oil emulsions*, Journal of Petroleum Science and Engineering, 53, 113-122

Dehkissia S., Larachi F., Rodrigue D., Chornet E., (2004) a. *Lowering the viscosity of Doba-Chad heavy crude oil for pipeline transportations - the hydrovisbreaking approach*, Energy & Fuels, 18, 1156-1168

Dehkissia S., Larachi F., Rodrigue D., Chornet E., (2004) b. *Characterization of Doba-Chad heavy crude oil in relation with the feasibility of pipeline transportation*, Fuel 83, 2157-2168

Dickinson E., (2009). *Hydrocolloids as emulsifiers and emulsion stabilizers*, Food Hydrocolloids 23, 1473–1482.

do Amaral M., (2004). *Assessing the environmental cost of recent progresses in emulsion polymerization*, Reactive & Functional Polymers 58, 197-202

Durand A. (2007). *Aqueous solutions of amphiphilic polysaccharides: Concentration and temperature effect on viscosity*, European Polymer Journal 43, 1744–1753

Eastoe J., (2005) . “Surfactant Aggregation and Adsorption at Interfaces” in *Colloid Science – Principles, Methods and Applications*, Cosgrove T. (Ed), Blackwell Publishing Ltd, 9600 Garsington Road, Oxford OX4 2DQ, (UK), 50-76

Eccleston G. M., (1997). *Function of mixed emulsifiers and emulsifying waxes in dermatological lotions and creams*, Colloids and surfaces A, 123-124, 169-182

Egelandsdal B., Langsrud Ø., Nyvold T., Sontum P. K., Sørensen C., Enersen G., et al. (2001). *Estimating significant causes of variation in emulsions’ droplet size distributions obtained by electrical sensing zone and laser low angle light scattering techniques*. Food Hydrocolloids, 15, 521–532.

Ferry J.D., (1980). *Viscoelastic properties of polymers*, John Wiley and sons, New York

Fingas M. and Fieldhouse B., (2009). *Studies on crude oil and petroleum product emulsions: Water resolution and rheology*, Colloids and Surfaces A: Physicochemical and Engineering Aspects, 333, 67-81

Fingas M., (1995). *Water-in-Oil emulsion formation: a review of physics and mathematical modeling*, Spill Science & Technology Bulletin, 2, 55-59

Fingas M., Fieldhouse B., (2003) a. *Studies of the formation process of water-in-oil emulsions*, Marine Pollution Bulletin 47, 369-396

Fingas M., Fieldhouse B., (2003) b. *Formation of water-in-oil emulsions and application to oil spill modelling*, Journal of Hazardous Materials 107, 37-50

Fingas M., Fieldhouse B., Mullin J., (1999). *Water-in-oil Emulsions Results of Formation Studies and Applicability to Oil Spill Modelling*, Spill Science & Technology Bulletin, 5,81-91

- Fingas, M., Fieldhouse, B., (2004). *Formation of water-in-oil emulsions and application to oil spill modelling*, Journal of Hazardous Materials, 107, 37-50.
- Ford, D.L, Borwankar, R., Martin, R.W.jr, Holcomb, D.N., (1997). Dressing and Sauces in “Food emulsions” by S.E Friberg and K. Larsson, Marcel Dekker, Inc., New York, · Basel
- Förster A. H., Herrington T. M., (1998). *Rheology of two commercial available cosmetic oil in water emulsion*, International Journal of Cosmetic Science 20, 317-326
- Fournanty S., Guer Y., Le El Omari K., and Dejean J.-P., (2008). *Laminar flow emulsification process to control the viscosity reduction of heavy crude oils*, Journal of Dispersion Science and Technology, 29,1355-1366
- Franco J. M., Guerrero A., Gallegos, C, (1995). *Rheology and processing of salad dressing emulsions*, Rheologica Acta, 34, 513–524
- Franco J.M., Raymundo A., Sousa I., Gallegos C., (1998). *Influence of processing variables on the rheological and textural properties of lupin protein-stabilized emulsions*, J. Agric. Food Chem. 46, 3109-3115
- Frasch-Melnik S., Spyropoulos F., Bakalis S., Norton I., (2009). *Fat crystal-stabilized W/O emulsions for controlled salt release*, Proceeding of the 5th International Symposium on Food Rheology and Structure, Zurich 15 – 18 June, 530-532
- Friberg S. E., Larsson K. (1976). Food emulsions – Third Edition, Revised and Expanded – Marcel Dekker, Inc. – New York · Basel
- Friberg S.E., (1997). *Emulsion Stability* in S.E. Friberg, K. Larsson, Food Emulsions, 3rd ed., Marcel Dekker Inc
- Gabriele D., Migliori M., Di Sanzo R., Oliviero Rossi C., Ruffolo S. A., de Cindio B. (2009). *Characterisation of dairy emulsions by NMR and rheological techniques*, Food Hydrocolloids, 23, 611-618
- Garti N., Binyamin H., Aserin A., (1998). *Stabilization of Water-in-Oil Emulsions by Submicrocrystalline α -Form Fat Particles*, Journal of American Oil Chemistry Society, 75, 1825-1831
- Gateau P., Hénaut I., Barré L., Argillier J. F., (2004). *Heavy oil dilution*, Oil & Gas Science and Technology- Rev. IFP, 59, 503-509

- Ghotra B.S., Dyal S.D., Narine S.S., (2002). *Lipid shortenings: a review*, Food Research International, 35, 1015-1048
- Guo J., Liu Q., Li M., Wu Z., Christy A. A., (2006). *The effect of alkali on crude oil/water interfacial properties and the stability of crude oil emulsions*, Colloids and Surfaces A, 273, 213-218
- Hannisdal A., Orr R., Sjöblom J., (2007). *Viscoelastic properties of crude oil-water interfaces. 1. The effect of dilution*, Journal of Dispersion Science and Technology, 28:1, 81-93
- Hee Lee J., Akoh C. C., Himmelsbach D. S., Lee K-T., (2008). *Preparation of Interesterified Plastic Fats from Fats and Oils Free of Trans Fatty Acid*, Journal of Agricultural and Food Chemistry 56, 4039–4046.
- Hemmingsen P.V., Auflem I. H., Sæther Ø., Westvik A., (2006). “Droplet Size Distributions of Oil-in-Water Emulsions under High Pressures by Video Microscopy” in *Emulsions and Emulsion stability* Edited by Johann Sjöblom Universitetet i Bergen, Norway, Taylor & Francis Group
- Hénaut I., Courbaron A-C., Argillier J. F., (2009). *Viscosity of concentrated emulsions: relative effect of granulometry and multiphase morphology*, Petroleum Science and Technology 27, 182–196
- Jahaniaval F., (2005). *Process for preparing high liquid oil, no trans, very low saturates, regular margarine with phospholipids*, patent US 2005/0233056 A1, international classification A23D007/00
- Johansson D., Bergenståhl B., Lundgren E., (1995). *Wetting of fat crystals by triglyceride oil and water. 1. The effect of additives*, Journal of the American Oil Chemists Society, 72, 921-931
- Kane V. K., (1969). *Method of moving viscous crude oil through a pipeline*, United States Patent No. 3,425,429
- Kim I-H, Lee S-M, Lee B-M, Park H-K, Kim J-Y, Kwon K-I, Kim J-W, Lee J-S, Kim Y-H, (2009). *Interesterification of Olive Oil with a Fully Hydrogenated Fat in a Batch Reactor Using Step Changes in Temperature*, Journal of Agriculture Food Chemistry, 56, 5942–5946

Kokal S., (2005). *Crude-oil emulsions: a state of the art review*, SPE Production & Facilities, Saudi Amarco, revision for publication of presentation at the 2002 SPE Annual Technical Conference and Exhibition, San Antonio, 29/09-02/10

Korhonen M., (2003). *Rheological properties of pharmaceutical creams containing sorbitan fatty acid ester surfactant*, Academic dissertation, Pharmaceutical Technology Division, Department of Pharmacy University of Helsinki, Finland

Langevin J. D., Poteau S., Hénaut I., Argillier J.F. (2004). *Crude oil emulsion properties application to heavy oil transportation*, Oil & Gas Science and Technology – Rev. IFP 59, 5, 511-521

Leal-Calderon F., Thivilliers F., Schmitt V., (2007). *Structured emulsions*, Current Opinion in Colloid & Interface Science 12, 206–212

Lee R. F., (1998). *Agents which promote and stabilize water-in-oil emulsions*, Spill Science & Technology Bulletin, 5, 117-126

Macrae A.R., (1983). *Lipase-Catalyzed Interesterification of Oils and Fats*, Journal of the American Oil Chemists Society, 60, 291-294

Marangoni A., (2009). *Novel strategies for nanostructuring liquid oils into functional fats*, Proceeding of the 5th International Symposium on Food Rheology and Structure, Zurich 15 – 18 june, 38-46

Masmoudi H., Piccerelle P., Le Dréau Y., Kister J., (2006). *A rheological method to evaluate the physical stability of Highly viscous pharmaceutical oil-in-water emulsions*, Pharmaceutical Research, 23, 1937-1947

Mat H. B., Samsuri A., wan Abdul Rahman W. A., Rani S. I., (2006). *Study on demulsifier formulation for treating Malaysian crude oil emulsion*, Project No. 02-02-06-0015 EA098/VOT 74004)

McClements D.J., (1999). *Food Emulsions – Principles, Practice and Techniques*, CRC Press, New York, Chapter 1.

McLean J. D., Kilpatrick P. K., (1997). *Effects of asphaltenes solvency on stability of water-in-crude-oil emulsions*, Journal of Colloid and Interface Science 189, 242-253

- Miller D., Wiener E.M., Turowski A., Thunig C., Hoffmann H., (1999). *O/W emulsions for cosmetics products stabilized by alkyl phosphates – rheology and storage tests*, Colloids and Surfaces A: Physicochemical and Engineering Aspects 152, 155–160
- Nädler M., Mewes D., (1996). *Flow induced emulsification in the flow of two immiscible liquids in horizontal pipes*, Int. J. Multiphase Flow, 23, 55-68
- Nordvik A. B., Simmons J. L., Bitting K. R., Lewis A., Strøm-Kristiansen T. (1996). *Oil and water separation in marine oil spill clean-up operation*, Spill Science & Technology Bulletin, 3, 107-122
- Norton I.T., Spyropoulos F., Alex E., Heuer K., Le Reverend B.J.D., Cox P.W., (2009). *Microstructure engineering of healthy everyday foods*, Proceeding of the 5th International Symposium on Food Rheology and Structure, Zurich 15 – 18 June, 10-16
- Norton J., Cox P.W., Fryer P.J., Parkinson J., (2009). *Engineered healthy indulgence: development and characterization of cocoa butter emulsions*, Proceeding of the 5th International Symposium on Food Rheology and Structure, Zurich 15 – 18 June, 228-232
- Ocampo-Barrera R., Villasenor R., Diego-Marin A., (2001). *An experimental study of the effect of water content on combustion of heavy fuel oil/water emulsion droplets*, Combustion and Flame 126, 1845-1855
- Pal R., (1998). *Short communication-Scaling of viscoelastic properties of emulsions*, Chemical Engineering Journal 70, 173-178
- Pal R., (2000). *Shear viscosity behaviour of emulsions of two immiscible liquids*, Journal of Colloids and Interface Science, 225, 359-366
- Pal R., (2007). *Rheology of double emulsions*, Journal of Colloid and Interface science 307, 509-515
- Quiñones-Cisneros S. E., Andersen S.I., Creek J, (2005). *Density and Viscosity Modeling and Characterization of Heavy Oils*, Energy & Fuels, 19, 1314-1318
- Quintana J.M., Califano A., and Zaritzky N., (2002), *Microstructure and stability of non-protein stabilized Oil-in-Water food emulsions measured by optical methods*, Journal Of Food Science, 67, 1130-1135

- Ramli M.R., Lin S.W., Yoo C.K., Idris N.A., Sahri M.M., (2008). *Physico-chemical Properties and Performance of High Oleic and Palm-Based Shortenings*, Journal of oleo science, 57, 605-612
- Riley J., (2005) . “Charge in Colloidal Systems” in *Colloid Science – Principles, Methods and Applications*, Cosgrove T. (Ed), Blackwell Publishing Ltd, 9600 Garsington Road, Oxford OX4 2DQ, (UK), 14-35
- Rodríguez-Abreu C., Lazzari M., (2008). *Emulsions with structured continuous phases*, Current Opinion in Colloid & Interface Science 13, 198–205
- Romero A., Cordobés F., Puppo M.C., Guerrero A., Bengoechea C., (2008). *Rheology and droplet size distribution of emulsions stabilized by crayfish flour*, Food Hydrocolloids 22, 1033–1043
- Romero N., Cárdenas A., Henríquez M., Rivas H., (2002). *Viscoelastic properties and stability of highly concentrated bitumen in water emulsions*, Colloids and Surfaces A, 204, 271-284
- Rousseau D., (2000). *Fat crystals and emulsion stability - a review*, Food Research International 33, 3-14
- Rubio-Hernández F.J., Gómez-Merino A.I., Ruiz-Reina E., (2000). *Electroviscous Effect in Dilute Suspensions of Alumina*, Journal of Colloid and Interface Science 222, 103–106
- Sajjadi S., (2006). *Effect of mixing protocol on formation of fine emulsions*, Chemical Engineering Science, 61, 3009-3017
- Salager J.L., Briceño M.I., Bracho C.L., (2001). “Heavy Hydrocarbon Emulsions. Making use of the State of the Art in Formulation Engine”, in *Encyclopedic Handbook of Emulsion Technology*, Sjöblom, J. (ed), Marcel Dekker, NewYork
- Salager J.L., Forgiarini A.F., Márquez L., Peña A., Pizzino A., Rodriguez M. P., Rondón-González M. (2004). *Using emulsion inversion in industrial process*, Advances in Colloid and Interfaces Science 108, 259-272
- Saniere A., Hénaut I., Argillier J.F., (2004). *Pipeline Transportation of Heavy Oils, a Strategic, Economic and Technological Challenge*, Oil & Gas Science and Technology, 59, 455-465

Satgé C., Granet R., Verneuil B., Champavier Y., Krausz P., (2004). *Synthesis and properties of new bolaform and macrocyclic galactose-based surfactants obtained by olefin metathesis*, Carbohydrate Research 339, 1243–1254

Schelero N., Lichtenfeld H., Zastrow H., Möhwald H., Dubois M., Zemb T., (2009). *Single particle light scattering method for studying aging properties of Pickering emulsions stabilized by catanionic crystals*, Colloids and Surfaces A: Physicochem. Eng. Aspects 337, 146–153

Schwering R., Blom A., Warr G.G., (2008). *Laterally nanostructured adsorbed layers of surfactant/surfmer mixtures before and after polymerization*, Journal of Colloid and Interface Science 328, 227–232

Sherman P., (1959). *The influence of emulsifying agent concentration on emulsion viscosity*, Kolloid-Zeitschrift, 165, 156-161

Shigemoto N., Al-Maamari R. S., Jibril B. Y., Hirayama A., Sueyoshi M., (2007). *Effect of water content and surfactant type on viscosity and stability of emulsified heavy Mukhaizna crude oil*, Energy & Fuels, 21, 1014-1018

Singh D., Rezac M. E., Pfromm P. H., (2009). *Partial hydrogenation of soybean oil with minimal trans fat production using a Pt-Decorated polymeric membrane reactor*, J Am Oil Chem Soc, 86, 93–101

Skogerson L., Boutte T., Robertson J., Zhang F., (2007). *Non-hydrogenated vegetable oil based margarine for puff pastry containig an elevated di-glyceride emulsifier*, USPTO Patent Application 20070148313, Class: 426602000 (USPTO)

Sotgia G, Tartarini P., Stalio E., (2008). *Experimental analysis of flow regimes and pressure drop reduction in oil–water mixtures*, International Journal of Multiphase Flow 34, 1161–1174

Steffe J.F., (1996). *Rheological methods in food process engineering*, Freeman Press, Michigan

Strausz O. P., Mojelsky T. W., Payzant J. D., (1999). *Upgrading of Alberta's heavy oils by superacid-catalyzed hydrocracking*, Energy & Fuels, 13, 558-569

Strayer et al., (2006), *Food fats and oils - Ninth edition*, Institute of Shortening and Edible Oils, Inc., 1750 New York Avenue, NW, Washington (U.S.A.)

- Tanner R.I., (1985). *Engineering Rheology*, Clarendon Press, Oxford
- Toda K., Furuse H., (2006). *Extension of Einstein's viscosity equation to that for concentrated dispersion of solutes and particles*, Journal of Bioscience and Bioengineering 102, 6, 524-528
- Vincent B., (2005). "Introduction to Colloidal Dispersion" in *Colloid Science – Principles, Methods and Applications*, Cosgrove T. (Ed), Blackwell Publishing Ltd, 9600 Garsington Road, Oxford OX4 2DQ, (UK), 1-13
- Wakabayashi T. (1997). *Viscosity correlation with specific gravity and molecular weight of crude oil fractions*, Fuel, 76, 1049-1056.
- Walther B., Cramer C., Tiemeyer A., Hamberg L., Fischer P., Windhab E. J., Hermansson A.M., (2005). *Drop deformation dynamics and gel kinetics in a co-flowing water-in-oil system*, Journal of Colloid and Interface Science 286, 378–386
- Wang Z., Fingas M., (1996). *Separation and characterization of petroleum hydrocarbons and surfactant in Orimulsion dispersion samples*, Environmental Science & Technology, 30, 3351-3361
- Washington C., (1992). *Particle size analysis in pharmaceuticals and other industries*, Ellis Horwood Limited, England
- Welch C.F., Rose G.D., Malotky D., Eckersley S.T., (2006). *Rheology of High Internal Phase Emulsions*, Langmuir 22, 1544-1550
- Ye A., Singh H., (2006). *Heat stability of oil-in-water emulsions formed with intact or hydrolysed whey proteins: influence of polysaccharides*, Food Hydrocolloids 20, 269–276
- Zaki N. N., (1997). *Surfactant stabilized crude oil-in-water emulsions for pipeline transportation of viscous crude oils*, Colloids and Surfaces A, 125, 19-25
- Zhou L., Chen H., Jiang X., Lu F., Zhou Y., Yin W., Ji X., (2009). *Modification of montmorillonite surfaces using a novel class of cationic gemini surfactants*, Journal of Colloid and Interface Science 332, 16–21

Chapter 2 – Isoenergetic emulsification: rheology and droplet size distribution

Abstract

Among the great number of applications involving the unstructured concentrated-in-oil emulsions, crude oil transportation is one of the most promising for industrial impact. The emulsification process can affect the droplet size distribution (DSD) of biphasic systems and as a consequence change their rheological properties. The aim of the present work is the study of the DSD and viscosity of concentrated oil in water emulsions produced by isoenergetically varying the specific power of mixing of the rotor stator device. A marked instability of emulsions produced at low power of mixing was found, and a progressive stabilisation was observed by increasing this parameter while maintaining the same energy level of mixing, although no significant changes in viscosity was observed.

2.1. Introduction

2.1.1. Different methods of emulsification: a general overview

Emulsions are biphasic systems widely used for many different industrial applications. Among them, the dispersion of crude oil in water in the form of concentrated emulsion (high oily phase content) is one of the most important methods for crude transportation in pipelines [Fournanty et al. 2008; Saniere et al., 2004; Nädler and Mewes, 1996; Dehkissia et al., 2004]. Conventional pipelines are not suitable for transporting heavy crudes from the reservoir to the refinery because of the high viscosity [Ahmed et al., 1999]. In order to limit pumping costs, pressure drop in pipes has to be as low as possible and travel along significant distances. In the case of heavy oils, pressure drop increases as viscosity increases and pumping single oil-phase becomes economically disadvantageous [Al-Roomi et al., 2004]. Therefore, emulsification can help in decreasing the viscosity of crude oil, reducing pressure drop in pipelines as a consequence. On the other hand, after transportation a de-emulsification process must be performed in order to separate the crude oil from the water; consequently, the desired emulsion should be stable under shear effect guaranteeing a safe pumping step, but phase separation should be easy to effect in

order to ensure a simple and cheap oil-phase recovery at the end of the transportation. The initial crude oil emulsification phase is really crucial because different emulsification conditions in water can produce stable or unstable emulsions. The aim of the present work is the study of the emulsification phase of a model oil where the emulsification conditions (speed and time of mixing) have been fixed with an isoenergetical criterion.

A wide literature has been written in order to study how emulsification influences the rheological and microscopic characteristics of emulsions. In fact, a lot of works focus on the study of DSD and its influence on the mechanical properties of emulsions by progressively varying the mixing speed (rpm) and, consequently, the power supplied during mixing.

Amongst the various mixing devices, the most used in the worldwide literature is the rotor-stator system (Ultra-Turrax, Figure 2.1) that disrupts droplets because of the high rotation speed of the rotor. The medium to be processed is automatically drawn axially into the dispersion head and then forced radially through the slots in the rotor/stator arrangement. The high accelerations acting on the material generate very high shear rates and thrust forces. In addition, high turbulence occurs in the shear gap between rotor and stator, providing optimum mixing of the emulsion.

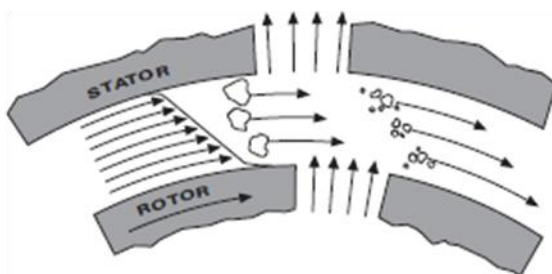


Figure 2.1: rotor-stator system

Hénaut et al. (2009) report how mixing speed changes the viscosity of emulsions preparing castor oil in water (70_{v/v}% oil) emulsions with an alkylphenol ethoxylated emulsifier (2_{w/w}%) and increasing the mixing speed from 500 to 13000 rpm without changing the emulsification time. They found that, depending on the stirring intensity, the emulsion may result either unimodal and multiple or unimodal and simple or bimodal and simple. Moreover, the authors found a marked dependence on the viscosity values and the mixing speed, and also they showed that the viscosity of a concentrated bimodal emulsion is lower than that with a unimodal size distribution.

Romero et al. (2008) used an Ultra-Turrax T-50 homogenizer from IKA (Germany) at different mixing speeds (3000 – 10000 rpm) and an emulsification time of 7 min to produce stable O/W concentrated emulsions. They observed the droplet size reduction due to the increase of the energy density supplied to the emulsion. The energy density E_V was defined as the energy input per unit of emulsion volume, obtained from the power input per unit of volume P_V up to an integrated fixed emulsification time t :

$$E_V = \int P_V(t) dt \quad [2.1.1]$$

Considering that during the emulsification phase the dispersed phase is added to the continuous one, from the eq. [2.1.1] it holds

$$E_V = \int \frac{\dot{W}(c, N, t)}{\frac{M_c}{\rho_c(c, t)} + \frac{M_o(t)}{\rho_o(t)}} dt \quad [2.1.2]$$

where M_c is the mass of emulsifier supplied as an aqueous dispersion, M_o is the amount of oil in the emulsion, c is the emulsifier flour concentration, N is the agitation speed, $\dot{W}(c, N, t)$ is the power consumption and $\rho_c(c, t)$ and $\rho_o(t)$ are the densities of the continuous and oil phases, respectively. The authors suggested that the relationship between the energy density and the (Sauter) volume-surface diameter can be expressed as follows:

$$d_{3,2} = a \cdot E_v^{-b} \quad [2.1.3]$$

with the constants a and b depending on the type of emulsifier, the properties of the continuous and the disperse phase and the emulsification equipment used.

Jafari et al. (2008) attribute the result of droplets disruption during the emulsification phase to the power density P_V and the residence time (t_{res}) in the emulsification zone:

$$d_{3,2} \propto P_v^{-b1} \cdot t_{res}^{-b2} \quad [2.1.4]$$

then, if $b1 \cong b2 \cong b$, the equation [2.1.4] can be written as a function of energy density as expressed in the equation [2.1.3] or as follows:

$$d_{3,2} = a \cdot E_v^{-b} \cdot \gamma^d \cdot \rho_c^{-e} \quad [2.1.5]$$

where b , C , d , and e are constants depending on the efficiency of droplet disruption and flow conditions in the emulsification zone of different systems and γ the interfacial tension.

Less (2003) studied DSD in water-in-crude oil emulsions produced by the Ultra-Turrax T25 mixing device by mixing at 65°C for 2 min and varying the speed from 6500 rpm to 21500 rpm. The authors characterised the prepared emulsions by using a lognormal distribution function of diameters in the range from 5 to 110 µm. Generally, a narrower distribution corresponded to a speed of mixing increase or a water cut decrease. Ni et al. (1998) analysed the droplet size and size distribution in methylmethacrylate dispersions in a batch oscillatory-baffled reactor (OBR), in which the fluid passes through a set of equally spaced orifice baffles generating eddies that promote the fluid mixing. Those periodically formed vortices can be controlled by a combination of geometrical and operating parameters; in particular the authors found a correlation between the Sauter diameter and X_0f , where f is the frequency of oscillation and X_0 the baffle thickness:

$$d_{32} = \propto (X_0f)^{-1.2} \quad [2.1.6]$$

Their results suggest that the oscillation amplitude and frequency play an equal part in controlling the droplet size, and the Sauter mean diameter in OBR can be approximated to the oscillatory velocity to a power of -1.2.

Bengochea et al. (2006) characterised highly concentrated O/W emulsions stabilised by proteins using linear dynamic viscoelasticity and DSD. DSD results showed lognormal bimodal profiles. A reduction in size and polydispersity (*polydispersity* indicates the broadness of a distribution: the higher the polydispersity, the broader the range of size) were obtained by increasing energy input or the concentration of either oil or protein, and the increase in mechanical energy produced higher values for the dynamic moduli. Franco et al. (1998) studied different processing conditions for the preparation of concentrated oil-in-water emulsions in a rotor-stator turbine (8000-20500 rpm, 3-10 min). All DSD curves obtained by the authors showed a bimodal shape with a secondary maximum at relatively low values of the droplet diameter and the maximum distribution value at higher sizes. Moreover, an initial increase in agitation speed produced a decrease in the average Sauter diameter (8000-14250 rpm), resulting in a significant increase of emulsion viscosity, firmness, and adhesiveness. Nevertheless, a further increase in the agitation speed produced only a slight decrease in the mean droplet diameter and does not qualitatively modify the DSD curves. Very similar results have been found in other works: Quintana et al. (2002) prepared O/W emulsions (40_{v/v}% of oily phase) increasing the mixing speed from 7800 to 16300 rpm for a mixing time of 2, 4 and 6 minutes. Ahmed et al. (1999) studied the stability of the Geisum crude oil-in-water emulsion (70_{v/v}%)

stabilised by a nonionic surfactant for three different mixing speeds, namely, 700, 1200, and 1700 rpm nominal speed of mixing at 60°C for 15 min at a fixed surfactant concentration (2.5%).

The authors found a progressive decrease of mean droplet diameter with the mixing speed and a consequent increase of emulsion stability.

[Maa and Hsu \(1996\)](#) focused on the preparation of the primary emulsion (W/O or O/W) using rotor/stator homogenisation as a first step for the double-emulsion microencapsulation process (W/O/W or O/W/O). The authors used Poly(methyl-methacrylate) and analytical-grade methylene chloride (MeCl₂) for the oily phase preparation, Polyvinyl alcohol (PVA) as an emulsifier and Bovine serum albumin (BSA) was used as a model protein. The authors found an initial reduction period (transition) of the obtained mean droplet diameter with the mixing speed, and subsequently a leveling-off period (equilibrium). The minimum droplet size obtained has been defined as the ultimate equilibrium emulsion droplet size. Its occurrence was also explained by [Vankova et al. \(2007\)](#) from a hydrodynamic point view. The disruption of droplets of the dispersed phase requires turbulent eddies. The scale of the turbulent eddies decreases with the increase of homogenisation intensity (power) until a critical point where the eddies are so small that further energy is lost through viscous dissipation. At a certain homogenization speed at which no further droplet size change is encountered, the turbulent eddies reach this critical scale. Consequently, homogenization at even higher speeds cannot generate turbulent eddies of a size smaller than the critical scale to further fragment the droplets.

In his work [Zaki \(1997\)](#) studied the stability and the viscosity of a surfactant stabilised viscous Geisum crude oil-in-water emulsion for pipeline transportation. Specifically, he studied the effect of five different mixing speeds (from 2000 to 6000 rpm) each maintained for 15 minutes, finding a linear increase of the emulsion viscosity with the mixing speed for the crude oil system.

The above presented literature review reports on studies of emulsification effects onto the rheological and microscopic characteristics of biphasic systems through an increase of mixing speed, without applying a criterion to fix the mixing conditions (power supplied, mixing time).

Thus, in this work the construction of isoenergetic curves of DSD parameters vs the specific power has been realised in order to study the main effect on emulsions rheology and *stability*.

2.1.2. DSD measurement and statistic analysis

As already mentioned, the DSD is one of the most important characteristics for the definition of emulsion characteristics such as stability [McClements, 1999], viscosity and rheological behaviour [Franco et al. 1998, Derkach 2009] colour and appearance [McClements, 2002]. The DSD is characterised by the ‘average’ particle (central tendency) and the variation between the particles’ dimensions (width of the distribution) in a polydisperse system that allow the mechanical behaviour of the sample to be defined. The mean value of a droplet size distribution $\langle d \rangle$ can be evaluated in different ways, already described in the Chapter 1 (paragraph 1.1.1) of the present thesis. The width of the distribution, related to its polydispersity, can be evaluated from the standard deviation value (σ) in the case of Gaussian distributions. In the case of multimodal distributions that cannot be described by conventional models, other empirical parameters are usually employed to describe the width of the distribution. Many authors [i.e. Mabile et al. (2000); Goubault et al. (2001); Romero et al. (2008)] uses an Uniformity index (expressed in percentage) in order to parameterize the polydispersity of the emulsion:

$$U = \frac{\sum_i V_i |d(v,0.5) - d_i|}{\sum_i V_i} \frac{1}{d(v,0.5)} \quad [2.1.7]$$

where $d(v, 0.5)$ is the is the median for the volume-based distribution, and V_i is the volume of droplets with a diameter d_i .

Washington (1992), Olesik and Bates (1994), and Vladisavljević and Schubert (2003) take into account the polydispersity of the distribution with the *Span* index, defined as

$$Span = \frac{d(0.9) - d(0.1)}{d(0.5)} \quad [2.1.8]$$

where the $d(0.1)$, $d(0.5)$ and $d(0.9)$ values indicate that 10%, 50% and 90% of the measured particles were less than or equal to the size stated.

In the case of the monomodal emulsions, particle size distributions may take many forms but there are few modelled distributions which are of particular interest. The study of these models allows the experimental data to be reduce to a few parameters, giving a complete sample characterisation. In many works the DSD is modelled by a log-normal distribution because it is well known that sequential break-up processes, such as grinding of solids or disruption of droplets under mechanical agitation, lead to a lognormal distribution of particles and drop sizes [Peña and Hirasaki, 2003]. This model supposes that

if the droplet diameter d is log-normally distributed, then $\ln(d)$ is normally distributed (Gaussian behaviour): likewise if a population counts a number N of unities, their logarithm is distributed in a normal way. The lognormal probability density function $f(d)$ is:

$$f(d) = \frac{1}{d \cdot \sigma_{\ln} \cdot \sqrt{2\pi}} \exp \left[\frac{-(\ln d - \bar{d}_g)^2}{2\sigma_{\ln}^2} \right] \quad [2.1.9]$$

in which σ_{\ln} is the standard deviation of the model and \bar{d}_g the geometrical mean of the distribution.

$$\bar{d}_g = \frac{\sum n_i d_{\ln,i}}{N} \quad [2.1.10]$$

$$\sigma_{\ln} = \sigma_g = \sqrt{\sum [n_i (d_{\ln,i} - \bar{d}_g)^2] / N} \quad [2.1.11]$$

n_i is the number of droplets in each size class, $d_{\ln,i} = \ln(d_i)$ and N is the total number of droplets, $N = \sum_i n_i$.

If the model is in a good accordance with the experimental data, a mean diameter and variance can be derived from the model parameters by applying the following rules [Walpole et al. 2007]:

$$\bar{d}_s = e^{\bar{d}_g + \sigma_{\ln}^2 / 2} \quad [2.1.12]$$

and

$$\sigma_s^2 = e^{2\bar{d}_g + \sigma_{\ln}^2} (e^{\sigma_{\ln}^2} - 1) \quad [2.1.13]$$

The 3-parameter lognormal distribution is a lognormal distribution used for data where the logarithms follow a normal distribution after subtracting a threshold value θ . The equation is very similar to the [2.1.9], and it's reported below.

$$f(d) = \frac{1}{(d-\theta) \cdot \sigma_{\ln} \cdot \sqrt{2\pi}} \exp \left\{ \frac{[-\ln(d-\theta) - \bar{d}_g]^2}{2\sigma_{\ln}^2} \right\} \quad [2.1.14]$$

As shown for the simple lognormal model, it is possible to derive a mean value and a variance of the distribution from the model parameters. The variance equation is the same used for the lognormal model (eqs. [2.1.13]), while the mean value equation is:

$$\bar{d}_s = \theta + e^{\bar{d}_g + \sigma_{\ln}^2 / 2} \quad [2.1.15]$$

Richter et al. (2007) studied O/W emulsions performing ultrasonic attenuation spectroscopy for the dispersed system characterization applying a lognormal model for the distribution. The lognormal distribution as a function of the median value is reported as follows:

$$f(d) = \frac{1}{d \cdot \sigma_{\ln} \cdot \sqrt{2\pi}} \exp \left[\frac{-\ln(d/d_{50})^2}{2\sigma_{\ln}^2} \right] \quad [2.1.16]$$

where the d_{50} is the median value and the σ_{ln} standard deviation of the model.

Peña and Hirasaki (2003) have characterized oilfield emulsions via NMR diffusion; the droplet size characterisation was interpreted by the Weibull distribution model and the lognormal distribution model by using d_{gV} (geometric volume-based mean diameter) and σ_{ln} as fitting parameters.

In order to study the droplet size distribution on sprays, Babinsky and Sojika (2002) present the modeling of DSD by using different probability density functions, such as the lognormal, root-normal, log-hyperbolic, Rosin-Rammler and so on. Focusing on the lognormal distribution, they introduce the three-parameter “upper limit distribution” like a modification of the lognormal distribution where a maximum limit drop size d_{max} is imposed. The equation is:

$$f(d) = \frac{\delta d_{max}}{\sqrt{\pi}d \cdot (d_{max} - d)} \exp\left\{-\delta^2 \left[\ln\left(\frac{ad}{d_{max} - d}\right)\right]^2\right\} \quad [2.2.17]$$

where $a = \frac{d_{max}}{\bar{d}}$ and $\delta = \frac{1}{\sqrt{2}(\ln \sigma_{distr})}$ where σ_{distr} is the width of the distribution.

Moreover, the root-normal distribution, widely used for the volume distribution of drops in sprays, was reported by the authors:

$$f(d) = \frac{1}{\sqrt{2\pi} \cdot 2\sigma_{distr} d} \exp\left\{-\frac{1}{2} \left[\left(\frac{\sqrt{d} - \sqrt{\bar{d}_g}}{\sigma_{distr}}\right)\right]^2\right\} \quad [2.2.18]$$

2.2. Materials and methods

2.2.1. Emulsions preparation

Two sets of O/W model emulsions (simulating a biphasic system for pipeline transportation [Gabriele et al, 2009]) were prepared by supplying two levels of energy of mixing: each set was prepared isoenergetically at different mixing speed (and, as a consequence different mixing power) with a rotor-stator system Ultra-Turrax T 25 (IKA, Germany). The mixing speed range chosen for the samples preparation was 12000/24000 rpm for the first isoenergetic curve and 10000/24000 rpm for the higher isoenergetic: the lower rpm value was chosen taking into account the stability of the samples that could not be maintained for the requested time at lower mixing speeds (at the investigated energy input value), whilst the upper value of the range corresponded to the maximum allowable by the instrument.

Raw materials were distilled water and commercial paraffin oil Finavestan A360B ($\rho(25^\circ\text{C})=0.864\pm 0.011$ Kg/l, $\mu(25^\circ\text{C}) = 0.157 \pm 0.002$ Pa·s, Total, France), a non-ionic hydrophilic emulsifier Tween 60 (polyoxyethilenesorbitan monostereate, HLB 14.9, gives O/W emulsions) purchased from Sigma Aldrich (Italy).

All samples (150 g for each batch) contained a total oil amount of 60_{v/v} %. Emulsions were prepared by the agent-in-water method [Yaghi and Al-Bemani, 2002], dissolving and stirring the emulsifier in water at 70°C using a magnetic-heater agitator (Heating Magnetic Stirred, Velp Scientific, Italy). The surfactant concentration (2_{w/w} %) was based on the total weight of the mixture. After the emulsifier was added, the solution was continuously stirred for 5 minutes. The oil (heated-up to 70°C) was then dropped to the water phase (for about 40s) by using an addition funnel (Schott Duran, Germany) and after that the homogenisation phase was prolonged for the necessary time.

After the sample preparation, all tests were performed after a rest time of three hours at room temperature.

2.2.2. Mixing conditions

Mixing speed and mixing time of emulsification were balanced in order to maintain fixed the total energy supplied to the sample.

The device is able to provide an output power of approximately 300 Watts at 24000 rpm. Assuming that the power P is a linear function of the mixing speed, the power could be evaluated correspondent to an arbitrarily assumed value of mixing speed of 15000 rpm. So the first sample was obtained imposing 15000 rpm and 7 min as operating conditions: the mixing time was chosen as a starting parameter.

Knowing these conditions, the mixing speed was just varied, as a consequence calculating the mixing time that allowed the requested energy input value to be obtained. In the table 2.1, the stirring conditions are listed indicating the mixing speed and the specific power Ps : the E1 samples are those prepared with this energy input value equal to 525 J/g, whilst the E2 set of samples were prepared by increasing energy input value of ~25%, equal to 657 J/g.

Sample ID	Mixing Speed, [rpm]	Mixing time [s]	P_s , [W/g]
E1_F126	12600	500	1.05
E1_F150	15000	420	1.25
E1_F176	17600	358	1.47
E1_F200	20000	315	1.67
E1_F240	24000	263	2.00
E2_F100	10000	788	0.83
E2_F126	12600	625	1.05
E2_F150	15000	525	1.25
E2_F200	20000	447	1.67
E2_F176	17600	394	1.47
E2_F240	24000	328	2.00

Table 2.1: samples stirring conditions

2.2.3. Rheological characterisation

A rheological characterisation was performed obtaining flow curves by averaging the step rate tests results performed at a fixed shear rate value. All rheological tests were carried out by using a controlled strain rheometer ARES-RFS (TA instrument, USA) equipped with a parallel plate geometry ($\Phi = 50$ mm, gap 1.5 mm). The shear rate range was $0.1-100$ s⁻¹ except when larger shear rates (at least 1s⁻¹) were required to measure torque values within the instrument sensitivity range (from 10^{-7} Nm to 0.1 Nm).

The ‘step rate test’ analyses the time dependence of the sample at a fixed shear rate. All tests were performed for 60s, and revealed that a steady values of viscosity is reached after more or less 10s from the beginning of the test. Therefore, viscosity value were calculated averaging the step rate tests data corresponding to the range 10 - 60s.

The flow curves were obtained from lower to higher shear rate values (‘direct’ sequence) and vice-versa (‘inverse’ sequence): if the two curves overlap each other, the system was assumed stable under the shear conditions applied. This allowed to measure a material property because the measure did not affect the mechanical behaviour of the sample. All tests were performed at 5, 10 and 25°C.

2.2.4. Microscopic characterisation: DSD

The morphology of the emulsion droplets was observed with a contrast phase microscopy (MX5000, MEIJI, Japan) equipped with phase contrast objective 40X and 100X. In order to produce photomicrographs without droplets aggregates and, as a consequence, which can be

easily analysed, samples were diluted (1:10, volume fraction) in distilled water. After that, all samples were placed onto a glass slide inside a cover imaging chamber (Sigma, Italy) on which a cover slide were put. Cover chamber forms a sealed volume for thick and freefloating specimens.

An image database software was used to detect the different particle sizes of droplets (*dhs* image database, Germany) by greyscale detection (Figure 2.2). In the following figures, an example of particles analysis is reported.

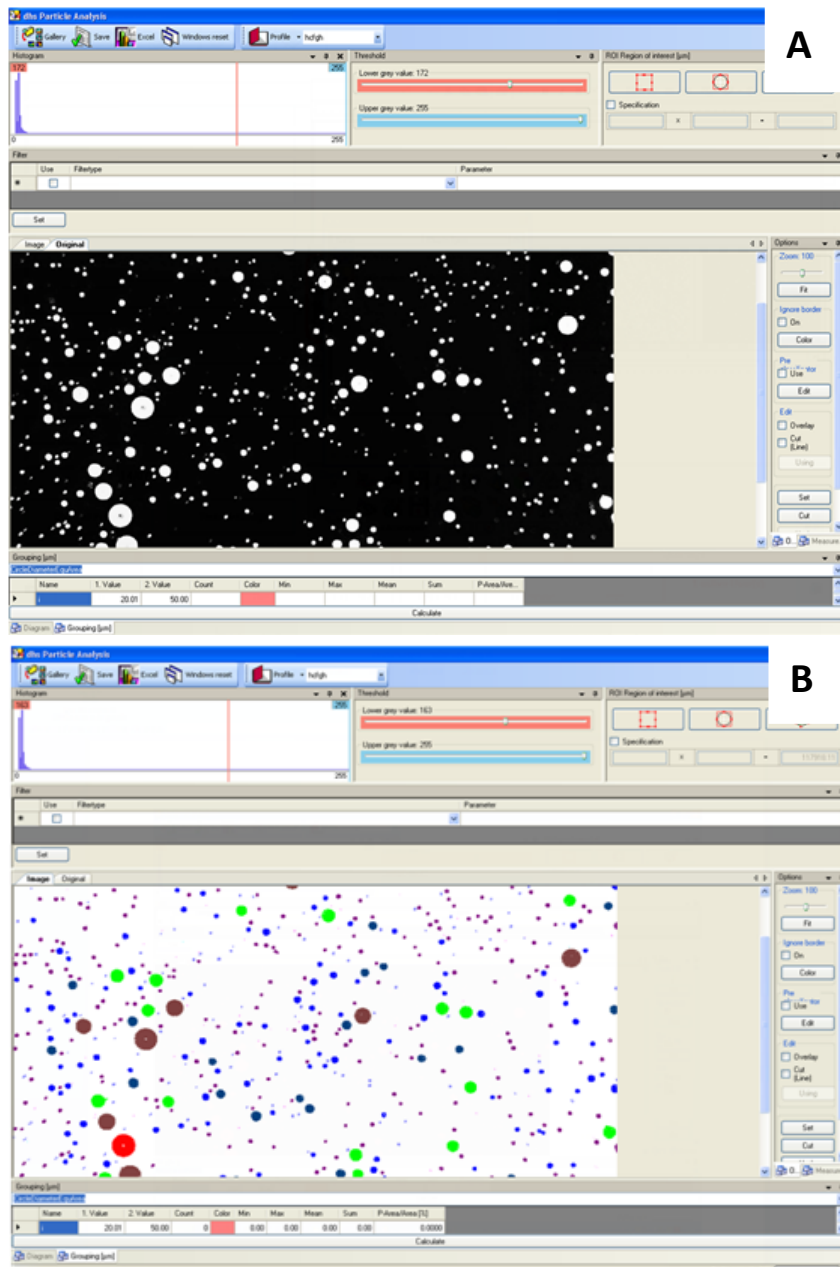


Figure 2.2: example of droplets size analysis by greyscale detection; in the image A the original photo is showed, in the image B the final analysis is presented: different sizes are discriminated by different colours.

The software measures the number-based surface equivalent diameter. A statistic software analysis was used to interpret the DSD raw data acquired from each emulsion batch (Statgraphics Centurion XV, version 15.2.13, USA). The first analysis for each sample used the descriptive statistic to find mean, mode, standard deviation, asymmetry and kurtosis of the data. Moreover, a frequency histogram was obtained where the number of the histogram bars, corresponding to the number of equal width intervals into which the data are divided, was chosen by applying the rule

$$n_b = 10 \cdot \log_{10}^{(4)}(N) \quad [2.2.1]$$

in which n_b is the total number of bars. This rule has to be used when the data set is composed of a great number of observations (at least 50).

Aiming at selecting the best-fitting equation, a statistic analysis was applied evaluating the Kolmogorov-Smirnov test as suggested by [Vigneau et al., \(2000\)](#). This test compares the cumulative distribution of the raw data to the cumulative distribution fitted by the chosen model evaluating two parameters [[Justel et al., 1997](#)]: D^+ , the maximum distance of the empirical cumulative distribution function (CDF) above the fitted CDF and D^- , the maximum distance of the empirical cumulative distribution function (CDF) below the fitted CDF. The lower $KS D$ the better the fitting model. In the present work the best-fitting model was tested by applying the above mentioned criteria, and the lognormal model was found to be the simplest and the more suitable model to describe the obtained DSD.

For all samples analysed, the DSD frequency histograms were obtained by the microscope raw data: 3 photos were taken on 3 different samples after the dilution evaluating for each image the mean diameter and standard deviation derived from of the droplet size distribution.

2.3. Results and discussion

2.3.1. Droplet size distribution: choice of the best fitting model

The number-based frequency histogram in figure 2.3 is referred, as an example, to the sample E1_F150, but the same statistical analysis was performed for all samples. In this figure, the normal, the lognormal and the 3-parameters lognormal model are plotted together with the raw data. The results show a good accord with both the lognormal and 3-parameters lognormal models, while the normal model is not appropriate as can be noticed.

The same curve shape was found for the other samples. The plot reported in figure 2.3 shows in fact an unimodal (one peak) and polydisperse behaviour of the investigated sample (as can be deduced by the width of the distribution).

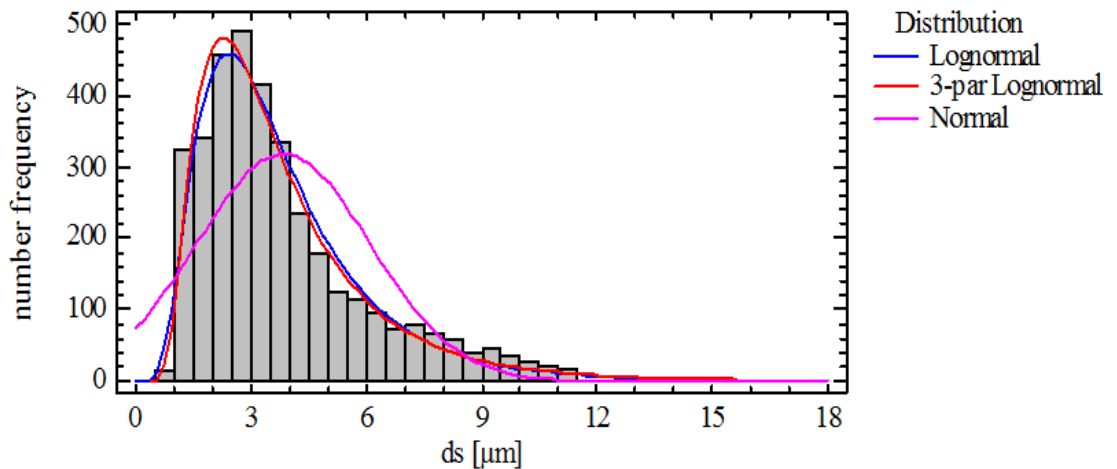


Figure 2.3: number frequency histogram for the sample E1_F150

The same characteristics were found for the other samples even at different mixing speed (corresponding to different specific powers of mixing) or increasing the energy input supplied to the samples.

The figure 2.4 summarises the results obtained comparing the DSD parameters (mean diameter and standard deviation) of the two models applied on the E1 set of samples. As can be seen, the mean diameter values (equations [2.1.12] and [2.1.15]) is not affected by the changing of the model, while the standard deviation curve shows a shift of the 3-parameters lognormal model with respect to the simple lognormal model slightly changing its shape. Even if the sample DSD can be modelled by both the equations (having very similar values of the $KS D$ parameter), and in some cases the equation [2.1.14] is the best fitting one, the simple lognormal model was chosen for its physical meaning that seems to be more appropriate for these kinds of distributions, as underlined by its widespread use in the literature [Hollingsworth and Johns, 2003; Clause et al. 2005; Melle et al., 2005; Egger and McGrath, 2006; Less et al., 2008].

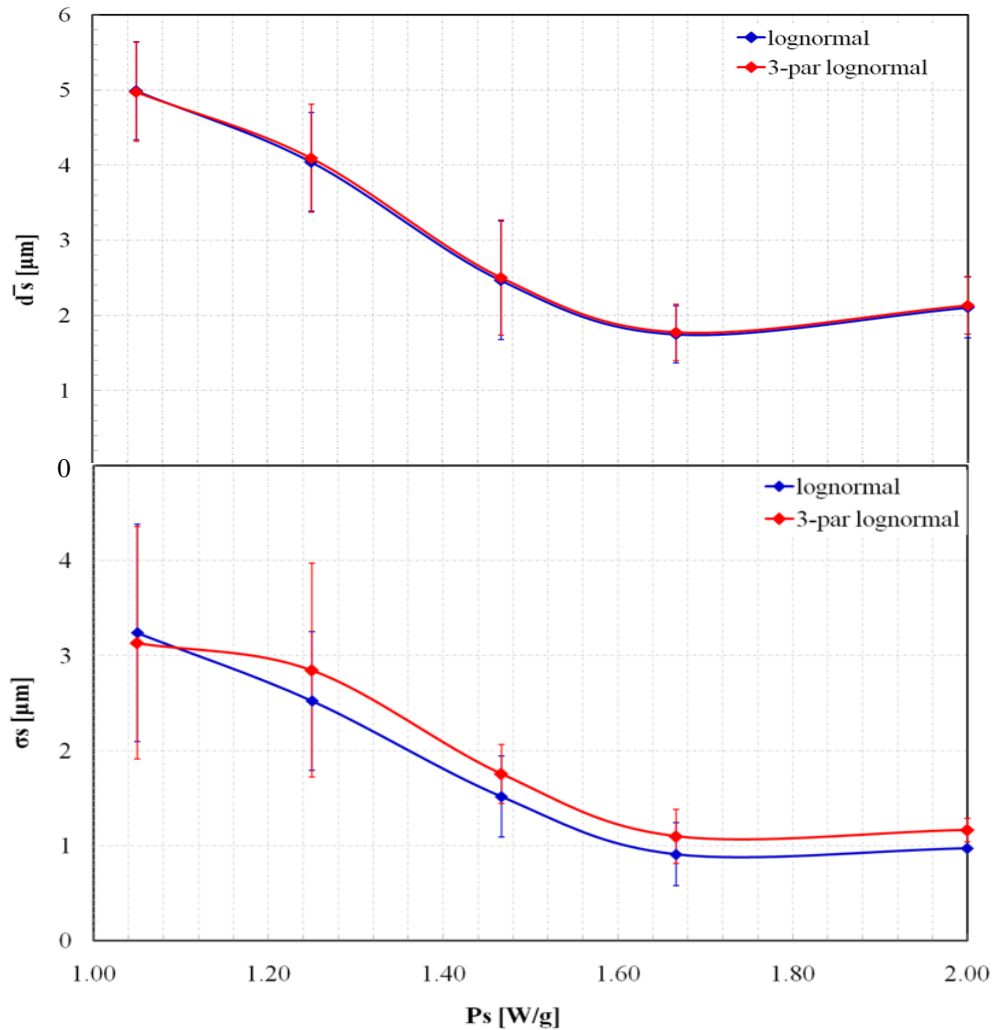


Figure 2.4: lognormal model parameters vs Specific Power

2.3.2. Droplet size distribution: physical meaning

A comparison of the mean diameters and the standard deviations values (from the lognormal model parameters) at different energy input values ($E_2 \cong 1.25 \cdot E_1$) is shown in figure 2.5. The reported plot shows that, at any constant energy value, low specific power input leads to a large mean droplet diameter and a broad distribution (high value of standard deviation). Increasing the power supplied to the system, the disruption of bigger droplets is favoured yielding to smaller mean droplet diameters and polydispersity.

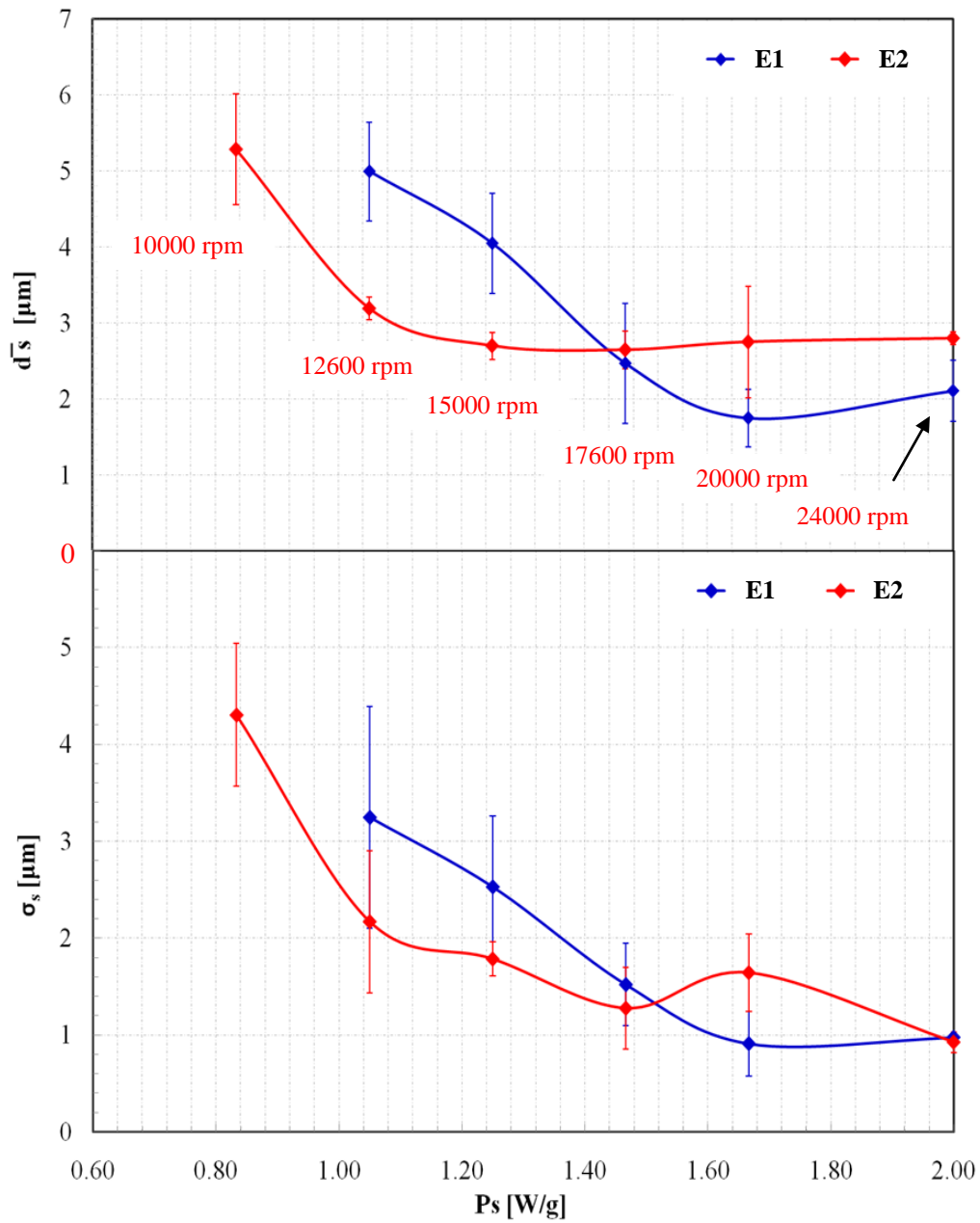


Figure 2.5: isoenergetic curves of lognormal model parameters

When increasing the specific input, a plateau value is encountered at a high power of mixing, 1.25 W/g for the E2 curve and about 1.7 W/g for the E1, confirming the results published by other authors [Maa and Hsu, 1996; Franco et al., 1998; Vankova et al., 2007]. Overcoming this threshold value, even if the specific power input is increased, there is not any further variation of the droplet diameter (even if the curve E1 seems to pass across a minimum value, the big error bar of the mean diameter values cannot justify any other conclusions). The same trend is encountered for the standard deviation curves, whose shape is very similar to those describing the mean droplet diameter behaviour.

Considering the energy of mixing, an interesting result was found comparing the two curves E1 and E2. The final DSD of any emulsion results from the equivalence of droplet disruption and coalescence rates [Al-Mulla & Gupta, 2000, Schubert and Engel, 2004]. At low specific power of mixing the energetic level E1 gives bigger DSD parameters with respect to the higher energetic level E2. Increasing the specific power of mixing at a constant energy level, an opposite behaviour is encountered, and a crossover of the two curves is shown. This phenomenon, described by Jafari et al. (2008), can be attributed to the “over-processing”, that is the increase in emulsion size by supplying more energy due to a high rate of re-coalescence of new droplets. It seems that the coalescence owing to the improved chance of droplet collisions prevails over the droplet disruption rate [Walstra, 1993].

The higher values of both the mean droplet diameters and standard deviations obtained at the lower power input justify the instability observed for these samples, that separated after a few hours after the preparation [Ahmed et al. 1999].

2.3.3. Rheological characterisation: viscosity

In order to consider whether deformation of the droplets in shear flow was significant or not, thereby influencing the analysis results, the equation proposed by Pal (1998) was used. The deformation of droplets can be calculated as:

$$E = \frac{5(19K+16)}{4(K+1)\sqrt{\left(\frac{20}{N_{Ca}}\right)^2+(19K)^2}} \quad [2.3.1]$$

where $K=\eta_d/\eta_c$ (η_d is the dispersed phase viscosity, and η_c the continuous phase viscosity), N_{Ca} is the Capillary number defined as $N_{Ca}=\eta_c R\dot{\gamma}/\sigma$ (R is the droplet radius, $\dot{\gamma}$ the shear rate and σ the interfacial tension). The deformation E is defined as

$$E = \frac{r_e-1}{r_e+1} \quad [2.3.2]$$

where r_e is the axis ratio L/B (L and B are the major and minor axes of the spheroidal droplet). From the application of the equation [2.3.1], E is evaluated, and then from the equation [2.3.2] the axis ratio can finally be calculated. For all the investigated samples over the entire imposed shear rate range, according to the model the smallness of deformation E value allowed the effects of deformation of mineral oil droplets to be neglected. In fact, for all the shear rate range, the parameter E varies from a minimum value of $5.2 \cdot 10^{-8}$ to a maximum of $6.0 \cdot 10^{-6}$ corresponding to N_{Ca} values of $4.4 \cdot 10^{-8}$ and $3.1 \cdot 10^{-6}$. Thus, flow curves were obtained avoiding any droplet deformation phenomenon.

An example of flow curve at different temperatures is reported below for the sample E1_F240.

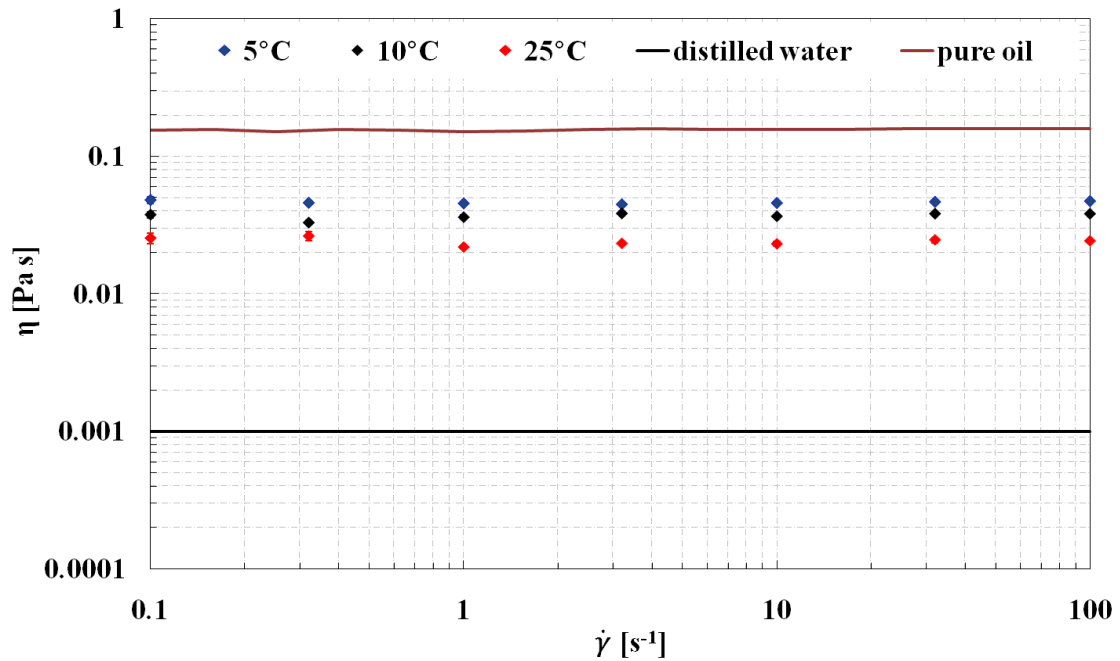


Figure 2.6: example of flow curve at different temperature for sample E1_F240

In the plot, the flow curve of pure paraffin oil (the same for all tests) and distilled water at 25°C are also reported, showing that the emulsions viscosity is always within the range defined by the two pure liquids also at a lower temperature improving the pipeline transportability of the biphasic system. Moreover, all the investigated samples exhibit a constant viscosity value at any imposed shear rates. It is worth noticing that, within the investigated O/W ratio, emulsions show an apparent newtonian behaviour when samples are fully emulsified [Pal, 2000, Romero et al., 2002]. On the contrary, at the same O/W ratio, a shear rate dependence should indicate an uncompleted emulsification leading to an “apparent” time dependent behaviour due to flow induced instability [Gabriele et al., 2009]. A decrease of viscosity with the increase of temperature is also evident: this confirms an already found behaviour [Yaghi and Al-Bemani, 2002].

For low values of specific power (i.e. E1_F126 and E2_F100) emulsions revealed a marked instability under shear. A comparison between the ‘direct’ and ‘inverse’ flow curves for sample E2_F100 at 25°C proposed in figure 2.7 confirms this experimental evidence.

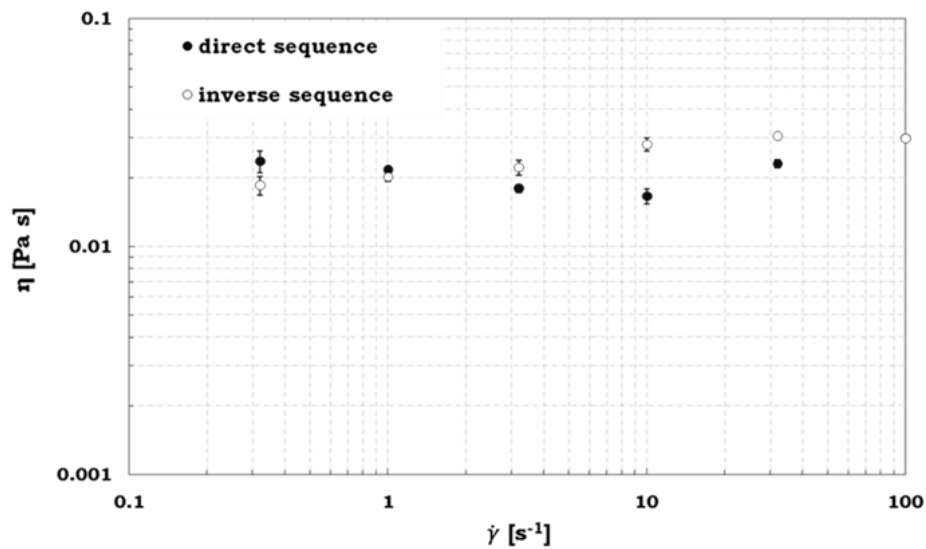


Figure 2.7: direct and inverse step rate test sequences for sample E2_F100: the difference between the direct and inverse sequence evidences the instability of the sample under the imposed shear rate conditions.

Exactly the same behaviour was found for the sample E1_F126.

Considering the apparent newtonian behaviour of all analysed samples, the “steady shear” viscosity was considered in order to compare the mechanical behaviour, as proposed in figure 2.8.

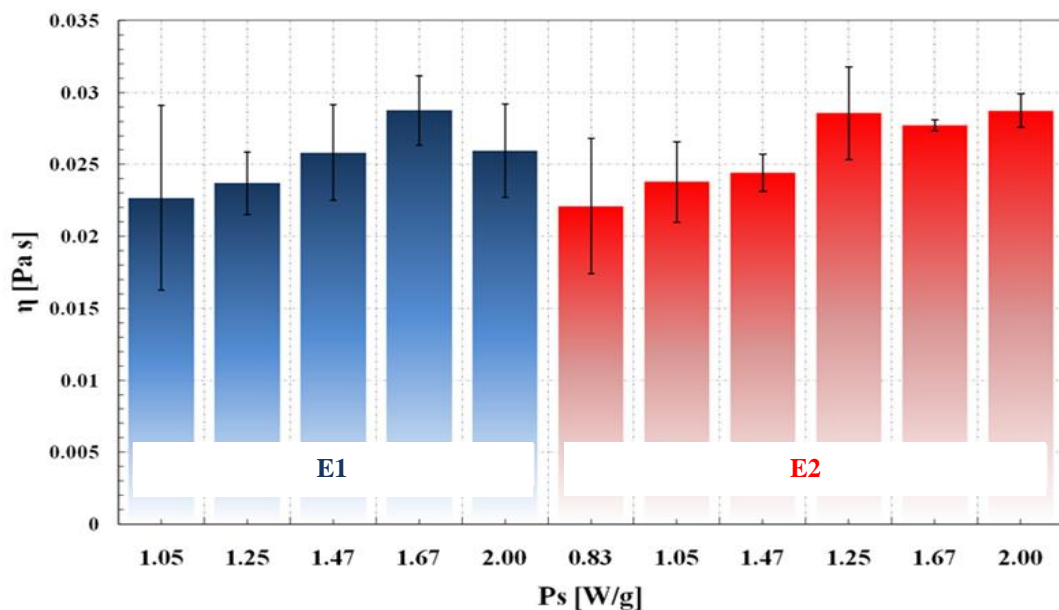


Figure 2.8: newtonian viscosities for all sample at 25°C

Despite a significant change in the DSD of the samples prepared at lower specific power, unstable, with respect to those stable prepared at higher specific power, viscosity values are all enclosed in a narrow range (from 0.022 Pa·s for the sample E2_F100, to 0.028 for the

sample E1_F200). The big error bars of the viscosities correspondent to the samples prepared at the lower power of mixing are justified by the high instability of the emulsions, as discusses before.

In figure 2.9 the relationship between the samples viscosities, the mean droplet diameters and the standard deviations are plotted.

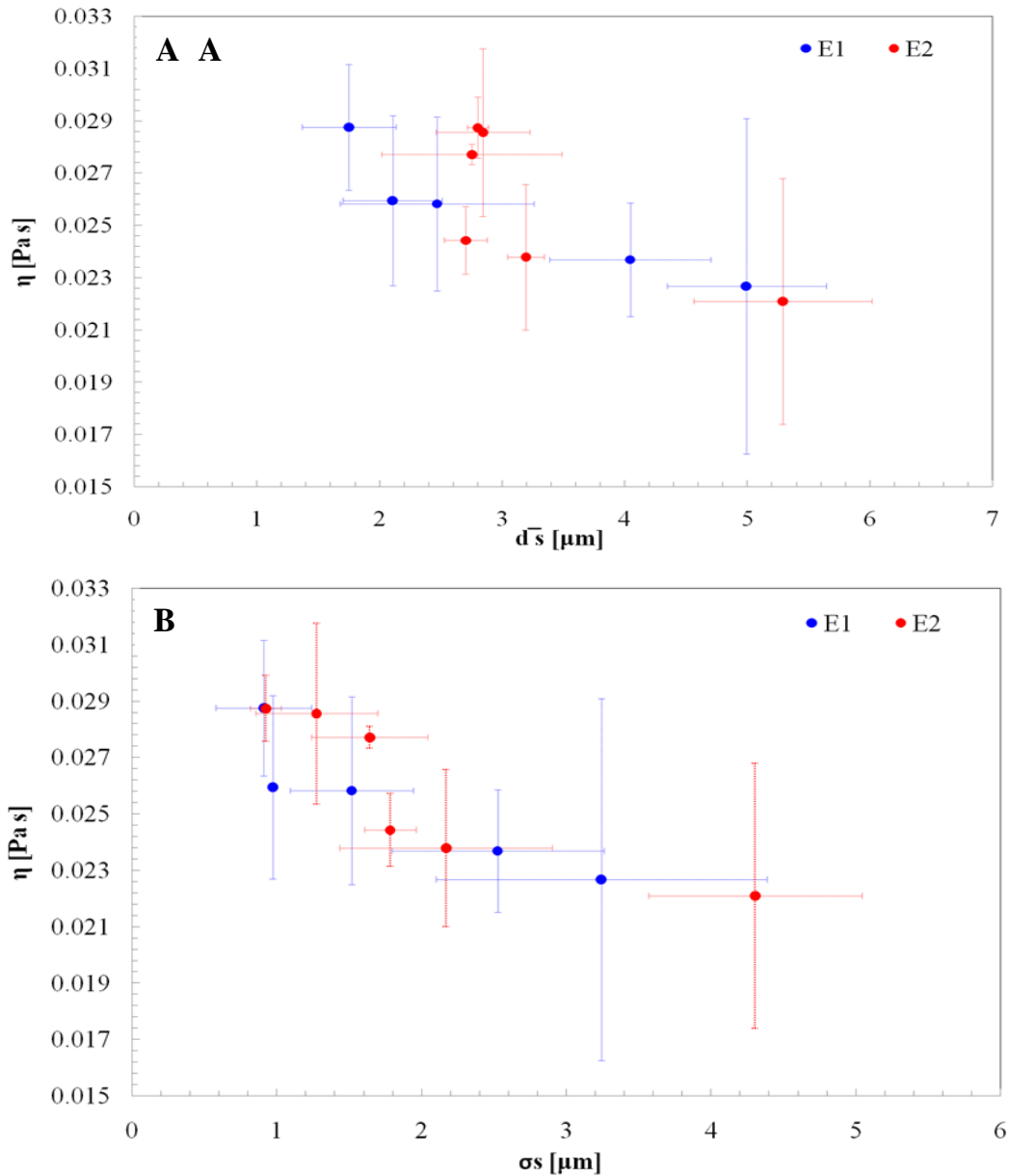


Figure 2.9: newtonian viscosities vs DSD parameters at 25°C

Drops of different dimensions allow a better dispersed phase packing and therefore viscosity decreases with the increase of polydispersity as reported in figure 2.9 A [Barnes, 2000]: moreover, it is well known that the viscosity increases if drop dimension decreases (figure 2.9 B) [Ford et al., 1997]. The same conclusions can be deduced for both the isoenergetic curves.

As can be observed by the plots shown above, a very important result is that the relationship between viscosity and DSD is independent of the energetic level.

Thus, the isoenergetic emulsification can be considered as an interesting aspect to be considered for producing emulsions at controlled stability, without excessively changing viscosity. This could be helpful in order to discriminate between the different phases of crude oil transportation, where a given emulsions stability is requested. In fact, as discussed before, the isoenergetic production of different samples can be performed at low or high specific powers of mixing: low specific power supplied yield low stable emulsions (big droplets lead to a fast coalescence), which could eventually separate during the pipeline transportation with serious technical and economical disadvantages.

On the contrary, a high excess of specific power supplied, can be avoided giving optimised processes from an economic, technical and environmental point of view. Thus, as shown by the reported results, after a certain threshold value a further increase of power does not change any longer the rheological and microscopic characteristics of the sample.

Conclusions

In the present work the emulsification of model oil-in-water emulsions has been studied in order to detect the influence of mixing speed, power and energy input on their rheological and microscopic properties. Emulsions were prepared by varying isoenergetically the specific power of mixing (P_s) in a rotor stator device, at two different energy levels. At a constant energy input, the specific power of mixing increase leads progressively to a DSD parameters decrease up to an invariance is reached, and a plateau region can be clearly individuated (starting from different points if we consider the two energy levels). A marked shear induced instability of emulsions prepared with low P_s has been found, and a progressive stabilisation has been obtained increasing the mixing speed (and the power of emulsification as a consequence). Moreover, an increase of energy of mixing corresponds to a decrease of the mean droplet diameter at low power input values, and an inversion of this behaviour has been found increasing the power supplied, owing to an over-processing effect. Finally, the relationship between viscosity and DSD is independent of the energetic level, and only slight viscosity changes have been found for all the investigated samples.

References

- Ahmed N. S., Nassar A. M., Zaki N. N., Gharieb H. K., (1999). *Formation of fluid heavy oil-in-water emulsions for pipeline transportation*, Fuel, 78, 593–600
- Al-Mulla, A., Gupta, R.K., (2000). *Droplet coalescence in the shear flow of model emulsions*, Rheologica Acta, 39, 20–25.
- Al-Roomi Y., George R., Elgibaly A., Elkamel A., (2004). *Use of a novel surfactant for improving the transportability/transportation of heavy/viscous crude oils*, Journal of Petroleum Science & Engineering 42, 235–243
- Babinsky E., Sojka P.E., (2002). *Modeling drop size distribution*, Progress in energy and combustion 28, 303–329
- Barnes H.A, (2000). *A handbook of elementary rheology*, The University of Wales, Institute of Non-newtonian Fluid Mechanics, Aberystwyth
- Bengochea C., Cordobés F., Guerrero A., (2006). *Rheology and microstructure of gluten and soya-based O/W emulsions*, Rheologica Acta 46, 13–21
- Clausse D., Gomez F., Pezron I., Komunjer L., Dalmazzone C., (2005). *Morphology characterization of emulsions by differential scanning calorimetry*, Advances in Colloid and Interface Science 117, 59 – 74
- Dehkissia S., Larachi F., Rodrigue D., Chornet E., (2004). *Characterization of Doba-Chad heavy crude oil in relation with the feasibility of pipeline transportation*, Fuel 83, 2157–2168
- Derkach S. R., (2009). *Rheology of emulsions*, Advances in Colloid and Interface Science, *in press*
- Egger H. and McGrath K.M., (2006). *Aging of oil-in-water emulsions: The role of the oil*, Journal of Colloid and Interface Science 299, 890–899
- Ford D.L, Borwankar R., Martin R.W.jr, Holcomb D.N., (1997). *Dressing and Sauces* in “Food emulsions” by S.E Friberg and K. Larsson, Marcel Dekker, Inc., New York, Basel

- Fournanty S., Guer Y., Le El Omari K., and Dejean J.-P., (2008). *Laminar flow emulsification process to control the viscosity reduction of heavy crude oils*, Journal of Dispersion Science and Technology, 29,1355–1366
- Franco J. M., Raymundo A., Sousa I., Gallegos C., (1998). *Influence of Processing Variables on the Rheological and Textural Properties of Lupin Protein-Stabilized Emulsions*, J. Agric. Food Chem., 46, 3109–3115
- Gabriele D., Migliori M., Lupi F.R., de Cindio B., (2009). *Rheological study of o/w concentrated model emulsions for heavy crude oil transportation*, Energy Sources, Part A: Recovery, Utilization, and Environmental Effects, *in press*.
- Goubault C., Pays K., Olea D., Gorria P., Bibette J., Schmitt V., Leal-Calderon F., (2001). *Shear rupturing of complex fluids: application to the preparation of quasi-monodisperse water-in-oil-in-water double emulsions*, Langmuir 17, 5184–5188
- Hénaut I., Courbaron A-C., Argillier J. F., (2009). *Viscosity of concentrated emulsions: relative effect of granulometry and multiphase morphology*, Petroleum Science and Technology 27, 182–196
- Hollingsworth K.G., Johns M.L., (2003). *Measurement of emulsion droplet sizes using PFG NMR and regularization methods*, Journal of Colloid and Interface Science 258, 383–389
- Jafari S. M., Assadpoor M., He Y., Bhandari B., (2008). *Review - Re-coalescence of emulsion droplets during high-energy emulsification*, Food Hydrocolloids 22, 1191–1202
- Justel A., Peña D., Zamar R., (1997). *A multivariate Kolmogorov-Smimov test of goodness of fit*, Statistics & Probability Letters 35, 251–259
- Less S., Hannisdal A., Bjørklund E., Sjöblom J., (2003). *Electrostatic destabilization of water-in-crude oil emulsions: Application to a real case and evaluation of the Aibel VIEC technology*, Fuel 87, 2572–2581
- Maa Y. F. and Hsu C., (1996). *Liquid-liquid emulsification by rotor/stator homogenization*, Journal of Controlled Release 38, 219–228

- Mabille C., Schmitt V., Gorria Ph., Leal Calderon F., Faye V., Deminière B., Bibette J., (2000). *Rheological and Shearing Conditions for the Preparation of Monodisperse Emulsions*, Langmuir, 16, 422–429
- McClements D.J., (1999). *Food Emulsions – Principles, Practice and Techniques*, CRC Press, New York, Chapter 7
- McClements D.J., (2002). *Theoretical prediction of emulsion color*, Advances in Colloid and Interface Science, 97, 63–89
- Melle S., Lask M., Fuller G. G., (2005). *Pickering Emulsions with Controllable Stability*, Langmuir 21, 2158–2162
- Nädler M., Mewes D., (1996). *Flow induced emulsification in the flow of two immiscible liquids in horizontal pipes*, Int. J. Multiphase Flow, Vol. 23 No. 1, pp. 55–68
- Ni X., Zhang Y., Mustafa I., (1998). *An investigation of droplet size and size distribution in methylmethacrylate suspensions in a batch oscillatory-baffled reactor*, Chemical Engineering Science, 53, 2903–2919
- Olesik J.W., Bates L.C., (1994). *Characterization of aerosols produced by pneumatic nebulizers for inductively coupled plasma sample introduction: effect of liquid and gas flow rates on volume based drop size distributions*, Spectrochimica Acta, 50B, 285–303
- Pal R., (1998). *A novel method to correlate emulsion viscosity data*, Colloids and Surfaces A: Physicochemical and Engineering Aspects, 137, 275–286
- Pal R., (2000). *Shear viscosity behaviour of emulsions of two immiscible liquids*, Journal of Colloids and Interface Science, 225, 359–366
- Peña A. A., Hirasaki G. J., (2003). *Enhanced characterization of oilfield emulsions via NMR diffusion and transverse relaxation experiments*, Advances in Colloid and Interface Science, 105, 103–150
- Quintana J.M., Califano A., and Zaritzky N., (2002). *Microstructure and stability of non-protein stabilized Oil-in-Water food emulsions measured by optical methods*, Journal Of Food Science, 67, 1130–1135

- Richter A., Voigt T., Ripperger S., (2007). *Ultrasonic attenuation spectroscopy of emulsions with droplet sizes greater than 10 μm* , Journal of Colloid and Interface Science 315, 482–492
- Romero N., Cárdenas A., Henríquez M., Rivas H., (2002). *Viscoelastic properties and stability of highly concentrated bitumen in water emulsions*, Colloids and Surfaces A, 204, 271–284
- Romero A., Cordobés F., Puppo M.C., Guerrero A., Bengoechea C., (2008). *Rheology and droplet size distribution of emulsions stabilized by crayfish flour*, Food Hydrocolloids 22, 1033–1043
- Saniere A., Hénaut I., Argillier J.F., (2004). *Pipeline Transportation of Heavy Oils, a Strategic, Economic and Technological Challenge*, Oil & Gas Science and Technology Rev. IFP, 59 (5), 455–465, Institute français du pétrole
- Schubert, H., Engel, R., (2004). *Product and formulation engineering of emulsions*, Trans IChemE, Part A, Chemical Engineering Research and Design, 82(A9), 1137–1143.
- Vankova N., Tcholakova S., Denkov N.D., Ivanov I.B., Vulchev V.D., Danner T., (2007). *Emulsification in turbulent flow I. Mean and maximum drop diameters in inertial and viscous regimes*, Journal of Colloid and Interface Science 312, 363–380
- Vigneau E., Loisel C., Devaux M.F., Cantoni P., (2000). *Number of particles for the determination of size distribution from microscopic images*, Powder Technology 107, 243–250
- Vladislavljević G. T., Schubert H., (2003). *Influence of process parameters on droplet size distribution in SPG membrane emulsification and stability of prepared emulsion droplets*, Journal of Membrane Science 225, 15–23
- Walpole R. E., Myers R. H., Myers S. L., Ye K., (2007). *Probability & Statistics for Engineers & Scientists – 8th edition*. Pearson Education International, Prentice Hall, USA
- Walstra P., (1993). *Principles of emulsions formation*, Chemical Engineering Science, 48, 333–349

Washington C., (1992). *Particle size analysis in pharmaceuticals and other industries*, Ellis Horwood Limited, England

Yaghi B. M., Al Bemani A., (2002). *Heavy crude oil viscosity reduction for pipeline transportation*, Energy Sources, 24, 93–102

Zaki N. N., (1997). *Surfactant stabilized crude oil-in-water emulsions for pipeline transportation of viscous crude oils*, Colloids and Surfaces A: Physicochemical and Engineering Aspects, 125, 19–25

Chapter 3 – Stability of concentrated O/W emulsions: a microscopic and rheological analysis

Abstract

Stability is an important characteristic for a great number of practical applications regarding emulsions. Concerning this, the stability of crude oil-in-water emulsions is a critical point for transportation along pipelines [Al-Roomi et al., 2004; Kokal, 2005]. In fact, the “ideal” emulsion should be stable under shear, guaranteeing a safe pumping step, but phase separation should be easily induced after the transportation, so ensuring oil-phase recovery. In the present work, two different emulsions stability tests were performed to separate the phases, aiming at comparing an accelerated method (by using the centrifugal force) to a ‘spontaneous’ long term test leaving the sample in a quiescent isothermal state. Two different oils (at different viscosity and density) and different volume fractions were used and rheological and microscopic characteristics were measured.

As a result of the treatment, a stratification of the samples was obtained with an upper “creamy layer” of concentrated emulsion (subjected to the tests) and a lower depleted water phase. The supernatant creamy layer exhibited a non-Newtonian behaviour and also a viscosity higher than the native oils, confirming the importance of the emulsion stability in crude oil transportation, where a very low viscosity sample, requested in conventional pipelines, may turn into a very viscous system [Gabriele et al., 2009]. The less dense and viscous oil showed a marked attitude to phase separation due to creaming effects enhanced by the centrifuged step, but a more significant Ostwald ripening phenomenon was observed in the case of emulsions prepared with the more viscous and dense oil. The same effect was found in the case of the long-term stability tests, where more polydisperse distributions of bigger droplets were found with respect to the centrifuged samples. A prevalent creaming effect justifies the increase of the samples viscosities in all cases.

3.1. Introduction

The term “emulsion stability” is widely used to describe the capability of an emulsion to maintain its properties with time. Depending on the emulsion droplet size, emulsions can

be divided into micro- (10–100 nm), mini- (nano-) (100–1000 nm), and macro-emulsions (0.5–100 μm) [Jafari et al., 2008]. In macro-emulsions, because of the large drop surface area, the high excess Gibbs energy cannot be compensated by entropy contributions as in micro-emulsions [Dukhin et al., 2006]. In fact, if we consider the case of a single big oil drop (assuming the same density of water) into a water volume, the free energy is given by:

$$G^i = G_O^i + G_W^i + G_I^i - TS_{config}^i \quad [3.1.1]$$

where the subscripts O , W , I refer to ‘oil’, ‘water’ and ‘interface’ respectively, T is the absolute temperature and S is the configurational entropy of the droplets in the system and the superscripts i refers to the initial state of the system. If the drop is broken into small ones, during emulsification, the final free energy is:

$$G^f = G_O^f + G_W^f + G_I^f - TS_{config}^f \quad [3.1.2]$$

where the superscripts f refers to the final state of the system.

The free energy of the bulk oil and water remains constant before and after homogenisation: $G_O^i = G_O^f$ and $G_W^i = G_W^f$ and the difference in free energy between the initial and final states is given by [McClements, 1999]:

$$\Delta G_{formation} = G^f - G^i = G_I^f - G_I^i - (TS_{config}^f - TS_{config}^i) = \Delta G_I - T\Delta S_{config} \quad [3.1.3]$$

By definition, the difference in interfacial free energy between the initial and final states (ΔG_I) is equal to the increase in surface area between the oil and aqueous phases (ΔA) multiplied by the interfacial tension ($\gamma_{O/W}$):

$$\Delta G_I = \gamma_{O/W} \Delta A \quad [3.1.4]$$

Hence [Ambrosone et al., 2007]

$$\Delta G_{formation} = \gamma_{O/W} \Delta A - T\Delta S_{config} \quad [3.1.5]$$

Therefore, the formation of an emulsion is always thermodynamically unfavorable, because of the increase in interfacial area after emulsification. It should be noticed that the term of configurational entropy can predominate on the interfacial free energy in emulsions in which the interfacial tension is extremely small and these systems, thermodynamically stable, are named *microemulsion* distinguished from thermodynamically unstable (macro)emulsion.

Emulsions stability has to be guaranteed for a wide number of applications: in the food industry, an emulsion has to maintain its aroma, texture and rheological characteristics for

the requested time (shelf life) [Robins, 2000; Mandala et al., 2004; Ambrosone et al., 2007], and also in the case of pharmaceutical [Masmoudi et al., 2006] and cosmetics products [Förster et al., 1998] a long stability (years) is requested. Another recent interesting application is the inclusion of crude oil in water as emulsion, aimed at crude transportation in pipelines [Saniere et al., 2004; Nädler and Mewes, 1997; Dehkissia et al., 2004]. The present work particularly focuses on the study of this application, being the main difference, with respect to other applications, that a de-emulsification is requested after the transportation, to recover the crude oil from the water. Therefore, the desired emulsion should be stable under shear and contemporarily it should be easy to break allowing the oil recovery.

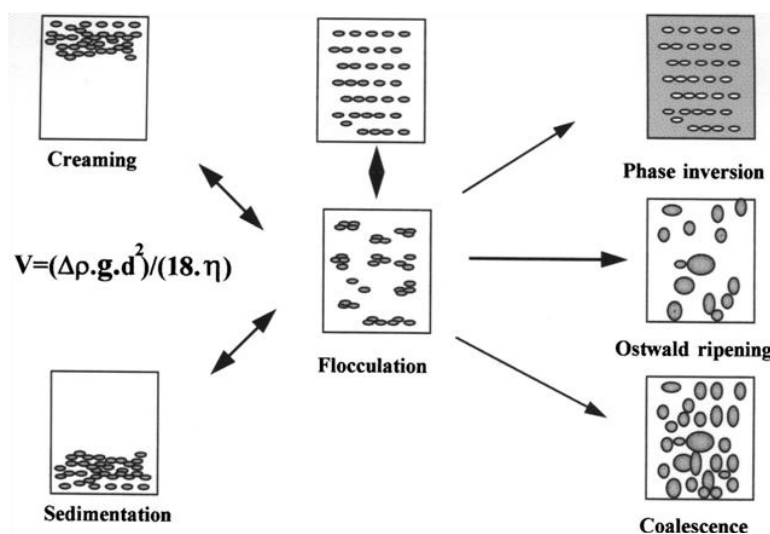


Figure 3.1: emulsions destabilisation mechanisms

Physical destabilisation mechanisms of emulsions (figure 3.1) include oil droplets size variation processes such as *coalescence* and *Ostwald ripening* and drop migration phenomena like *flocculation*, *sedimentation* and *creaming* [Imhof and Pine, 1997; Dukhin et al., 2006; Tadros, 2004].

Flocculation is a reversible instability phenomenon. It is the aggregation of droplets in form of flocs, and sometimes it can be followed by creaming or sedimentation according to the respective densities of the dispersed and continuous phases. Coalescence between two droplets can be spontaneous or stress-induced. Spontaneous coalescence is more probable when the emulsifier is not enough to guarantee droplets separation due to electrostatic repulsions, or when the adsorption kinetics of surface-active molecules at the interface is slow and does not protect it. Stress-induced coalescence, already discussed in the previous chapter of this PhD thesis, can be promoted by applying either compression or shear [Al-Mulla and Gupta, 2000]. Moreover, it is well known that the coalescence rate increases with increasing drop size, and polydispersity [Langevin et al., 2004]. Ostwald ripening is the process whereby

large droplets grow at the expense of small ones because of mass transport of dispersed phase from one droplet to another through the intervening continuous phase [McClements, 1999]. Considering a droplet of radius R dispersed in an immiscible liquid, the droplet internal pressure is P_i and the bulk pressure P_0 . The oil/water interfacial tension is $\gamma_{o/w}$ and the total energy of the system can be evaluated by the balance equation

$$G = \frac{4\pi R^3}{3}(P_0 - P_i) + 4\pi R^2\gamma_{o/w} \quad [3.1.6]$$

at the equilibrium conditions

$$\frac{dG}{dR} = 0 = 4\pi R^2(P_0 - P_i) + 8\pi R\gamma_{o/w} \quad [3.1.7]$$

from which the *Capillary pressure* elsewhere defined as *Laplace equation* can be calculated [Walstra, 1993]

$$(P_0 - P_i) = \frac{2\gamma_{o/w}}{R} \quad [3.1.8]$$

Equation [3.1.8] can be applied on spherical droplets, while in the case of irregularly shaped droplets (e.g. ellipsoids), two curvature radii R_1 and R_2 have to be considered:

$$(P_0 - P_i) = \gamma_{o/w} \left(\frac{1}{R_1} + \frac{1}{R_2} \right) \quad [3.1.9]$$

Thus, the mass transport is promoted by the pressure gradient, inversely to the droplet radii. This explains the Ostwald ripening phenomenon.

When there is a significant difference between the two phases densities, and the droplets are bigger than $1\mu\text{m}$ (for smaller droplets Brownian motions dominate the effects of gravity), they can settle down to the bottom of the vessel (sedimentation) or rise to the top (creaming), giving sample instability [Langevin et al., 2004]. The rate at which an isolated spherical particle creams in an ideal liquid is determined by a balance of forces. When a particle has a lower density than the surrounding liquid, an upward gravitational force acts upon it [McClements, 1999]:

$$V(\rho_d - \rho_c)g = \pi \frac{d^3}{6}(\rho_c - \rho_d)g \quad [3.1.10]$$

where d is the diameter and V the volume of the droplet, ρ_c and ρ_d are the continuous and the dispersed phase density respectively and g the gravitational constant. The particle motion is resisted by a hydrodynamic frictional force related to the solvent viscosity.

$$f_f = 3\pi\eta_c dv \quad [3.1.11]$$

where v is the creaming velocity and η_c the continuous phase viscosity. The particle reaches a constant velocity (Stokes equation [3.1.12]), where the forces due to gravity balance the downward force due to friction (i.e. $f_g=f_f$). Thus [Schramm, 2005]:

$$v_{Stokes} = \frac{gd^2(\rho_c-\rho_d)}{18\eta_c} \quad [3.1.12]$$

Centrifugal force, is proportional to the mass and the coefficient $\omega^2 R$, where ω is the angular velocity (rev. per sec.) and R is the distance of the particle from the axis of rotation. Thus, the driving force for creaming and sedimentation becomes

$$\pi \frac{d^3}{6} (\rho_c - \rho_d) \omega^2 R \quad [3.1.13]$$

and the terminal velocity [Schramm, 2005]:

$$v_{centr} = \frac{d^2}{18} \left(\frac{\rho_c - \rho_d}{\eta_c} \right) \omega^2 R \quad [3.1.14]$$

Many authors studied the forced destabilisation of emulsions, aiming at reproducing on a lab-scale the natural destabilisation of these systems. During ‘*bottle test*’, widely used in oil applications, different chemicals are added in an emulsion bottle to determine the effectiveness in breaking or separating an emulsion [Hurtevent et al., 2006]. In addition, different amounts of chemical can be added to bottle samples to evaluate the minimum amount required to efficiently break the emulsion. Auflem et al. (2001) studied the emulsions stability by using the bottle test for W/O emulsions homogenised with a Silverson L4RT emulsifier, and toluene as destabilising chemical for its affinity with resins and asphaltenes. For all experiments, the amount of toluene in the crude oil phase was varied. The separation was carried out in 100-ml sealed cylinder, and was monitored visually as volumes of water separated from the emulsion as a function of time.

Gafonova and Yarranton (2001) investigated the role of asphaltenes, resins and native solids such as sand, clay, silica, and organic particles in the stabilisation of W/O emulsions by measuring the water separated after heating and centrifugation steps as a function of time. They found that asphaltenes and native solids act as emulsion stabilisers while resins destabilise emulsions. Moreover, the asphaltenes appear to be adsorbed as a monolayer with interfacial configurations (or packing densities) that depend on the asphaltenes concentration. Kang et al. (2006) used phenol-formaldehyde resin polyoxyethylene and polyoxypropylene or

polyoxyethylene polyoxypropylene polymers as demulsifiers in bottle tests performed to breakup synthetic water in oil (W/O) crude oil emulsions.

In addition to these techniques, centrifugation is a diffused analysis for emulsions stability study. In fact, centrifugation is able to induce emulsions destabilisation by simply accelerating the natural process without any other external factor: when high centrifugal force is applied, the aqueous phase is separated from the emulsion and the oil globules come into close contact in distorted polyhedral shapes.

Owing to its simplicity, this stability analysis has been used for a long time. [Merrill \(1943\)](#) used centrifugation (1000, 3000 and 3600 rpm centrifuging time 100 minutes) to compare the stability properties of different soap emulsifiers varying the oil density (dispersed phase) and viscosity. [Hahn and Mittal \(1979\)](#) studied the destabilisation of emulsions prepared using three different non-ionic and anionic emulsifier by centrifugating, at 2000 rpm at room temperature, for a time ranging from 15 minutes to 3 h. The authors monitored the DSD in the creamy layer as a function of centrifugation time, finding that the creamy layer stratified with varying sizes of oil globules along the centrifuge axes. Moreover, they concluded that the droplets size reaches a plateau ("steady state" particle size), and subsequently the rate of oil separation decreases considerably, proportionally to the concentration emulsifier. [McLean and Kilpatrick \(1997\)](#) applied a modified stability test adding an heating and recentrifugation steps to the standard protocol: the standard stability protocol consists in centrifuging the emulsions for 30 minutes at 15000 rpm, while the modified protocol adds a heating step of 18h in a water bath followed by a recentrifugation. A more recent work was proposed by [Tcholakova et al. \(2004\)](#) on the destabilisation of protein stabilised emulsions determining the DSD by NMR tests. They compared the short-term stability, measured by centrifugation immediately after emulsion preparation, to long-term stability (after a shelf-storage up to 60 days). The authors concluded that there is no general relation between the emulsion stability and the changes in the mean drop diameter upon shelf-storage of protein emulsions. The higher short-term stability corresponds to higher long-term stability for emulsions stabilised by the same type of emulsifier. [Nour et al. \(2009\)](#) investigated the potential of centrifugation method in demulsification of O/W emulsions in order to extract oil without using chemicals. The centrifuged speed was varied from 6000 to 12000 rpm and the centrifugation time was varied from 30 to 105 min.

The stability of model O/W emulsions, simulating an emulsified crude oil system for pipeline transportation, was investigated by modifying the procedure proposed by [Gafonova and Yarranton \(2001\)](#). The majority of the open literature works deal with W/O emulsions

destabilisation as an interesting issue to recover crude oil from water after oil spill tragedies. Nevertheless, it is also important to study the emulsions stability in the case of crude oil transportation in pipelines, where, owing to phase instability issues, a low viscosity O/W system may turn into a very viscous one leading, at worst, to the transportation process shutdown. Therefore, the aim of the present work is the rheological and microscopic analysis of the destabilisation of O/W model emulsions by centrifugation with short-term stability test (STSTs). A comparison was made between the characteristics of the upper creamy layer found after the centrifugation steps to the ones of the layer obtained leaving the same samples in a quiescent state (long-term stability tests, LTSTs). The effect of oil viscosity and density, and the dispersed phase volume fraction on the system stability were investigated in detail. In fact, different crude oils have different physical properties that may enhance the destabilisation of the emulsions where they are dispersed.

3.2. Materials and Methods

O/W model emulsions were prepared using distilled water and two different commercial paraffin oil, Finavestan A360B (Total, France) and Arum HT 220 (Agip, Italy): the physical characteristics of both the oils are reported in table 3.1. The surface tensions σ and the oil/water interfacial tensions $\gamma_{o/w}^E$ were measured by using a drop-shape-analysis of pendant drops of emulsifier-in-water solution immersed in oil, using a FTA 200 (USA) pendant drop equipped with a completely automatic image analysis software (FTA 32 Video 2.0, USA).

Oil	μ [Pa s]	ρ [kg/m ³]	σ [mN/m]	$\gamma_{o/w}^E$ [mN/m]
Finav. A360B	0.157 ± 0.002	0.864 ± 0.011	35.08 ± 0.69	10.10 ± 0.20
Arum HT 220	0.596 ± 0.012	0.974 ± 0.012	29.63 ± 0.14	6.82 ± 0.11

Table 3.1: physical properties of oils at 25°C

The nonionic hydrophilic emulsifier was Tween 60 (polyoxyethylenesorbitan monostereate, HLB 14.9, gives O/W emulsions) purchased from Sigma Aldrich (Italy). Different samples (a total amount of 200 g) were prepared by varying the oil/water ratio and the oil type, without changing the emulsifier amount (2_{w/w}% based on the total weight of the mixture). Emulsions were prepared by the agent-in-water method [Yaghi and Al-Bemani, 2002], dissolving and stirring the emulsifier in water at 70°C using a magnetic-heater agitator (Heating Magnetic Stirred, Velp Scientific, Italy). After the emulsifier addition, the solution was stirred for 5 minutes. The oil was, then, slowly dropped to the water phase and the homogenisation phase took place for 10 minutes, using a mixing device able to provide an output power of

approximately 300 Watts (blender ‘Minipimer’ Braun, Germany). The geometrical characteristics of the mixing device head are shown in figure 3.2. After preparation, all samples were stored at room temperature for a rest time of 3 h.

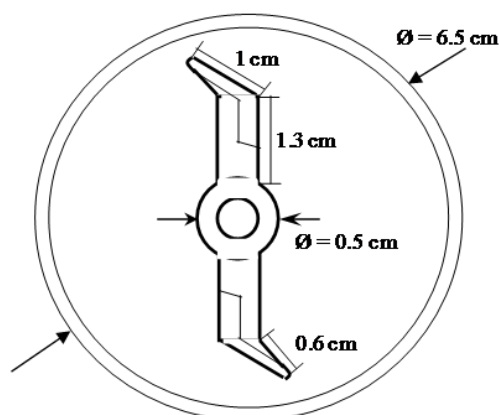


Figure 3.2: sketch of blade mixer configuration

The fresh samples were subjected to a forced destabilisation under centrifugation (STSTs) or left in a quiescent state (LTSTs) allowing them to be naturally destabilised.

For each sample, both for the original (control) and the destabilised ones, rheological and microscopic analysis were performed. The emulsions destabilisation caused the formation of a creamy concentrated-in-oil layer, on which all the tests were executed (figure 3.3). Moreover, the volumetric concentration of oil in the upper creamy layer was evaluated in order to analyse its effects on the rheological and microscopic characteristics of the emulsions. The control samples (freshly prepared and not yet destabilised) are listed in table 3.2: they are all labelled with the post-fix ‘*ref*’ in the following results discussion.

Sample ID	Oil volume [%]	Oil type
F_50_ref	50	Finavestan A360B
F_60_ref	60	Finavestan A360B
A_50_ref	50	Arum HT 220
A_60_ref	60	Arum HT 220

Table 3.2: *ref*-samples identification

In the STSTs, *ref* samples were centrifugated once at 2000 rpm for 10 minutes (centrifuge Eppendorf 5810, Germany) alternated by 1 hour of rest time. In the following part of the present work, these samples will be labelled as ‘*X_YZ_1_C*’, where *X* will be ‘*F*’ or ‘*A*’ whether the used oil is Finavestan A 360 B or Arum HT 220 respectively, *YZ* will be ‘50’ or ‘60’ whether the oil volume fraction is 0.5 or 0.6. After the rest time (1 hour) a second centrifugation was performed (label ‘*X_YZ_2_C*’) and the same protocol was applied for the

third centrifugation step (label 'X_YZ_3_C'). The post-fix 'C' indicates the Centrifuge procedure.

The LTSTs were performed leaving in a quiescent state the sample at a constant temperature of 5°C for 15 days (label 'X_YZ_15_d' in the result discussion).

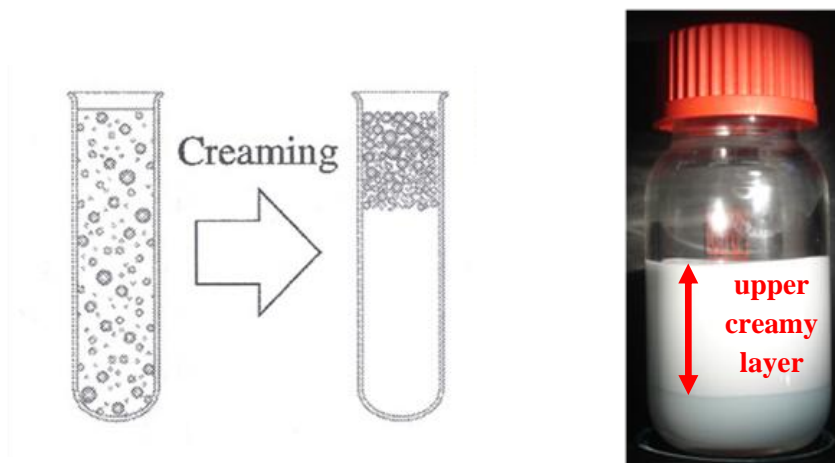


Figure 3.3: formation of a creamy layer due to the density difference between the oil and water phases.

3.2.1. Rheological characterisation

Viscosity was measured as a function of shear rate (flow curves) at a constant temperature, by averaging the step rate tests results performed at fixed shear rate values. The 'step rate test' investigates the transient behaviour of the sample at a fixed (and imposed) shear rate. All tests were performed for 60s, and revealed that steady state viscosity was reached after 10s from the beginning of the test for any of the investigated samples. Therefore, the viscosity value at any shear rate was obtained by averaging the step rate tests data corresponding to the range 10 – 60s.

Rheological tests were done by using a controlled strain rheometer ARES-RFS (TA instrument, USA) equipped with a parallel plate geometry ($\Phi = 50$ mm, gap 1.5 mm). The shear rate range was $0.1-100 \text{ s}^{-1}$ except when a higher limit (at least 1 s^{-1}) was necessary to measure torque values within the instrument range (from 10^{-7} Nm to 0.1 Nm).

All tests were performed at 25°C; in the case of the LTSTs, all samples were analysed after the rest time requested to reach the temperature of 25°C from the storage one (about 4°C).

When a linear trend of viscosity η versus shear rate $\dot{\gamma}$ in a log-log plot was found, a "power law" model was used [Barnes et al., 1989]:

$$\eta = k \cdot \dot{\gamma}^{n-1} \quad [3.2.1]$$

where k and n are consistency and flow indices respectively. k is equal to viscosity value at 1 s^{-1} , n can be calculated as the slope of the curve and its value is always positive and lower than one in the case of shear thinning materials. From a physical point of view, the lower is the n value the higher is the curve slope, indicating a great tendency to in-flow destructuration (sharp decrease of viscosity when increasing shear rate).

3.2.2. Microscopic characterisation: DSD

The morphology of the emulsion droplets was observed with a contrast phase microscopy (MX5000, MEIJI, Japan) equipped with phase contrast objective 40X and 100X. In order to produce photomicrographs without droplets aggregates, difficult to be analysed, samples were diluted in distilled water. The effects of dilution on DSD characterisation were preliminarily tested, and the results showing that the analysis is not affected by the dilution are presented in the following paragraph.

All samples were inserted onto a glass slide inside a cover imaging chamber (Sigma, Italy) on which a cover slide was placed. An image database software was used to detect the different droplet sizes (*dhs* image database, Germany) by greyscale detection (see the previous chapter for a more detailed description) giving as a result the number-based surface equivalent diameter. Oil immersion objective was used in the case of 100X magnification. The DSD was interpreted by the lognormal model [Hollingsworth and Johns, 2003; Clause et al. 2005; Melle et al., 2005; Egger and McGrath, 2006; Less et al., 2008] reported in the equation 3.2.2.

$$f(d) = \frac{1}{d \cdot \sigma_{ln} \cdot \sqrt{2\pi}} \exp \left[\frac{-(\ln d - \bar{d}_g)^2}{2\sigma_{ln}^2} \right] \quad [3.2.2]$$

where \bar{d}_g and σ_{ln} (the geometrical mean droplet diameter and the standard deviation respectively) are the model parameters. A mean diameter \bar{d}_s and variance σ_s^2 can be derived from the model parameters by applying the following rules [Walpole et al. 2007]:

$$\bar{d}_s = e^{\bar{d}_g + \sigma_{ln}^2 / 2} \quad [3.2.3]$$

$$\sigma_s^2 = e^{2\bar{d}_g + \sigma_{ln}^2} (e^{\sigma_{ln}^2} - 1) \quad [3.2.4]$$

The square root of the variance is the standard deviation σ_s , and it is commonly considered as an index of polydispersity. The raw data were analysed with Excel 2007 (USA) and with the statistic software Statgraphics Centurion XV, version 15.2.13, (USA).

3.2.3. Oil extraction procedure

In order to measure the oil amount in the upper creamy layer of emulsion after the destabilisation, a solvent-extraction technique with petroleum ether was used.

10 ml of emulsion sample was poured in a round-bottomed flask filled up to 500 ml with distilled water. The sample was then diluted 50 times. 100 ml of this diluted emulsion was poured in a 250 ml separating funnel (Schott Duran, Germany). 80 ml of petroleum ether (Fluka, Switzerland) was then added, and the stratification of the sample took place. The separated aqueous phase was removed and the supernatant was put into a 250 ml Erlenmeyer flask (Schott Duran, Germany) with a small quantity of anhydrous sodium sulphate (Sigma Aldrich, Italy) in order to eliminate any water. The petroleum ether was then added in two steps (50 ml the first and 30 ml the second one) in order to guarantee the total recovery of the oily phase. The extract was then decanted in the perfectly clean flask through a paper filter (adding more anhydrous sodium sulphate). Finally, the petroleum ether was evaporated in a rotary evaporator (Buchi 011, Italy) and then the flask was completely dried in an oven in order to evaporate any petroleum ether residual. The flask was then weighed and the total amount of oil was calculated by difference.

3.3. Results and discussion

3.3.1. Dilution effect on the DSD results

Aiming at evaluating the emulsion dilution effects on the DSD, some preliminary tests were performed on the sample *A_60_ref*. The fresh sample was diluted in distilled water with a volumetric ratio of 1:5 and 1:10. A comparison between the lognormal model obtained by fitting the DSD histograms of the three samples is reported in figure 3.4.

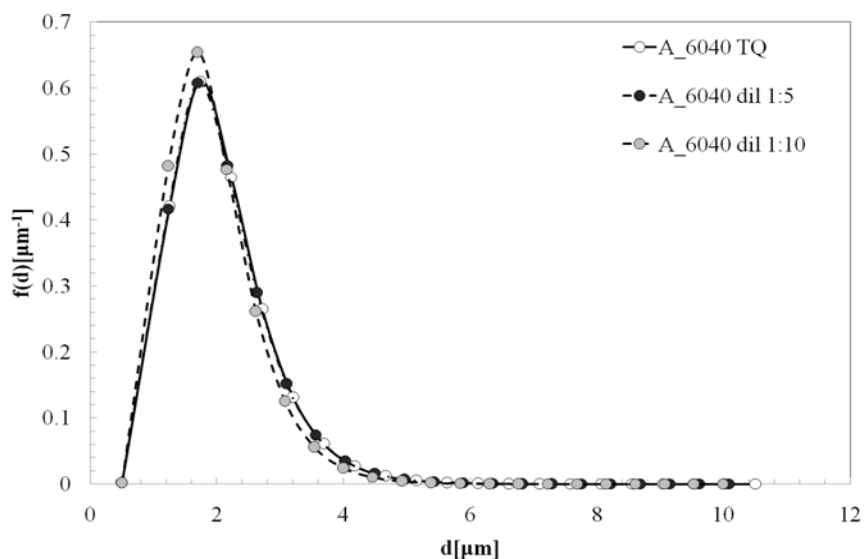


Figure 3.4: lognormal model obtained by the DSD of sample *A_60_ref* with and without dilution

It can be noticed that the dilution of the sample does not affect its DSD. The centrifugation concentrates the emulsions in the upper creamy layer of the batch, therefore all samples were diluted with a volumetric ratio of 1:10 in order to obtain suitable photomicrographs without droplets aggregates that could be interpreted as a single big drop by the imaging software.

3.3.2. STSTs: effect of oil characteristics

The effect of the different properties of the two oils on the rheological and microscopic characteristics of emulsions was investigated. Samples *F_50_ref* and *A_50_ref* were prepared with an equal oily phase volume fraction having different viscosities and densities. The number-based mean diameter and the standard deviation obtained from the lognormal model are reported in figure 3.5.

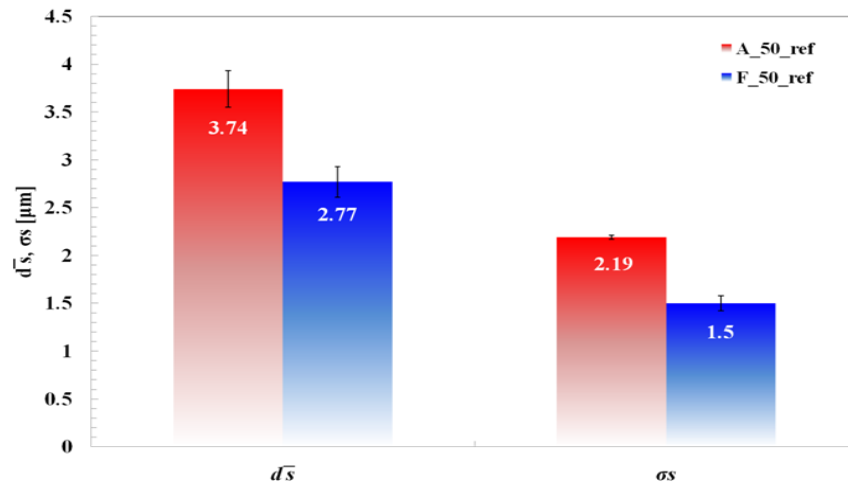


Figure 3.5: effect of oil characteristics on fresh samples DSD parameters

As shown, different oils produce emulsions with different DSDs. In particular the sample produced with Arum HT 220 is characterised by bigger and more polydisperse droplets with respect to the emulsion prepared with the less viscous oil. Both the emulsions were produced with the same homogenisation conditions, thus, an increase in the specific energy should be required to produce emulsions with a higher viscosity of the continuous phase in order to obtain a similar DSD [Romero et al., 2008]. The drop size broadly distributed, allows a better dispersed phase packing and a lower viscosity as a consequence [Barnes, 2000] and moreover, the viscosity increases when the mean drop size decreases [Ford et al., 1997].

Thus, the parameters of figure 3.5 justify the slightly lower viscosity value of the emulsions *A_50_ref* compared with *F_50_ref* as reported in figure 3.6.

As already found in the previous chapter of the thesis, emulsions show an apparent Newtonian behaviour within the investigated O/W ratio [Pal, 2000 a; Romero et al., 2002]. Thus, it is worthy noticing that the DSD affects the rheological behaviour of the sample more than the raw materials viscosity [Pal, 1998].

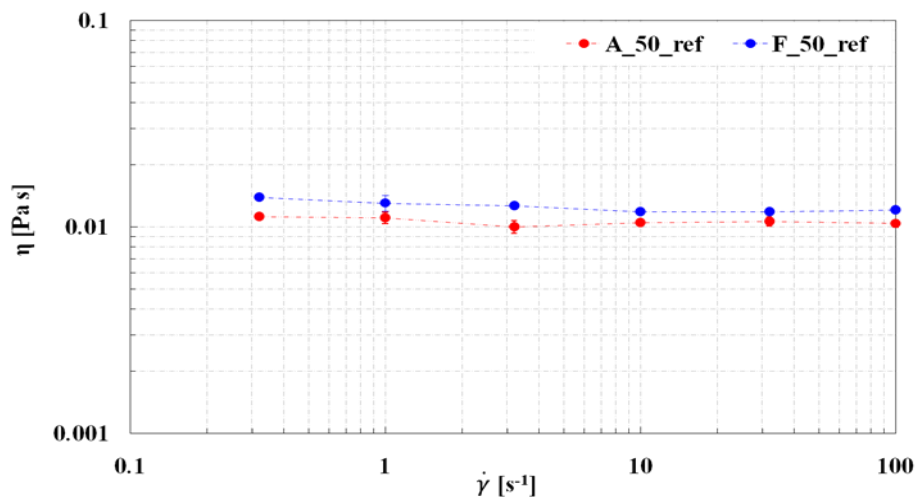


Figure 3.6: effect of oil characteristics on fresh samples viscosities

As far as DSDs results is concerned, after any centrifugations the samples produced with *Arum HT 220* always led to bigger and broadly distributed droplets with respect to *Finavestan A360B*. The mean droplet diameters and the standard deviations of centrifuged samples are shown in figure 3.7.

It can be observed, for both the samples the mean droplets diameter \bar{d}_s is less affected by centrifugation than standard deviation, which continues to increase up to the second step.

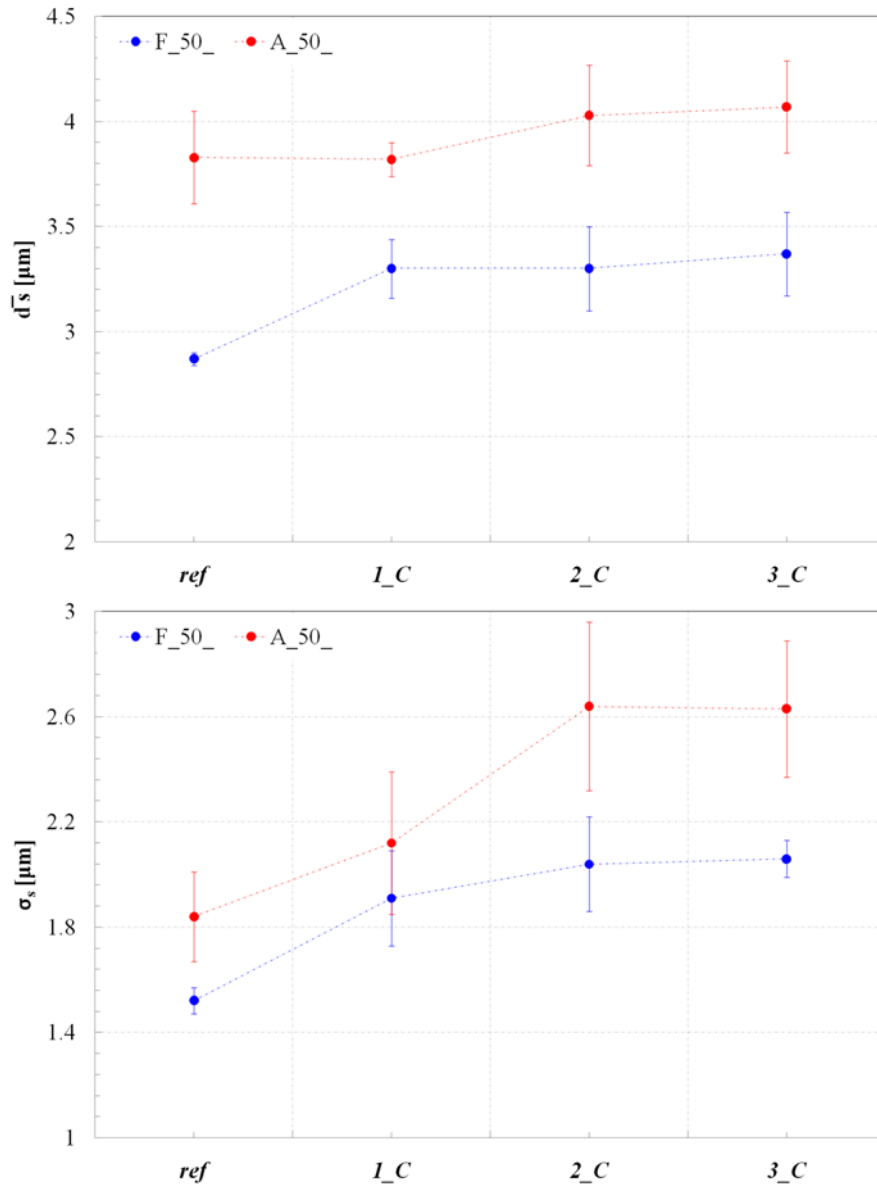


Figure 3.7: a comparison between samples F_50_ and A_50_ for the short term stability test

The observed DSD parameters changes, are due to the Ostwald ripening effect. In fact, the small droplets are “included” in the large ones (numerically fewer in any lognormal DSD, and, as a consequence less important in the final evaluation of the DSD number-based parameters) allowing a small increase in mean droplet diameter, and, furthermore increasing

the standard deviation. Thus, it can be deduced that standard deviation is affected by Ostwald ripening phenomenon more than mean droplet diameter. This phenomenon can be better understood with the scheme sketched in figure 3.8.

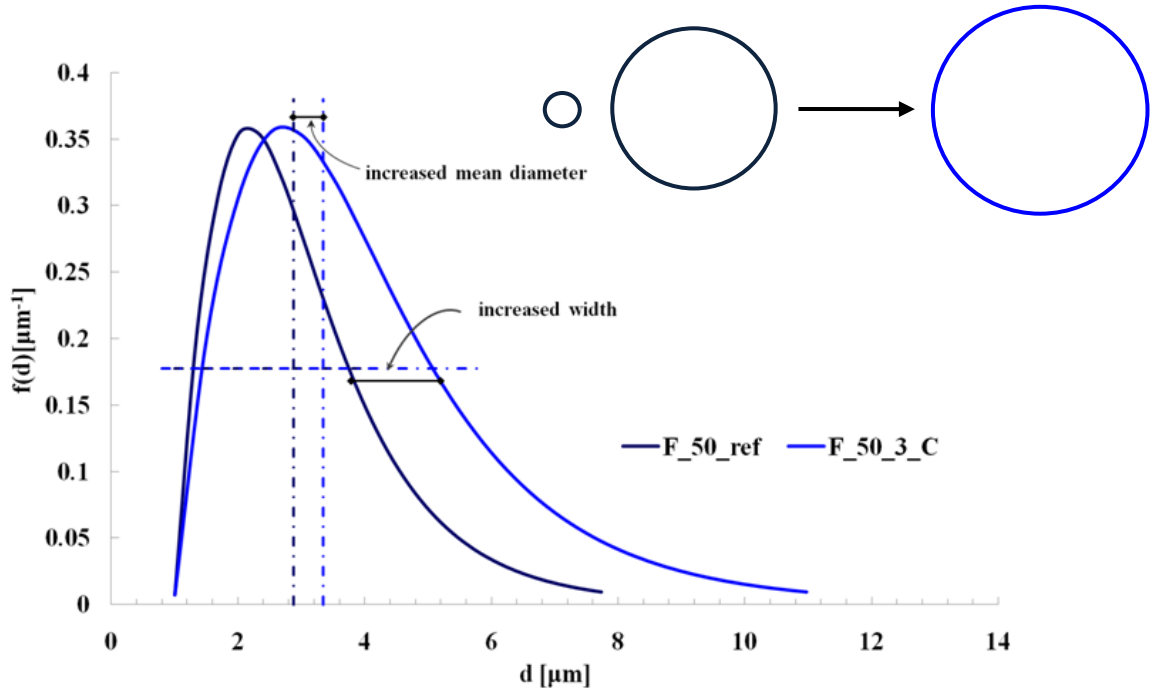


Figure 3.8: Ostwald ripening phenomenon scheme and its effects on the number-based parameters of a lognormal distribution for sample *F_50_ref* and after the 3rd centrifugation

From figure 3.7 it can be noticed that the polydispersity increase is more significant for *Arum HT 200*-based emulsions, as evidenced by the standard deviation curves. In fact the increase for the emulsion prepared with oil Finavestan A360B is about 36%, with respect to about 43% for samples prepared with *Arum HT 220*. This conditions were detected also increasing the oily phase volumetric fraction in the fresh sample.

Thus, because \bar{d}_s exhibits a reduced variation, it can be concluded that the Ostwald ripening effect is more significant for the emulsions produced with the more dense and viscous oil.

As for the flow behaviour of the samples, flow curves at each destabilisation step are reported in figure 3.9. After the first centrifugation a significant increase in viscosity (higher than the starting oil viscosity in all the investigated shear rate range) was observed together with a marked shear thinning behaviour. This is due to the effect of droplets concentration on the viscosity of concentrated emulsions, also related to the maximum packing fraction [Barnes, 2000; Derkach, 2009]. In fact, it is well known that suspensions (of hard spheres) have a maximum packing fraction close to 0.63, while monodisperse emulsions of deformable droplets can reach a maximum packing fraction of 0.74 [Barnes et al., 1989] for hexagonally

packed droplets, the value of 0.84 can be reached in the case of polydisperse emulsions where small droplets can fill the empty spaces among the large ones [Aomari et al., 1998]. Viscosity exhibits a significant increase and can show a shear thinning behaviour when the actual packing fraction is close to the maximum one [Barnes, 2000; Pal, 2000, b]. Therefore, the water depletion concentrates the dispersed phase allowing this threshold value to be approached.

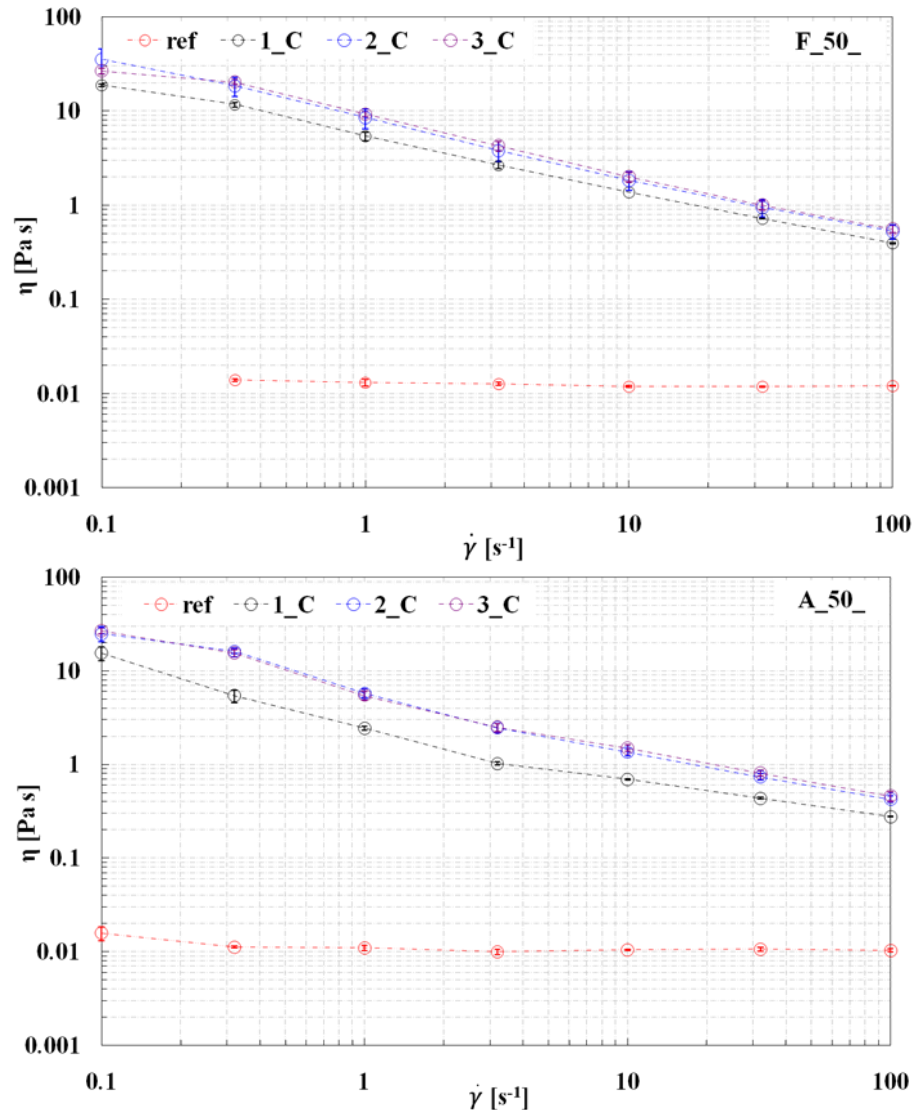


Figure 3.9: flow curves of short-term stability tests at each centrifugation; after the first centrifugation the increased concentration of the dispersed phase in the upper creamy layer leads the emulsions to behave as a power law shear thinning fluid

Moreover, for both the samples the most significant variations in the flow curve can be encountered just up to the second centrifugation, confirming the DSD parameters results

(figure 3.7). A comparison between parameters k and n of the power law model (eq. [3.2.1]) used to fit the centrifuged samples flow curves data is reported in figure 3.10.

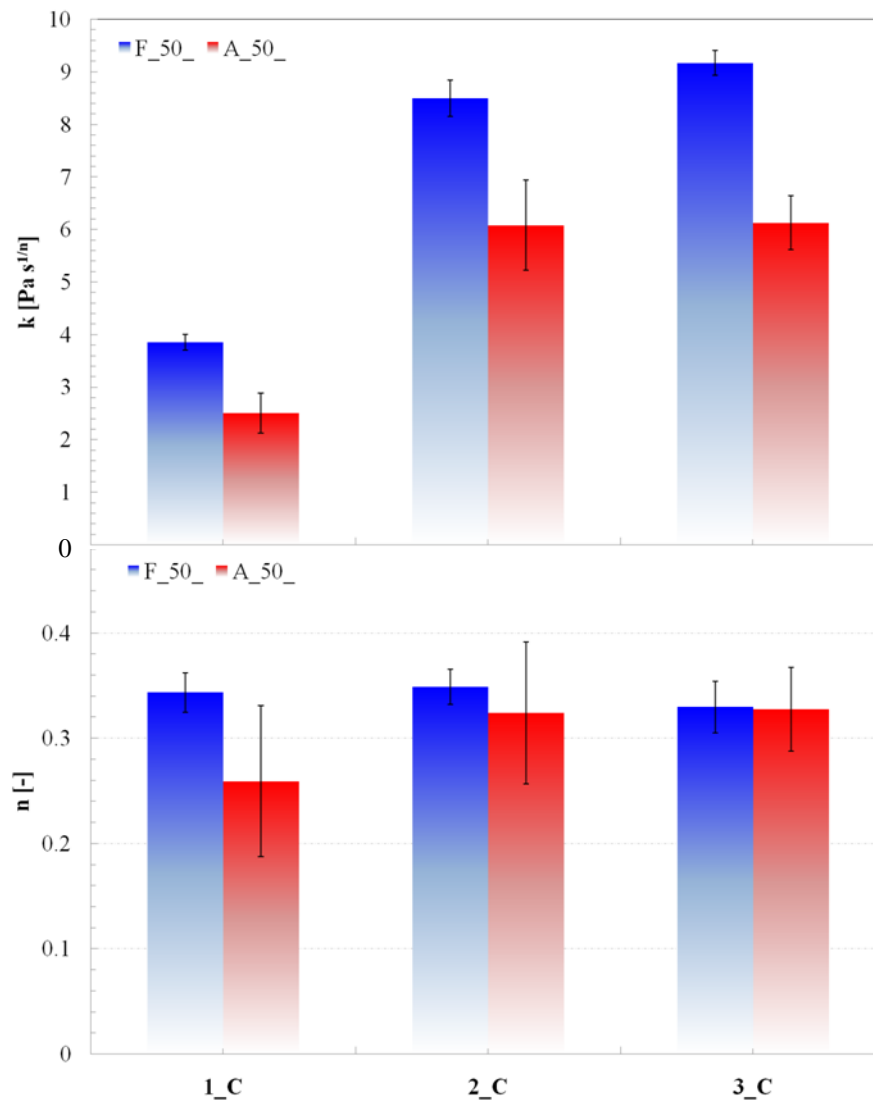


Figure 3.10: k and n parameter of the power-law model for samples A_50_ and F_50_

As expected, owing to creaming, a significant increase in k is encountered when progressing with centrifugation, whilst a less evident effect is found on the flow index parameter. When analysing the effect of centrifugation/destabilisation on samples viscosity, the water loss during separation has to be taken into account together with DSD changes. In fact, if only the changes in the mean droplet size and standard deviation should be considered, a little decrease in the viscosity value should be expected. Moreover, as shown in the 2nd chapter of the present PhD thesis, small variations of the viscosity may correspond to significant changes in DSD. Therefore, it is clear that the viscosity changes are mostly due to the water depletion under the action of the centrifugal force (creaming effect), and, considering the slight

variations of the DSD parameters, the Ostwald ripening can be neglected. In order to confirm this assumption, the oil fraction in the concentrated creamy layer was measured (figure 3.10).

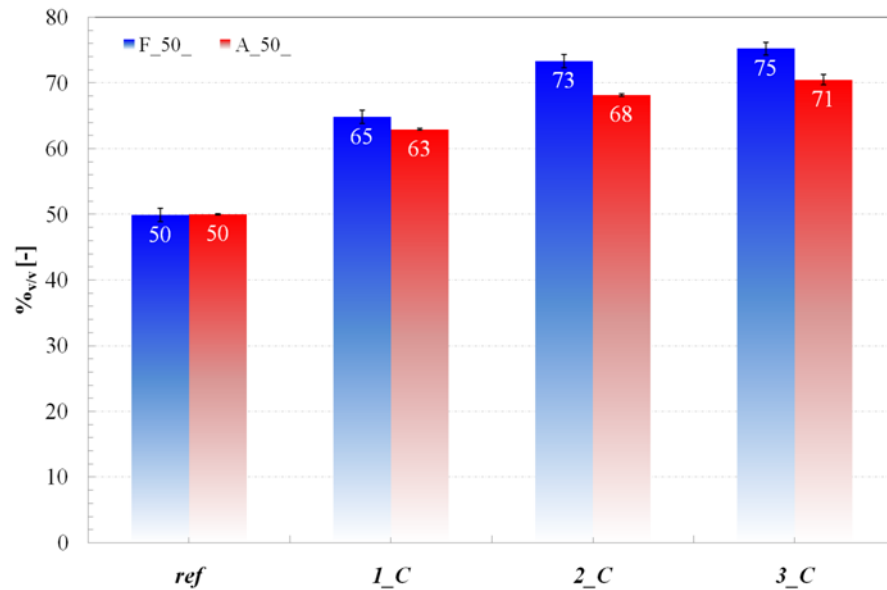


Figure 3.10: oil volumetric percentage in the creamy layer for samples A_50_ and F_50_: a plateau is reached after the second centrifugation

It appears that water depletion takes place less for the emulsions prepared with the more dense and viscous oil (samples A_50_): if equation [3.1.13] is considered, the driving force for centrifugation accounts for the difference between the continuous and the dispersed phase densities and the more viscous the oil, the less effective will be the centrifugation. Thus, from the proposed results it is clear that the effect of oil characteristics on emulsions stability can be split into two cases: if creaming is considered, emulsions prepared with the less viscous and dense oil are less stable and water depletion is more evident, even from a rheological point of view (an increase in samples viscosity is encountered). On the contrary if the Ostwald ripening phenomenon is analysed, the more viscous and dense oil produces less stable emulsions giving bigger and more polydisperse droplets.

3.3.3. STSTs: effect of oil fraction

The effect on the system destabilisation of the increased oily phase volume fraction without changing the total amount of emulsifier was analysed. The mean drop diameter and the standard deviation of the lognormal distribution model for the sample F_60_ compared with the same samples produced with a lower oil fraction are reported in figure 3.11.

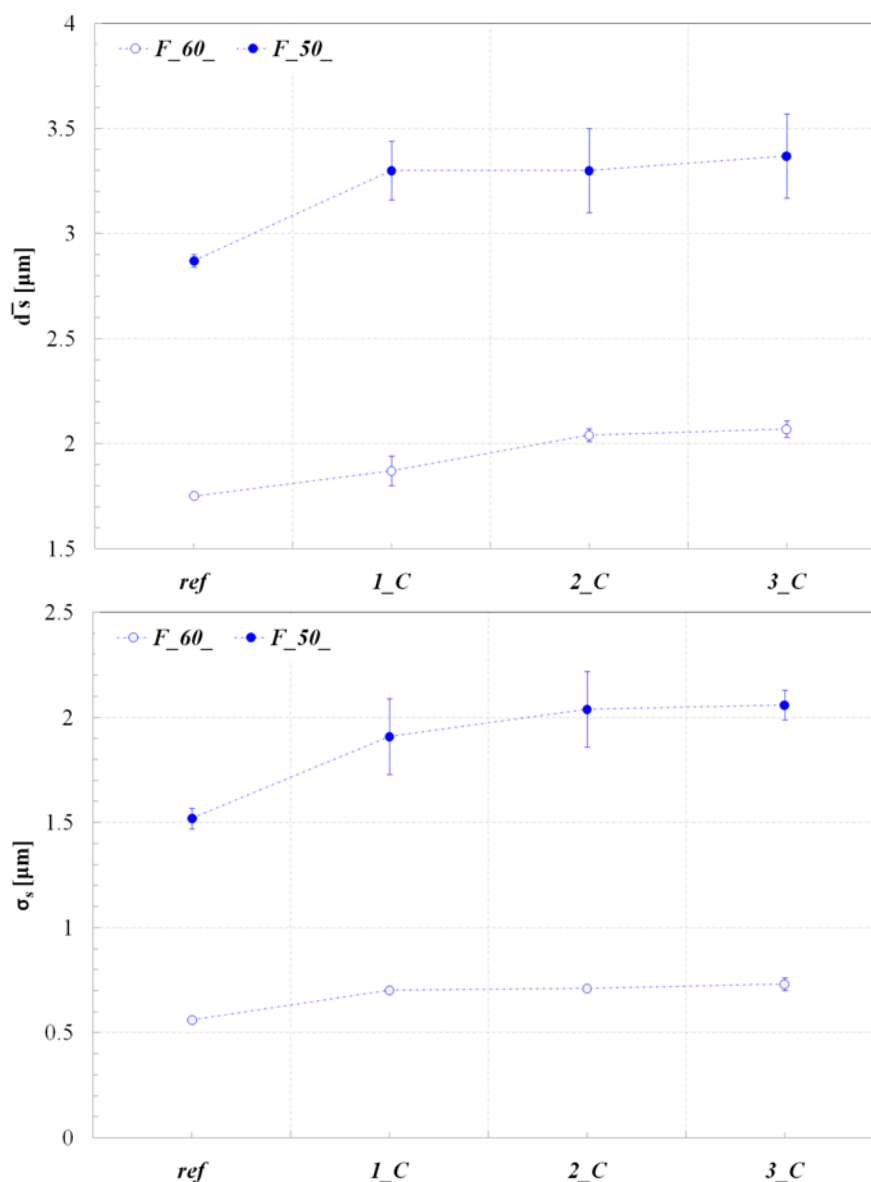


Figure 3.11: a comparison between samples *F_60_* and *F_50_* DSDs.

In this case, an increase of the oil concentration leads to less polydisperse emulsions characterised by a smaller mean droplet diameter. A similar result was found by Zaki (1997) for Geisum crude oil-in-water emulsions using the same oily phase volume fraction. The author concluded that the emulsions prepared with an oil content value of 60_{v/v}% were more stable than those prepared with 50_{v/v}% (the more stable the emulsion, the smaller its mean droplets diameter, as found in the 2nd chapter of the PhD thesis). This result can be explained if the effect of the surfactant is considered. The surfactant concentration with respect to the total volume of the emulsions was kept constant (2_{w/w}%), but considering the concentration in the aqueous continuous phase (water), it increased as the oil content increased. Thus, the actual surfactant concentration with respect to the aqueous phase passed from 4.69_{w/w}% at an

oil fraction of 60_{v/v}% to 3.80_{w/w}% at an oil fraction of 50_{v/v}%. It is known that a lower amount of emulsifier leads to bigger droplets (a lower surface to volume ratio) [Barnes, 2000]. Figure 3.11 shows that at a lower oil concentration a constant value of the mean diameter was reached after the 1st centrifugation, while at a higher oily phase volume fractions a further homogenisation step is requested (2nd centrifugation). The same conclusions can be derived by the analysis of the samples produced with the high viscous oil, for which a more significant effect of destabilisation is encountered up to the 2nd centrifugation at the higher oily phase volume fraction. The DSDs of these emulsions are shown in figure 3.12.

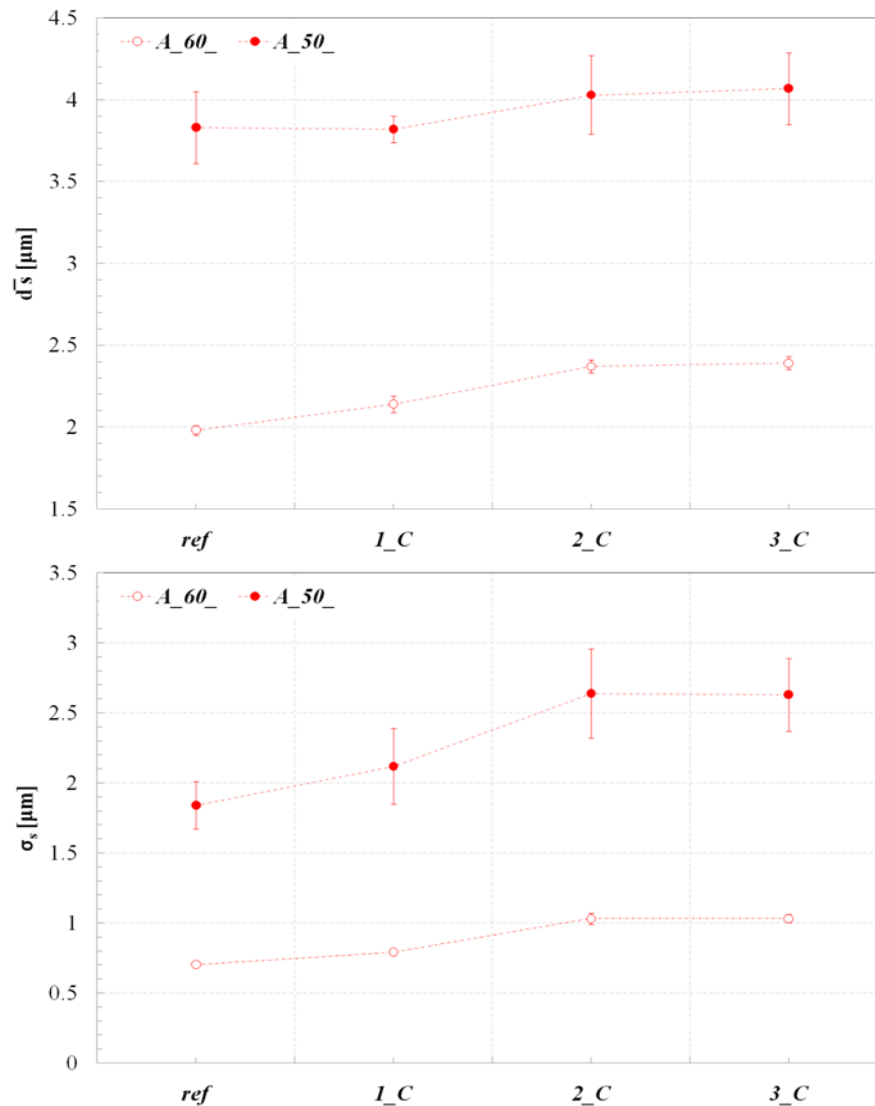


Figure 3.12: a comparison between samples A_60_ and A_50_ DSDs

The flow curves of the samples prepared with high oily phase fractions are reported in figure 3.13. Even in the case of more concentrated emulsions, a significant viscosity increase due to the water depletion was observed. Considering the slight variations of the DSD parameters, the most important contribution to the emulsions destabilisation and viscosity increase is

given by the creaming effects, the Ostwald ripening phenomenon being not so important as to justify any viscosity variations.

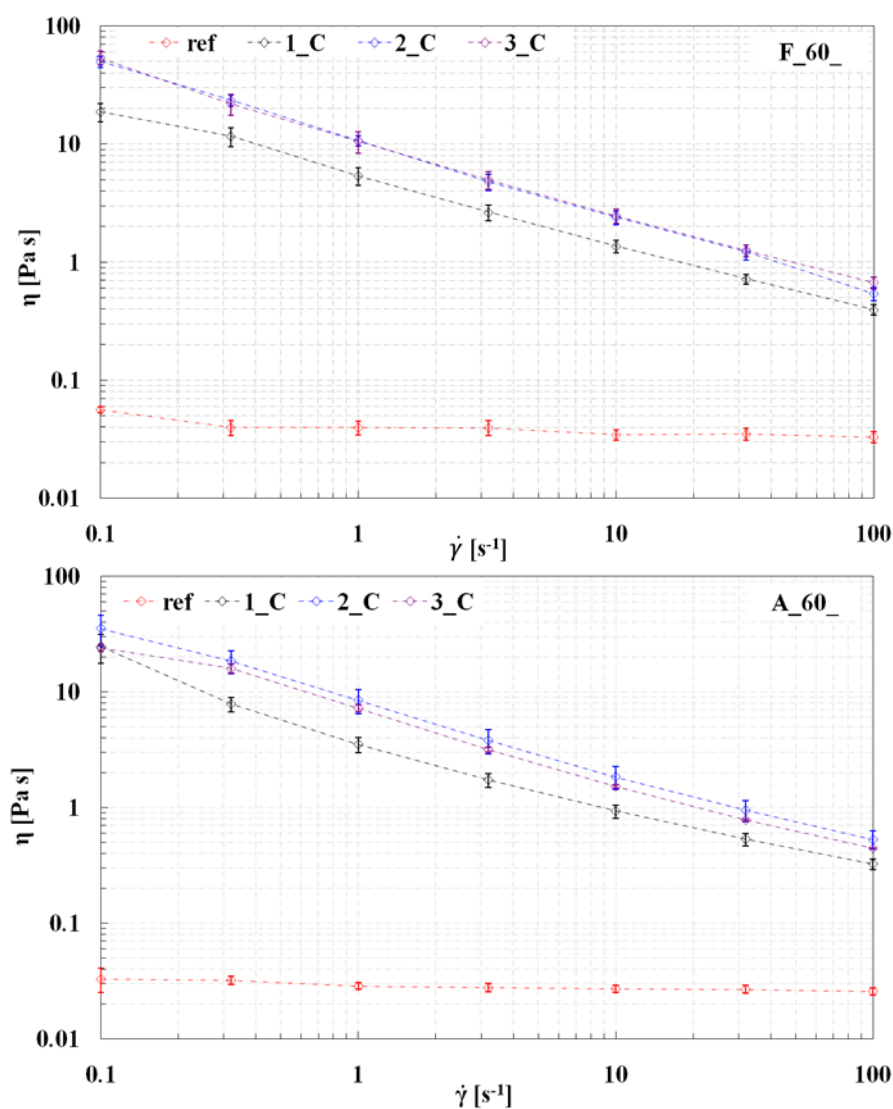


Figure 3.13: short-term stability tests: flow curves at each centrifugation for samples with an increased oily phase percentage

The *power law* model parameters for the shear thinning flow curves of emulsions F_{60} are reported in the following figure 3.14 compared with those of the emulsions prepared at a lower oil concentration.

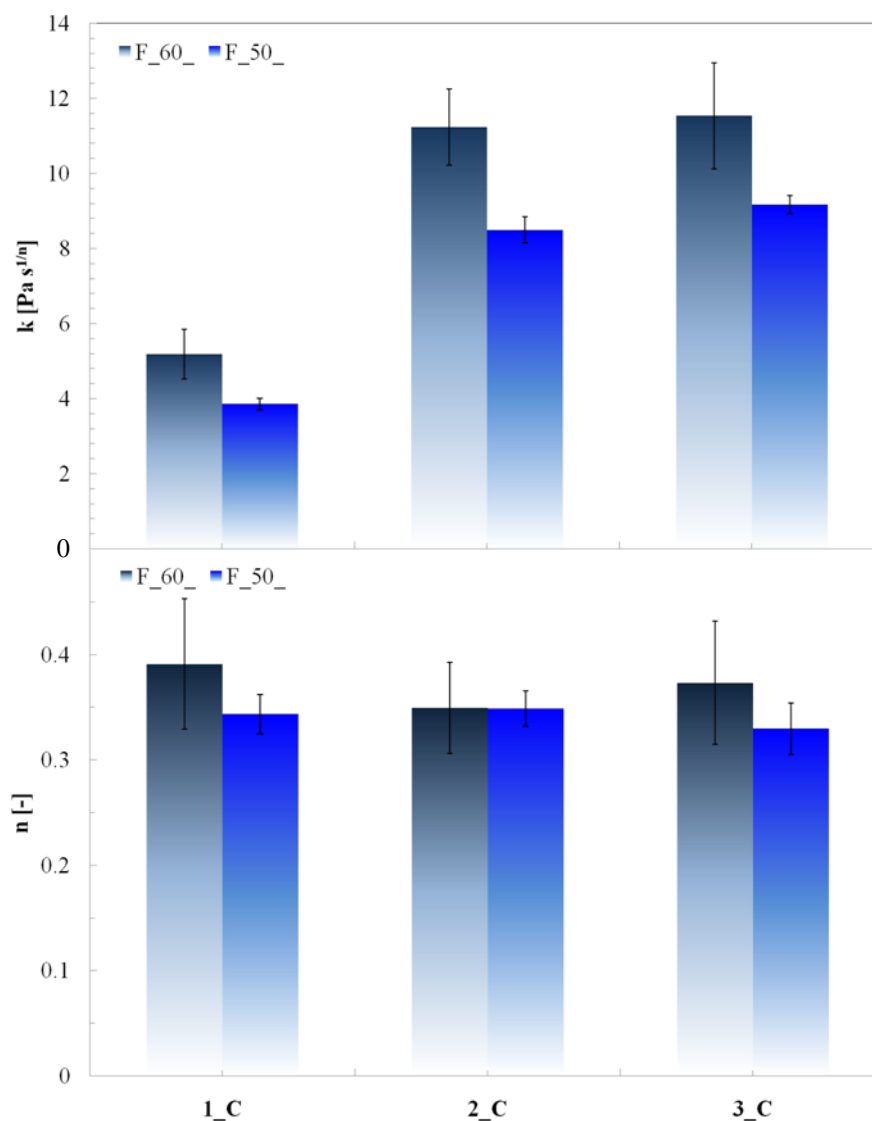


Figure 3.14: k and n parameter of the power-law model for samples F_{60} and F_{50}

As found in samples prepared with a low oily phase volume fraction, an increase in the consistency index k after the first centrifugation was measured, while the flow index n is not significantly affected by the creaming destabilisation.

As expected, a bigger k value is encountered at a higher oily phase volume fraction, while n has the same value for both the oil contents.

Similar results were found for the most viscous oil; the power-law model parameters are reported in figure 3.15.

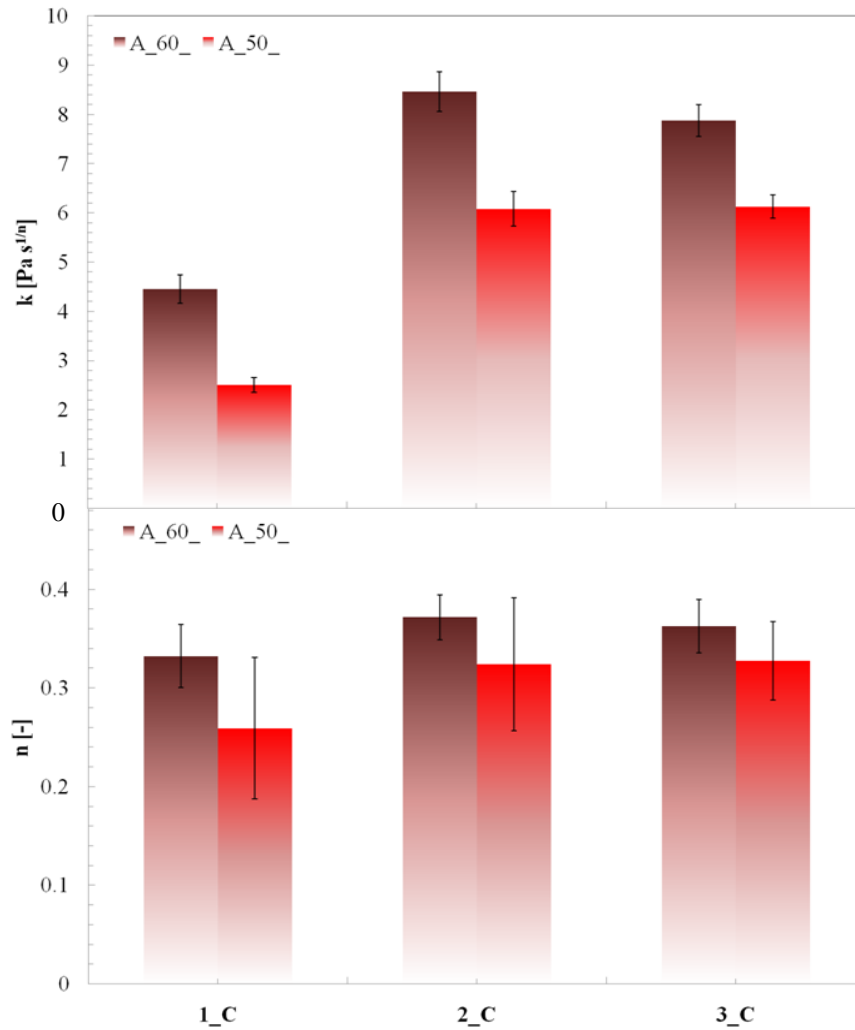


Figure 3.15: k and n parameter of the power-law model for samples A_60_ and A_50_

The oil volume fraction of the more concentrated emulsions was detected and reported in figure 3.16.

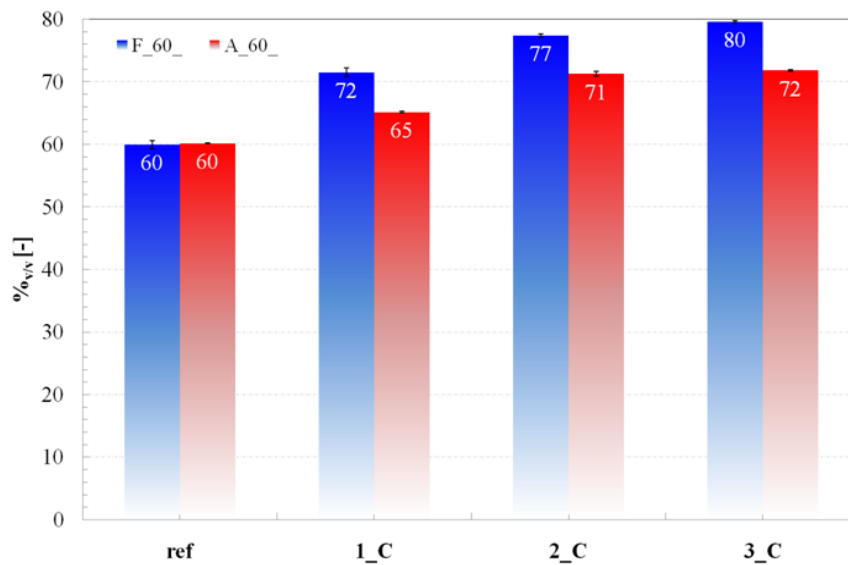


Figure 3.16: oil volumetric percentage in the creamy layer for samples A_60_ and

As found for the previously analysed samples, the efficiency of extraction is higher for the sample prepared with the less dense oil, and, obviously, a greater quantity of oil was found in these samples with respect to those prepared at a lower oily phase volume fraction.

3.3.4. LTSTs

A comparison between the forced destabilisation of the STSTs and the natural destabilisation occurring during the LTSTs is proposed. Figure 3.17 reports, as an example, the DSD parameters for samples *A_50_ref* and *A_50_15_d*.

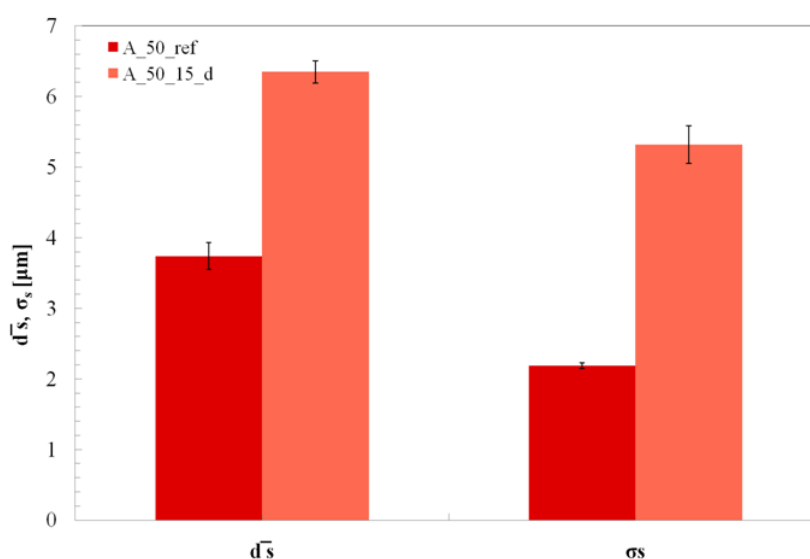


Figure 3.17: DSD parameters of LTSTs for sample *A_50_*

Significant differences are present between the DSD of sample *A_50_15d* and the native one. In fact, both \bar{d}_s and σ_s increased with time giving a more polydisperse distribution of bigger droplets. It is probable that, in the case of natural destabilisation, the storage time was enough to allow the droplets to aggregate for the Ostwald ripening effect as well as creaming phenomenon, while the destabilisation exerted by centrifugal forces, in the STSTs, were able to evidence only the creaming effect. In fact, the coalescence among drops in an immiscible liquid medium takes place in 4 different stages, each of them is characterised by different timescale from system to system [Less et al., 2008]. In the first stage, the droplets come into very close proximity, under long range flocculation forces, before the second stage of film thinning can occur. When the film reaches a critical thickness, any significant disturbance or instability will cause the breakage and the coalescence takes place.

Despite the significant differences among the creaming and Ostwald ripening phenomena in the two destabilisation tests (LTSTs and STSTs), if the effect of oil characteristics is

considered, even in the case of LTSTs, the more dense and viscous oil gives larger droplets increasing polydispersity and confirming the STSTs results. The DSD parameters of the samples prepared with the same volume fraction of different oils are shown in figure 3.20.

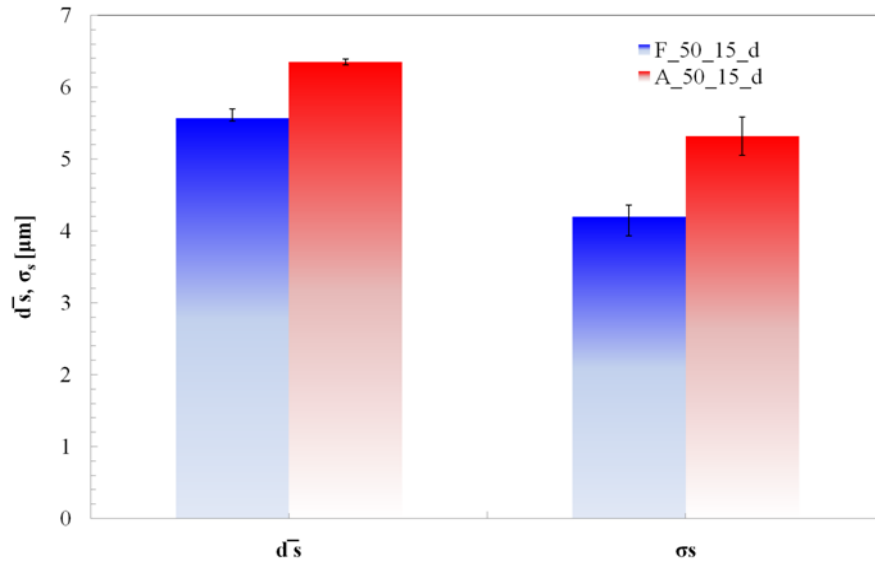


Figure 3.20: DSD parameters for LTST: effect of oil characteristics

Analysing the effect of the dispersed phase volume fraction variation, samples produced with a higher oily phase amount presented a more polydisperse distribution of larger droplets for any oil used (figure 3.21 and 3.22). As already stated in the case of STSTs, this behaviour is certainly due to the emulsifier amount dispersed in the aqueous phase.

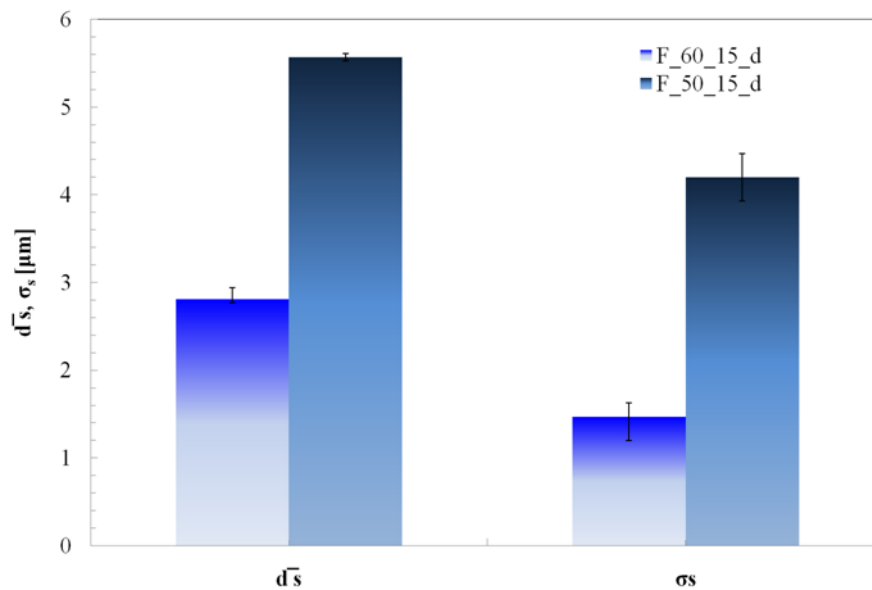


Figure 3.21: DSD parameters for LTST: effect of oil fraction (Finavestan A360B)

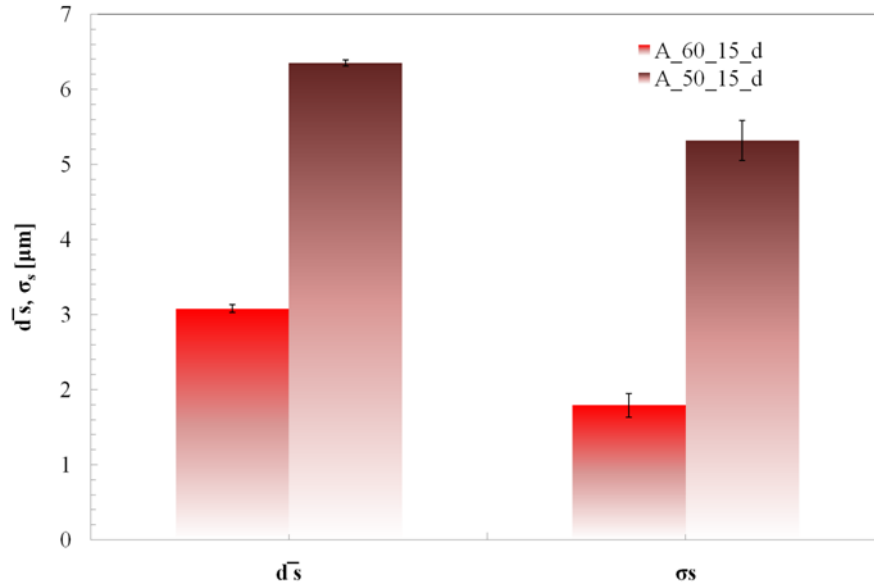


Figure 3.22: DSD parameters for LTST: effect of oil fraction (Arum HT 220)

Figure 3.23 reports viscosity results as flow curves of sample *A_50_15_d* compared with the viscosities of the native sample and the same sample after the 1st centrifugation step. The viscosity of the centrifuged sample is higher than the viscosity of the naturally destabilised one, showing a shear thinning behaviour. This is in good accordance with the total water amount separated by centrifugation, higher than the water volume naturally separated (figure 3.24), and the DSDs of the two samples (the sample having the higher viscosity value has the smaller and less polydisperse droplets).

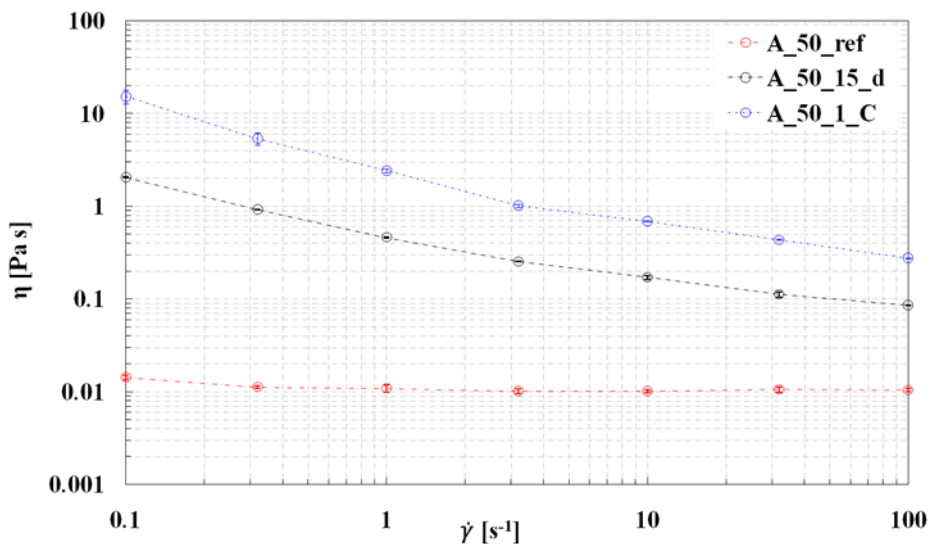


Figure 3.23: flow curves of samples at different stability evaluation

In figure 3.24 the total oily phase volume fraction is shown. It can be noticed that a greater water amount was separated from the emulsions produced with a lower oily phase volume

fraction. Moreover, a value slightly below 70_{v/v}% of the oily phase concentration seems to be a threshold limit that can be recovered.

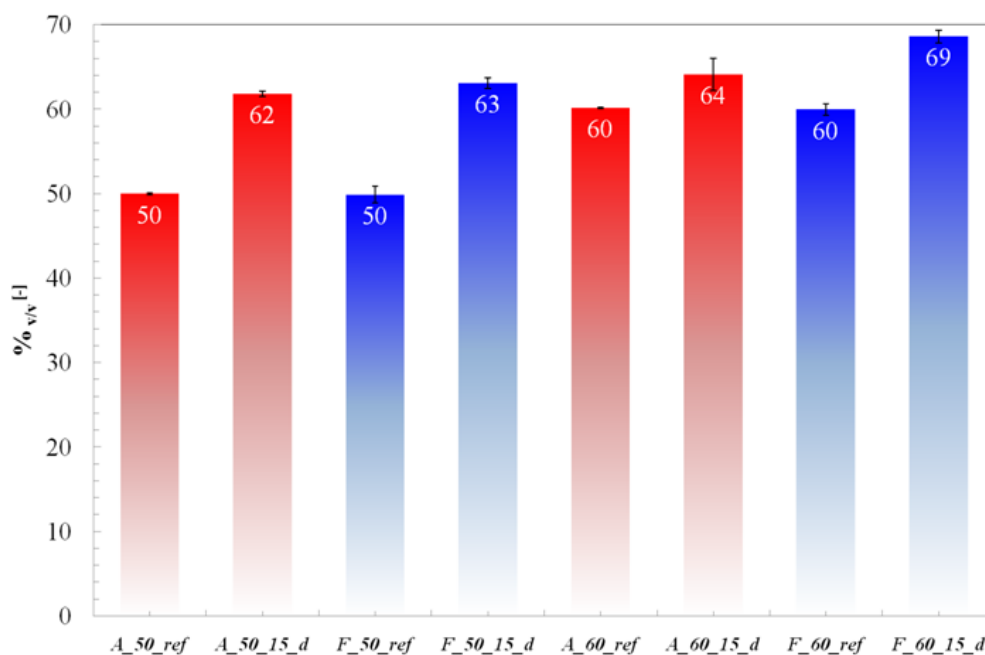


Figure 3.24: oil volumetric percentage in the creamy layer for long term stability tests

From the oily phase concentration and the DSDs parameters reported, it is clear that different samples have different viscosity values. The power law parameters of the examined samples are reported in figure 3.25.

In accord with STSTs results, samples produced with the less viscous oil are characterised by higher k parameter, moreover k increases with the oil volume fraction. The flow index n is not affected by oil characteristics and its volume increase does not give any further variation, confirming again the STSTs results.

Finally, it can be concluded that STSTs and LTSTs gives important information on emulsions destabilisation. Both the tests evidence a significant creaming effect that leads to a phase separation producing an upper concentrated O/W layer and a lower water phase layer. Moreover, STSTs enhances the creaming phenomena giving slight DSDs changes: from a rheological point of view, the shear-thinning behaviour of the destabilised emulsions can be attributed only to the water depletion. On the contrary, LTSTs showed a more significant contribution of Ostwald ripening phenomenon to the viscosity changes observed after destabilisation.

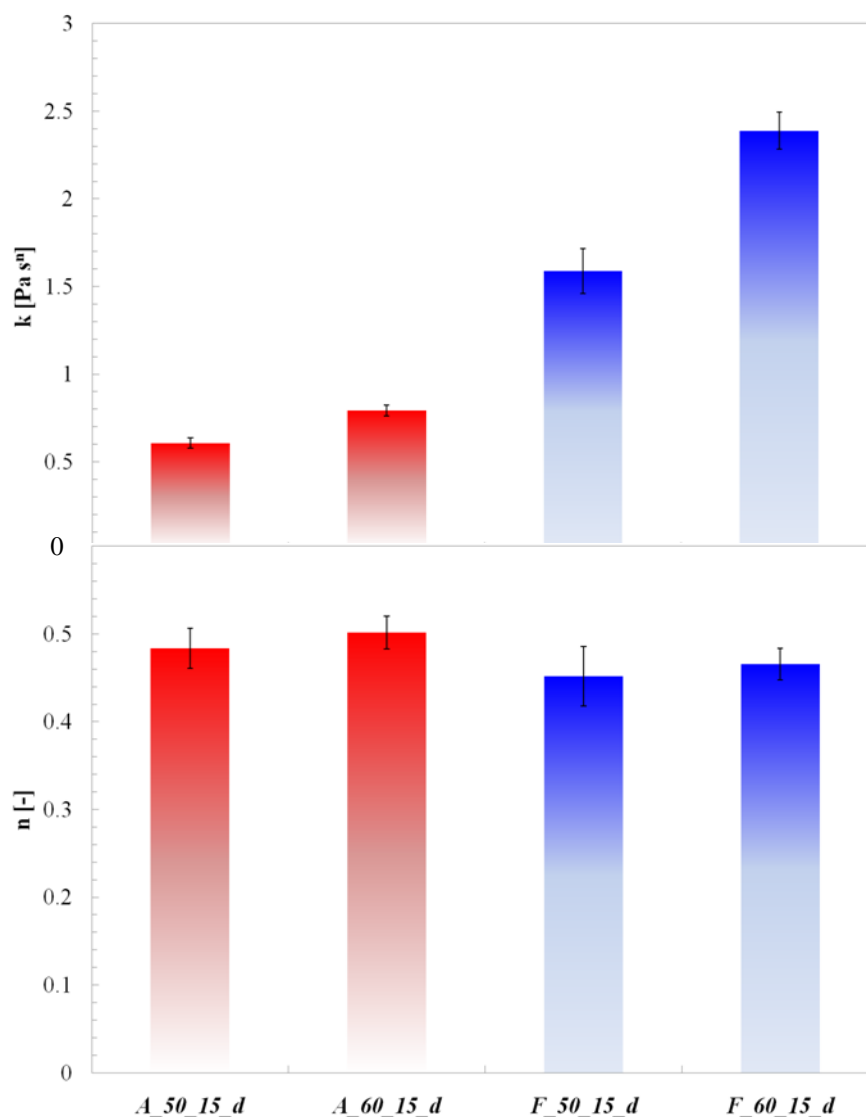


Figure 3.25: LTSTs power-law parameters at 25°C

Conclusions

In this chapter the destabilisation of model O/W emulsions has been studied. Crude oil emulsions have to be stable during oil transportation in pipelines in order to reduce pressure drops as a consequence of a lower viscosity, but an easy destabilisation should be accomplished to recover oil from water. Two different stability tests were studied: a short-term one by applying the centrifugal force on stable emulsions, and a long-term one by storing the fresh sample at controlled temperature in a quiescent state for 15 days. Emulsions destabilised with these two techniques were compared by measuring the rheological and microscopic characteristics of the formed upper creamy layer. Two different oils (different in viscosity and density) were chosen, and two different oil amounts were used to prepare the emulsions. For all the tests a pronounced creaming destabilising phenomenon, more evident

for the less dense oil, has been found, while the emulsions produced with the more dense and viscous oil has been characterised by a more polydisperse distribution of bigger droplets with a consequent greater tendency to be destabilised by the Ostwald ripening. For both the oils, in LTSTs, a marked Ostwald ripening destabilisation mechanism has been detected. In both the destabilisation tests, an increase in viscosity owing to the creaming effect has been observed, and the less viscous and dense oil produced emulsions characterised a higher viscosity value. Therefore, owing to different ratios between emulsifier amount and water phase volume fraction (into which emulsifier was dispersed), an increase of the oily phase volume fraction has given less polydisperse distributions of smaller droplets. The viscosity of all samples varied during the destabilisation: the fresh samples have shown a Newtonian behaviour, while after the water depletion, the samples became shear thinning and much more viscous with respect to the native oil. Thus, it is obvious that these unstable systems cannot be transported in conventional pipelines and a study of emulsions stability beforehand is recommended in order to avoid an undesired pipelines shutoff.

References

- Abismail B., Canselier J.P., Wilhem A.M., Delmas H., Gourdon C., (1999). *Emulsification by ultrasound: drop size distribution and stability*, Ultrasonics Sonochemistry 6, 75-83
- Al-Mulla, A., Gupta, R.K., (2000). *Droplet coalescence in the shear flow of model emulsions*, Rheologica Acta, 39, 20-25.
- Al-Roomi Y., George R., Elgibaly A., Elkamel A., (2004). *Use of a novel surfactant for improving the transportability/transportation of heavy/viscous crude oils*, Journal of Petroleum Science & Engineering 42, 235-243
- Ambrosone L., Mosca M., Ceglie A., (2007). *Impact of edible surfactants on the oxidation of olive oil in water-in-oil emulsions*, Food Hydrocolloids 21, 1163–1171
- Aomari N., Gaudu R., Cabioc'h F., Omari A., (1998). *Rheology of water in crude oil emulsions*. Colloids and Surfaces A: Physicochemical and Engineering Aspects 139, 13–20
- Auflem I. H., Kallevik H., Westvik A., Sjöblom J., (2001). *Influence of pressure and solvency on the separation of water-in-crude-oil emulsions from the North Sea*, Journal of Petroleum Science and Engineering 31, 1–12

Barnes H.A, (2000). *A handbook of elementary rheology*, The University of Wales, Institute of Non-newtonian Fluid Mechanics, Aberystwyth.

Barnes H.A., Hutton J.F., Walters, K., (1989). *An Introduction to Rheology*, Elsevier Science Publishers B.V., Amsterdam, NL

Clausse D., Gomez F., Pezron I., Komunjer L., Dalmazzone C., (2005). *Morphology characterization of emulsions by differential scanning calorimetry*, *Advances in Colloid and Interface Science* 117, 59 – 74

Dehkissia S., Larachi F., Rodrigue D., Chornet E., (2004). *Characterization of Doba-Chad heavy crude oil in relation with the feasibility of pipeline transportation*, *Fuel*, 83, 2157-2168.

Derkach S. R., (2009). *Rheology of emulsions*, *Advances in colloid and interface science*, in press

Dukhin S. S., Sjöblom J., Sæther Ø., (2006). *Theoretical approach to the dynamic behavior of emulsions* in “Emulsions and emulsions stability”, CRC Press Taylor & Francis Group, Boca Raton, U.S.A, Chapter 1

Egger H. and McGrath K.M., (2006). *Aging of oil-in-water emulsions: The role of the oil*, *Journal of Colloid and Interface Science* 299, 890–899

Ford D.L, Borwankar R., Martin R.W.jr, Holcomb D.N., (1997). *Dressing and Sauces* in “Food emulsions” by S.E Friberg and K. Larsson, Marcel Dekker, Inc., New York, Basel

Förster A.H., Herrington, T.M., (1998). *Rheology of two commercial available cosmetic oil in water emulsions*, *International Journal of Cosmetic Science*, 20, 317-326

Gabriele D., Migliori M., Lupi F.R., de Cindio B., (2009). *Rheological study of o/w concentrated model emulsions for heavy crude oil transportation*, *Energy Sources, Part A: Recovery, Utilization, and Environmental Effects*, in press.

Gafonova O. V., Yarranton H. W., (2001). *The stabilization of water-in-hydrocarbon emulsions by asphaltenes and resins*, *Journal of Colloid and Interface Science*, 241, 469-478

Hahn A. U., Mittal K. L., (1979). *Mechanism of demulsification of oil-in-water emulsion in the centrifuge*, *Colloid & Polymer Sci.* 257, 959-967

Hollingsworth K.G., Johns M.L., (2003). *Measurement of emulsion droplet sizes using PFG NMR and regularization methods*, Journal of Colloid and Interface Science 258, 383–389

Hurtevent C., Rousseau G., Bourrel M., Brocart B., (2006). *Production issues of acidic petroleum crude oils*, in “Emulsions and emulsions stability”, CRC Press Taylor & Francis Group, Boca Raton, U.S.A, Chapter 13

Imhof A., Pine D. J., (1997). *Stability of Nonaqueous Emulsions*, Journal Of Colloid And Interface Science 192, 368–374

Jafari S. M., Assadpoor M., He Y., Bhandari B., (2008). *Review - Re-coalescence of emulsion droplets during high-energy emulsification*, Food Hydrocolloids 22, 1191–1202

Kang W., Jing G., Zhang H., Li M., Wu Z., (2006). *Influence of demulsifier on interfacial film between oil and water*, Colloids and Surfaces A: Physicochem. Eng. Aspects 272, 27–31

Kokal S., (2005). *Crude-oil emulsions: a state-of-the-art review*, SPE Production & Facilities, 20, 5-13

Langevin J. D., Poteau S., Hénaut I., Argillier J.F., (2004). *Crude oil emulsion properties application to heavy oil transportation*, Oil & Gas Science and Technology, 59 511-521

Less S., Hannisdal A., Bjørklund E., Sjöblom J., (2008). *Electrostatic destabilization of water-in-crude oil emulsions: Application to a real case and evaluation of the Aibel VIEC technology*, Fuel 87, 2572–2581

Mandala I.G., Savvas T.P., Kostaropoulos A.E., (2004). *Xanthan and locust bean gum influence on the rheology and structure of a white model-sauce*, Journal of Food Engineering 64, 335–342

Masmoudi H., Piccerelle P., Le Dréau Y., Kister J., (2006). *A rheological method to evacuate the physical stability of highly viscous pharmaceutical oil-in-water emulsions*, Pharmaceutical Research, 23, 1937-1947

McClements D.J., (1999). *Food Emulsions – Principles, Practice and Techniques*, CRC Press, New York, Chapter 7

- McLean J. D., Kilpatrick P. K., (1997). *Effects of asphaltenes solvency on stability of water-in-crude-oil emulsions*, Journal of Colloid and Interface Science 189, 242-253
- Melle S., Lask M., Fuller G. G., (2005). *Pickering Emulsions with Controllable Stability*, Langmuir 21, 2158-2162
- Merrill R., (1943). *Determining mechanical stability of emulsions. A rapid quantitative method*, Ind. Eng. Chem. Anal. Ed., 15, 743-746
- Nädler M., Mewes D., (1997). *Flow induced emulsification in the flow of two immiscible liquids in horizontal pipes*, Int. J. Multiphase Flow, 23, 55-68
- Nour A. H., Mohammed F.S., Yunus R.M., Arman A., (2009). *Demulsification of Virgin Coconut Oil by centrifuging method: a feasibility study*, International Journal of Chemical Technology, 1, 1-6
- Pal R., (1998). *A novel method to correlate emulsion viscosity data*, Colloids and Surfaces A: Physicochemical and Engineering Aspects, 137, 275-286
- Pal R., (2000) a. *Shear viscosity behaviour of emulsions of two immiscible liquids*, Journal of Colloids and Interface Science, 225, 359-366
- Pal R., (2000) b. *Relative viscosity of non-newtonian concentrated emulsions of noncolloidal droplets*, Ind. Eng. Chem. Res., 39, 4933-4943
- Robins M. M., (2000). *Lipid emulsions*, Grasas y Aceites, 51, 26-34
- Romero A., Cordobés F., Puppó M.C., Guerrero A., Bengoechea C., (2008). *Rheology and droplet size distribution of emulsions stabilized by crayfish flour*, Food Hydrocolloids 22, 1033–1043
- Romero N., Cárdenas A., Henríquez M., Rivas H., (2002). *Viscoelastic properties and stability of highly concentrated bitumen in water emulsions*, Colloids and Surfaces A, 204, 271-284
- Saniere A., Hénaut I., Argillier J.F., (2004). *Pipeline transportation of heavy oils, a strategic, economic and technological challenge*, Oil & Gas Science and Technology, 59, 455-465.

Schramm L.L., (2005). *Emulsions, Foams, and Suspensions: Fundamentals and Applications*, WILEY-VCH Verlag GmbH & Co. KGaA, Weinheim, Germany

Tadros T., (2004). *Application of rheology for assessment and prediction of the long-term physical stability of emulsions*, *Advances in colloid and Interface Science*, 108-109, 227-258

Tcholakova S., Denkov N., Ivanov I. B., Marinov R., (2004). *Evaluation of Short-Term and Long-Term Stability of Emulsions by Centrifugation and NMR*, *Bulg. J. Phys.* 31, 96–110

Walpole R. E., Myers R. H., Myers S. L., Ye K., (2007). *Probability & Statistics for Engineers & Scientists – 8th edition*. Pearson Education International, Prentice Hall, USA

Walstra P., (1993). *Principles of emulsions formation*, *Chemical Engineering Science*, 48, 333–349

Yaghi B. M., Al Bemani A., (2002). *Heavy Crude Oil Viscosity Reduction for Pipeline Transportation*, *Energy Sources*, 24, 93–102

Zaki N. N., (1997). *Surfactant stabilized crude oil-in-water emulsions for pipeline transportation of viscous crude oils*, *Colloids and Surfaces A*, 125, 19-25

Chapter 4 – Effect of waxes addition on rheological properties of O/W concentrated model emulsions

Abstract

Because of the continuous depletion of light oil reservoirs, heavy crude oil usage is increasing in importance. As heavy oil contains different impurities that increase the viscosity, pipeline transportation becomes economically disadvantageous. O/W emulsification, adopted as cost reduction transportation technique, may take advantage of the presence of natural components of heavy crudes, asphaltenes and resins as emulsifiers and waxes as stabilisers, decreasing the emulsions viscosity with respect to the pure-oil one. This chapter aims at investigating the effect of waxes addition on the viscosity of model O/W emulsions produced in bench-scale, using two different emulsification techniques.

4.1. Introduction

Upstream of conventional heavy oils, emulsification occurs when crude oil is mixed with water already present or injected in the reservoir, at well bore, in pipelines, and at surface facilities. If the dispersed phase of the emulsion is water, the system viscosity increases with respect to the oil-one and this may cause high pressure drops throughout the pipeline [Al-Sahhaf et al., 2009]. On the contrary, emulsification of the oily phase in water is a reliable method to decrease the fluid viscosity for crude oil transportation in pipelines [Saniere et al., 2004]. In fact, emulsions pumping (up to 75_{v/v}% of oil in water) [Langevin et al., 2004] and separation in situ, seems to be the most interesting technique, always considering that, after transportation, oil must be separated from water.

Concerning the crude oil composition, there are many components naturally present in the raw crude oil that can act as emulsifiers or stabilisers materials in different cases. In fact, emulsions characteristics (stability formation mechanism, drop size distribution) can be significantly affected by the presence of asphaltenes, resins, waxes and inorganic solids.

Moreover, viscosity of heavy oils may widely range from 0.1 Pa·s⁻¹ to 100 Pa·s⁻¹, [Wakabayashi, 1997; Ahmed et al., 2005; Quiñones-Cisneros et al., 2005], also showing shear thinning behaviour, depending upon type and amount of minor components (such as

waxes, resins, asphaltenes, sand or eventually hydrates). Asphaltenes are present in crude oils mixtures in the form of colloidal dispersed particles, soluble in toluene and precipitate in presence of aliphatic solvents [Hannisdal et al., 2007]. During emulsion formation, asphaltenes interact with resins, forming an interfacial film surrounding droplets that are then protected against coalescence [McLean and Kilpatrick, 1997]. Resins are polar and non volatile compounds, soluble in n-pentane, n-heptane and aromatic solvents and insoluble in methanol and propanol.

Waxes are natural components of high viscous crude oil, and their deposition at the pipe wall, under certain conditions during crude transportation, can cause serious damage to conventional pipelines [Burger et al., 1981; Kané et al., 2003] as shown in figure 4.1.

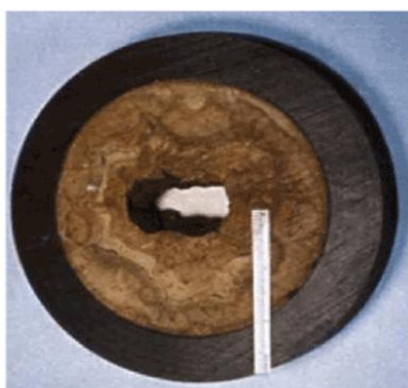


Figure 4.1: wax deposition blockage in pipelines

This class of compounds is solid at room temperature and it can be divided into microcrystalline or macrocrystalline [Thanh et al., 1999]. Macrocrystalline waxes are mainly n-alkanes with chain length within the range C20–C50. Microcrystalline or amorphous waxes have a high amount of isoparaffins and naphthenes within the range C30–C60 [Coto et al., 2008]. Waxes can be classified also according to their solubility in pentane. The pentane-soluble waxes contain predominantly n-alkanes (<C40-C45) whilst the insoluble ones contain mainly microcrystalline waxes (>C40). This fact is mainly responsible for deposition phenomena. A schematic configuration of the different kinds of waxes is shown in figure 4.2.

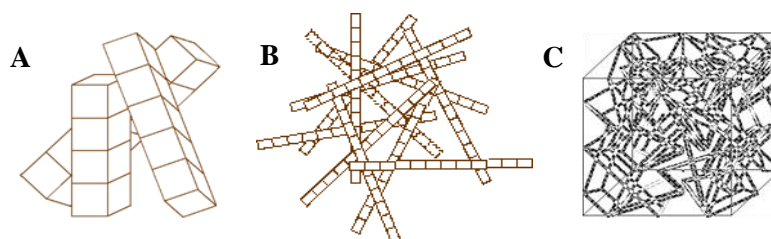


Figure 4.2: macrocrystalline (A), microcrystalline (B), and crystal deposit network of wax (C)

In the case of emulsions formation, waxes can co-adsorb at the oil/water interface improving the film stability. A wide literature has been written in order to clarify the role of wax crystals on the water-in-oil emulsions stability, but there are no recent papers dealing with oil-in-water emulsification for crude oil transportation. [Visintin et al. \(2008\)](#) studied the effect of water cut on the rheological and structural behaviour of water in waxy crude oil emulsions, finding that water above a threshold value can greatly enhance gel formation in crude oil, changing both the pour point temperature and the yield strength. [Paso et al. \(2009\)](#) found that the superior stability of emulsions (up to a 70% water cut) produced with waxy crude oils is likely a consequence of the greater abundance of asphaltenes that interact with waxes. Similar conclusions were reached by [Lee \(1998\)](#) who reports that, for a Kuwait crude oil, an asphaltenes concentration of 0.01g/ml did not produce a stable water-in-oil emulsion, but stability was improved when waxes (0.05 g/ml) were added; a consequent conclusion is that waxes cannot act as emulsifier by themselves, but they are good stabilisers for both O/W and W/O emulsions. For the same sample a concentration of asphaltenes containing 0.03 g/ml produced stable emulsions with no waxes. At low temperature, wax crystals ($>1_{w/w}\%$) may promote droplets coalescence as they break the interface protruding into the disperse phase drop. On the contrary, at higher temperatures, it was observed that the droplet size decreases with wax concentration. In fact, [Li et al. \(2009\)](#) showed that waxes are liquid-like during the high temperature emulsification process, but during the cooling phase wax crystals appear around the oil/water interface stabilizing the droplet. The aim of this chapter is the investigation of the effect of n-paraffins ($\approx C40$) addition into the oily phase onto rheological properties of a model O/W concentrated emulsion. Samples containing different amounts of waxes are produced both in batch and in flow by using a lab-scale loop plant and viscosity measurement were performed. The lab-scale plant allows samples to be collected at different emulsification times and this allows the effect of waxes on the emulsion formation to be investigated.

4.2. Materials and methods

4.2.1. Materials

O/W emulsions (simulating a biphasic system for pipeline transportation [[Gabriele et al., 2009](#)]) were prepared using commercial products and tap water; the total amount of the

sample was 200g. Paraffin oil was purchased from Total (Finavestan A360B, France, $\rho(25^{\circ}\text{C})=0.864\pm 0.011$ Kg/l, $\mu(25^{\circ}\text{C})=0.157\pm 0.002$ Pa·s) and waxes were paraffin cut (Carlo Erba Reagenti, Italy) ranging from C-20 to C-40. Emulsifier (simulating the natural emulsifying effect of asphaltenes and resins) was hydrophilic nonionic Tween 60 (polyoxyethylenesorbitan monostereate, HLB 14.9). Volume ratio of oil and water was fixed at 1.5 and, keeping a constant emulsifier quantity (2%), waxes content was varied (0.5% and 1%). Both emulsifier and wax are weight percentage referred to the oil amount. Table 4.1 shows emulsions composition and sample ID as used in the rest of the paper: *Bx* indicates batch prepared emulsions and *Ex* labels in-flow prepared ones. In addition, in order to clarify the effect of waxes addition onto oil viscosity, wax-in-oil solutions were tested for a wax content of 0.5% and 1%.

Sample ID	paraffin oil [v/v %]	water [v/v %]	wax [w/w %]	Emuls. Method
B1	60	40	0	Batch
B2	60	40	0.5	Batch
B3	60	40	1	Batch
E1	60	40	0	Flow
E2	60	40	0.5	Flow
E3	60	40	1	Flow

Table 4.1: samples ID

4.2.2. Batch Emulsification

Both water and oil were obtained separately. The two phases were heated-up to 70°C in two cylindrical beakers (volume 600 ml). The hydrophilic emulsifier was gently added to water, while waxes were melted into the hot oil. The resulting solutions were kept under stirring for 5 minutes. Homogenisation of the emulsion was then performed by using a commercial blender (Minipimer Braun MR 404 Plus, Germany) having a nominal power of 300W for 10 minutes. During heating and stirring water evaporation was prevented by placing a lid over the beaker. Rheological characterisation was performed after 3 hours rest from the emulsification completion at room temperature (Samples B1-3).

4.2.3. Flow emulsification

Flow emulsification on laboratory scale was performed using the experimental home-made system. Oil and water were mixed using a module (labelled as M in the general flow loop scheme of figure 4.3), produced for this purpose.

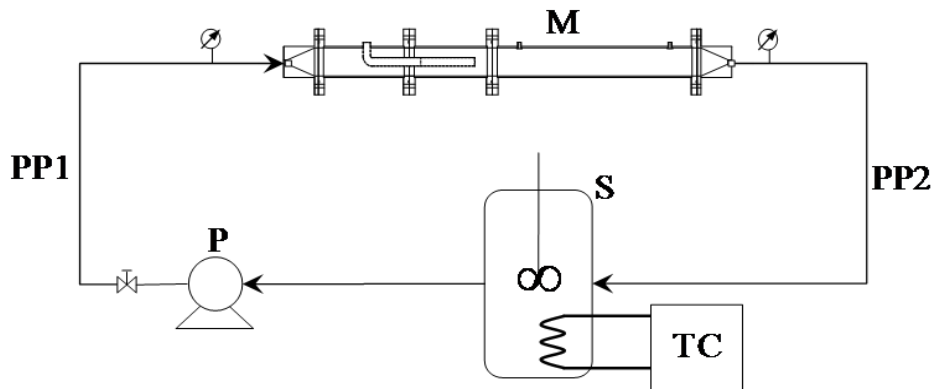


Figure 4.3: plant flowsheet

The module consists of an external cylindrical PMMA vessel (ID^V 64 mm, OD^V 70 mm) with an internal coaxial copper pipe (ID^P 20 mm, OD^P 22 mm) as shown in figure 4.4.

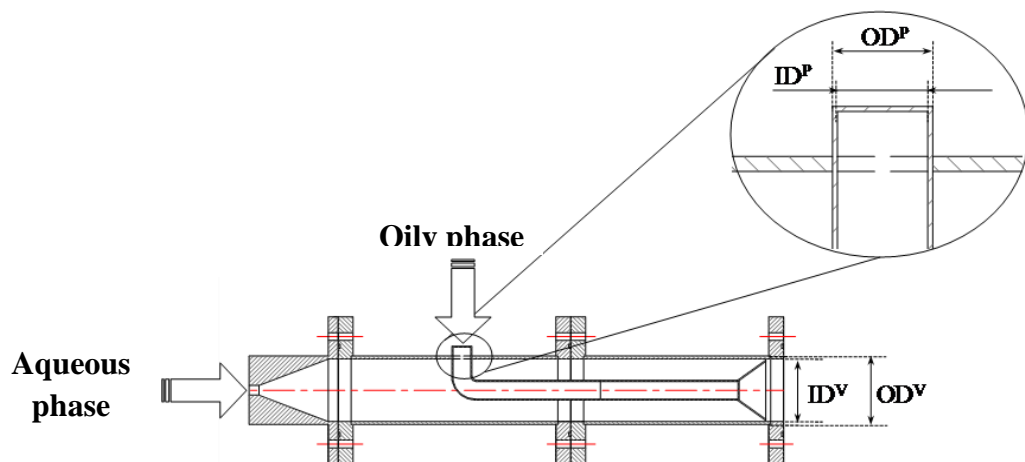


Figure 4.4: nozzle section for feeding pure phases

During the start-up, when the two phases were still to be mixed, the oily and aqueous phase were fed at room temperature from separate reservoir and pumped through the vessel (water) and copper pipe (oil) into the loop. Oil was pumped by a peristaltic pump (Watson Marlow 323Du, USA) running at 400 rpm, equipped with a series of 4 pumping head (type 313-X), whilst water was fed using a centrifugal pump having a nominal power of 0.5 hp (Tecno 05/4M, Italy). According to the oil/water ratio, as specified in table 4.1, 6 litres of oily phase and 4 litres of aqueous phase were used. Start-up management was mainly affected by the limiting flow rate of the peristaltic pump ($1 \text{ l} \cdot \text{min}^{-1}$). Therefore, a start-up time of 6 minutes

was necessary to empty the oil vessel, and water flow rate was adjusted to $0.67 \text{ l}\cdot\text{min}^{-1}$ to keep the same emptying time. At the end of the start-up phase, when both the pure fluid reservoirs were empty, the loop was full of oil-water mixture to be emulsified. During normal operation, the mixture was continuously re-circulated, from the reservoir S (volume 20 l) to the module M by the same pump P used to feed water during the start up. The reservoir S was equipped with a shaft agitator (Heidolph, Germany) to prevent potential spontaneous de-emulsification, especially at the early stages of the process when the system was quite unstable. Temperature control of the reservoir was guaranteed by cold water (15°C) flowing in a coil from a thermostatic bath TC (Neslab, USA), this solution maintained the temperature inside the tank always below 27°C . The module M was connected to the reservoir by the pipeline PP1 (length 3.73 m), the length of the pipe PP2 connecting the pump exit to the module M was 1.75m; both pipe were made of Rilsan[®] (ID 10 mm). The sampling for rheological test was performed from the reservoir S at different times (measured from start-up end on) as reported in table 4.2 (*Px* samples) for any of the E1-3 recipes.

Sample ID	<i>E1</i>	<i>E2</i>	<i>E3</i>
P1	0	0	0
P2	11	15	16
P3	65	54	57
P4	151	134	132

Table 4.2: sampling time in minutes during in-flow emulsification

4.2.4. Rheological characterisation

Flow curves were performed using a controlled strain rheometer ARES-RFS (TA instrument, USA) equipped with a Couette Cylinder geometry (internal bob diameter 32 mm, gap 1 mm). Viscosity as a function of shear rate was measured at two temperatures 10 and 25°C , by using a thermostatic bath (Julabo, USA). The shear rate range was $1\text{--}100 \text{ s}^{-1}$ and preliminary “step shear rate” test at 1 s^{-1} , was performed to evaluate the time needed to reach the steady state before measurement. For all samples, a time of 10 s was found to be sufficient to reach the time independent viscosity value and steady shear viscosity was averaged over 10 s sampling time. All test were performed three times and flow curves of Bx samples were preceded by a pre-shear step (500s^{-1} for 180 s) in order to prevent phases separation during viscosity measurements.

4.3. Results and discussion

4.3.1. Oil and wax mixture

In table 4.3 the viscosity of wax-in-oil mixtures at 25°C are presented. It clearly appears that the wax addition does not determines any changes of the oily-phase viscosity, the total paraffin amount added to the oil being not high enough to thicken it.

<i>Wax content [w/w %]</i>	<i>Viscosity [mPa·s]</i>
0	155 ± 3
0.5	154 ± 3
1	154 ± 1

Table 4.3: oil-wax mixture viscosity at 25°C

4.3.2. Batch produced emulsions

Batch produced emulsions viscosity showed an apparent Newtonian behaviour [Gabriele et al., 2009]. Table 4.4 reports viscosity values averaged throughout the investigated shear rate range. A comparison with Table 4.3 shows that emulsification process reduces the viscosity at about one fifth of the waxy oil value. In addition, it is noteworthy that viscosity increases by adding 0.5% of wax, with respect to the pure-oil/water emulsion, whilst no further effect is observed when the wax content is increased up to 1%. As found by Li et al. (2009), the heat produced during the emulsification process makes the wax melt, while in the following cooling process, the wax crystallises near the oil/water interface, which protects the droplets from coalescence increasing therefore emulsions viscosity.

<i>Sample ID</i>	<i>Viscosity [mPa·s]</i>
B1	28.0 ± 0.5
B2	34.6 ± 1.3
B3	34.9 ± 1.3

Table 4.4: apparent Newtonian viscosity of batch produced emulsions at 25°C

4.3.3. In-flow produced emulsions

Table 4.2 reports sampling time for all the produced emulsion and the P_x ID is used throughout the text. It is important to clarify that the last sample (P4) is always collected after

the emulsification process completion, i.e. when emulsion showed apparent Newtonian behaviour and no further viscosity change were observed when increasing process.

Figure 4.5 shows viscosity evolution over time for sample E1, E2 and E3 respectively. For reader convenience, in the same plot is also reported the value of the correspondent batch prepared emulsion as well as the viscosity value of pure emulsion phases, water and (waxy) oil.

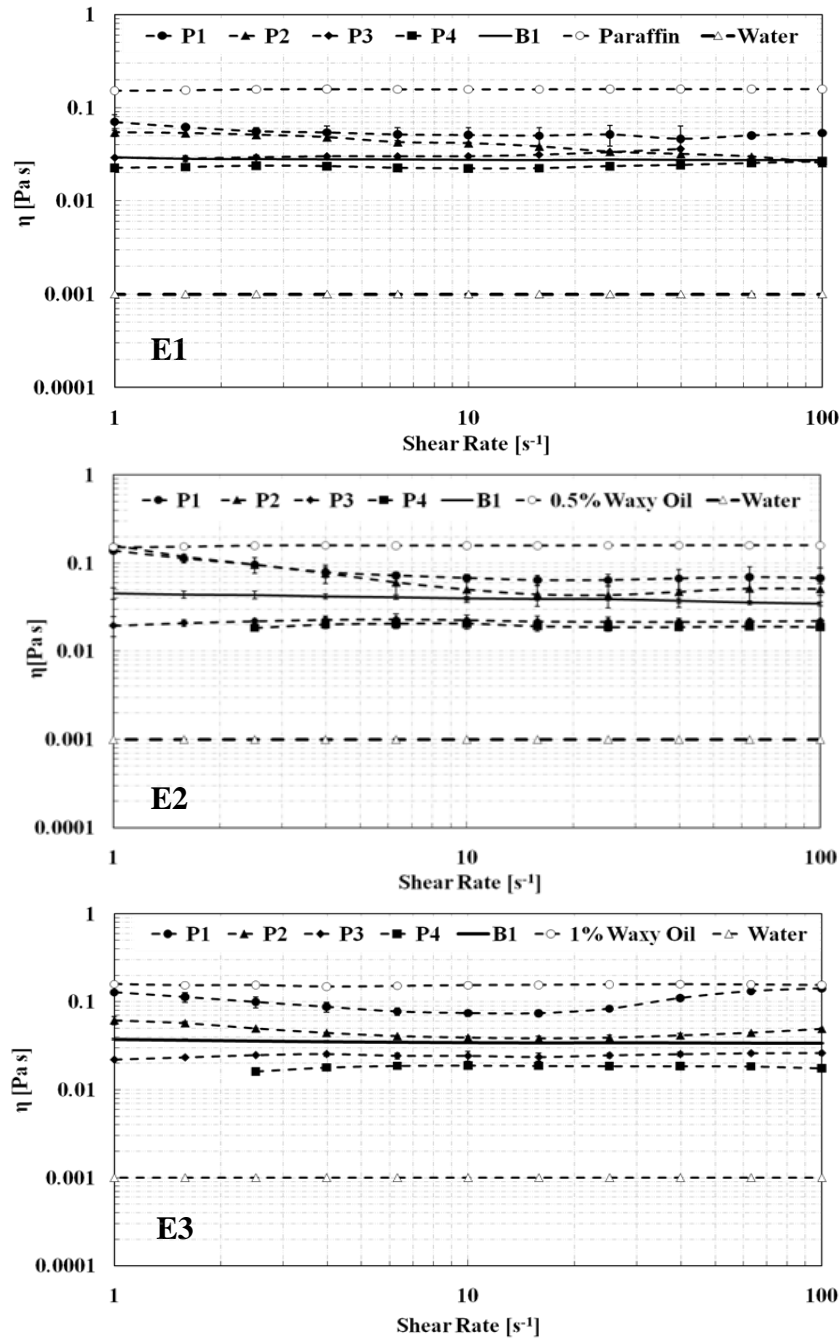


Figure 4.5: flow curves for tests E1, E2 and E3 compared to paraffin oil, 0.5% waxy oil and 1%waxy oil respectively and batch tests

All the investigated samples showed a decrease of viscosity when increasing the residence time in the emulsification loop. As for the viscosity data at low emulsification time (P1 and P2), the sample without wax exhibits an apparent Newtonian behaviour straightaway, indicating a good sample stability during measurements. On the contrary, samples prepared with waxy oil exhibit a decreasing-increasing viscosity path in the early stage of the emulsification process. This phenomenon indicates a poor material stability during measurements due to flow-induced drop size distribution change of the disperse phase caused by the destabilising effect of wax crystals formed at room temperature [Li et al., 2009]. On the contrary, when considering the time of emulsification completion (P4 data in Table 4.2), it clearly appears that the addition of waxes acts positively, as the time requested to achieve a time-independent viscosity value (assumed as indication of the emulsification process end) is significantly reduced. In fact, the addition of wax reduces of about 20 minutes the completion time (from 150 min of E1 sample) and this effect does not depend on the wax amount in the investigated range. Moreover, it can be seen that, especially for E2 and E3 samples, the “in-flow” test viscosity value under-crossed the batch test values. This evidence can be explained if the DSD (droplet size distribution) is considered [Ford et al., 1997]. In fact, drops of different dimensions allow a better dispersed phase packing and therefore viscosity decreases below the batch sample value as consequence [Barnes, 2000]. In addition the observed viscosity decrease could be ascribed to the increased drop dimension [Ford et al., 1997] due to coalescence phenomena.

Moreover, the effect of the wax addition can be observed when evaluating the ratio Ω of the apparent Newtonian viscosity of batch and long time in-flow process (P4).

$$\Omega = \frac{\eta_{Ex}|_{P4}}{\eta_{Bx}} \quad [4.1.1]$$

Data of table 4.5 shows that Ω decreases when increasing the wax content in the oily phase. Thus, wax addition allows the viscosity to be reduced during in-flow process. In addition, it is worthy of note that the phenomenon becomes more relevant as the wax amount is increased. If the emulsions are prepared at low temperature, as in the case of in-flow samples, at the added waxes concentrations ($\leq 1_{w/w}\%$), few crystals are present in the oily phase that cannot significantly reduce the oil droplets size acting as Pickering stabilisers and giving, therefore, low viscous systems [Li et al., 2009]. For emulsions produced at higher temperatures (the batch ones), wax melting and adsorption on oil/water interface is favoured by the heat produced during the emulsification process. This can produce smaller droplets leading to more viscous emulsions.

<i>Wax content [w/w %]</i>	<i>Ω [-]</i>
0	0.85
0.5	0.51
1	0.42

Table 4.5: final viscosity ratio of batch and in flow emulsification processes

Conclusions

In this paper the effect of waxes (long chain paraffinic compounds) on the viscosity of concentrated O/W emulsion is presented. The research work aims at supporting the knowledge in the field of “heavy oil” transportation techniques and waxes are one of the more relevant minor components in heavy oil. Model emulsions O/W were prepared and two different emulsification methods, batch and in-flow loop, were used in order to investigate the effect of different amounts of waxes in the oily phase. The addition of a small amount of wax did not affect the oily phase viscosity and this should be considered when analysing emulsion behaviour. Samples of O/W emulsion prepared in batch all exhibited a constant viscosity vs shear rate behaviour, whilst, during in-flow emulsification, time-dependent behaviour of viscosity was observed. This effect was found for the samples containing wax and at low process time. Therefore, it was concluded that, in the early stage of the emulsification, waxes seem to reduce the system stability under shear. As for the emulsification completion, it was observed that the wax addition reduces the time requested to reach a constant apparent Newtonian behaviour. This evidence did not depend on the amount, but only on the presence, of waxes. When comparing long term viscosity of the two emulsification methods, it was found that addition of wax promoted the viscosity drop of the emulsion prepared using the in-flow technique, with respect to the batch one. This effect was more evident when increasing the wax amount and can be attributed to a variation of the emulsion polydispersity in the two preparation methods and to the different thermal histories according to which the emulsions were prepared.

References

Ahmed N. S., Nassar A. M., Zaki N. N., Gharieb H. K., (1999). *Formation of fluid heavy oil-in-water emulsions for pipeline transportation*, Fuel, 78, 593-600

Al-Mulla, A., Gupta, R.K., (2000). *Droplet coalescence in the shear flow of model emulsions*, Rheologica Acta, 39, 20–25.

Al-Sahhaf, T. A., Fahim M. A., and Elsharkawy A. M., (2009). *Effect of Inorganic Solids, Wax to Asphaltene Ratio, and Water Cut on the Stability of Water-in-Crude Oil Emulsions*, Journal of Dispersion Science and Technology 30,597-604

Barnes H.A, (2000). *A handbook of elementary rheology*, The University of Wales, Institute of Non-newtonian Fluid Mechanics, Aberystwyth

Burger, E.D., Perkins, T.K., and Striegler, J.H. (1981). *Studies of Wax Deposition in the Trans Alaska Pipeline*, Journal of Petroleum Technology 33, 1075-1086

Coto, B., Martos, C., Peña, J. L., Espada, J. J., and Robustillo M. D., (2008). *A new method for the determination of wax precipitation from non-diluted crude oils by fractional precipitation*, Fuel 87, 2090-2094

Ford, D.L, Borwankar, R., Martin, R.W.jr, Holcomb, D.N., (1997). *Dressing and Sauces* in “Food emulsions” by S.E Friberg and K. Larsson, Marcel Dekker, Inc., New York, Basel

Gabriele D., Migliori M., Lupi F.R., de Cindio B., (2009). *Rheological study of o/w concentrated model emulsions for heavy crude oil transportation*, Energy Sources, Part A: Recovery, Utilization, and Environmental Effects, *in press*

Hannisdal A., Orr R., and Sjöblom J. (2007). *Viscoelastic Properties of Crude Oil Components at Oil-Water Interfaces. 1. The Effect of Dilution*, Journal of Dispersion Science and Technology 28,81–93

Kané M., Djabourova M., Volleb J.-L., Lechaire J.-P., Frebourg G. (2003). *Morphology of paraffin crystals in waxy crude oils cooled in quiescent conditions and under flow*, Fuel 82, 127–135

Langevin J. D., Poteau S., Hénaut I., Argillier J.F. (2004). *Crude oil emulsion properties application to heavy oil transportation*, Oil & Gas Science and Technology – Rev. IFP 59, 5, 511-521

Lee R. F., (1998). *Agents which promote and stabilize water-in-oil emulsions*, Spill Science & Technology Bulletin, 5, 117-126

Li C., Liu Q., Mei Z., Wang J., Xu J., and Sun D. (2009). *Pickering emulsions stabilized by paraffin wax and Laponite clay particles*. Journal of Colloid and Interface Science 336, 314–321

McLean J. D., Kilpatrick P. K., (1997). *Effects of asphaltenes solvency on stability of water-in-crude-oil emulsions*, Journal of Colloid and Interface Science 189, 242-253

Paso K., Silset A., Sørland G., de A. L. Gonçalves M., Sjöblom J., (2009). *Characterization of the Formation, Flowability, and Resolution of Brazilian Crude Oil Emulsions*. Energy & Fuels, 23, 471–480

Quiñones-Cisneros S. E., Andersen S.I., Creek J, (2005). Density and Viscosity Modeling and *Characterization of Heavy Oils*, Energy & Fuels, 19, 1314-1318

Saniere A., Hénaut I., and Argillier J.F. (2004). *Pipeline Transportation of Heavy Oils, a Strategic, Economic and Technological Challenge*. Oil & Gas Science and Technology 59, 455-465.

Thanh N. X., Hsieh M., and Philp R.P. (1999). *Waxes and asphaltenes in crude oils*. Organic Geochemistry 30, 119-132.

Visintin R. F. G., Lockhart T. P., Lapasin R., D'Antona P., (2008). *Structure of waxy crude oil emulsion gels*, J. Non-Newtonian Fluid Mech. 149, 34–39.

Wakabayashi T. (1997). *Viscosity correlation with specific gravity and molecular weight of crude oil fractions*, Fuel, 76, 1049-1056

Chapter 5 – Structuring water phase: olive oil emulsions as puff pastry shortening replacer

Abstract

Amongst the possible biphasic systems that can be produced with a high oil fraction, many efforts have been addressed to the study of structured food emulsions.

Structured emulsions are biphasic systems of one liquid dispersed in another immiscible one, where droplets interact in a network that play a crucial role in emulsion stability, rheology and microstructure. Owing to the possibility of controlling the structural properties, the design of food emulsions with improved kinetic stability and/or novel functional properties becomes possible. One of the possible applications of structured food emulsions is the production of olive oil-based systems as healthy foods. Amongst them, olive oil-based emulsions as shortenings replacers in puff pastry production are studied in the present work.

Puff pastry production uses high melting point “solid fats” (shortenings) based on hydrogenated fatty acids with mechanical properties suitable for sheeting or calendering processes. Because of their dangerous characteristics for consumers’ health, hydrogenated fats are being replaced, in many foods, by healthy products rich in unsaturated fatty acids and characterised by a low melting point, such as olive oil. They are liquid at room temperature and not suitable for a direct application in traditional industrial processes, thus, olive oil emulsions have been produced and characterised with the aim of designing healthy foods.

First of all, water-in-oil emulsions were prepared structuring the water phase with polysaccharides and trying to increase the final consistency in order to obtain a margarine-like product (from a rheological point of view). Considering that the most consistent W/O emulsion produced did not reach the desired consistency (even if a good structuration was obtained), other possible ways to produce the olive oil emulsion with the proper rheological characteristics were also investigated: fat crystallised W/O emulsions (discussed in the next chapter) and inverted O/W systems structuring the water phase with different kind of polysaccharides.

5.1. Introduction

5.1.1. Puff pastry and shortenings

Puff pastry, also called *pâte feuilletée*, or *pâte feuilletage*, is a dough which is spread with solid fats and repeatedly folded and rolled out. Thus, it consists of alternating layers of dough (wheat flour and water) separated by alternating layers of a solid-like fat, margarine, designed to obtain the proper rheological matching. The shortening is not mixed into the unleavened flour or dough but is placed on top of the dough and folded to form several alternating layers of dough and fat. The fat keeps the layers of dough separate and flaky and the moisture contributes the ‘puff’ as it turns to steam during the baking process [Ghotra et al. 2002].

In figure 5.1 the distinction of the alternate layers is well shown thanks to the microstructural image of a commercial puff pastry (Buitoni, Italy) performed by an NMR analysis on a Bruker Avance 300 (Bruker, Germany) wide-bore spectrometer equipped with a standard microimaging probe.

Belonging to the impulse sequence used to observe the proton signal, the intensity of the pixel brightness of the image can be related to the water quantity of the material (GEFI tests) or alternatively to the transverse relaxation time T_2 (MSME tests). Figure 5.1-A reports an MRI (magnetic resonance image) image of an axial section of puff pastry dough obtained with a GEFI experiment. The signal intensity is proportional, in this case, only to the proton density differences. As can be seen, the image shows the structure of the pastry, revealing the structural composition of the system composed of alternative layers of dough and fats. Figure 5.1-B shows an MRI image “weighed on T_2 ”, obtained by MSME experiments on the puff pastry. In this case the stratification of the aqueous dough is more evident with respect to the fat phase.

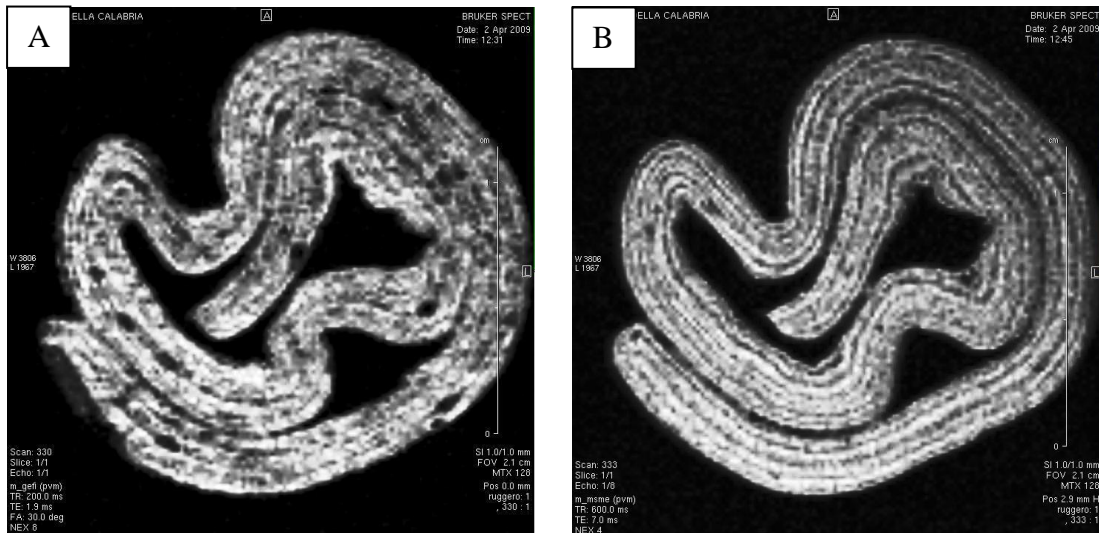


Figure 5.1: NMR image analysis of a commercial puff pastry

Margarines are W/O structured emulsions with a dispersed phase ratio of less than 20_{wt}%. If the water phase amount is higher than this threshold limit, W/O emulsions, called “spreads”, cannot be considered as margarines, but they can be commercialised as spreading shortenings [Borwankar, 1992].

The taste of margarines and food spreads is due to water-soluble flavours, oil soluble flavours and salt in the water phase [Blanco Muñoz, 2004]. The rheological characteristics are given by the high melting point of saturated fats in the oily phase; crystals interact and form a three-dimensional network surrounding water droplets and stabilising the biphasic system, giving a hard gel-like character to these foods.

The high consistency of margarine is obtained with a certain amount of fully saturated triglycerides (triglycerides or triacylglycerol are conveniently called TAGs) that allow a better molecular interaction and, as a consequence, a better packing (see paragraph 1.4.2, Chapter 1) giving a more ordered structure. The traditional process employed to saturate the TAGs is generally hydrogenation (described in the next chapter) from which *cis* and *trans* isomers (TFAs) can be obtained. In general, fats containing a majority of saturated fatty acids (SFA) are solid at room temperature, and those containing mostly unsaturated fatty acids (oils) are usually liquid at room temperature [Ghotra et al., 2002].

Different data indicates that TFAs are not metabolically equivalent to the natural *cis* isomers and that they promote the development of atherosclerosis and predispose to coronary heart disease and other not well-known risks [Blanco Muñoz, 2004]. The substitution of TFAs crystals with different rheological structures giving the same rheological characteristics but producing at the same time healthy foods is one of the most relevant problems for food designers [Norton, 2009].

Unlike margarines, olive oil is a mixture of different unsaturated triglycerides, mainly oleic acid (73% for the best quality oils), palmitic acid and linoleic acid [Azadmard-Damirchi, 2007]. Olive oil and products based on it are promoted as part of the Mediterranean diet which is currently viewed as making a favourable dietary contribution. Thus, in this respect, olive oil in the diet can be recommended, and has a positive image in terms of consumer appeal [Blanco Muñoz, 2004].

5.1.2. Structured emulsions: a brief introduction

The structuration of emulsions can be achieved by structuring the water phase with gelling agents and/or hydrocolloids [Rodriguez-Abreu and Lazzari, 2008], structuring the oily phase by fat crystallisation [Coupland, 2002] or by concentrating the dispersed phase up to volume fractions much higher than the volume fraction ϕ^* , corresponding to the closer packing of an equivalent suspension of hard spheres [Pal, 1998 a]. The rheological characterisation of the first group of materials is the aim of this chapter, while the second case will be treated in the next one.

The important function of many hydrocolloid ingredients as a stabiliser and structuring/thickening/gelling agent in the aqueous medium, in conjunction with added ‘weighting agents’ to match the densities of oil and aqueous phases is generally well recognised. The main effect of these additives, mainly polysaccharides, is based on the control of the rheology of the aqueous phase [Dickinson, 2003]. In figure 5.2 the chemical structure of two commonly used polysaccharides is shown.

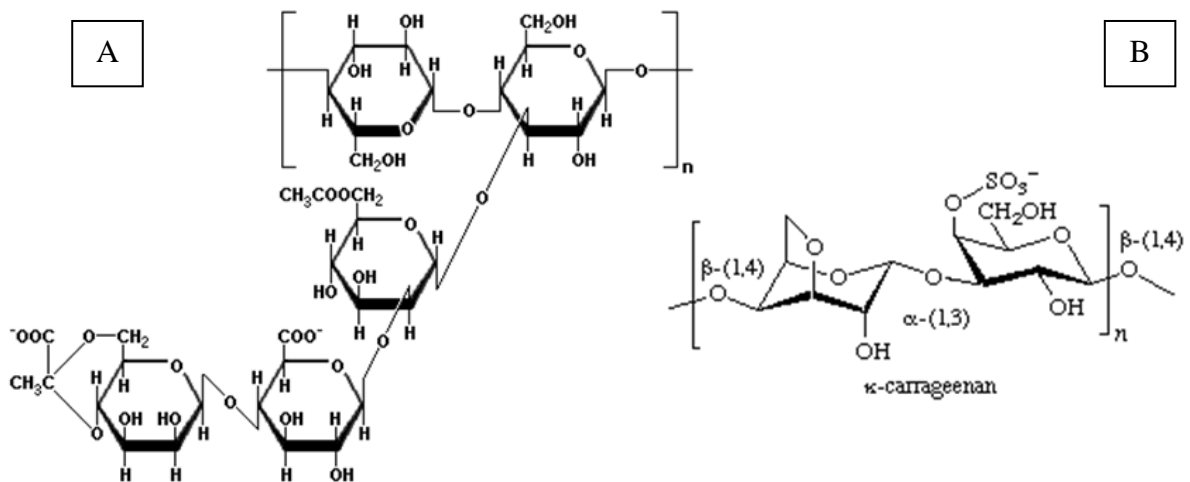


Figure 5.2: the repeating unit of Xanthan Gum (A) and κ -carrageenan (B)

In the figure 5.3 a schematic representation of emulsions is sketched [Kokini and van Aken, 2006]. If water is continuous phase, a structured emulsion can be imagined as an entangled polysaccharide network and the buoyancy force acting on each droplet is insufficient to overcome the yield stress of the surrounding gel giving a solid-like system [Leal-Calderon et al., 2007].

In the case of a dispersed water phase in a diluted system (made by non-interacting particles) on the contrary, an increase of its structuration leads to an increase of the emulsions viscosity up to a plateau value given by the Einstein's equation for suspensions [Toda and Furuse, 2006]. If the dispersed phase volume fraction is greater than the limit where the Einstein equation can be applied ($5_{v/v}\%$), droplets can interact and the rheological characteristics will be clearly different as a result giving a bulk viscosity that can overcome the plateau described by the Einstein equation. Moreover, a possible formation of interconnections between droplets, given by fat crystallisation, can give highly viscous emulsions even at low ϕ values.

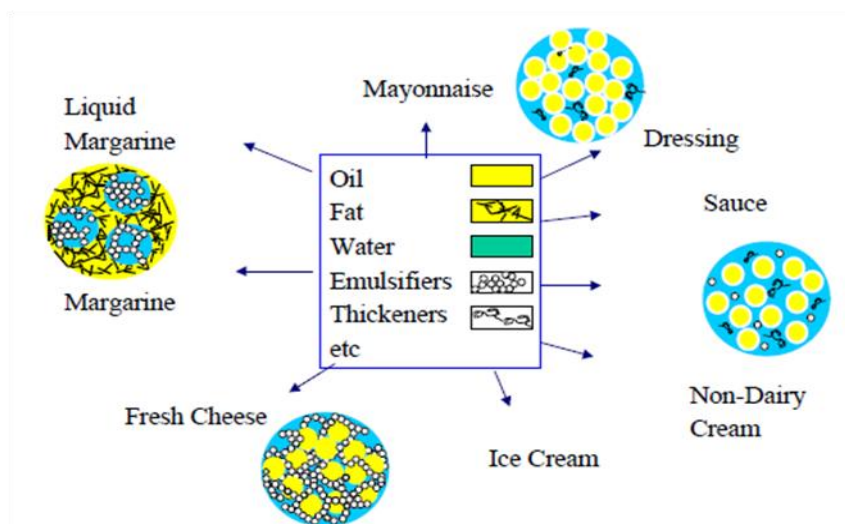


Figure 5.3: O/W and W/O typical scheme

Aiming at enhancing the viscosity of an emulsion, also the shape of the droplets have a crucial role in the rheological characteristics of emulsions and suspension. Marti et al. (2005) studied the effect of replacing part of the spherical particles in a non-Brownian suspension by fibre-shaped particles, finding a dramatic increases in the zero shear viscosity as a function of the mixing ratio and overall particle concentration; an evident increase in the relative viscosity η_r with the increase of fibre disperse particles with respect to the round-shaped ones was found. Similarly Walther et al. (2005) investigated the possibility of deforming κ -carrageenan aqueous solution drops in sunflower oil under shear flow in a smooth narrowing deformation channel of a fast continuous flow process

by quenching the system up to the gelling temperature. Therefore, they “froze” the droplet in a ellipsoid shape obtained by varying the flow conditions (and Capillary number) with the possibility of modifying the rheological properties of the emulsion or suspension. These systems, called “gelled emulsions” show a very interesting behaviour, allowing emulsions to be converted in a suspension of non-spherical droplets. [Wierenga et al. \(1998\)](#) described the rheological behaviour of aqueous dispersions of boehmite rods with two different aspect ratios affirming that those systems could form self-sustaining gels at very low particle volume fractions, as a function of the particle and lithium chloride concentration. Moreover, they found an increase of the elastic modulus increasing the volume fraction of the rods. In the present work gelled emulsions were prepared as W/O emulsion using gelling hydrocolloids in order to harden the water phase and change the rheological properties of the final system.

5.1.3. Interaction between the more common hydrocolloids and emulsions characteristics

Many authors studied the interactions of hydrocolloids with emulsifiers and the other components of emulsions in order to improve their stability and change the rheological properties. [Knoth et al. \(2005\)](#) studied water-in-sunflower oil emulsions stabilized by WPI (whey protein isolate) and Xanthan gum, finding that emulsions were more stable and smaller in droplet size when they contained WPI in water, and the droplet size was further reduced by combining WPI with Xanthan gum in the aqueous phase.

As far as O/W systems are concerned, [Romero et al. \(2008\)](#) studied Crayfish flour (source of proteins) stabilised O/W emulsions. They found that these emulsions followed a gel-like behaviour, characterized by G' being about one order of magnitude higher than G'' within the experimental frequency range. This behaviour was characteristic of highly concentrated emulsions showing bridging flocculation.

[Gu et al. \(2005\)](#) studied the influence of pH and carrageenan type (ι , κ and λ) on the stability of O/W emulsions, while [Singh et al. \(2002\)](#) focused attention on the production of O/W emulsions formed with mixtures of milk proteins and κ -carrageenan. The authors found that addition of κ -carrageenan up to 0.4_{w/w}%, before homogenisation, slightly increased the average droplet size. The addition of low levels of κ -carrageenan (< 0.2_{w/w}%) caused extensive flocculation of oil droplets, which resulted in very low creaming stability.

At higher κ -carrageenan concentrations, the creaming stability increased, apparently due to the formation of a network of flocculated droplet.

For O/W emulsions Xanthan gum is especially effective for its stabilising role. For low oil volume fractions the simple rheological control mechanism is most effective; in fact, individual droplets are separately immobilized in an entangled biopolymer network. For concentrated emulsions, emulsion stability and rheological characteristics strictly belong to the total amount of hydrocolloids in the aqueous phase. For very low concentrations (less than 0.1_{w/w}% for Xanthan Gum), the added hydrocolloid has a destabilising property because of the depletion flocculation induced by the non-adsorbing hydrocolloid that causes enhanced serum separation of the emulsion [Dickinson, 2009; Blijdenstein et al., 2004 a]. In fact, for beverages emulsions [Chanamai and McClements, 2006], the addition of polysaccharides like Dextran [Blijdenstein et al., 2004 b] or Arabic gum, that do not adsorb at the emulsion droplets, can induce a depletion interaction between the emulsion droplets and an increase in viscosity of the aqueous phase [Blijdenstein et al., 2004 b]. However, at higher added hydrocolloid concentrations (still <0.1_{w/w}% for Xanthan gum), when the depletion interactions are stronger, creaming is inhibited due to the viscoelastic character of the interconnected regions of emulsion droplets that have become flocculated into a gel-like network.

As mentioned before, the main purpose of the present work is the study of an olive oil emulsion with suitable rheological characteristics for a sheeting product. First of all, W/O gelled emulsions were studied where the internal phase is structured with wheat flour; in order to have a further increase of the consistency of the system, the system was inverted, producing more stable O/W emulsions with κ -carrageenan and Xanthan gum as gelling agents.

5.2. Materials and Methods

5.2.1. Samples ingredients and identification

First of all, W/O oil emulsions were prepared with mono- and di-glycerides of fatty acids by varying the water phase content up to a maximum weight concentration of 30% in order to produce an emulsion with a high oily phase percentage. The water phase was structured by adding different amounts of wheat flour (up to 10_{w/w}%). Then, the water phase (further structured with Xanthan gum and κ -carrageenan) was used in olive O/W

emulsions in order to study how the phase inversion can influence the rheological characteristics of an emulsion prepared with the same raw materials, but a different emulsifier agent (polyoxyethylene sorbitan monostearate) was used. The emulsification optimisation is one of the main purposes of the product design, aiming at obtaining rheological properties similar to those of commercial fats (also tested).

Samples preparation was performed using the following raw materials: as main constituents of the two phases, distilled water and a virgin olive oil (De Santis S.p.A., Italy); as emulsifiers mono- and di-glycerides of fatty acids (Myverol 18 04, Kerry Group, Ireland) and a polyoxyethylene sorbitan monostearate (Admul T60 K Kerry Group, Ireland), as stabilisers and structuring agent a commercial wheat flour (Barilla, Italy) and a thermal treated flour (kindly supplied by Soavegel s.r.l, Italy); moreover, two gelling agents (κ -carrageenan, Sigma, Germany and Xanthan gum, Danisco, Denmark) were used as gelling and thickening agents of the water phase. All samples, listed in table 5.1, were prepared with 3_{w/w}% of emulsifier in the oily phase (the maximum amount that can be used in a foodstuffs recipe according to Italian rules).

Aiming at reproducing the mechanical behaviour of commercial fats, a rheological characterisation of two different kinds of margarines, (Flora, Unilever, Spain and Vallè, France) was also performed. The first one (Flora) contains 20_{w/w}% olive oil, while the second one contains 18_{w/w}% butter.

Sample	Oily phase	Water+flour	Hydroc.	Hom. steps	Type of emulsions
Emu 1	90	9+1*	-	1	W/O
Emu 2	90	9+1	-	1	W/O
Emu 3	70	24+6	-	1	W/O
Emu 4	70	24+6	-	2	W/O
Emu 5	70	21+9	-	2	W/O
Emu 6	70	21+9**	-	2	W/O
Emu 7	70	21+9**	-	2	O/W
Emu 8	60	27+12**	1 (κ -carr.)	2	O/W
Emu 9	60	27+12**	1 (Xanth.)	2	O/W
Emu 10	60	21+9**	10 (κ -carr.)	2	O/W

Table 5.1: Samples identification. All quantities are reported in weight percentage. The symbol * indicates that the two phases were mixed at room temperature. The symbol ** indicates that structuration was achieved by using a treated (tempered) wheat flour

5.2.2. Samples preparation

A 200 g batch was prepared for all samples. The two different phases were obtained separately: the lipophilic emulsifier was added to the oil at 70°C for a mixing time of 5 minutes on a heating magnetic stirrer (Velp scientific, Italy), while preliminarily sieved flour (mesh 125 µm, Bicasa, Italy) and the structuring agents (when present) were added to the water at room temperature. For the first 6 samples listed in table 5.1, the emulsifier used (Myverol 18 04, HLB 3.7) was chosen for its capability to produce W/O emulsions [Constantinides and Yiv, 1994], while the high HLB value of the emulsifier used for the other samples (Admul T60 K, HLB = 15) gave O/W emulsions.

Sample *Emu 1* was prepared by mixing the two phases for 5 minutes at room temperature on a magnetic-heater agitator (Heating Magnetic Stirred, Velp Scientific, Italy), and heating up the heterogeneous systems to 70°C. The system showed an evident phase separation, therefore the same sample preparation was modified producing *Emu 2*. In this sample, first of all, the water phase (including the flour) was heated up to 70°C and maintained at this temperature for 2 minutes to allow the changing of the material toward more “solid-like” behaviour as a consequence of temperature induced starch gelatinisation and gluten network formation [Migliori et al., 2009]. After that the gelatinised water phase was mixed to the warm oily phase (for 5 minutes) and then further homogenised with a blades mixing device (Minipimer, Braun, Germany) for 10 minutes. Aiming at increasing the consistency of the sample (see the ‘result and discussion’ section), the structured water phase amount was increased from 10 to 30_{w/w}% and the flour mass fraction in the aqueous phase was doubled, obtaining the sample *Emu 3*. A further homogenisation step (sample *Emu 4*) guaranteed an evident increase in the sample consistency, therefore it was applied to all the other samples. The structuring effect of flour on the water phase was analysed in the emulsion *Emu 5*, where the mass fraction of flour was enhanced by 10%. Finally, *Emu 6* was produced by substituting the commercial wheat flour with an industrial thermal treated flour (with a small amount of salt included).

Despite the good results obtained with sample *Emu 6* from a the rheological point of view, the desired consistency was not reached with W/O systems, and therefore O/W emulsions made with the same raw materials (from sample *Emu 7* to sample *Emu 10*) were also studied. The samples *Emu 7* – *Emu 10* were prepared with Admul T60K that seems able to give a more homogenous structure at the first step of emulsification (performed with the centrifugal mixer IKA RW 20, Germany), which, as a consequence, was reduced to 60 s.

Sample *Emu 7* was prepared with the same quantities as sample *Emu 6*. Lowering the oily phase percentage, *Emu 8* was prepared increasing the structuring flour, and adding κ -carrageenan by means of a Hobart mixer (N-50 CE, Hobart, USA): the final aqueous phase therefore was composed of 2.5_{w/w}% κ -carrageenan, 30_{w/w}% flour and the rest of water. In sample *Emu 9* Xanthan gum instead of κ -carrageenan was used, and finally in sample *Emu 10* the consistency was further enhanced by a huge increase in the final κ -carrageenan amount. All samples were studied after a rest time of 24h at 5°C.

5.2.3. Rheological characterisation

The rheological characterisation of the samples *Emu 1/Emu 9* was performed using a controlled strain rheometer ARES-RFS (TA Instruments, U.S.A.). The rheometer was equipped with parallel plates geometry (parallel plates $\phi=50$ mm, gap=2 mm). The characterisation of the sample *Emu 10* was performed using a controlled stress rheometer DSR 500 (Rheometric Scientific, U.S.A.) equipped with serrated parallel plates ($\phi=40$ mm, gap=2mm). For both the rheometers the temperature control ($\pm 0.1^\circ\text{C}$) was guaranteed by a Peltier system acting under the lower plate. Finally, the rheological characterisation of the commercial margarine ‘Flora’ was performed with a controlled stress rheometer Mars (Haake, Germany) equipped with a serrated parallel plates geometry of $\phi=35$ mm with a gap of 2 mm.

Dynamic tests include a Strain (or Stress) sweep test at the fixed frequency of 1 Hz, in order to evaluate the linear viscoelastic range of the material. Frequency sweep tests were performed at constant strain (or stress) within the linear viscoelastic region in the frequency range 0.1-10 Hz. When materials are tested in the linear range, material functions do not depend on the magnitude of the stress, the magnitude of the deforming strain, or the rate of application of the strain [Steffe, 1996].

Both tests were performed at 20°C as a representative temperature for process conditions. In order to observe the structure evolution with the temperature, a dynamic temperature ramp test (Time cure) was also performed at the fixed frequency of 1 Hz, increasing the temperature from 20°C to 80°C in order to simulate cooking conditions with a rate of 1°C/min, and decreasing the temperature from 20°C to -10°C (20°C to -15°C for the O/W emulsions) with a rate of -1°C/min, in order to simulate freezing conditions. The applied strain (or stress) was adjusted according to the temperature change during the test in order

to guarantee the linear viscoelastic regime. The frequency sweep test analysis was carried out by applying the *Weak Gel* model.

According to [Gabriele et al. \(2001\)](#), rheological properties of the material can be obtained by considering the sample as a weakly structured 3-D network. The mechanical characteristics of this network are determined by considering the number of the interacting units inside the structure and the strength of the connections among them. At any temperature T , if the complex modulus G^* is considered as a combination of the elastic modulus G' and the dissipative one G'' , data can be fitted using a two-parameter power law:

$$G^*(T) = \sqrt{G'(T)^2 + G''(T)^2} = A(T) \cdot \omega^{1/z(T)} \quad [5.2.1]$$

According to the Weak Gel model, the parameter z is related to the number of interacting rheological units within the 3-D network and A is the strength of these interactions.

When A increases the interaction forces within the network are increasing whilst a high z value indicates a large number of interacting units cooperating and increasing the network connectivity. All data fitting was performed through Table Curve 2D Software (Jandel Scientific, USA).

As will be shown in the next paragraph of the present chapter, sample *Emu 10* has the best properties from a rheological point of view when compared with the commercial margarines. Aiming at giving a complete characterisation, the flow curve of sample *Emu 10* was also performed. Unfortunately a slippage at the solid interface was evident and the measurement became unreliable at high shear values.

To overcome these problems an approximate method of manipulating experimental data was used, based on the possibility of relating dynamic and shear data [[Peressini et al., 2002](#)]. It is well known that for several polymeric systems the so-called Cox–Merz rule applies [[Cox and Merz, 1958](#)] stating, as a rule of thumb, that complex and shear viscosity coincide by assuming:

$$\dot{\gamma} = \omega \quad [5.2.2]$$

In this case, instead of using this equation, the following one should be used:

$$\dot{\gamma} = a_{\dot{\gamma}} \omega \quad [5.2.3]$$

where $a_{\dot{\gamma}}$ is a shift factor. At low shear rate values, in addition to the viscosity data obtained by flow tests, it was possible to obtain some shear viscosity values at 20°C by performing creep tests at different applied stresses. In a creep test, material is subjected to a constant stress and the corresponding strain is measured as a function of time; thus, with this test it is possible to observe properly any eventual slippage phenomena and to

individuate the time necessary to reach the linear response to stress correspondent to the long time viscous flow of the material from which the Newtonian viscosity can be evaluated [Steffe, 1996].

The experimental data, reported in terms of creep compliance versus time, were analysed by using a one-element Kelvin–Voigt model [Gabriele et al., 2001, b]:

$$J(t) = J_0 + J_1 \left(1 - e^{-\left(\frac{t}{\lambda_{ret}}\right)} \right) + \frac{t}{\eta} \quad [5.2.4]$$

where J_0 is the instantaneous compliance, J_1 is the retarded compliance, λ_{ret} is the retardation time of the Kelvin component, and η is the Newtonian viscosity [Steffe, 1996]. From the inverse of the slope, η , of the creep test obtained after a long time, it is possible to calculate the shear rate

$$\dot{\gamma} = \frac{\tau_0}{\eta} \quad [5.2.5]$$

Thus the shear viscosity can be computed and reported in the same plot together with the dynamic complex viscosity defined as:

$$\eta^* = \sqrt{\eta'^2 + \eta''^2} \quad [5.2.6]$$

where

$$\eta' = \frac{G''(\omega)}{\omega} \text{ and } \eta'' = \frac{G'(\omega)}{\omega} \quad [5.2.7]$$

The steady shear viscosity and the dynamic one show a very similar slope, thus it is possible to overlap those curves by a horizontal shift. It is allowed even to make an adjustment of the slope [Rao, 1999], but in this case it was not necessary.

The obtained flow curve can be then modelled by a modified Cross model [Barnes et al., 1989] where the η_∞ plateau is not present.

$$\eta = \frac{\eta_0}{1 + (\lambda\dot{\gamma})^m} \quad [5.2.8]$$

in which η_0 refers to the asymptotic value of viscosity at very low shear rates, λ is a constant parameter with the dimension of time and m is a dimensionless constant.

All the tests were performed three times, and the average values with the correspondent standard deviations were evaluated.

5.3. Results and Discussion

5.3.1. Rheological characterisation of commercial margarines

In order to define a range of proper rheological characteristics of the final sample necessary to allow the sheeting process, the rheological characterisation of commercial

fats is proposed. As an example, the results of the oscillatory tests for the ‘Flora’ fat are reported in the figure 5.4 in terms of complex modulus G^* versus frequency at the indicated temperature (20°C). Both the investigated samples show a typical solid-like behaviour, the elastic modulus G' being always greater than G'' , the loss modulus, by almost an order of magnitude in a log–log plot of dynamic moduli versus the applied frequency. Moreover, an almost linear trend in the tested frequency range for the moduli is encountered.

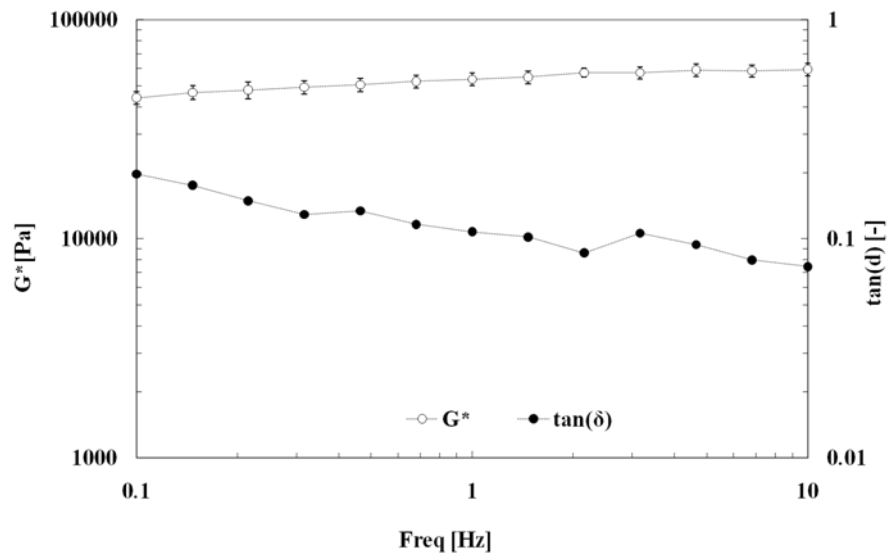


Figure 5.4: frequency sweep test of the commercial margarine ‘Flora’

The Weak Gel model parameters obtained by the equation [5.2.1] for both the samples are reported in figure 5.5.

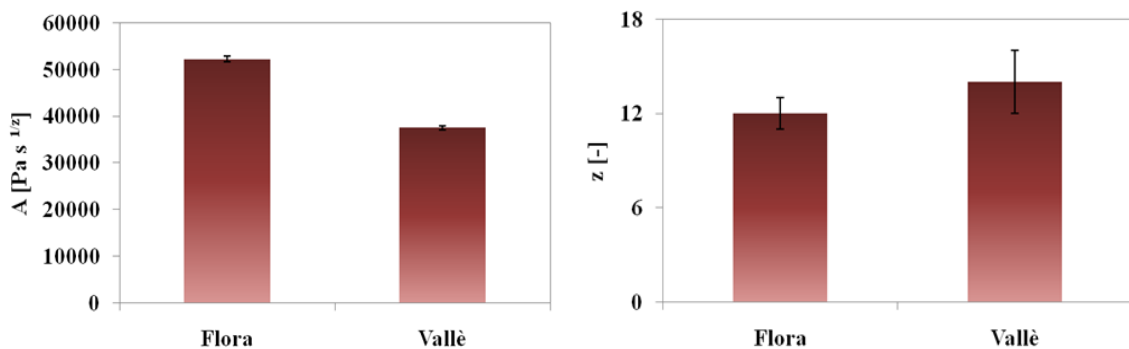


Figure 5.5: Weak Gel model parameters for two commercial fats

It can be deduced from the results shown that the two samples show a different strength but more or less the same extension of the network, indicating a possible range into which the properties of the produced sample should fall.

5.3.2. Rheological characterisation of the W/O emulsions

Sample *Emu 1* was not characterised because of its high instability encountered after a few hours from preparation.

After a rest time of 24h, a visual inspection of sample *Emu 2* revealed an increase in consistency.

The strain sweep tests at different temperatures for sample *Emu 2* are reported in figure 5.6: the linear viscoelastic region is not affected by the temperature change, and a constant strain value of 0.063% was chosen and set also for the temperature cure test.

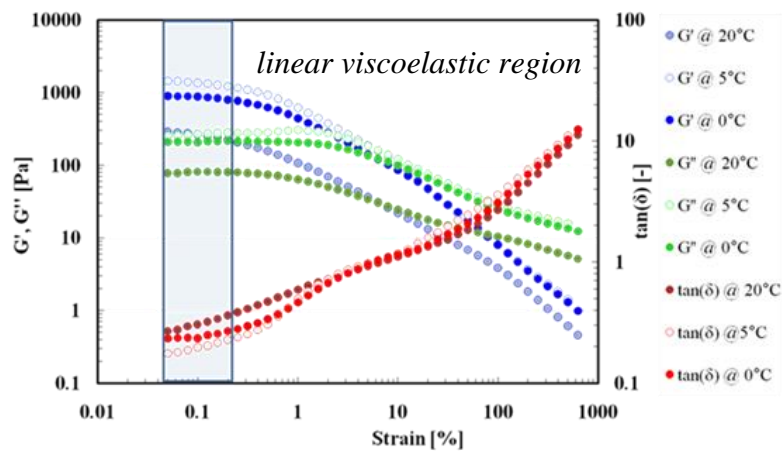


Figure 5.6: Strain sweep tests at different temperatures for sample *Emu 2*

After the evaluation of the linear viscoelastic region, a frequency sweep test was performed and it is reported in figure 5.7.

The frequency sweep test of the sample shows a solid-like behaviour, with a $\tan(\delta)$ value always lower than 1.

The parameters A and z are respectively $A = 240 \pm 2 \text{ Pa}\cdot\text{s}^{1/z}$ and $z = 5.2 \pm 0.2$, very far from the rheological characteristics required.

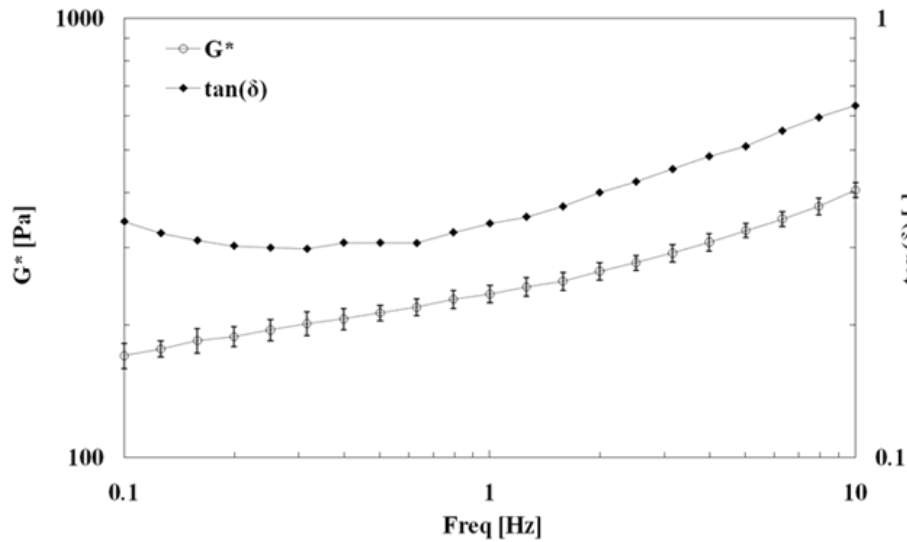


Figure 5.7: Frequency sweep test at 20°C for sample *Emu 2*

The Time cure test for sample *Emu 2* is reported in figure 5.8.

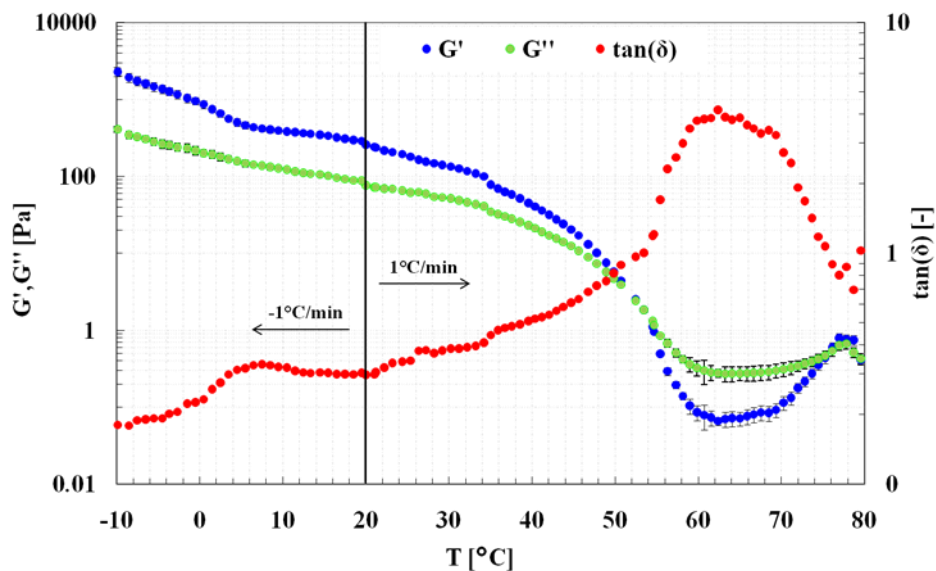


Figure 5.8: Temperature cure test for sample *Emu 2*

It can be noticed that from the lower temperatures to about 52°C the moduli show a constant decrease with G' being always greater than G'' , thereby confirming the solid-like behaviour. A crossover is then encountered at about 52°C, where G'' is higher than G' , and a new inversion is evidenced at 60°C after a further increase in both moduli, owing to a probable further gelatinisation of the starch not completed in the preparation step of the aqueous phase.

Aiming at increasing both the strength and the extensions of the network, sample *Emu 3* was prepared increasing the structured water phase amount (from 10 to 30_{w/w}%) and the mass fraction of flour in the aqueous phase. A comparison between the frequency sweep tests of these two samples is then proposed in figure 5.9.

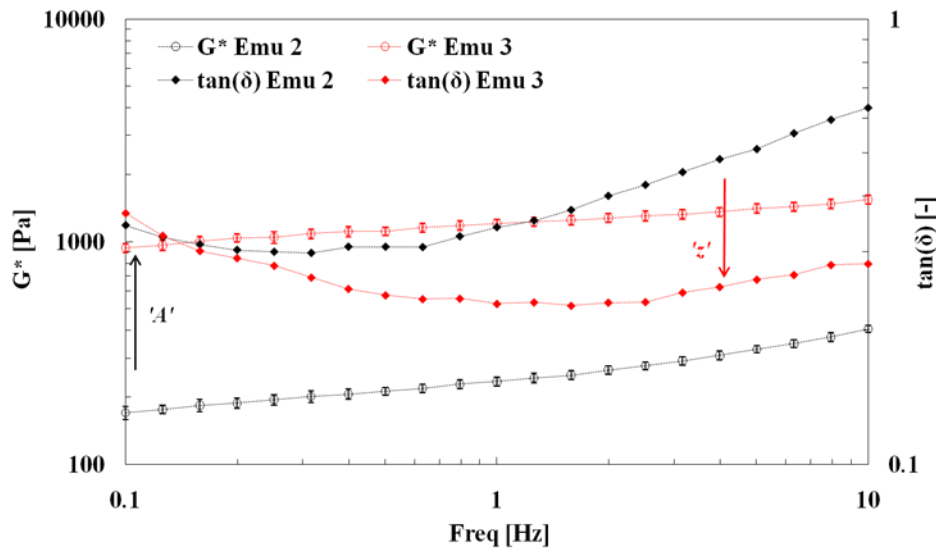


Figure 5.9: Frequency sweep test at 20°C: a comparison between samples *Emu 2* and *Emu 3*

As a result of the aqueous phase structuration (increase of flour amount) and the increase of the dispersed phase mass fraction there is a ‘thickening’ of the sample, as can be deduced by the upper shift of the G^* curve of *Emu 3* with respect to *Emu 2*. Contemporarily an increase in bulk ‘structuration’ (extension of the network) is given by the lowering of the curve describing the loss tangent.

An interesting result can be deduced if samples *Emu 3* and *Emu 4* are compared: both the samples are, in fact, produced with the same formulation, but in the second one a further homogenisation step is performed at room temperature. The homogenisation at room temperature can improve the rheological characteristics because the shape of the particles and diameter of the final sample produced with the previous step was modified by the second step of homogenisation (increasing the moduli values as a consequence) [Walther et al., 2005; Erni et al., 2009]. In fact, it is probable that the water phase, more consistent and structured at a lower temperature, can be ‘broken’ under the effect of the mixing device into irregular shaped particles that allow a worst packing, enhancing the bulk consistency as a consequence [Ford et al., 1997]. Indeed, it is known from the literature data that the rheological behaviour of aqueous dispersions of fibres [Wierenga et al., 1998] or ‘shaped drops’ [Walther et al., 2004] (that allow a low packing degree) form self-sustaining gels with an increased elastic modulus. Moreover, other tests not shown (unpublished data) revealed a better action of the used emulsifier at a low temperature.

In figure 5.10 a microscopic image of sample *Emu 4* is shown. The picture was taken with a contrast phase microscope (Leica DHIL, Germany).

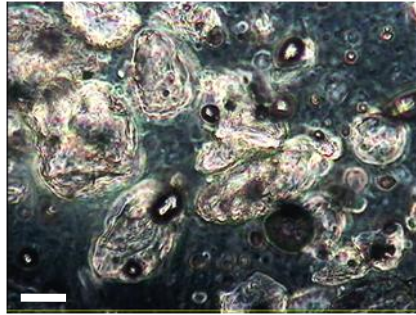


Figure 5.10: Particles distribution for sample *Emu 4* observed with contrast phase microscopy: the control bar is 50 μm

As can be observed in figure 5.11, the second homogenisation step is able to increase the strength of the network by about one order of magnitude (big increase of the complex modulus), on the contrary slightly decreasing its extension (slight decrease of the $\tan(\delta)$ curve).

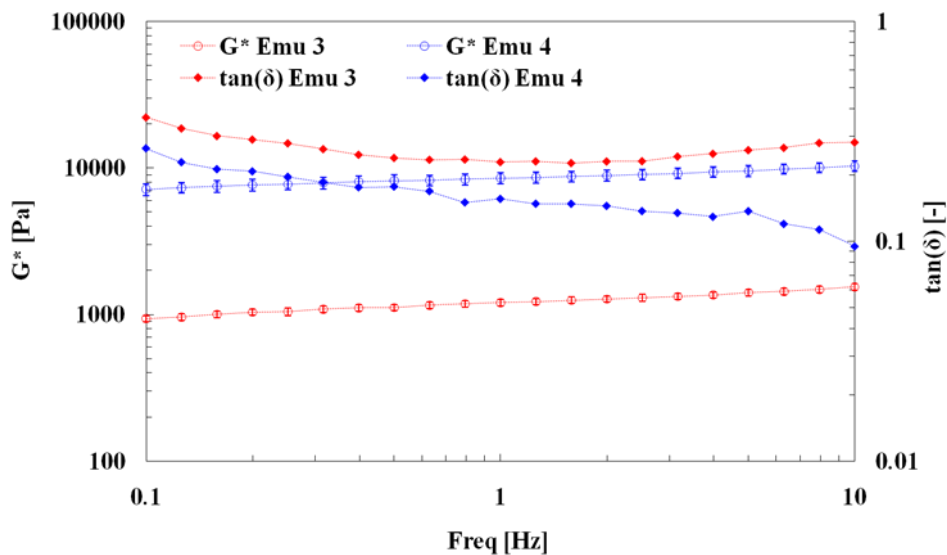


Figure 5.11: Frequency sweep test at 20°C: a comparison between samples *Emu 3* and *Emu 4*

The effect of the increase of the structuring agent (flour) on the mechanical characteristics of the emulsion was analysed with sample *Emu 5*. As can be noticed in figure 5.12, the final characteristics of the emulsion presented in terms of complex modulus and loss tangent are only slightly influenced by the structuration of the inner phase.

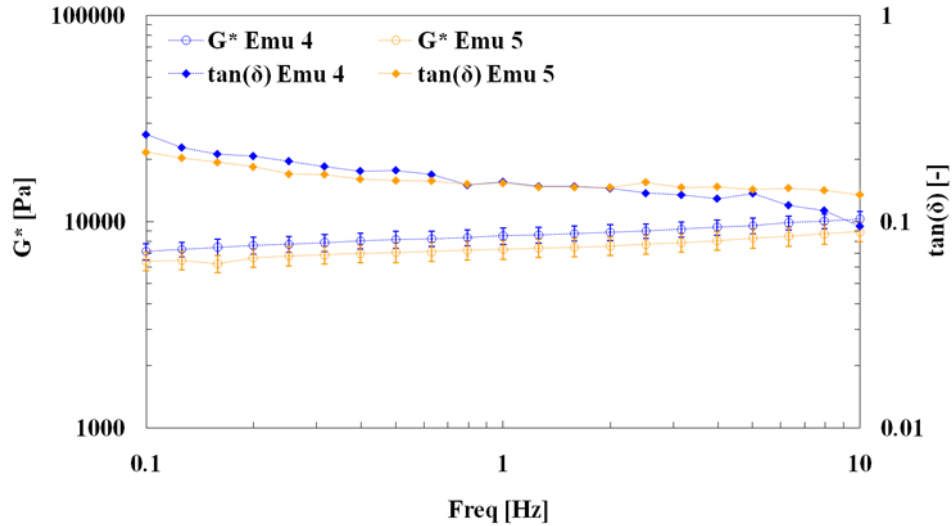


Figure 5.12: Frequency sweep test at 20°C: a comparison between samples *Emu 4* and *Emu 5*

The last W/O emulsion studied was produced by simply substituting the commercial wheat flour with an industrial thermally treated flour (with added salt). As a result the frequency sweep test of the two compared emulsions is reported in figure 5.13.

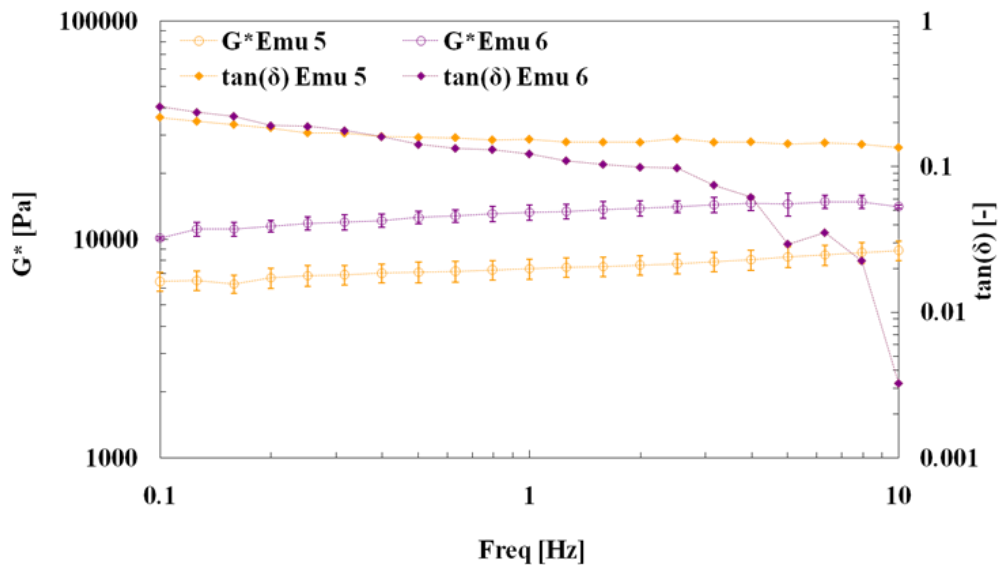


Figure 5.13: Frequency sweep test at 20°C: a comparison between samples *Emu 5* and *Emu 6*

The treated flour is able to increase the complex modulus value without drastically changing the phase angle. The $\tan(\delta)$ curves of both the samples are, in fact, almost similar: the unexpected decrease of the curve referred to *Emu 6* at higher frequencies is due to the decrease of G'' modulus, probably attributable to slippage phenomena. The temperature cure test for this sample is shown in figure 5.14.

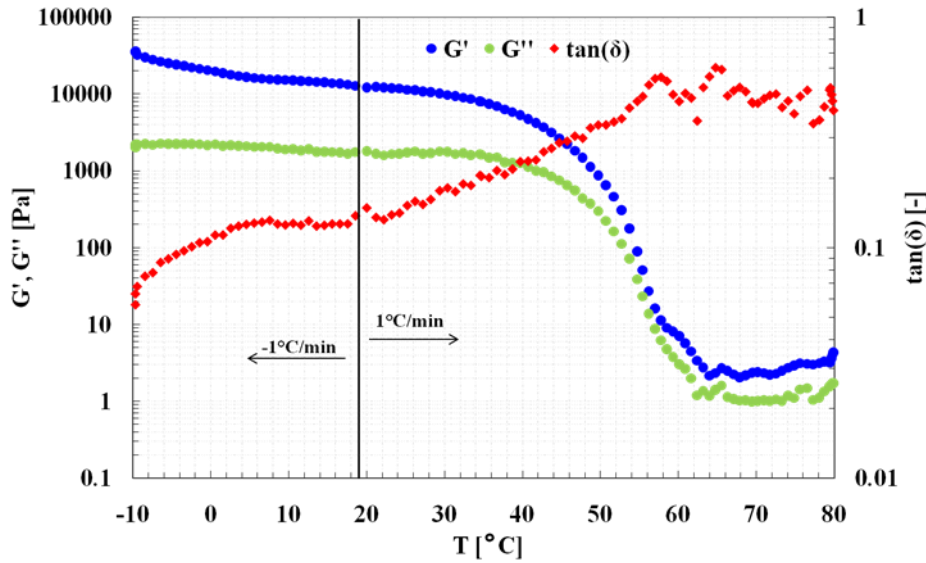


Figure 5.14: Temperature cure test for sample *Emu 6*

In this case the sample shows a solid-like behaviour for all the whole tested range, and unlike sample *Emu 2*, it does not indicate a cross between the moduli curves. Thus, the thermal treatment to which the flour was subjected clearly affected the structure of the whole system, which appears more consistent and which does not show any further gelatinisation effect.

In figure 5.15, all Weak gel parameters are presented in order to give a final overview of the obtained results.

The strength of the network (parameter A) correspondent to the W/O gelled emulsions does not reach the value of the two commercial margarines, even in the case of the more consistent sample *Emu 6* at the investigated temperature. Nevertheless, as far as the z parameter is concerned the difference between the samples and the margarine is much lower, indicating a proper structuration of the samples given by the network extension. Thus, it is clear that these emulsions can be employed in the sheeting process used for pastries production only after a profound change of the conventional devices and/or process operative variables.

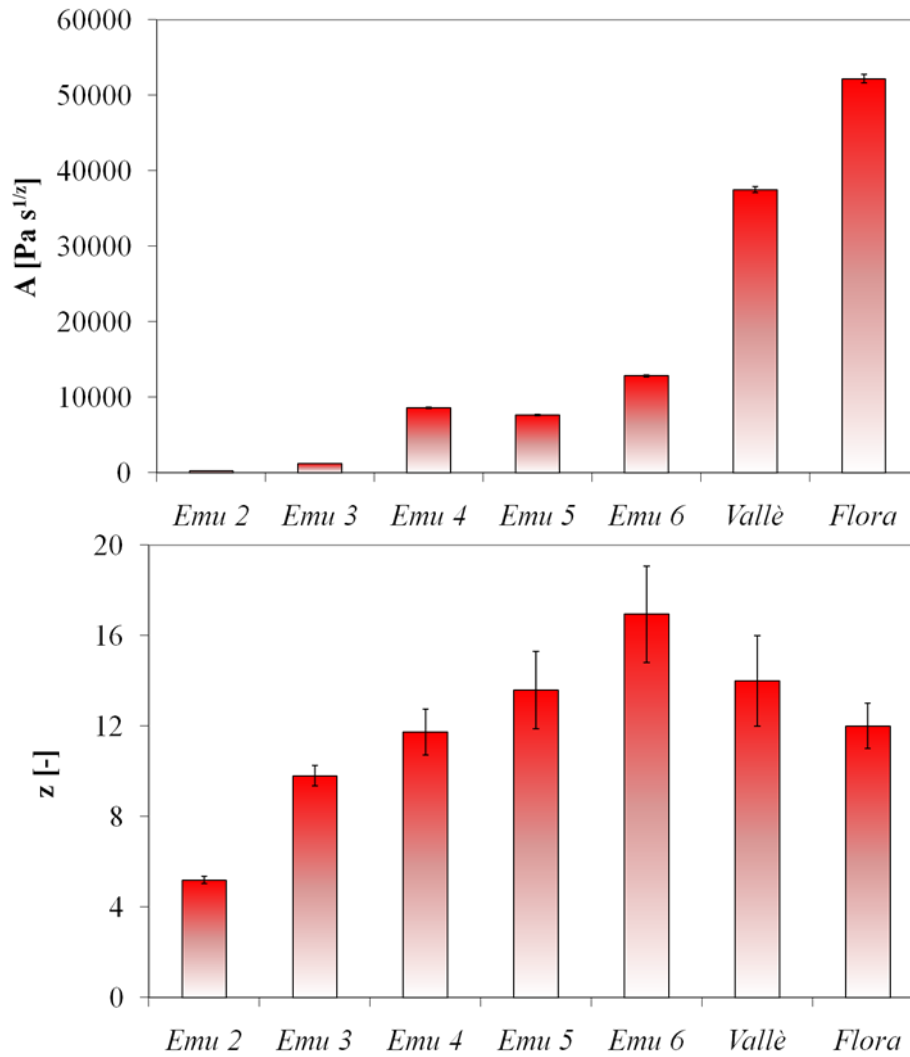


Figure 5.15: Weak gel model parameters histogram for all the investigated W/O samples

5.3.3. Rheological characterisation of the O/W emulsions

Sample *Emu 6* is the most consistent W/O emulsion obtained. A further increase of the water phase, or a great deformation of the droplets inside the continuous phase could probably enhance the mechanical properties of the system giving more similar characteristics to those of a commercial margarine. Nevertheless, it seems very difficult to obtain such a huge increase of the consistency of the sample without a fundamental changing on the emulsion properties. For this reason, O/W emulsions were produced changing the emulsifier with a new one that could give stability to the samples even after the first step of emulsification. The O/W emulsions are not gelled, and thus there is no need to further emulsify the sample with the second step of homogenisation. Moreover, two different hydrocolloids were added in order to create a structured emulsion by

constructing a network of interacting unities. Sample *Emu 7* was prepared with the same quantities as sample *Emu 6*, but the first step of homogenisation was reduced to 60 s.

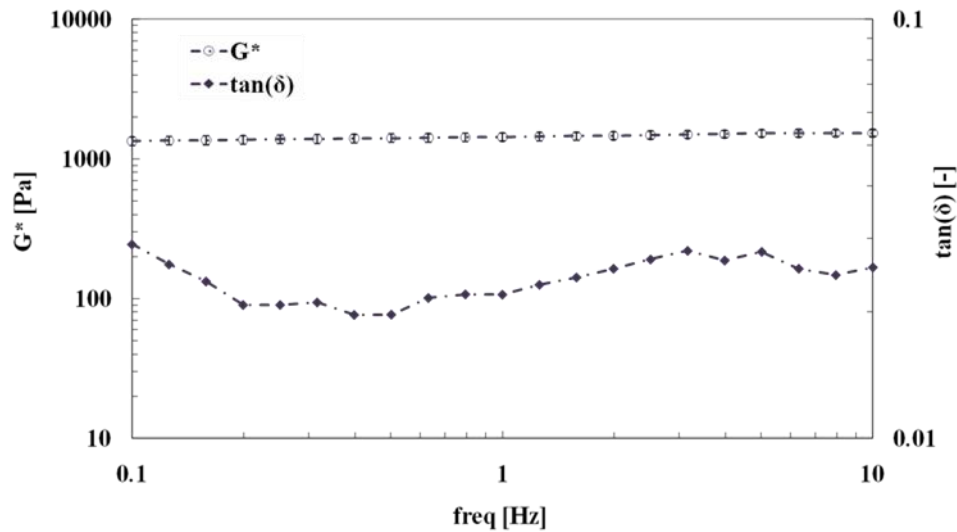


Figure 5.16: Frequency sweep test at 20°C of sample *Emu 7*

As shown by figure 5.16, the investigated sample is characterised by a lower consistency with respect to sample *Emu 6* (lower value of the G^* modulus at all the investigated range of frequency). The $\tan(\delta)$ curve is always lower than 1, evidencing a solid-like behaviour. The Weak gel parameters of this sample are $A=1460 \pm 13 \text{ Pa}\cdot\text{s}^{1/z}$ and $z=18 \pm 2$. As a consequence the phase inversion has a strong effect on the rheological characteristics of the emulsion, lowering the final consistency of the sample but increasing its structuration. The sample behaviour at the lower temperatures is described by the plot in figure 5.17-A. It is evident that the O/W emulsion shows a sudden increase of both the moduli at -8.5°C circa, probably due to the freezing effect of the external water phase, which is not encountered in the W/O emulsions, where the water phase is more “protected” against freezing. Moreover, Ghosh et al. (2006) affirm that O/W emulsions frequently show considerable oiling-off following a freeze-thaw cycle, owing to the freezing of the outer phase.

In this particular case the same sample was subjected to a freeze-thaw cycle (cooling from 20°C to -15°C at $-1^\circ\text{C}/\text{min}$, rest time at -15°C of 5 minutes and thawing from -15°C to 20°C at $1^\circ\text{C}/\text{min}$) in order to test the stability of the sample. Figure 5.17-B shows, as a result, that there are no changes in the G^* modulus and $\tan(\delta)$ at $T>12^\circ\text{C}$ after the whole cycle, guaranteeing a good stability of the product in the temperature range of consumption improved by the flour action on the emulsion.

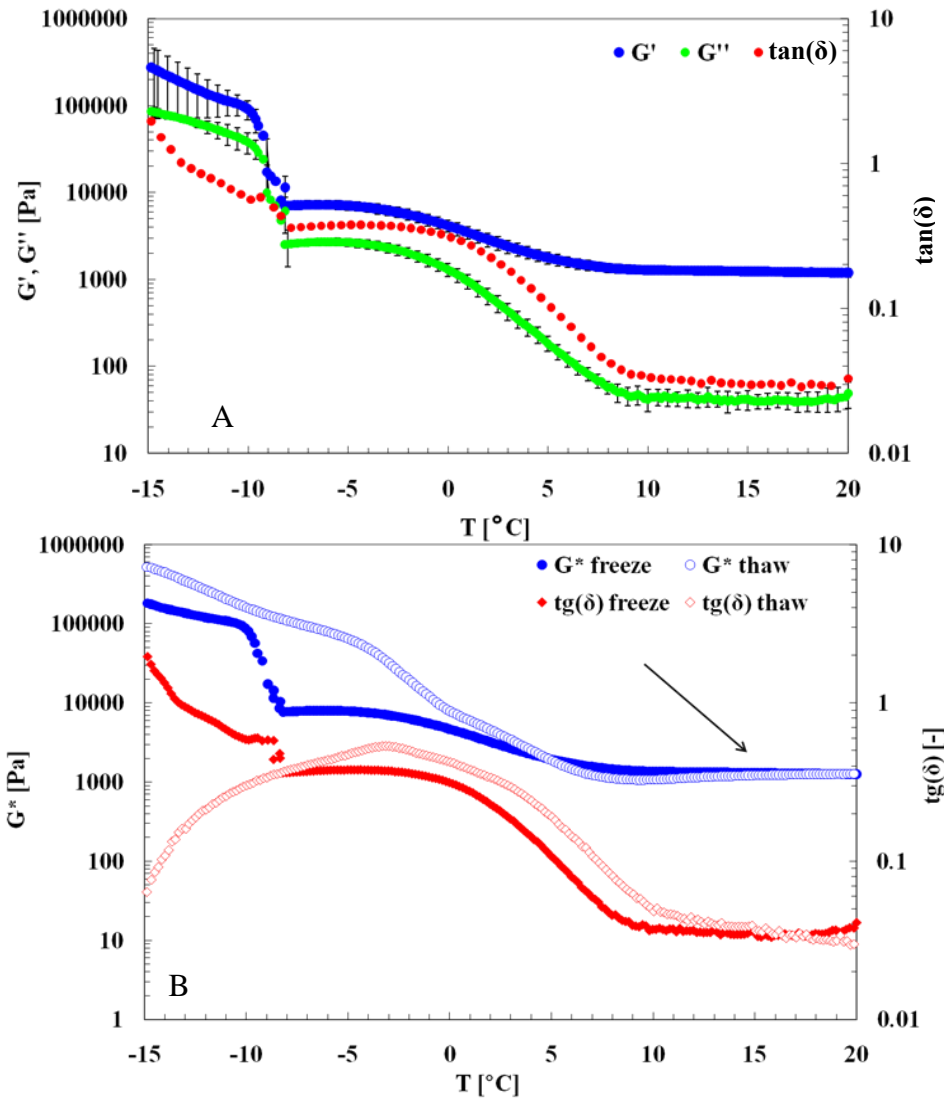


Figure 5.17: Temperature cure test for sample *Emu 7* (A), freeze and thaw cycle (B), in this last figure the standard deviation bar is omitted for a better readability.

In emulsion *Emu 8* the water phase was augmented: even if the emulsion moduli are increased by the internal phase volume fraction increase [Pal, 1998 b], it was decided to strengthen the network by adding more water phase and, as a consequence, more structuring agents in the system adding 1_{w/w}% of κ -carrageenan. This hydrocolloid is commonly perceived to slow down or even prevent creaming by modifying the rheology of the continuous phase. In O/W emulsions, in fact, this simple rheological control mechanism is most effective at low oil volume fractions, where individual droplets are separately immobilized in an entangled biopolymer network [Dickinson, 2009]. Thus, as expected, sample *Emu 8* showed a higher consistency and structuration with respect to sample *Emu 7* (figure 5.18), giving the weak gel parameter $A=3830 \pm 40 \text{ Pa}\cdot\text{s}^{1/z}$ and $z = 22 \pm 3$. Emulsion *Emu 9* was structured with Xanthan gum. The Weak gel parameter obtained where $A=2990 \pm 15 \text{ Pa}\cdot\text{s}^{1/z}$ and $z= 22 \pm 2$.

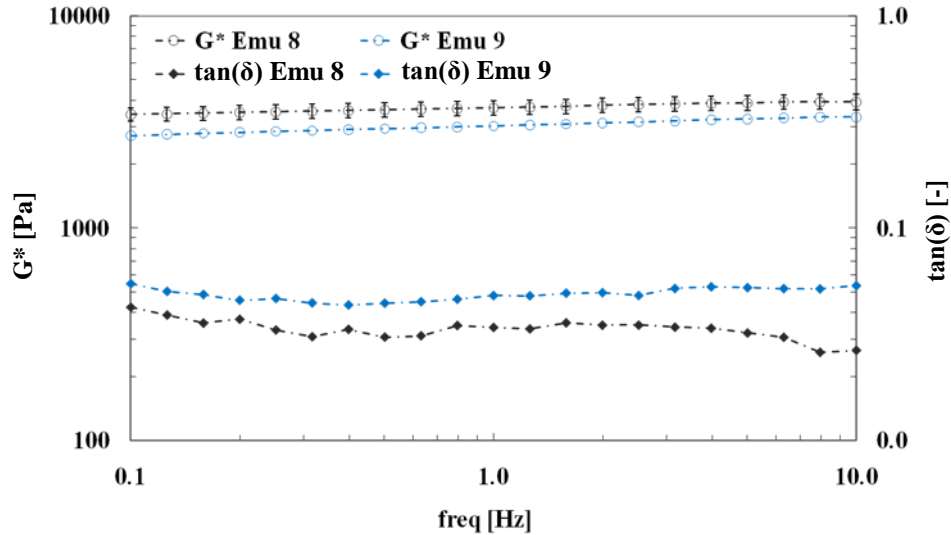


Figure 5.18: Frequency sweep test at 20°C: a comparison between samples *Emu 8* and *Emu 9*

The sample is less consistent than the one prepared with the carrageenan, while the structuration remains the same, confirming that carrageenan exerts a greater effect on the elastic behaviour of the samples with respect to xanthan gum, because of its gel-forming properties response [Rodríguez-Hernández and Tecante, 1999]. For this reason, aiming at increasing the parameter A , it was chosen to use a large amount of κ -carrageenan (10_{w/w}%), obtaining $A=30300 \pm 300 \text{ Pa}\cdot\text{s}^{1/z}$ and $z=10 \pm 1$ (sample *Emu 10*).

For this sample the flow curve (figure 5.19) was obtained by matching the apparent viscosities evaluated by the creep tests, the oscillatory tests and the flow curve tests in the same plot. The shift factor is $a_{\dot{\gamma}} = 0.048$.

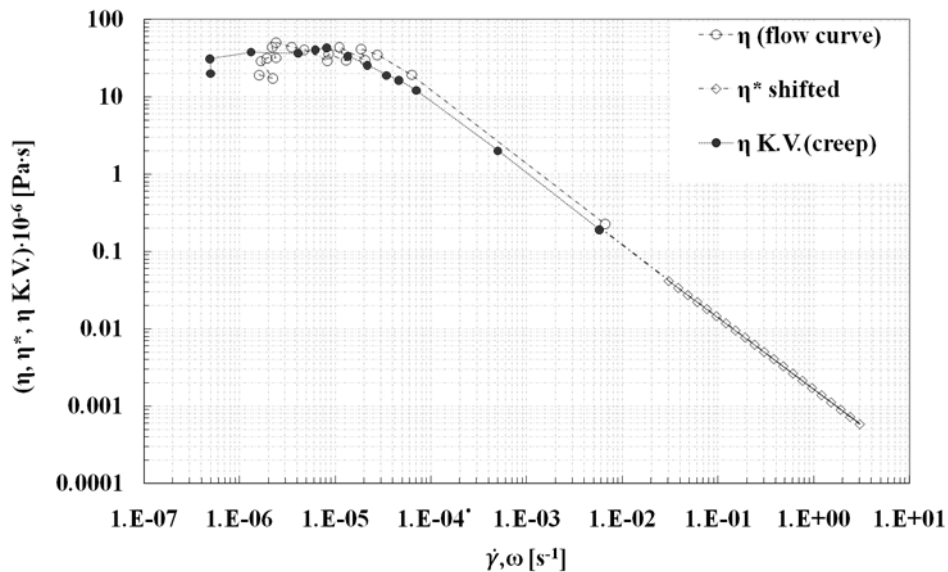


Figure 5.19: flow curve for sample *Emu 10*

The modified Cross parameters (eqn. [5.2.8]) for this sample are reported in the following table 5.2.

Sample	η_0 [Pa·s]	λ [s]	m [-]
Emu 10	$3.4 \cdot 10^7 \pm 3.4 \cdot 10^6$	$3.0 \cdot 10^4 \pm 9.3 \cdot 10^3$	0.97 ± 0.38

Table 5.2: Modified Cross model for viscosity correlation

The huge increase of gelling agent allowed a big increase to be obtained in the consistency of the system. It is worth noticing that the increase of structuring agents gives a lower value of the network extension, really similar to that of the commercial margarine.

The aqueous phase of sample *Emu 10* is a very strong gel, much more difficult to mix to the oily phase with respect to samples *Emu 8* and *Emu 9*, if the same mixing conditions are chosen. In fact, an increase in the specific energy should be required to produce emulsions with a higher viscosity of the continuous phase [Romero et al., 2008]. This can justify the lowering of parameter z , owing to structural change of the sample characteristics. While the samples previously described can be considered as gelled emulsions (*Emu 1 – Emu 6*) or structured emulsions (*Emu 7 – Emu 9*), the last produced sample can be defined as a very strong network where the oily phase is entrapped.

In order to summarise the obtained results, in the diagrams in figure 5.20, the Weak Gel parameter values are reported.

Therefore, it seems that the emulsion *Emu 10* has better sheetable properties, having rheological characteristics similar to one of the two commercial fats (Vallè). Moreover, some sheeting tests were performed on a calendering machine in the ‘Soavegel s.r.l. Company’ (Brindisi, Italy) revealing a good rheological matching with the wheat dough, but a failed ‘puff’ process of the dough: the emulsion is probably absorbed by the dough because of its inner structure (the oil should be the continuous phase). This suggested W/O emulsions should be produced with a structured oily phase, which will be presented in the next chapter of the present work.

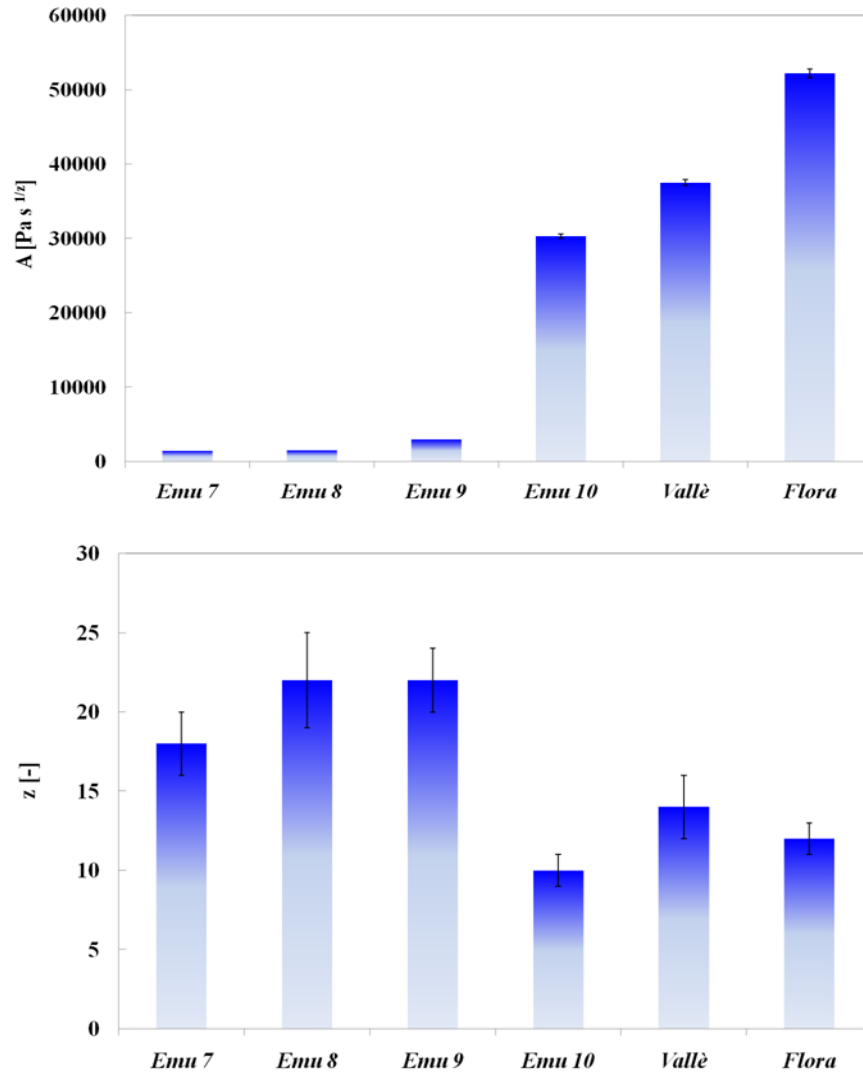


Figure 5.20: Weak gel model parameters histogram for all the O/W samples investigated

Conclusions

In the present chapter two different kinds of emulsions are studied in order to obtain a shortening replacer for puff pastry production. To this purpose, interesting conclusions have been drawn on the rheology of W/O gelled emulsions and O/W structured emulsions with a high percentage of oily phase. In the first case gelled emulsions were obtained structuring the water phase with wheat flour. Two kinds of wheat flour were tested revealing better thickening properties of the thermal treated one, as confirmed by the temperature cure test. An improvement of both the consistency and the structuration of the samples were guaranteed by a second step of homogenisation performed at room temperature, probably owing to the effect that the mixing device has on the dimension and shape of the particles. An increase of the dispersed phase mass fraction enhances the rheological properties of the sample in W/O emulsions.

A phase inversion was obtained using a hydrophilic emulsifier: the resulting O/W emulsion was less consistent and more structured than the W/O one. Finally, the effect of two different hydrocolloids were tested, and the κ -carrageenan gives a more consistent system with respect to the Xanthan gum without changing its structuration. The sample showing the more appropriate rheological properties was an O/W emulsion with the 10_{w/w}% of κ -carrageenan characterised by the same structuration and a consistency of the same order of magnitude as a commercial margarine.

References

- Azadmard-Damirchi S., (2007). *Olive Oil - Phytosterols, Tracing of Adulteration with Hazelnut Oil and Chemical Interesterification*, Doctoral thesis, Swedish University of Agricultural Sciences, Uppsala, Acta Universitatis Agriculturae Sueciae 2007, 36
- Barnes H.A., Hutton J.F., Walters K. (1989). *An Introduction to Rheology*. Elsevier Science Publishers B.V., Amsterdam, NL
- Blanco Muñoz M. A. (2004), *Olive oil in food spreads*, *Grasas y Aceites* 55, 92–94
- Blijdenstein T. B. J., Veerman C., van der Linden E., (2004) a. *Depletion–Flocculation in oil-in-water emulsions using fibrillar protein assemblies*, *Langmuir*, 20, 4881–4884
- Blijdenstein T.B.J., Zoet F.D., van Vliet T., van der Linden E., van Aken G.A., (2004) b. *Dextran-induced depletion flocculation in oil-in-water emulsions in the presence of sucrose*, *Food Hydrocolloids* 18, 857-863
- Borwankar R.P., Frye L. A., Blaurock A.E., Sasevich F.J., (1992). *Rheological characterization of melting of margarines and tablesreads*, *Journal of food engineering* 16, 55–74
- Chanamai R. and McClements D.J, (2006). *Depletion Flocculation of Beverage Emulsions by Gum Arabic and Modified Starch*, *Journal of Food Science*, 66, 457–463
- Constantinides P.P. and Yiv S.H., (1994). *Particle size determination of phase-inverted water-in-oil microemulsions under different dilution and storage conditions*, *International Journal of Pharmaceutics*, 115, 225–234
- Coupland J.N., (2002). *Crystallization in emulsions*, *Current Opinion in Colloid and Interface Science* 7, 445–450

- Cox W. P. and Merz E. H., (1958). *Correlation of dynamic and steady flow viscosities*. Journal of Polymer Science 28, 619-622.
- Dickinson E., (2003). *Hydrocolloids at surfaces and the influence on the properties of dispersed system*, Food Hydrocolloids, 17, 25–39
- Dickinson E., (2009). *Hydrocolloids as emulsifiers and emulsion stabilizers*, Food Hydrocolloids 23, 1473–1482
- Erni P., Cramer C., Marti I., Windhab E. J., Fischer P., (2009). *Continuous flow structuring of anisotropic biopolymer particles*, Advances in Colloid and Interface Science, 150, 16–26
- Ford, D.L, Borwankar, R., Martin, R.W.jr, Holcomb, D.N., (1997). *Dressing and Sauces* in “Food emulsions” by S.E Friberg and K. Larsson, Marcel Dekker, Inc., New York, Basel
- Gabriele D., Curcio S., de Cindio B. (2001) b. *Optimal design of single screw extruder for liquorice candy production: a rheology based approach*. Journal of Food Engineering, 48, 33–44
- Gabriele D., de Cindio B., D’Antona, P., (2001) a. *A weak gel model for foods*. Rheol. Acta 40, 120-127
- Ghosh S., Cramp G.L., Coupland J.N., (2006). *Effect of aqueous composition on the freeze-thaw stability of emulsions*, Colloids and Surfaces A: Physicochem. Eng. Aspects 272, 82–88
- Ghotra B.S., Dyal S.D., Narine S.S., (2002). *Lipid shortenings: a review*, Food Research International, 35, 1015–1048
- Gu Y. S., Decker E.A., McClements D. J., (2005). *Influence of pH and carrageenan type on properties of b-lactoglobulin stabilized oil-in-water emulsions*, Food Hydrocolloids 19, 83–91
- Knoth A., Scherze I., Muschiolik G., (2005). *Stability of water-in-oil-emulsions containing phosphatidylcholine-depleted lecithin*, Food Hydrocolloids 19, 635–640
- Kokini J., van Aken G, (2006). *Discussion - Discussion session on food emulsions and foams*, Food Hydrocolloids 20, 438–445

- Leal-Calderon F., Thivilliers F., Schmitt V., (2007). *Structured emulsions*, Current Opinion in Colloid & Interface Science 12, 206–212
- Marti I., Höfler O., Fischer P., Windhab E., (2005). *Rheology of concentrated suspensions containing mixtures of spheres and fibres*, Rheol Acta, 44, 502–512
- Migliori M., Gabriele D., Baldino N., Lupi F. R., de Cindio B., (2009). *Rheological properties of batter dough: effect of egg level*, Journal of Food Process Engineering, *in press*
- Norton I.T., Spyropoulos F., Alex E., Heuer K., Le Reverend B.J.D., Cox P.W., (2009). *Microstructure engineering of healthy everyday foods*, Proceeding of the 5th International Symposium on Food Rheology and Structure, Zurich 15- 18 June, 10-16
- Pal R., (1998) a. *A novel method to correlate emulsion viscosity data*, Colloids and Surfaces A: Physicochemical and Engineering Aspects, 137, 275–286
- Pal R., (1998) b. *Short communication-Scaling of viscoelastic properties of emulsions*, Chemical Engineering Journal 70, 173–178
- Peressini D., Sensidoni A., Pollini C. M., Gabriele D., Migliori M., de Cindio B., (2002). *Filled-snacks production by co-extrusion-cooking. Part 3. A rheological-based method to compare filler processing properties*, Journal of Food Engineering 54, 227–240
- Rao M. A., (1999). *Rheology of fluid and semisolid foods. Principles and applications*. Gaithersburg, MD: Aspen Publishers
- Rodríguez-Abreu C., Lazzari M., (2008). *Emulsions with structured continuous phases*, Current Opinion in Colloid & Interface Science 13, 198–205
- Rodríguez-Hernández A.I. and Tecante A., (1999). *Dynamic viscoelastic behavior of gellan-*l*-carrageenan and gellan-xanthan gels*, Food Hydrocolloids 13, 59–64
- Romero A., Cordobés F., Puppo M.C., Guerrero A., Bengoechea C., (2008). *Rheology and droplet size distribution of emulsions stabilized by crayfish flour*, Food Hydrocolloids 22, 1033–1043
- Romero N., Cárdenas A., Henríquez M., Rivas H., (2002). *Viscoelastic properties and stability of highly concentrated bitumen in water emulsions*, Colloids and Surfaces A, 204, 271–284

Singh H., Tamehana M., Hemar Y., Munro P.A., (2003). *Interfacial compositions, microstructures and properties of oil-in-water emulsions formed with mixtures of milk proteins and k-carrageenan: 1. Sodium caseinate*, Food Hydrocolloids 17, 539–548

Steffe J.F., (1996). *Rheological methods in food process engineering*, Freeman Press, Michigan

Toda K., Furuse H., (2006). *Extension of Einstein's viscosity equation to that for concentrated dispersion of solutes and particles*, Journal of Bioscience and Bioengineering 102, 524–528

Walther B., Cramer C., Tiemeyer A., Hamberg L., Fischer P., Windhab E. J., Hermansson A.M., (2005). *Drop deformation dynamics and gel kinetics in a co-flowing water-in-oil system*, Journal of Colloid and Interface Science 286, 378-386

Walther B., Hamberg L., Walkenström P., Hermansson A.M., (2004). *Formation of shaped drops in a fast continuous flow process*, Journal of Colloid and Interface Science 270, 195–204

Wierenga A., Philipse A.P., Lekkerkerker H.N.W., (1998). *Aqueous Dispersions of Colloidal Boehmite: Structure, Dynamics, and Yield Stress of Rod Gels*, Langmuir, 14, 55-65

Chapter 6 – Structuring oily phase: water in olive oil emulsions as puff pastry shortening replacer

Abstract

Margarines used in puff pastry production derive their consistency from a fat crystal network obtained with a certain amount of fully saturated triglycerides (TAGs). TAGs allow a better molecular interaction and packing to give a more ordered structure. Traditionally TAGs saturation is performed by hydrogenation from which *cis* and *trans* isomers (TFAs) can be obtained. In particular TFAs raise the plasma levels of total and low-density lipoproteins (LDL), while decreasing the plasma level of high-density lipoproteins (HDL). Their presence promotes the development of atherosclerosis and a predisposition to coronary heart disease and other not well-known risks [Blanco Muñoz, 2004]. In general, fats containing a majority of saturated fatty acids (SFA) are solid at room temperature, and those containing mostly unsaturated fatty acids (oils) are usually liquid at room temperature [Ghotra et al., 2002].

Olive oil is a typical ingredient of the Mediterranean diet, and it is recognised as a healthy food. From a rheological point of view it is a Newtonian liquid and it cannot be used in the traditional sheeting process. The production of emulsions with a structured water phase as an olive oil shortening replacer was considered in the previous chapter. Nevertheless, the aim of the present work is the production and the rheological and microstructural characterisation of W/O emulsions (shortenings) structuring the oily phase with a natural *trans-free* fat source. A previous unemulsified oily phase characterisation is presented, in order to clarify the effect of added hard fats and emulsifier on crystallisation and its effect on emulsions rheology. It is clear that these emulsions should be highly concentrated in oil in order to guarantee the lubrication of the alternating layers of dough of puff pastries (see the previous chapter for a more detailed description).

6.1. Introduction

6.1.1. Margarine and margarine substitutes: a state of the art

Structuring W/O emulsions is a well-known technique for puff pastries shortenings production. Margarine is one of the best known fats for leavening and baking products. Its production process passes through different steps aiming at obtaining W/O emulsions with a dispersed phase ratio less than 20_{w/w}%. The rheological characteristics are given by the high melting point of saturated fats in the oily phase organised in crystals aggregates that form an interacting ordered structure. Therefore, these aggregates form a three-dimensional network surrounding and stabilising the water droplets, and giving a hard gel-like character to these foods (Figure 6.1).

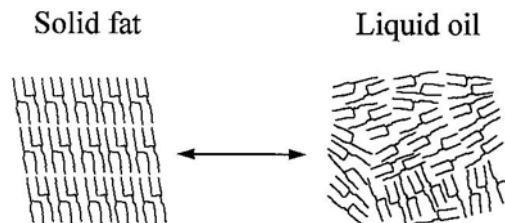


Figure 6.1: a comparison between the structure of solid hard fats (ordered) and liquid oil (disordered)

In the figure 6.2 an image of a commercial margarine is proposed: it is well visible the inner structure of the system.

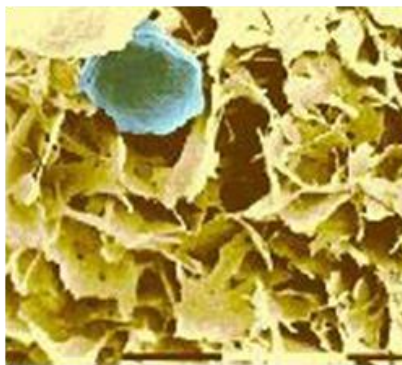


Figure 6.2: fat crystalline network (yellow) and a water droplet (blue) in a margarine observed by Cryo-Scanning EM. The shell around the water droplet has a crystalline structure. The open spaces in the structure indicate the areas where oil had originally been present before it was removed during the preparation of the sample for electron microscopy

Three different methods are currently employed in food processing industries in order to obtain the hardening of the oily phase:

- partial hydrogenation of vegetable oils
- catalytic interesterification of vegetable oils and completely saturated fats

- addition of solid fats materials to the starting liquid oil

The most used technique among those listed before, is the catalytic hydrogenation of double bounds of the unsaturated fatty acids chains. Industrial hydrogenation of vegetable oil (fish oil occasionally) is a process involving three phases (gas–solid–liquid) carried out in a batch autoclave over nickel based catalyst as a slurry at 110–190°C, 30–70 psi H₂ pressure, with 0.01– 0.15_{wt}% Ni [Singh et al., 2009]. The process may imply the movement of double bonds in their positions on the fatty acid carbon chain, producing positional and geometrical isomers, *trans* fatty acids (TFAs, figure 6.3), dangerous for consumers' health [Blanco Muñoz, 2004].

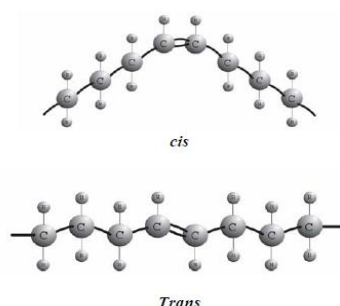


Figure 6.3: *cis*- and *trans*- configuration of a fatty acid

A more detailed introduction about this argument was already treated in the 1st chapter of the present PhD thesis work (paragraph 1.4.2).

As already said, in the case of W/O emulsions one of the methods that could be applied to enhance their mechanical characteristics is the addition of hard fats in the oily liquid phase with an opportune emulsifier and stabilising agent.

Jahaniaval (2005) in his patent suggests a recipe for the preparation of healthy margarine and butter substitutes based on liquid oils (at room temperature) like olive oil and phospholipids as stabilisers. The final consistency of the resulting margarine is increased by mixing at high temperature the oil and added hard fat like cocoa butter. Skogerson et al. (2007) propose the emulsification of W/O emulsions with a glyceride emulsifier having an elevated di-glyceride portion especially useful in preparing puff pastry products.

Mono- and di-glyceride of fatty acids are very common emulsifiers widely employed in food industry. They are produced by the reaction of glycerol with vegetal oil and fats, whose composition strictly depends on the characteristics of the starting fruit from which the oil is obtained [Clogston et al., 2000]. This lipophilic emulsifier has a HLB value of about 3.7 allowing the formation of W/O emulsions [Constantinides & Yiv, 1994; Friberg, 1997].

The molecules of mono- and di-glyceride of fatty acids are characterised by a hydrophilic water-attracting head and a hydrophobic water-rejecting tail and exhibit a specific aggregation behaviour determined by their geometry (Figure 6.4). The more interesting way in the structuring of food products is the one involving more or less cylindrically shaped molecules (Figure 6.4-B). In that case emulsifiers like mono- and di-glyceride can enclose water layers between bi-layered structures, which give rise to a so-called lamellar phase (Figure 6.4-D) [<http://www.isaac-heertje.nl/structure/>].

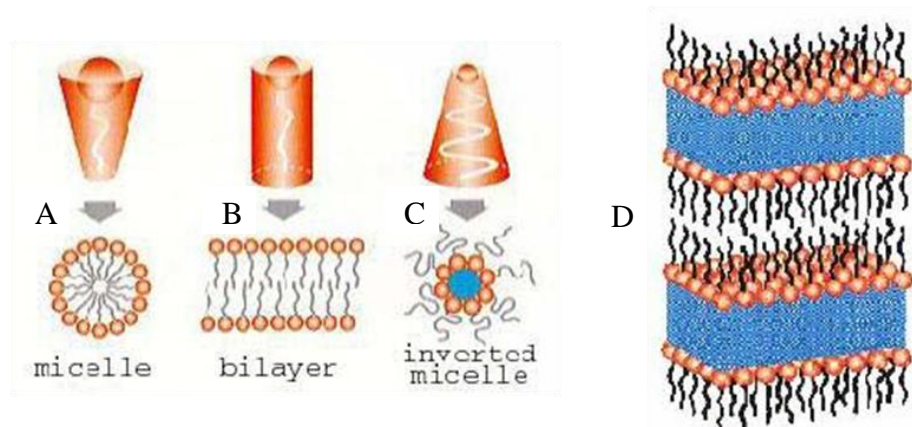


Figure 6.4: A - Head group larger than the tail: micelle formation in water; B – Cylinder-shaped molecule: formation of parallel bi-layers; C – Head group smaller than the tail: formation of inverted micelles enclosing water; D – Schematic drawing of a lamellar phase

The interaction between emulsifiers and fat crystals is not very clear. One of the probable interpretations is shown in the schematic picture of figure 6.5. Here the stabilisation mechanism of fat particles linked to the emulsifier molecules is reported: belonging to [Garti et al. \(1998\)](#) emulsifiers are the molecular bridges that allow the fat crystals to be linked to the dispersed phase droplets. It is clear that the fat particles play an important role in the Pickering stabilisation mechanism.

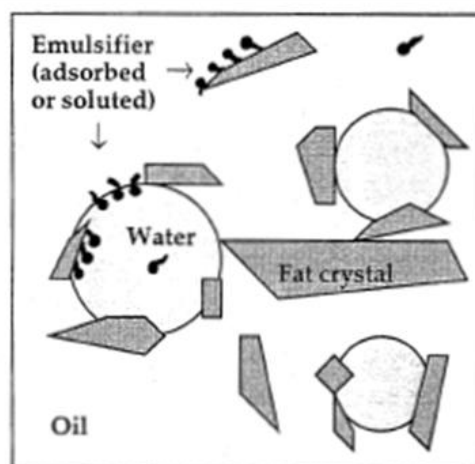


Figure 6.5: a schematic picture of margarine structure: interaction between water droplets, fat crystals and emulsifiers

Olive oil and products based on it are worldwide recognised as healthy foods and promoted as part of the Mediterranean diet which is currently viewed as making a favourable dietary contribution. Therefore, in this respect, olive oil can be recommended in the diet, and has a positive image in terms of consumer appeal.

Although the product “margarine with olive oil” still exists in foreign market, the maximum percentage of olive oil contained into these original recipes is 21_{w/w}%. In table 6.1 some different brands of shortenings containing olive oil are listed; the total amount of olive oil is reported on a weight basis.

Brand	made in	Name	% olive oil
Biona	U.S.A.	<i>Organic Olive Extra Spread</i>	12.7
Migros	Switzerland	<i>Margarine Sanissa Olive</i>	15
Kaiku-Benecol	Spain	<i>Margarina con Aceite de Oliva</i>	15
Flora (Unilever)	Spain	<i>Margarina Oliva</i>	20
Bertolli	Italy	<i>Spread Olive Oil</i>	21

Table 6.1: some brands of olive oil shortenings in the foreign market

Olive oil is a mixture of TAGs of different fatty acids, mainly oleic acid (about 73_{w/w}% for extra-virgin oil), palmitic and linoleic acid [<http://www.oliveoilsource.com>].

Obviously the exact composition of the oil depends on the stage of maturity of the raw fruit and on the cultivar quality; in table 6.2 is reported an average TAGs composition of a standard olive oil, while in table 6.3 the average composition of olive oil in terms of fatty acids is listed [Cappelli and Vannucchi, 2000; Azadmard-Damirchi, 2007].

Triglyceride	Quantity [_{w/w} %]	Name
OOO	40-59	1,2,3-trioleoylglycerol
POO	12-20	2,3-dioleoyl-1-palmitoylglycerol
OOL	12.5-20	1,2-dioleoyl-3-linoleoylglycerol
POL	5.5-7	2-oleoyl-3-linoleoyl-1-palmitoylglycerol
SOO	3-7	2,3-dioleoyl-1-stearoylglycerol

Table 6.2: average TAGs composition of olive oil, other TAGs can be present in small traces

Acid	Quantity [_{w/w} %]	Typology
oleic	>65	Monounsaturated
palmitic	<17	Saturated
linoleic	<13.5	Polyunsaturated
stearic	<3.5	Saturated
linolenic	<1.5	Polyunsaturated
palmitoleic	0.3 – 3	Monounsaturated

Table 6.3: some of the most important fatty acids of olive oil

The most common triglycerides used to enhance the consistence of the oily phase of W/O emulsions for shortenings production is palm stearin or fully hydrogenated tristearin [Garti et al., 1998; Johansson et al., 1995; Ramli et al., 2008]. As already mentioned, Jahaniaval (2005) proposed the adding of cocoa butter or cocoa butter equivalents aiming at producing margarines or shortenings.

6.1.2. W/O emulsions with cocoa butter

Cocoa butter, also called “theobroma oil” or “theobroma cocoa”, is a pale yellow pure edible vegetable fat extracted from the cocoa bean (containing a total amount of butter of 50/60_{w/w}%). Cocoa butter crystallises in different forms as a function of processing condition, time and storage temperature. The fatty acids chains forming the cocoa butter TAGs can be packed in different crystal structures. Literature data about the different polymorphic forms of cocoa butter crystals have a no uniform nomenclature. Six polymorphic forms have been identified: these are recognised like polymorph I-VI [Fessas et al., 2005] or α , β (distinguished in β_1 and β_2), β' (also distinguished in β'_1 , β'_2) and γ . Schenk and Peschar (2004) unify the different polymorphs calling them γ , α , β' , $\beta(V)$ and $\beta(VI)$. The unstable forms I (melting point 16 – 18 °C) and II (22 – 24°C) transform slowly into III (24 – 26 °C) and IV (26 – 28 °C), all possessing less stable polymorphs but upon optimal tempering sets in a more stable form V (32 – 34 °C) polymorph, optimal for chocolate production [Afoakwa et al., 2009]. The different crystals are collected referring to their melting point in table 6.4.

Crystal	melting point [°C]
β_1 (VI)	34-36
β_2 (V)	32-34
β'_1 (IV)	26-28
β'_2 (III)	24-26
α (II)	22-24
γ (I)	16-18

Table 6.4: different polymorphs of cocoa butter and their melting points

In figure 6.6, a complete scheme of a static isothermal phase transition is reported [Schenk and Peschar, 2005]. In the case of margarine, the oily phase should be crystallised in the β' form which possesses smooth mouthfeel, gives hardness to the final

margarine and also traps a large amount of liquid oil because of its spherulitic nature [Wiederman, 1978; Schenk and Peschar, 2004; Borwankar et al., 1992]. Nevertheless Garti et al. (1998) affirm that α -form crystals of hydrogenated fat can be obtained by a flash-cooling process in the oily phase, and that in the presence of food emulsifiers W/O emulsions (like margarines) can be stabilised by α -form (mixed with β' -form) submicronial crystals. Hindle et al. (2000) studied emulsified cocoa butter crystallised in the α -form, while Coupland (2002) studied palm oil and lard emulsions with β -crystals.

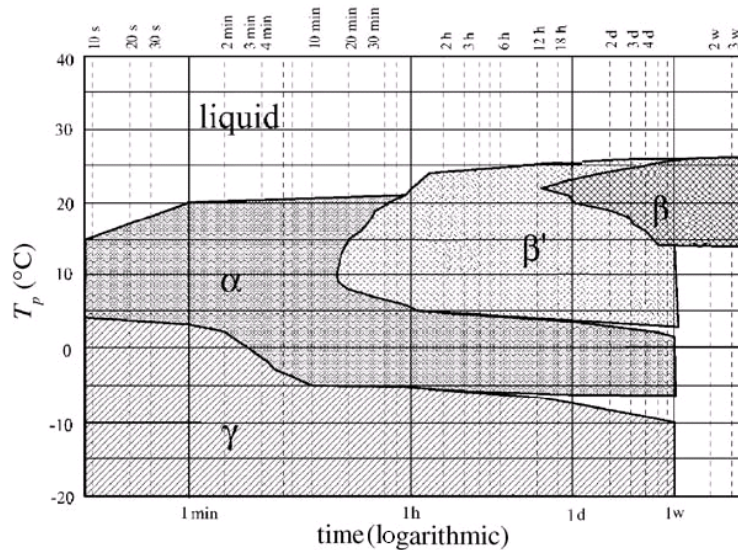


Figure 6.6: static phase transition of cocoa butter qualitative scheme. The darker zones represent the solid phase after an isotherm crystallisation time

Obviously cocoa butter is composed of a large quantity of saturated fatty acids TAGs, the most present fatty acid is the stearic one. Lipp et al. (2001) studied the average composition of different cocoa butters, whose composition is shown in table 6.5.

Triglyceride	Quantity [w/w %]	Name
POP	18.27	1,3-dipalmitoyl-2-oleylglycerol
PLP	1.82	2-linoleyl-1,3-palmitoylglycerol
POS	42.07	2-oleyl-3-stearoyl-1-palmitoylglycerol
POO + PLS	5.58	2,3-dioleyl-1-palmitoylglycerol 2-linoleyl-3-stearoyl-1-palmitoylglycerol
SOS	26.39	1,3-distearoyl-2-oleylglycerol
SOO + SLS	4.64	2,3-dioleyl-1-stearoylglycerol 1,3-distearoyl-2-linoleylglycerol
OOO	1.23	1,2,3-trioleylglycerol

Table 6.5: average TAGs composition of cocoa butter

In another work Lipp and Anklam (1997) analysed the average composition of cocoa butters from different countries chosen between the most important producer of this material in terms of fatty acids. Their results are summarised in table 6.6.

Acid	Ecuador	Brazil	Ghana	Ivory coast	Malaysia	Java	Average
Palmitic acid	25.6	25.1	25.3	25.8	24.9	24.1	25.13
Stearic acid	36.0	33.3	37.6	36.9	37.4	37.3	36.42
Oleic acid	34.6	36.5	32.7	32.9	33.5	34.3	34.08
Linoleic acid	2.6	3.5	2.8	2.8	2.6	2.7	2.83
Linolenic acid	0.1	0.2	0.2	0.2	0.2	0.2	0.18
Arachidic acid	1.0	1.2	1.2	1.2	1.2	1.2	1.17
Behenic acid	0.1	0.2	0.2	0.2	0.2	0.2	0.18

Table 6.6: average fatty acids composition (_{w/w}%) of cocoa butter from different countries

Margarine production process follows consecutive steps: the first one is the catalytic hydrogenation of vegetable oils which can be prolonged for several days. After that, the emulsification phase is done at 100°F (about 38°C) and the obtained emulsion is sent to the “Votator”, where it is cooled by using NH₃ at its boiling point. Within two minutes the mixture reaches 45-50°F (7-10°C). The obtained material is then pumped into a second vat, where it continues to crystallise and it is occasionally agitated but generally left to sit still and form its semi-solid state [Wiederman, 1978]. It is worth noting that a slow cooling rate can lead, in a quiescent state, directly to the polymorph β' , but slow cooling rates and low annealing temperatures allow a more disordered network to be produced giving a final product with a small elastic modulus [Fessas et al., 2005]. Thus, it is clear that the chilling process is divided into a first quenching step in order to obtain a huge number of small α crystals and a second slower step to convert these crystals in more stable and useful β' crystals.

While the previous chapter was mainly focused on the structuration of the water phase of both W/O and O/W emulsions in order to study and characterise puff pastries shortening replacers, the main purpose of the present work is the characterisation of W/O emulsions with a structured continuous oily phase, the structuration of the internal phase being not adequate to give the suitable mechanical properties of a commercial solid fat (one of the main results of the previous chapter). In this chapter, a previous rheological characterisation of the unemulsified oily phase is presented in order to evaluate the effects of added hard fats and emulsifier on its crystallisation and structuration. The oily phase structuration was achieved by adding cocoa butter to olive oil together with mono- and diglyceride of fatty acids as emulsifier. Thus, fixing the oily phase composition, process conditions were varied, such as the cooling rate of the melted oily phase and shear rate during crystallisation. After that, different emulsions were prepared, optimising first the emulsions preparation methods fixing the ingredients fractions, and then changing the oily

phase composition in order to reach the desired rheological characteristics of the shortening.

6.2. Materials and methods

6.2.1. Samples ingredients and identification

The raw materials used for samples preparation were: as main constituents of the two phases, distilled water and a virgin olive oil (Carbonell, Spain), cocoa butter (Icam S.P.A., Italy), mono- and diglycerides of fatty acids (Myverol 18 04, Kerry Group, Ireland, 3_{w/w}% for all samples) as emulsifiers, NaCl (Panreac, Spain) 0.1 M added to the water in order to identify the mutual position of the two phases by an electric conductivity technique (emulsions W/O or O/W). The analysed samples are listed in table 6.7.

Sample	Oil + Myverol	Water	Cocoa Butter	Homog. steps
Emu 1	86	12	2	1 st 70°C + 2 nd 25°C
Emu 2	86	12	2	25°C SCR
Emu 3	86	12	2	20°C, FCR, gently mixing
Emu 4	86	12	2	20°C, FCR, static
Emu 5	78	12	10	20°C, FCR, gently mixing
Emu 6	68	12	20	20°C, FCR, gently mixing

Table 6.7: samples identification. All quantities are reported in weight percentage. The last column refers to the homogenisation steps conditions. The reported temperature is that of the sample. SCR is “slow cooling rate” of the oily phase, while FCR is “fast cooling rate”

6.2.2. Samples preparation

As usual, the two phases were obtained separately. Different samples (a total amount of 200 g) were prepared by varying the sample preparation or the oil/cocoa butter/water ratio without changing the emulsifier amount (3_{w/w}%). The oily phase was prepared melting the cocoa butter and the emulsifier added contemporary [Garti et al., 1998] to the continuously stirred oil at 70°C with a magnetic-heater agitator (Agimatic E, Selecta, Spain). After the cocoa butter and the emulsifier were completely melted (under a visual inspection), the mixing was prolonged for a further 5 minutes. The water phase was obtained dissolving the right amount of NaCl into the water at room temperature for a mixing time of 5 minutes.

The emulsification step was performed with a rotor stator system (Ultra-Turrax T 50, IKA, Germany) optimised with the different samples characterisation. Sample *Emu 1* was prepared by adding the water phase to the oily one at 7600 rpm at 70°C for a mixing time of 5 minutes. At these mixing conditions a marked system instability was encountered, therefore a second step of homogenisation was necessary (at 25°C for 5 minutes) to produce a stable emulsion. Sample *Emu 2* was prepared by mixing the two phases at 25°C. The oily phase was slowly cooled from 70°C to 25°C (leaving the hot sample at room temperature for the time necessary to reach the thermal equilibrium). Sample *Emu 3* was produced applying a fast cooling rate to the gently stirred oily phase, quenching it in a thermostatic cold bath (at 0°C) up to the final temperature of 20°C. The oily phase was poured into a round size aluminium container ($\phi=15$ cm), where the final thickness of the cold hard fat phase reached a maximum value of about 1 cm.

Sample *Emu 4* was prepared in the same way, but leaving the oily phase in a static state. In samples *Emu 5* and *Emu 6* the total amount of cocoa butter was increased up to the 10_{w/w}% in the first case and the 20_{w/w}% in the second case, following the same preparation steps used for sample *Emu 3*.

6.2.3. Rheological characterisation

The rheological characterisation of all the investigated emulsions was performed using a controlled stress rheometer Mars (Haake, Germany) equipped with a serrated parallel plates geometry of $\phi=35$ mm with a gap of 2 mm. Temperature was fixed at 20°C for all tests and the thermal control was obtained using a thermostatic bath connected to the parallel plate geometry.

The unemulsified oily phase was analysed too. Its characterisation was performed on a controlled strain rheometer ARES-RFS (TA Instruments, U.S.A.) equipped with parallel plates geometry (parallel plates $\phi=50$ mm, gap=2 mm) and the temperature control ($\pm 0.1^\circ\text{C}$) was guaranteed by a Peltier system acting under the lower plate.

Dynamic tests include a Stress (or Strain in the case of the oily phase characterisation) sweep test at the fixed frequency of 1 Hz, in order to evaluate the linear viscoelastic region of the material. Frequency sweep tests were performed at a constant stress (or strain) within the linear viscoelastic range in the frequency range 0.1-10 Hz. Both tests were performed at 20°C as a representative temperature for process conditions.

The frequency sweep test analysis was effected by applying the *Weak Gel* model.

According to [Gabriele et al. \(2001\)](#), rheological properties of the material can be obtained by considering the sample as a weakly structured 3-D network. Mechanical characteristics of this network are determined by considering the number of the interacting units inside the structure and the strength of the connections among them. At any temperature T , if the complex modulus G^* is considered as a combination of the elastic modulus G' and the dissipative one G'' , data can be fitted using a two parameters power law:

$$G^*(T) = \sqrt{G'(T)^2 + G''(T)^2} = A(T) \cdot \omega^{1/z(T)} \quad [6.2.1]$$

From the Weak Gel model, the parameter z is related to the number of interacting rheological units within the 3-D network and A is the strength of these interactions.

When A increases the interaction forces within the network are increasing whilst a high z value indicates a large number of interacting units cooperating and increasing the network connectivity. All data fitting is performed through Table Curve 2D Software (Jandel Scientific, USA).

In order to observe the structure evolution of the unemulsified oily phase with the temperature, a dynamic temperature ramp test (Time cure) was also performed at the fixed frequency of 1 Hz, cooling the sample from 70°C to 20°C with a fast (-5°C/min) and a slow (-1°C/min) ramp rate. The applied strain was adjusted according to the temperature change during the test in order to guarantee the linear viscoelastic regime.

Also the flow behaviour of the oily phase was investigated in its dependence on temperature. In fact *Step rate temperature ramp tests* were performed at the different fixed shear rates of 1, 5, 10, 100 s⁻¹ in the same temperature interval and applying the same cooling rates of the dynamic tests. Starting from the melted oily phase, it was cooled thanks to the Peltier system of the rheometer during the measurement of its structure evolution up to 20°C.

As far as viscosity measurements are concerned, flow curves were obtained in the shear rate range 0.01-1000 s⁻¹ for samples *Emu 1 – Emu 4*. The obtained flow curves were linear in a log-log plot, up to high shear rate values, where a Newtonian plateau was reached. Thus, the more suitable model used for the data-fitting was the Sisko equation, used in other works to model the flow behaviour of emulsions [[Barnes, 1989](#); [Gabriele et al., 2008](#)] and proposed as it follows:

$$\eta = \eta_{\infty} + k\dot{\gamma}^{n-1} \quad [6.2.2]$$

where k and n are consistency and flow indices respectively. The parameter k can be considered as an index of the material “consistency”. n is always positive and lower than one. From a physical point of view, the lower the n value, the higher the curve slope,

meaning a sharper decrease of viscosity when increasing shear rate (greater tendency to in-flow destructure).

As shown in the previous chapter, two commercial fats were analysed as control materials. The two studied fats were the margarine “Flora” (Unilever, Spain) and Vallè (with 18_{w/w}% of butter, France). For sample *Emu 6* the flow behaviour was also analysed, but considering the evident slippage phenomena at the solid interface, the measurement became unreliable at high shear rate values. Therefore, a method of manipulating experimental data was used, based on the possibility of relating dynamic and shear data [Peressini et al., 2002] that relates complex and shear viscosity. In fact, it is well known that for several polymeric systems the so-called Cox–Merz rule applies [Cox and Merz, 1958] stating, as a rule of thumb, that complex and shear viscosity coincide by assuming:

$$\dot{\gamma} = \omega \quad [6.2.3]$$

where $\dot{\gamma}$ is the shear rate and ω the frequency of oscillation. In this case, instead of using this equation, the following should be used:

$$\dot{\gamma} = a_{\dot{\gamma}} \omega \quad [6.2.4]$$

where $a_{\dot{\gamma}}$ is a shift factor. It was possible to obtain some shear viscosity values at 20°C by performing creep tests at different fixed stresses by applying the Kelvin –Voigt model.

The experimental data, reported in terms of creep compliance versus time, were analysed by using a one-element Kelvin –Voigt model [Gabriele et al., 2001, b]:

$$J(t) = J_0 + J_1 \left(1 - e^{-\left(\frac{t}{\lambda_{ret}}\right)} \right) + \frac{t}{\eta} \quad [6.2.5]$$

where J_0 is the instantaneous compliance, J_1 is the retarded compliance, λ_{ret} is the retardation time of the Kelvin component, and η is the Newtonian viscosity [Steffe, 1996].

From the inverse of the slope, η , of the creep test obtained after a long time, it is possible to calculate the shear rate

$$\dot{\gamma} = \frac{\tau_0}{\eta} \quad [6.2.6]$$

Thus the shear viscosity can be computed and reported in the same plot together with the dynamic complex viscosity defined as:

$$\eta^* = \sqrt{\eta'^2 + \eta''^2} \quad [6.2.7]$$

where

$$\eta' = \frac{G''(\omega)}{\omega} \quad \text{and} \quad \eta'' = \frac{G'(\omega)}{\omega} \quad [6.2.8]$$

The steady shear viscosity and the dynamic ones show a very similar slope, thus it is possible to overlap those curves by a horizontal shift.

The obtained flow curves were then modelled by a modified Cross model [Barnes et al., 1989] without the η_{∞} plateau.

$$\eta = \frac{\eta_0}{1+(\lambda\dot{\gamma})^m} \quad [6.2.9]$$

in which η_0 refers to the asymptotic value of viscosity at very low shear rates, λ is a constant parameter with the dimension of time and m is a dimensionless constant. All tests were repeated three times and the reported results are the average values; the error bars are also reported.

6.2.4. Microscopy tests

In order to study the internal microstructure of the emulsions, an optical microscopy analysis was also performed. The droplet size distribution of the produced W/O emulsions could not be analysed, but anyway a qualitative inspection allowed a reasonable interpretation of the rheological data to be given. The samples were diluted in olive oil (the same used as a raw material for the samples preparation) with a weight ratio of 1:5 and gently stirred in order to guarantee a better separation of the droplet agglomerates linked by fat crystals. The microphotographs were taken by using an optical microscope Olympus BX 51 (U.S.A) with an objective magnification of 50X.

6.2.5. Study of the phases placement

The mutual placement of the phases was tested in order to be sure that the water phase was the internal one. The confirmation of this important characteristic of the biphasic system was achieved by the electric conductivity analysis.

The electric conductivity of samples was tested by the conductimeter inoLab pH/Cond Level 1 (WTW, Germany). All samples were in fact prepared with a solution 0.1 M NaCl at a known conductivity value ($\sigma=10.7$ mS/cm circa at 25°C) [Ozawa et al., 1997; Eicke et al. 1989], while, as known, the oily phase is not an electric conductor: thus, the water phase being the internal one, the samples electric conductivity could not be detected by the instrument. For all the analysed samples the electric conductivity was zero, confirming that they were all W/O emulsions as expected.

6.3. Results and discussion

The rheological characterisation of the commercial fats has been already proposed in the Chapter 5 of the present Ph.D. thesis. The Weak Gel parameters of the commercial fats are listed in the table 6.8.

Commercial fat	A [$\text{Pa}\cdot\text{s}^{1/z}$]	z [-]
Flora	52200±600	12±1
Vallè	37500±400	14±2

Table 6.8: Weak Gel parameters of the commercial fats

6.3.1. Oily phase rheological characterisation

The mechanical and rheological characteristics of the W/O emulsions with a structured oily phase are strictly related to the crystals formation within the oily phase [Macierzanka et al., 2009; Coupland, 2002; McClements, 1999]. Thus, aiming at studying the crystallisation and, mostly, its consequence on rheology of the structured phase, a rheological characterisation of the oily phase needed to produce samples *Emu 1-Emu 4* was accomplished. It was chosen to examine only the oily phase of these samples because the optimisation of the emulsions preparation was achieved thanks to their production. In fact, samples *Emu 5* and *Emu 6* were prepared maintaining the same operating conditions and changing the amount of cocoa butter in the oily phase. In the figure 6.7 the oily phase time cure is reported.

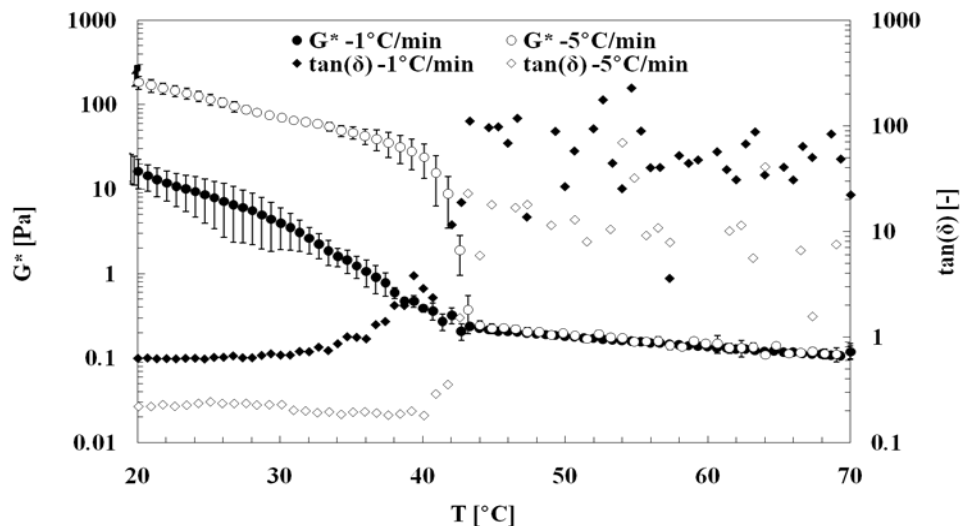


Figure 6.7: Time cure of the oily phase of samples *Emu1-Emu4* at different cooling rates

A liquid-like behaviour, confirmed by a loss tangent value greater than one, can be observed for both the tests up to the beginning of crystallisation. Aiming at identifying the temperature of initial crystallisation the moduli crossover, i.e. the loss tangent equal to one, is usually assumed as a transition criterion from liquid-like to solid-like behaviour. However, in the present case interest is mainly focused on the nucleation and initial growth of crystals, and not on the real transition between the two different behaviours probably related to the formation of a significant crystals mass. Therefore, an alternative criterion should be proposed. Experimental data evidence, for both tests, an almost constant value of loss tangent at high temperature and a sharp decrease when a critical temperature is reached. This should be due to the beginning of crystallisation phenomena as confirmed also by the simultaneous change in complex modulus slope associated with a potential increase in solid content. As a consequence, the beginning of crystallisation was identified by the sharp decrease of the loss tangent, corresponding to the temperature at which a slop change in the G^* modulus was encountered. The critical temperature identified in this way is approximately 43°C for both the cooling conditions. It can be noticed that the transition temperature is much higher than that of the pure cocoa butter, for which the maximum crystallisation temperature, measured in static conditions, is about 36°C for the β crystalline form [Afoakwa et al., 2009]. This behaviour could be explained thanks to the interactions of cocoa butter with mono- and di-glyceride of fatty acids and olive oil.

As revealed by previous works on cocoa butter crystallisation [Baldino et al., 2009], a greater consistency of the oily phase at a fast cooling rate with respect the slow one can be imputed to the presence of smaller fat crystals with a smaller surface area that can create a more rigid network with a greater number of interconnections. This is because the nucleation rate increases more rapidly with decreasing temperature than the crystallisation rate. Even the flow behaviour of the system after its crystallisation point is affected by the cooling rate, giving, as a consequence, a more or less viscous material that can be broken under the shear action. Figure 6.8 reports the step rate temperature ramp tests of the oily phase at two different cooling rates and fixing the shear rate value at 10 s⁻¹. The same conditions (shear rate and thermal history) were used in other works [Paso et al., 2009; Tarabukina et al., 2009] in order to measure the onset of the crystallisation from a melted oily phase.

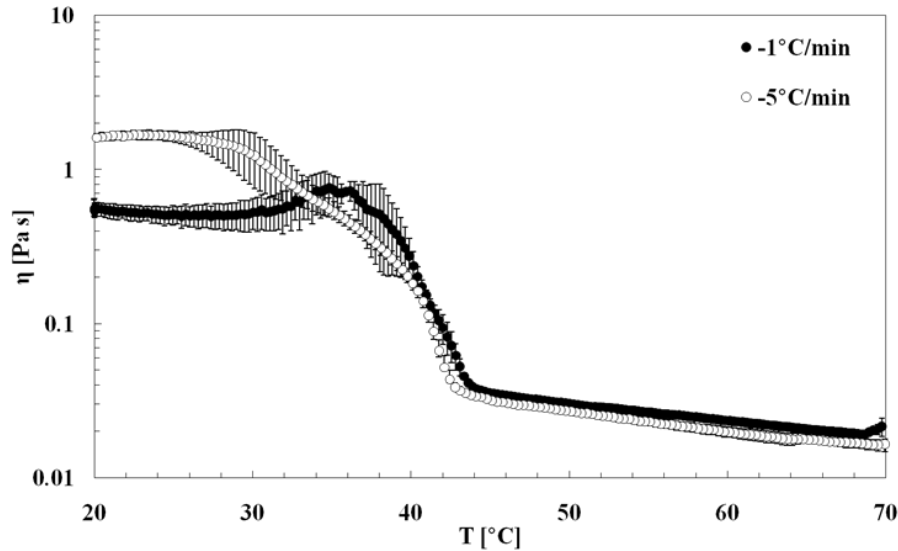


Figure 6.8: Step rate temperature ramp test of the oily phase of samples *Emu1-Emu4* at different cooling rate

In the first zone of the plot (from 70 to ~ 43°C), the oily phase is in the molten state, which is characterised by a Newtonian behaviour.

The viscosity varies with the temperature according to the law derived from the Arrhenius one [Steffe, 1996]:

$$\eta = \eta_0 \cdot e^{\frac{E_a}{kT}} \quad [6.3.1]$$

η being the viscosity of the oily phase at a given temperature T , E_a being the activation energy, k being the Boltzmann constant, and η_0 being a constant. An activation energy equal to $4.22 \cdot 10^{-20} \text{ J} \pm 1.06 \cdot 10^{-21} \text{ J}$ was calculated. This value falls into the range of activation energies for low molecular weight Newtonian liquids (for example, $E_a = 8.3 \cdot 10^{-20} \text{ J}$ for glycerine and $5.1 \cdot 10^{-20} \text{ J}$ for Palm oil [Tarabukina et al., 2009]). After the Newtonian region, a huge increase in the viscosity value is encountered for both the applied cooling rate values, but at lower temperature conditions ($T < 30^\circ\text{C}$) a higher viscosity is encountered for the fast cooling rate imposed. The crystallisation transition is the same for the flow tests and the dynamic ones, suggesting that the onset of crystallisation is not affected by the kinematic conditions in which the sample is analysed. Aiming at better understanding the flow behaviour of the oily phase with the shear rate, different step rate temperature ramp tests (at a cooling rate of $-5^\circ\text{C}/\text{min}$) were performed at different fixed shear rate values. Figure 6.9 shows the results.

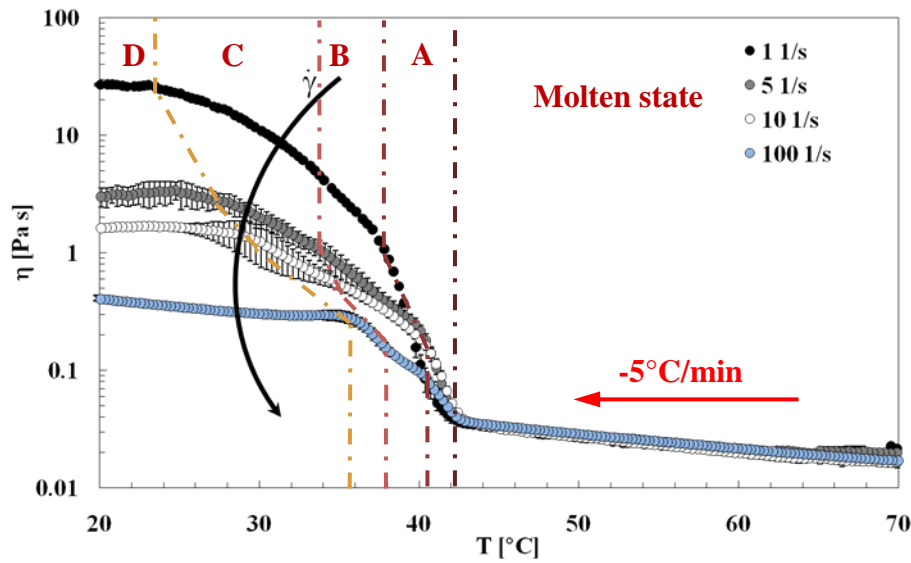


Figure 6.9: step rate temperature ramp of the oily phase of samples *Emu 1-Emu 4* at the cooling rate of $-5^{\circ}\text{C}/\text{min}$ at different shear rate values

The different microstructural modifications owing to shear rate and temperature changing are grouped into zones delimited by the broken lines. In the zone ‘A’ a viscosity jump occurs, signing the onset of the crystallisation for all the samples (independent of the shear rate values). The zone ‘B’, is delimited by the zone ‘A’ and the broken line passing through the slope change points of the curves (more marked at higher shear rate values). After the slope change, the zone ‘C’ shows another viscosity increase and finally a plateau (the steady state) is reached in the zone ‘D’. This behaviour, already described by Tarabukina et al. (2009) for palm oil cooling under fixed shear rates, but leaving isothermal conditions after the starting of crystallisation, is strictly related to the samples microstructural changes. Cooling the molten phase, the crystallisation temperature T_c is reached, and first of all crystals (α form) and spherulites are formed increasing progressively in number and size (zone ‘A’) during cooling. Crystals move as individual bodies, while spherulites start to meet because of the increase of crystalline fraction forming aggregates composed of a few spherulites. As already noticed, the onset of crystallisation in the zone ‘A’ (1st crystallisation) is of the applied shear rate, while the second increase in viscosity (2nd crystallisation) delimited by the broken line between the zones ‘B’ and ‘C’, changes with the shear rate. During cooling the crystallisation proceeds through α nucleation and successive $\alpha \rightarrow \beta'$ polymorphic transformation. Shear had no effect on the onset of α crystallization (1st crystallisation) [Tarabukina et al., 2009], but accelerated the polymorphic transition (2nd crystallisation). At low shear rates, aggregates of α nuclei have time to be formed delaying the $\alpha \rightarrow \beta'$ transformation, whereas at larger shear rates, α nuclei remain as individual crystals, which can more easily be transformed

on β' crystals. This explains that the phase transition in the zone 'C' appears sooner when the shear rate is increased [Tarabukina et al., 2009].

Finally, spherulites aggregates have a slower movement due to a collaborative motion, and after their growth is accomplished, all the aggregates are connected together and form a network (defined by the plateau region 'D') [Brunello et al., 2003]. If high shear rate values are applied, a shear-induced destructurement of the formed crystalline network can be found, giving as a consequence a lowering in the viscosity value.

The nucleation stage of the crystals can be *homogeneous* or *heterogeneous*. The last type starts when an impurity acts as a catalyst of crystal growth, such as mono-glyceride micelles [McClements, 1999]. It was often found that the homogeneous crystallisation starts later than the heterogeneous one.

In figure 6.10 a comparison between the oily phase with and without the emulsifier is shown. It seems that, at these conditions, the sample prepared without emulsifier does not have structural changes owing to the fat crystallisation, but only a viscosity increase due to kinetics effects; the crystallisation process is maybe retarded as previously stated.

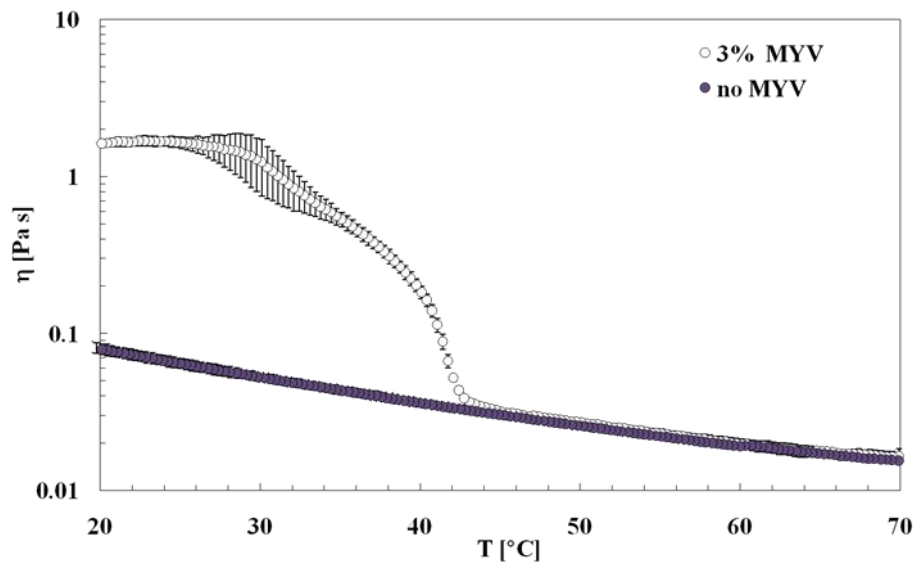


Figure 6.10: Step rate temperature ramp of the oily phase with and without emulsifier at a cooling rate of $-5^{\circ}\text{C}/\text{min}$

6.3.2. Emulsions rheological characterisation

The frequency sweep test for sample *Emu 1* is reported in figure 6.11.

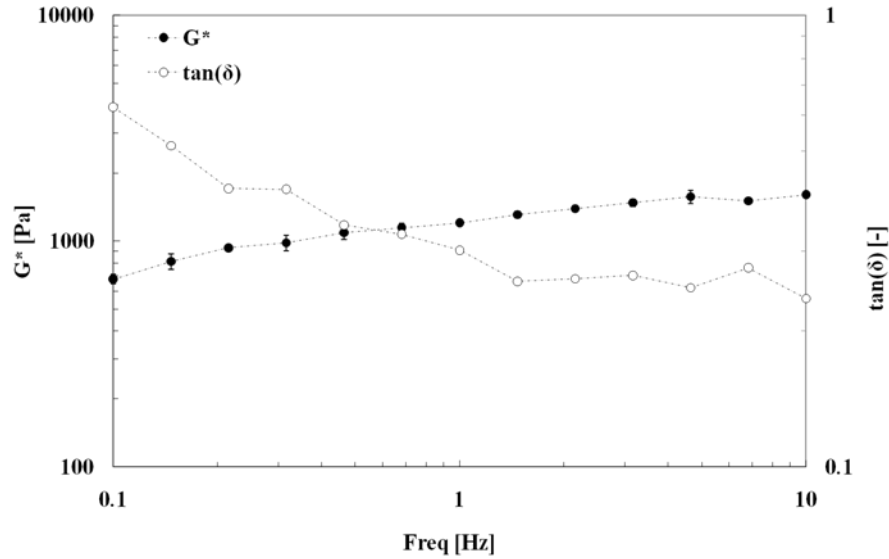


Figure 6.11: Frequency sweep test at 20°C of sample *Emu 1*

As shown, the sample is characterised by a solid-like behaviour, being G' , the elastic modulus, always greater than G'' , the loss modulus in the frequency range investigated. The loss tangent, always smaller than the unity, confirms this behaviour. The parameters of the Weak Gel model are $A=1171\pm 15 \text{ Pa}\cdot\text{s}^{1/z}$ and $z=6.0\pm 0.3$, both really different from the reference values listed in table 6.8.

A similar rheological behaviour was found for the sample *Emu 2*, as can be observed in figure 6.12.

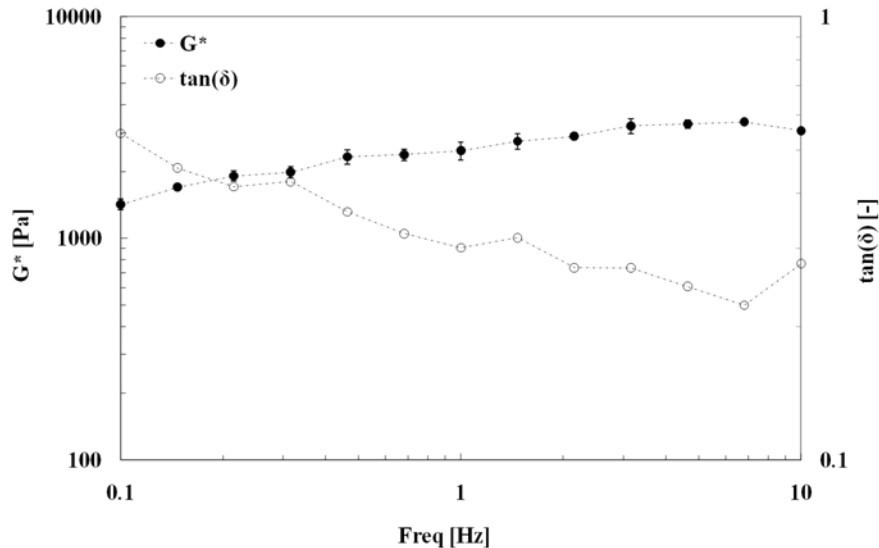


Figure 6.12: Frequency sweep test at 20°C of sample *Emu 2*

The Weak Gel parameters are $A=2481\pm 40 \text{ Pa}\cdot\text{s}^{1/z}$ and $z=6.8\pm 0.5$. The direct emulsification at 25°C increases the strength of the network without varying its extensions, giving an increase of the consistency as a consequence. The effect of the

cooling rate on the final consistency and structuration of the samples can be analysed by a comparison of samples *Emu 2* and *Emu 3*, given in the plot of figure 6.13.

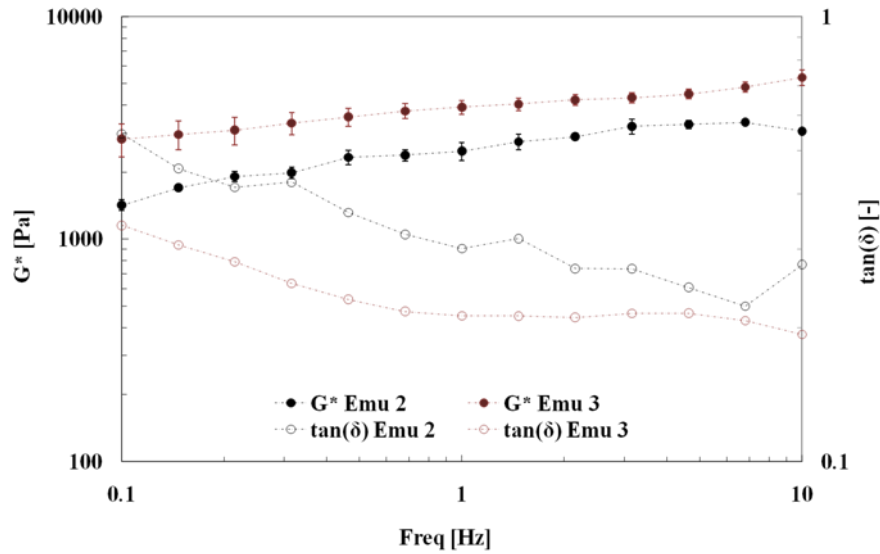


Figure 6.13: Frequency sweep test at 20°C of samples *Emu 2* and *Emu 3*

As shown, the fast cooling rate applied for quenching the oily phase results in increasing both the strength and the extension of the network, as confirmed by the Weak Gel parameters $A = 3741 \pm 52 \text{ Pa}\cdot\text{s}^{1/z}$ and $z = 7.6 \pm 0.5$. Thus, as already said in the case of the unemulsified oily phase, a fast cooling rate gives a bigger number of small crystals, which, together with the water droplets, can be interpreted as rheological unities interacting amongst them and forming a more structured and consistent network [<http://www.isaac-heertje.nl/structure/>]. Moreover, it is known that smaller crystals are likely to provide better coverage on the droplets surface than larger crystals, giving more stable Pickering emulsions [Rousseau, 2000].

Sample *Emu 3* was prepared stirring the oily phase during quenching, while in sample *Emu 4* the oily phase was left in a static state. The effects of these two methods of preparation on the samples rheology is shown in figure 6.14.

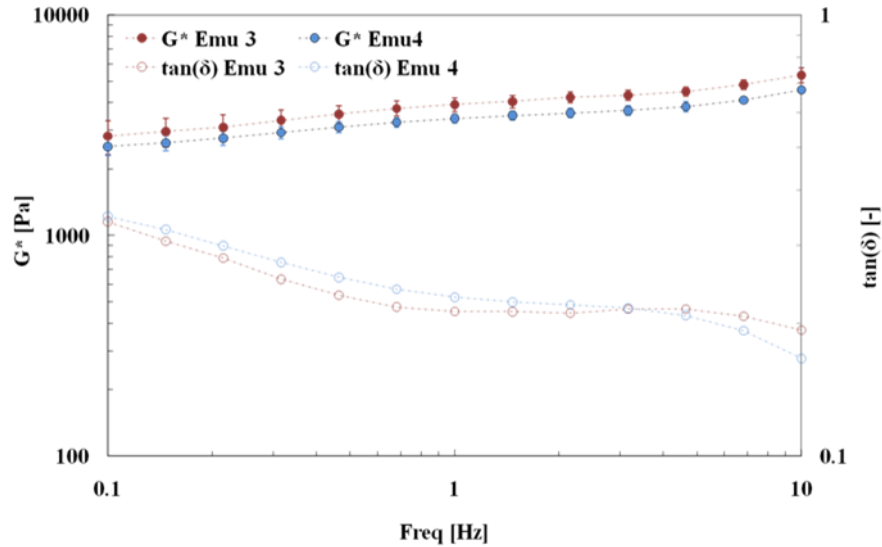


Figure 6.14: Frequency sweep test at 20°C of samples *Emu 3* and *Emu 4*

It is clear from the plot that the gently mixing of the oily phase is able to give a very slight increase to the strength of the network without changing its extension. The mixing allows a better dispersion of the produced nuclei favouring the nucleation step, and moreover enhancing the $\alpha \rightarrow \beta'$ transformation that results in a more consistent system [De Graef et al., 2009].

The samples prepared with higher fractions of cocoa butter in the oily phase were produced following the same procedure described for sample *Emu 3*. The cocoa butter content was 10_{w/w}% in sample *Emu 5*, while the total amount of cocoa butter was increased up to 20_{w/w}% in sample *Emu 6*. The frequency sweep test of the obtained emulsions is reported in figure 6.15.

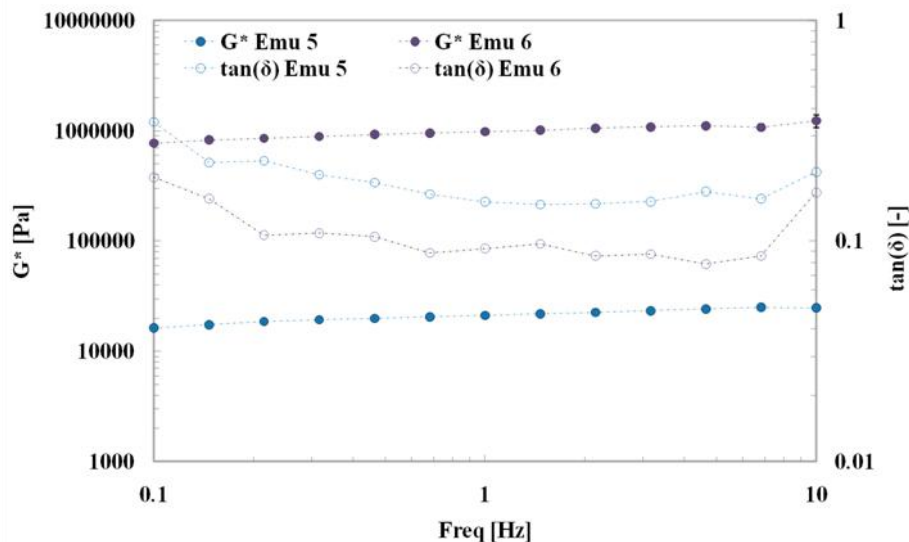


Figure 6.15: Frequency sweep test at 20°C of samples *Emu 5* and *Emu 6*

As expected, the increased fraction of cocoa butter enhances the final consistency of the W/O emulsion of different orders of magnitude. A comparison between the complex moduli and the loss tangents of the analysed samples and the commercial fats is proposed in figure 6.16.

The amount of cocoa butter used in emulsion *Emu 6* is greater than the quantity necessary to obtain the desired rheological characteristics of a typical shortening. In fact, a cocoa butter fraction slightly larger than 10_{w/w}% seems to be enough to produce a suitable shortening replacer, ensuring consequently a low amount of total added hard fats with respect to the common shortenings for pastry production.

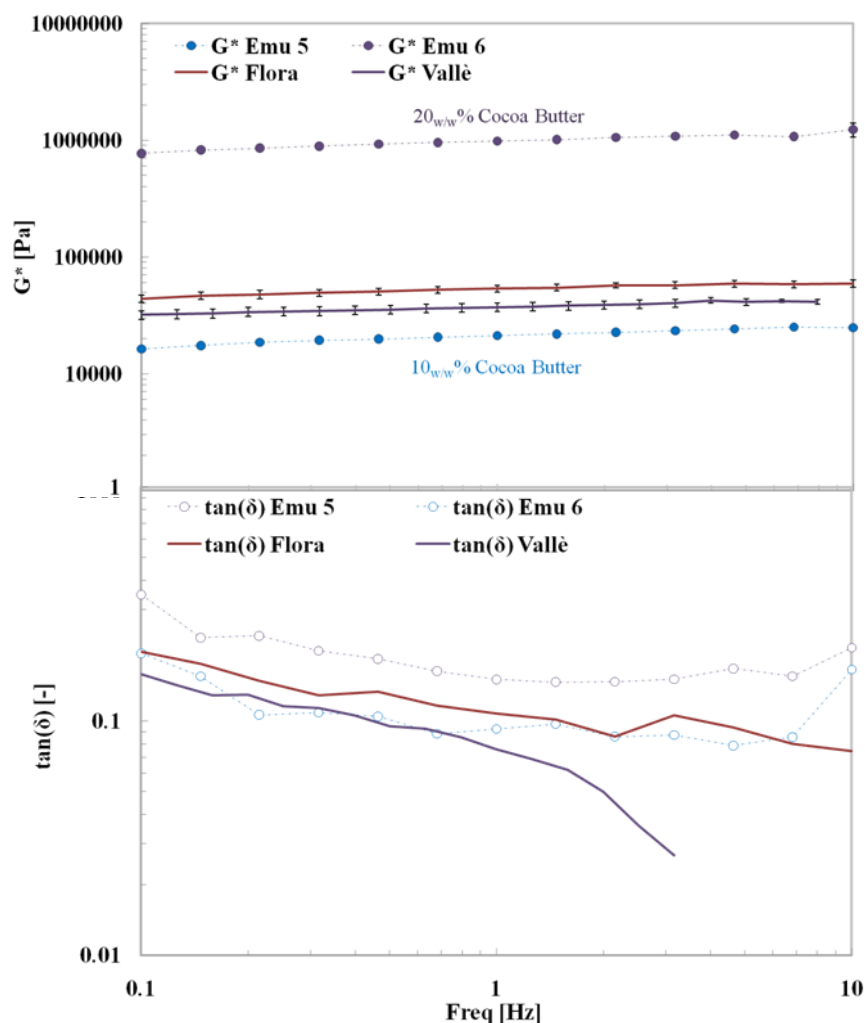


Figure 6.16: Frequency sweep test at 20°C of samples *Emu 5* and *Emu 6* compared with the commercial fats

In figure 6.17 the Weak Gel parameters of samples *Emu 1* – *Emu 5* are resumed. A comparison between *Emu 6* and the commercial shortenings is then proposed in figure 6.18.

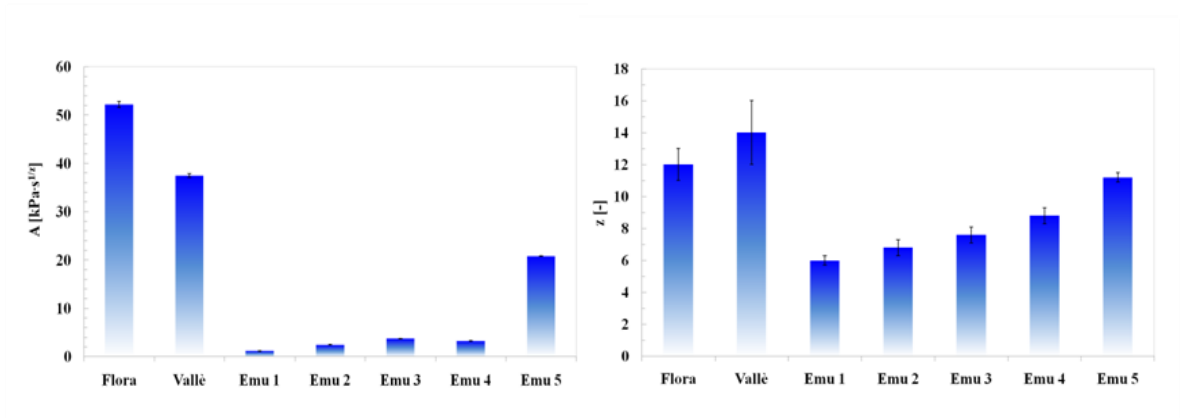


Figure 6.17: Weak Gel parameters for the samples *Emu 1-Emu 5* and the commercial fats

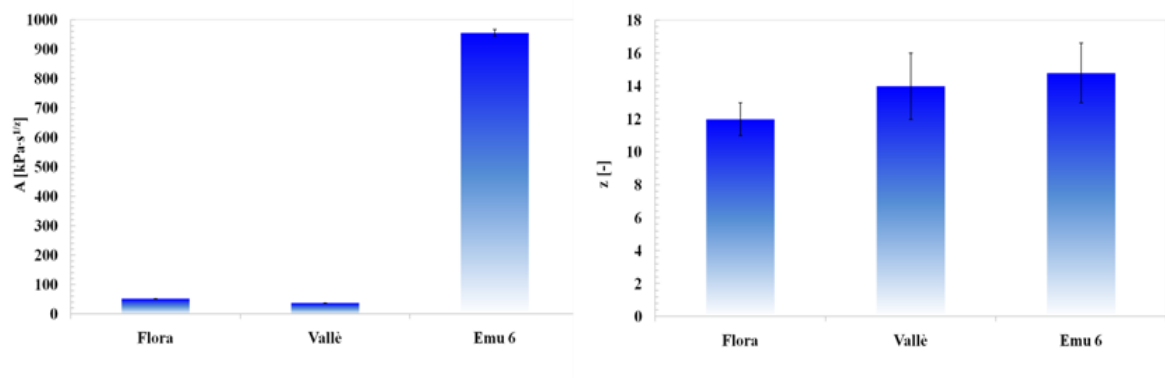


Figure 6.18: Weak Gel parameters for sample *Emu 6* and the commercial fats

Samples *Emu 5* and *Emu 6* seems to reach the right network extension, being the z parameters similar to those of the two fats. On the contrary the network strength is much more increased by the further addition of cocoa butter.

The flow properties of the samples *Emu 1 – Emu 4* were also tested. In the plot in figure 6.19 the flow curves of the different emulsions are shown.

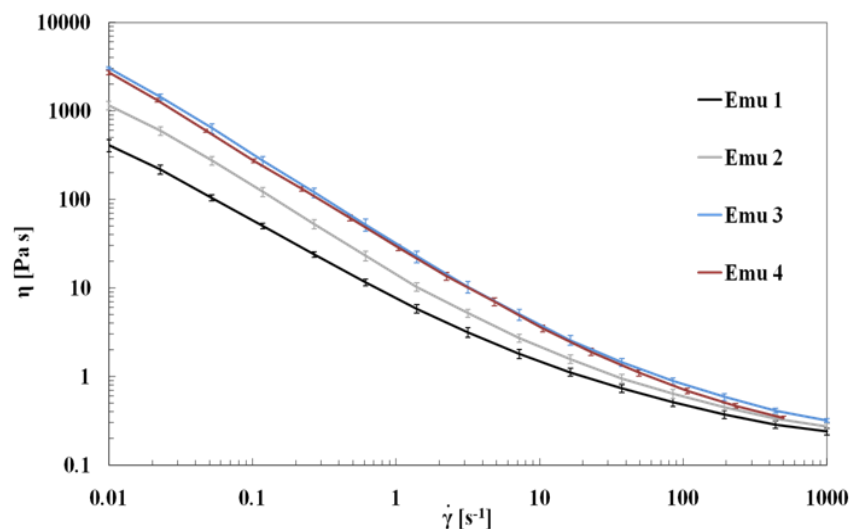


Figure 6.19: Flow curves for samples *Emu 1 - Emu 4*

In table 6.9 the Sisko equation parameters are listed for each sample.

Sample	η_{∞} [Pa·s]	k [Pa·s ⁿ]	n [-]
Emu 1	0.17±0.01	6.01±0.82	0.35±0.04
Emu 2	0.19±0.02	9.39±1.68	0.32±0.05
Emu 3	0.21±0.02	19.4±3.10	0.25±0.04
Emu 4	0.19±0.02	24.1±4.30	0.26±0.04

Table 6.9: Sisko model parameters of samples *Emu 1* – *Emu 4*

The parameters of the Sisko model show an invariance of the Newtonian plateau value for all the investigated samples, correspondent to the complete destruction of the network [McClements, 1999]. Confirming the results obtained by the Weak Gel model application, an increase of the consistency index was found, while the flow index n is constant. The flow curve of the more viscous emulsions (*Emu 5* and *Emu 6*) could not be obtained by using the conventional steady state tests for evident slippage phenomena at the solid interface, thus dynamic and shear data were combined. The flow curve of the sample *Emu 6* is reported in figure 6.20.

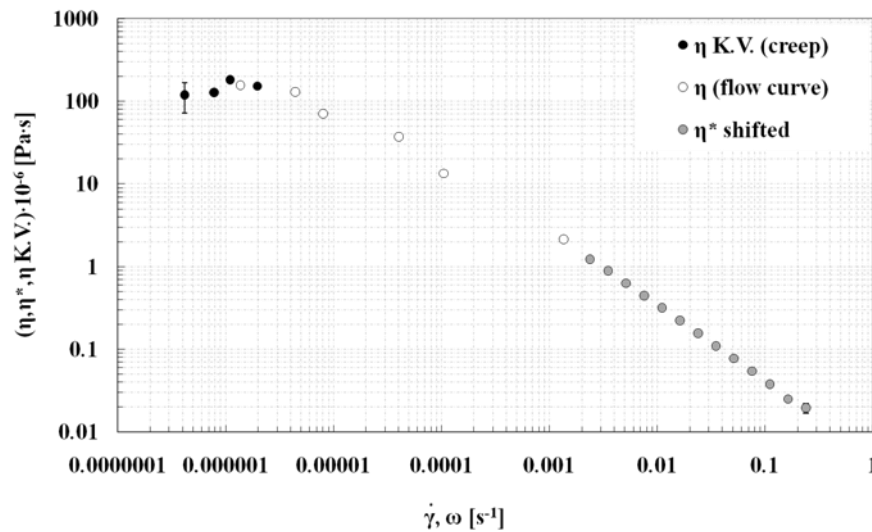


Figure 6.20: Flow curve of sample *Emu 6*

The modified Cross model parameters of sample *Emu 6* are listed in table 6.10. It can be surely concluded that the high fraction of added cocoa butter leads to a huge increase of the sample viscosity with respect to the other samples analysed.

Sample	η_0 [Pa·s]	λ [s]	m [-]
Emu 6	$2.1 \cdot 10^8 \pm 2.5 \cdot 10^7$	$1.1 \cdot 10^5 \pm 4.3 \cdot 10^4$	0.92 ± 0.14

Table 6.10: Modified Cross model parameters of sample *Emu 6*

6.3.3. Microstructural characterisation

Aiming at performing a qualitative characterisation of the internal microstructure of the samples, a microscopic analysis was achieved. In figure 6.21 the microphotographs of all the samples is shown.

It can be deduced that there are no significant differences between the DSD (droplet size distribution) of the emulsions *Emu 1* and *Emu 2*, while comparing the samples *Emu 2*, *Emu 3* and *Emu 4* a remarkable decrease of the droplets average dimension is encountered. It is clear that the increase in both the strength and extension values of the weak gel network owed to the production of a big number of small crystals at fast cooling rate (samples *Emu 2* and *Emu 3*) results in a consequent decrease of the water droplets inside the network, moreover the droplets dimensions in samples *Emu 3* and *Emu 4* are quite similar. Finally, the smallest droplets aggregates can be found in the sample *Emu 6* with the stronger and more structured network, because of the big cocoa butter fraction.

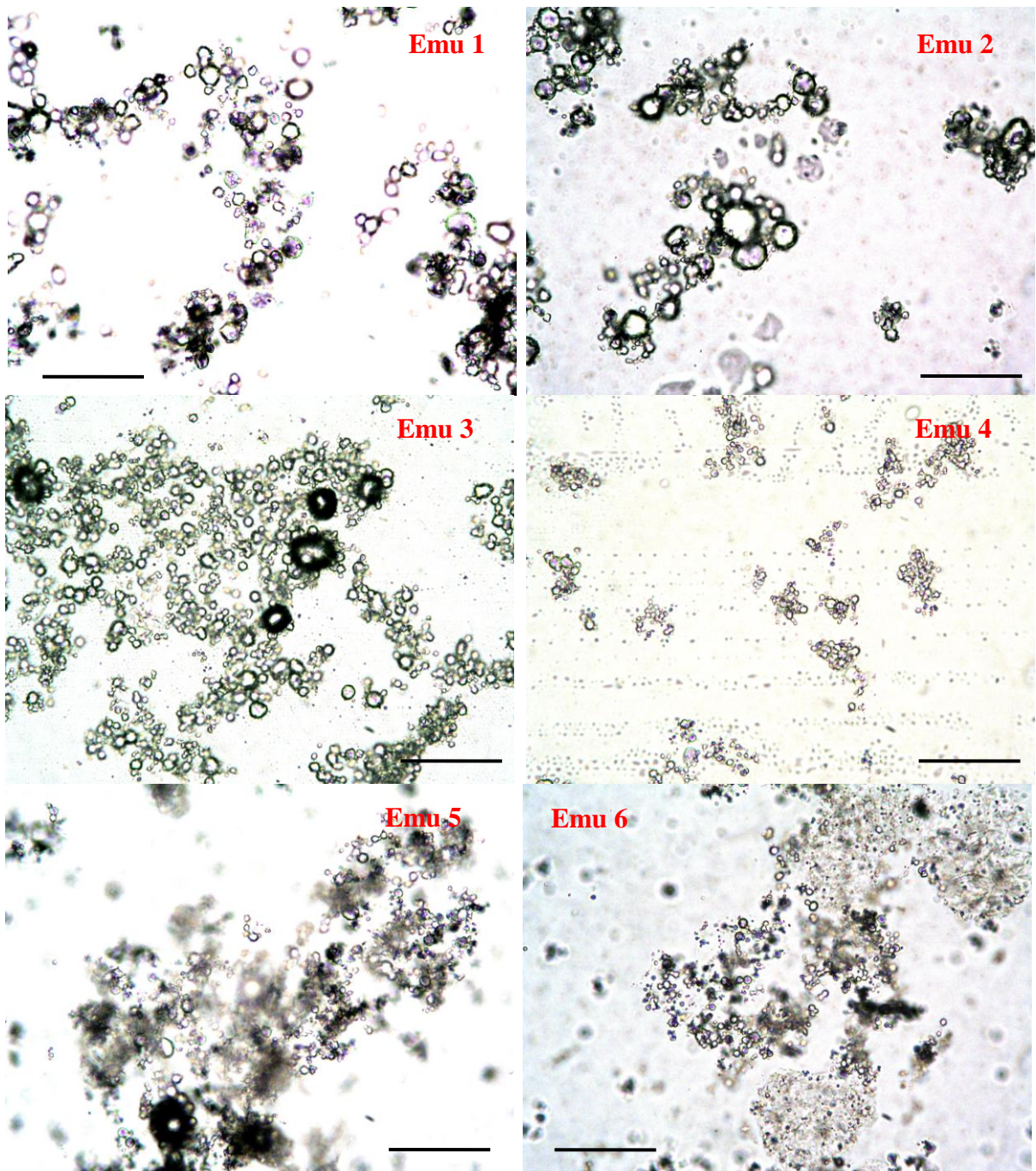


Figure 6.21: Microphotographs of samples *Emu 1- Emu 6* (magnification 50X). The control bar is 50 μm

Conclusions

In this work the production of W/O emulsions with a high structured oily phase fraction as a puff pastry shortening replacer have been optimised following the Weak Gel rheological model.

The oily phase structuration has been achieved by adding cocoa butter and mono- and di-glycerides of fatty acids.

The unemulsified oily phase was studied first, with the main purpose of understanding the complex fat crystallisation process. Then, the effect of both the preparation procedure and the total amount of cocoa butter on the rheological characteristics of the final emulsions was investigated, finding interesting conclusions. A fast cooling rate of the oily phase was necessary to produce small crystals of a cocoa butter-mono-glyceride complex, giving, finally, smaller water droplets and producing a strong and structured network. A range of cocoa butter fraction added to the oily phase (from 10_{w/w}% to 20_{w/w}%) has been individuated for the new shortening production in order to obtain rheological properties similar to those of two commercial characterised fats.

References

- Afoakwa E. O., Paterson A., Fowler M., Vieira J., (2009). *Influence of tempering and fat crystallization behaviour on microstructural and melting properties in dark chocolate systems*, Food Research International 42, 200–209
- Azadmard-Damirchi S., (2007). *Olive Oil - Phytosterols, Tracing of Adulteration with Hazelnut Oil and Chemical Interesterification*, Doctoral thesis, Swedish University of Agricultural Sciences, Uppsala, Acta Universitatis Agriculturae Sueciae 2007: 36
- Baldino N., Gabriele D., Migliori M., de Cindio B., (2009). *Influence of process and formulation on chocolate rheology*. Proceeding of the 5th International Symposium on Food Rheology and Structure, Zurich 15th- 18th June, 250-253
- Barnes H.A., Hutton J.F., Walters K. (1989). *An Introduction to Rheology*. Elsevier Science Publishers B.V., Amsterdam, NL
- Blanco Muñoz M. A. (2004). *Olive oil in food spreads*, Grasas y Aceites 55, 92–94
- Borwankar R.P., Frye L. A., Blaurock A.E., Sasevich F.J., (1992). *Rheological characterization of melting of margarines and tablesreads*, Journal of food engineering 16, 55–74
- Brunello N., McGauley S. E., Marangoni A., (2003). *Mechanical properties of cocoa butter in relation to its crystallization behavior and microstructure*, Lebensm.-Wiss. u.-Technol. 36, 525–532

- Cappelli P., Vannucchi V., (2000). *Chimica degli Alimenti: conservazione e trasformazione*, Zanichelli ed. (italian language)
- Clogston J., Rathman J., Tomasko D., Walker H., Caffrey M. (2000). *Phase behaviour of a monoacylglycerol (Myverol 18-99K)/water system*, Chemistry and Physics of Lipids 107, 191–220
- Constantinides, P. P., Yiv S. H. (1994). *Particle size determination of phase-inverted water-in-oil microemulsions under different dilution and storage conditions*, International Journal of Pharmaceutics 115, 225-234
- Coupland J. N., (2002). *Crystallization in emulsions*, Current Opinion in Colloid and Interface Science 7, 445–450
- Cox W. P. and Merz E. H., (1958). *Correlation of dynamic and steady flow viscosities*. Journal of Polymer Science 28, 619-622.
- De Graef V., Van Puyvelde P., Goderis B., Dewettinck K., (2009). *Influence of shear flow on polymorphic behavior and microstructural development during palm oil crystallization*, Eur. J. Lipid Sci. Technol., 111, 290–302
- Eicke H-F., Borkovec M., and Das-Gupta B., (1989). *Conductivity of water-in-oil microemulsions: a quantitative charge fluctuation model*, J. Phys. Chem., 93, 314–317
- Friberg S.E., (1997). *Emulsion Stability* in S.E. Friberg, K. Larsson, Food Emulsions, 3rd ed., Marcel Dekker Inc.
- Fessas D., Signorelli M., Schiraldi A., (2005). *Polymorphous transitions in cocoa butter a quantitative DSC study*, Journal of Thermal Analysis and Calorimetry, Vol. 82, 691–702
- Gabriele D., de Cindio B., D'Antona, P., (2001) a. *A weak gel model for foods*. Rheol. Acta 40, 120-127
- Gabriele D., Curcio S., de Cindio B. (2001) b. *Optimal design of single screw extruder for liquorice candy production: a rheology based approach*. Journal of Food Engineering, 48, 33–44
- Gabriele D., Migliori M., Di Sanzo R., de Cindio B., (2008). *Effetto degli stabilizzanti sulle proprietà reologiche di emulsioni a base latte* (Italian language). Proceeding of the 10th Italian Conference on Rheology (S.I.R.), Ravenna (Italy) 18th- 21th May, 295-300

Garti N., Binyamin H., Aserin A., (1998). *Stabilization of Water-in-Oil Emulsions by Submicrocrystalline α -Form Fat Particles*, Journal of American Oil Chemistry Society, 75, 1825–1831

Ghotra B.S., Dyal S.D., Narine S.S., (2002). *Lipid shortenings: a review*, Food Research International, 35, 1015–1048

Hindle S., Povey M.J.W., Smith K., (2000). *Kinetics of crystallization in n-hexadecane and cocoa butter oil-in-water emulsions accounting for droplet collision-mediated nucleation*, Journal of Colloid and Interface Science 232, 370–380

Jahaniaval F., (2005). *Process for preparing high liquid oil, no trans, very low saturates, regular margarine with phospholipids*, patent US 2005/0233056 A1, international classification A23D007/00

Johansson D., Bergenståhl B., Lundgren E., (1995). *Wetting of fat crystals by triglyceride oil and water. 1. The effect of additives*, Journal of the American Oil Chemists Society, 72, 921–931

Lipp M. and Anklam E., (1997). *Review of cocoa butter and alternative fats for use in chocolate-Part A. Compositional data*, Food Chemistry, 62, 73–97

Lipp M., Simoneau C., Ulberth F., Anklam E., Crews C., Brereton P., de Greyt W., Schwack W., Wiedmaier C., (2001). *Composition of Genuine Cocoa Butter and Cocoa Butter Equivalents*, Journal of food composition and analysis, 14, 399–408

Macierzanka A., Szelağ H., Szumala P., Pawłowicz R., Mackie A. R., Ridout M.J., (2009). *Effect of crystalline emulsifier composition on structural transformations of water-in-oil emulsions: Emulsification and quiescent conditions*, Colloids and Surfaces A: Physicochem. Eng. Aspects 334, 40–52

McClements D.J., (1999). *Food Emulsions – Principles, Practice and Techniques*, CRC Press, New York, Chapter 4

Ozawa K., Solans C., Kunieda H., (1997). *Spontaneous formation of highly concentrated oil-in-water emulsions*, Journal of Colloid and Interface Science 188, 275–281

- Paso K., Silset A., Sørland G., de A. L. Gonçalves M., Sjöblom J., (2009). *Characterization of the Formation, Flowability, and Resolution of Brazilian Crude Oil Emulsions*. *Energy & Fuels*, 23, 471–480
- Peressini D., Sensidoni A., Pollini C. M., Gabriele D., Migliori M., de Cindio B., (2002). *Filled-snacks production by co-extrusion-cooking. Part 3. A rheological-based method to compare filler processing properties*, *Journal of Food Engineering* 54, 227–240
- Ramli M.R., Lin S.W., Yoo C.K., Idris N.A., Sahri M.M., (2008), *Physico-chemical Properties and Performance of High Oleic and Palm-Based Shortenings*, *Journal of oleo science*, 57, 605–612
- Rousseau D., (2000). *Fat crystals and emulsion stability - a review*, *Food Research International* 33, 3-14
- Schenk H., Peschar R., (2005). *Understanding the structure of chocolate*, *Radiation Physics and Chemistry* 71, 829–835
- Singh D., Rezac M. E., Pfromm P. H., (2009). *Partial hydrogenation of soybean oil with minimal trans fat production using a Pt-Decorated polymeric membrane reactor*, *J Am Oil Chem Soc*, 86, 93–101
- Skogerson L., Boutte T., Robertson J., Zhang F., (2007). *Non-hydrogenated vegetable oil based margarine for puff pastry containing an elevated diglycerides emulsifier*, USPTO Patent Application 20070148313, Class: 426602000 (USPTO)
- Steffe J.F., (1996). *Rheological methods in food process engineering*, Freeman Press, Michigan
- Tarabukina E., Jego F., Haudin J.-M., Navard P., Peuvrel-Disdier E., (2009). *Effect of shear on the rheology and crystallization of palm oil*, *Food Engineering and Physical Properties*, 74, 405-416
- Wiederman L. H., (1978). *Margarine and Margarine Oil, Formulation and Control*, *Journal Of The American Oil Chemists' Society*, 55, 823–829

Conclusions

In the present PhD thesis the rheological and microscopic study of highly-concentrated-in-oil emulsions has been reported. The high concentration of phases does not identify their mutual position: in fact, the main constituent of the system can be either the dispersed or the continuous phase. The thesis is developed by subdividing the main subject into two opposites parts: the rheological and microscopic study of unstructured and concentrated O/W emulsions, and the analysis of the progressive structuration of the aqueous and oily phase of food emulsions. Two different case studies have been taken into account: crude oil emulsification for its transportation in pipelines, and the formulation and production optimisation of a new-*trans-fats-free* puff pastry shortening replacer.

The first case study was discussed in chapters 2, 3 and 4. First of all an isoenergetic emulsification was studied, finding interesting considerations upon the possibility of constructing a more or less stable system without changing drastically the final viscosity of the emulsion (Chapter 2). It is noteworthy that the relationship between emulsions viscosity and droplet size distribution (DSD) is independent of the energetic level of mixing, and only slight viscosity changes have been found for samples produced at different powers of mixing but the same energetic level.

Then, the destabilisation study of apparent Newtonian model O/W emulsions was considered comparing two different destabilisation tests: a long-term and an accelerated short-term one in centrifuge (Chapter 3). The destabilised samples showed a marked creaming effect leading to a notable stratification with the production of an upper creamy layer for both the stability tests. Thus, the huge increase of the upper creamy layer viscosity has been attributed only to the creaming effect even if the Ostwald ripening phenomenon was detected.

Successively, a batch and a flow induced emulsification processes in order to simulate the pipeline behaviour of model crude oil-in-water emulsions with paraffin waxes added was analysed (Chapter 4). It has been concluded that, as far as flow emulsification, waxes seemed to reduce the time requested to reach a constant apparent Newtonian behaviour.

The other two chapters dealt with the production of W/O and O/W emulsions with a structured water phase, and W/O crystallised emulsions with a structured oily phase for the production of a puff pastry shortening replacer (Chapters 5 and 6).

If compared with two commercial shortenings, the best results from a rheological point of view have been obtained with an O/W emulsion having the water phase structured with wheat flour and κ -carrageenan, and a W/O crystallised emulsions produced by structuring the oily phase with a mono- and di-glyceride/cocoa butter complex.

International Journals

Gabriele D., Migliori M., **Lupi F. R.**, de Cindio B., (2009). *Batch And Flow-Induced Emulsification Of O/W Concentrated Emulsions For Crude Oil Transportation*, Oil & Gas Science and Technology. *In press*.

Migliori M., Gabriele D., Baldino N., **Lupi F. R.**, de Cindio B., (2009). *Rheological Properties of Batter Dough: Effect of Egg Level*, Journal of Food Process Engineering. *In press*.

Proceedings of International Conferences

F. R. Lupi, N. Baldino, D. Gabriele, M. Migliori, B. de Cindio, (2009), *Olive oil emulsions as puff pastry shortening replacer*, ISFRS 2009, 15 - 18 June, Zurich, (CH)

D. Gabriele, M. Migliori, **F.R. Lupi**, B. De Cindio, (2008), *Olive oil based emulsions in frozen puff pastry production*, The XV International Congress on Rheology, Monterey, California (U.S.A.), 3 - 8 August, 2008

M. Migliori, D. Gabriele, N. Baldino, **F. R. Lupi**, B. de Cindio, (2008), *Rheological study of batter dough for yorkshire pudding*, The XV International Congress on Rheology, Monterey, California (U.S.A.), 3 - 8 August, 2008

F. R. Lupi , M. Migliori, D. Gabriele, N. Baldino, R. Di Sanzo, B. de Cindio,(2007), *Oil in water emulsions characterisation for heavy oil in pipeline transportation*, 4th Annual European Rheology Conference, 12-14 April, Naples, (I)

M. Migliori , D. Gabriele, N. Baldino, R. Di Sanzo, **F. R. Lupi**, B. de Cindio, S. Corraera, (2007), *Viscosity of multi-component solutions of simple and complex sugars in water*, 4th Annual European Rheology Conference, 12-14 April, Naples, (I)

M. Migliori , **F. R. Lupi**, D. Gabriele, N. Baldino, R. Di Sanzo, B. de Cindio, (2007), *Thermo-viscoelastic stresses in "short pasta": rheological modelling*, 4th Annual European Rheology Conference, 12-14 April, Naples, (I)

M. Migliori, D. Gabriele, N. Baldino, **F. R. Lupi**, R. Di Sanzo, B. de Cindio, (2007), *Biaxial extensional characterization of flour dough*, 4th Annual European Rheology Conference, 12-14 April, Naples, (I)

N. Baldino , D. Gabriele, M. Migliori, R. Di Sanzo, **F. R. Lupi**, B. de Cindio, (2007), *Application of creep test to chocolate structure determination*, 4th Annual European Rheology Conference, 12-14 April, Naples, (I)

N. Baldino, D. Gabriel , M. Migliori, R. Di Sanzo, **F.R. Lupi**, B. de Cindio, D. Vuozzo, (2007), *Rheological modelling of foam expansion*, 4th Annual European Rheology Conference, 12-14 April, Naples, (I)

N. Baldino, Rosa Di Sanzo, D. Gabriele , M. Migliori, **F. R. Lupi**, B. de Cindio, (2007), *A rheological quality control of microwave heating of foods*, 4th Annual European Rheology Conference, 12-14 April, Naples, (I)

R. Di Sanzo , D. Gabriele, M. Migliori, N. Baldino, **F. R. Lupi**, B. De Cindio, D. Vuozzo, (2007), *Rheological properties of dairy emulsions for whipping products*, 4th Annual European Rheology Conference, 12-14 April, Naples, (I)

R. Di Sanzo , M. Migliori, D. Gabriele, N. Baldino, **F. R. Lupi**, B. de Cindio, (2007), *A rheology assisted approach to fruit extract production*, 4th Annual European Rheology Conference, 12-14 April, Naples, (I)

Proceedings of Italian Conferences

F. R. Lupi, M. Migliori, D. Gabriele, B. de Cindio (2008), *Caratterizzazione di emulsioni olio in acqua con aggiunta di cere per il trasporto di greggi pesanti in condotte*, GRICU 2008, 11-14 September, Le Castella (Kr)

D. Gabriele, M. Migliori , **F.R.Lupi**, N. Baldino, C. Oliviero Rossi, B. de Cindio (2008), *Analisi reologica di emulsioni modello per applicazioni in campo petrolifero*, X Convegno Nazionale di Reologia, 18-21 may, Ravenna

F. R. Lupi, D. Gabriele, M. Migliori, B. de Cindio (2008), *Studio della struttura di un'emulsione cosmetica mediante misure di creep e di XRD*, X Convegno Nazionale di Reologia, 18-21 May, Ravenna

F.R.Lupi, D. Gabriele, M. Migliori, B. de Cindio (2008), *Analisi reologica di un'emulsione a base di olio di oliva per pasta sfoglia surgelata*, X Convegno Nazionale di Reologia, 18-21 may, Ravenna

M. Migliori, D. Gabriele, N. Baldino, **F. R. Lupi**, B. de Cindio (2008), *Proprietà reologiche di "Yorkshire Pudding"*, X Convegno Nazionale di Reologia, 18-21 may, Ravenna

N. Baldino , M. Migliori, D. Gabriele, **F.R. Lupi**, B. de Cindio, M. Veneri, G. Chidichimo (2008), *Analisi reologica di stucchi compositi per il restauro di dipinti*, X Convegno Nazionale di Reologia, 18-21 may, Ravenna